Ministry for Primary Industries
Manatū Ahu Matua

Future Forest Systems

MPI Technical Paper No: 2012/40

Prepared for the Ministry for Primary Industries
by Scion
June 2012

ISBN No: 978-0-478-40454-8 (online)
ISSN No: 2253-3923 (online)

November 2012

Disclaimer

The information in this publication is for consultation only: it is not government policy. While every effort has been made to ensure the information in this publication is accurate, the Ministry for Primary Industries does not accept any responsibility or liability for error of fact, omission, interpretation or opinion that may be present, nor for the consequences of any decisions based on this information. Any view or opinion expressed does not necessarily represent the view of the Ministry for Primary Industries.

Requests for further copies should be directed to:

Publications Logistics Officer
Ministry for Primary Industries
PO Box 2526
WELLINGTON 6140

Email: brand@mpi.govt.nz
Telephone: 0800 00 83 33
Facsimile: 04-894 0300

This publication is also available on the Ministry for Primary Industries website at http://www.mpi.govt.nz/news-resources/publications.aspx

SCION
forests • products • innovation

CLIENT REPORT
Future Forest Systems

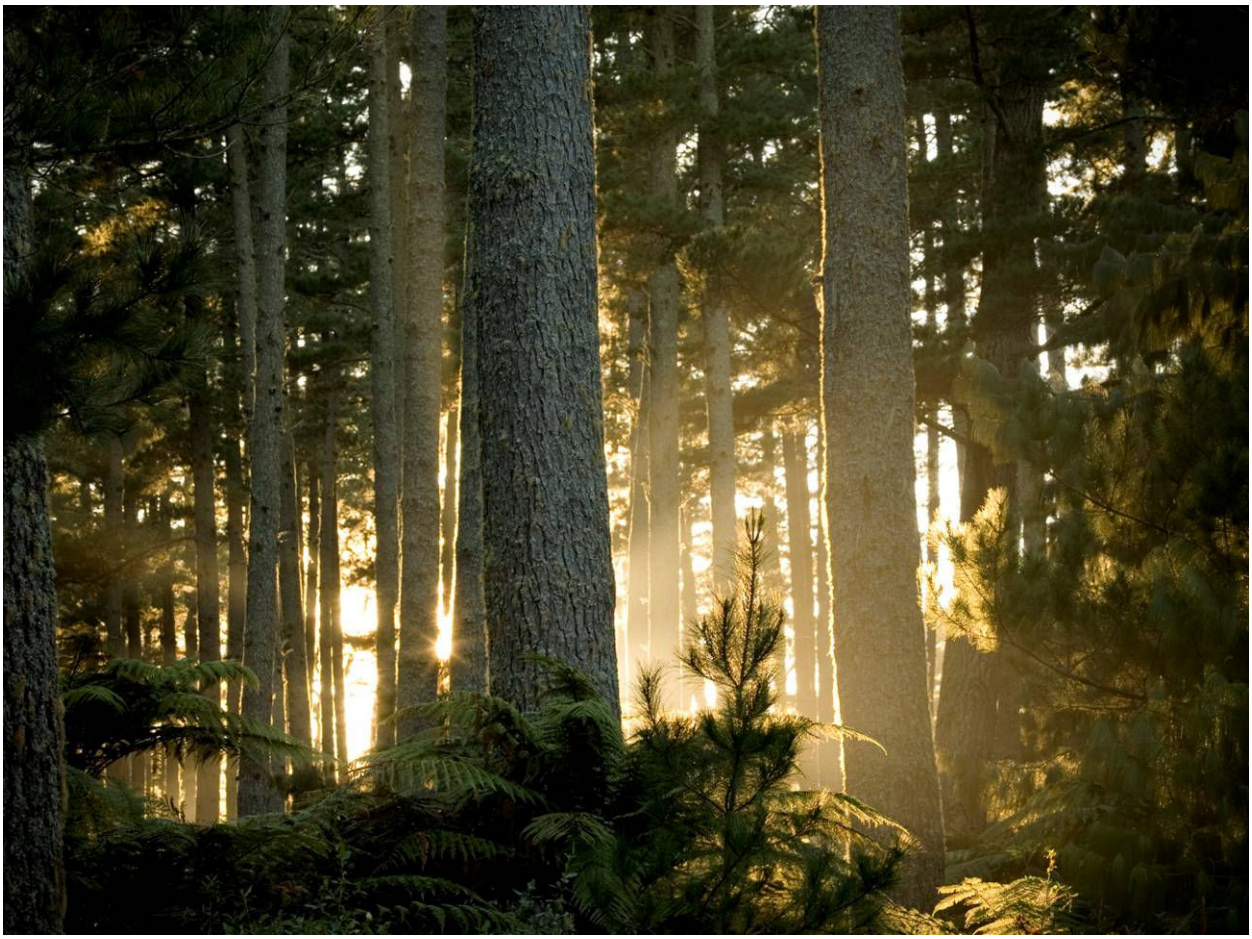

www.scionresearch.com

REPORT INFORMATION SHEET

REPORT TITLE	FUTURE FOREST SYSTEMS
AUTHORS	AUTHORS: WATT, M.S., KIRSCHBAUM, M.U.F., MEASON, D., JOVNER, A. PEARCE, H.G., MOORE, J.R., NICHOLAS, I., BULMAN, L. ROLANDO, C., PALMER, D.J., HARRISON, D., HOCK, B.K., TAIT, A., AUSSEIL, A.E., SCHULER, J.
CLIENT	MPI
CLIENT CONTRACT NO:	
FRST CONTRACT NO:	PROP-20499-SLMACC-FRI
SIDNEY OUTPUT NUMBER	
SIGNED OFF BY	JOHN MOORE
DATE	JUNE 2012
CONFIDENTIALITY REQUIREMENT	

Disclaimer

The information and opinions provided in the Report have been prepared for the Client and its specified purposes. Accordingly, any person other than the Client uses the information and opinions in this report entirely at its own risk. The Report has been provided in good faith and on the basis that reasonable endeavours have been made to be accurate and not misleading and to exercise reasonable care, skill and judgment in providing such information and opinions.

Neither Scion, nor any of its employees, officers, contractors, agents or other persons acting on its behalf or under its control accepts any responsibility or liability in respect of any information or opinions provided in this Report.

Future Forest Systems

Watt, M.S.
Scion, PO Box 29237, Christchurch
June, 2012

Table of Contents

EXECUTIVE SUMMARY

The problem

The aim of this research was to quantify the direct and indirect effects of climate change on plantation productivity and develop a decision support tool that can be used to optimise forestry systems under a changing climate for both plantation and native systems.

This objective was achieved by the following steps: (i) using GIS surfaces the area suitable for future afforestation was quantified and mapped, (ii) the three most suitable exotic plantation species for the East Coast of the North Island (as this area has a large proportion of future afforestable land) were selected, (iii) process-based growth models were used to estimate future productivity for these three species and also for the native species mānuka/kānuka as this has high potential for further afforestation, and (iv) we examined the likely impacts of key diseases, fire and wind on plantation productivity. The key results from the report were integrated into a decision support system (DSS) that allows end-users to optimise species, end-use and rotation length for a particular site under climate change.

Major results

Area suitable for future afforestation

Within New Zealand three potential afforestation scenarios were developed in which delineated areas ranged from ca. 0.7 million ha to 1.1 M ha and 2.9 M ha. All three scenarios targeted non-arable land classes for afforestation that have limitations for sustainable use under perennial vegetation. For the current plantations the mean national 300 Index (mean annual volume increment at age 30 for a stand growing at 300 stems ha^{-1}) was 27.4 m^3 ha^{-1} yr^{-1}. A spatial surface of 300 Index showed that the identified areas had a 300 Index that was on average between 2 to 6% higher than that of currently established plantations.

Three most useful exotic forest species

The three most suitable plantation species for the south eastern North Island (Gisborne, Hawke's Bay, Taranaki, Manawatu/Wanganui and Wellington regions) hill country were identified as this region includes a large area of marginal land suitable for future afforestation. Key attributes examined as part of the selection process were health, siting and productivity. Based on these criteria the species selected as being most suitable were *Pinus radiata*, *Sequoia sempervirens* and *Eucalyptus fastigata*.

Climate change and tree growth

Process-based growth models were used to spatially estimate productivity under current and future climate for all exotic and native species. Future climatic inputs to the process based models were derived from a factorial combination of various Global Climate Models (GCMs) and the three emissions scenarios B1 (low), A1B (mid-range) and A2 (high) with projections made to 2040 and 2090. Projections of growth for all species examined were made under the assumption of (i) no response to increasing CO_2 (modelled by holding CO_2 constant under climate change) and (ii) a growth response to increases in CO_2, with this scenario bracketing the upper end of expected changes in productivity.

The physiologically-based growth model CenW was used to simulate wood-productivity responses of *Pinus radiata* to climate change. With constant CO_2, there were only slight growth responses to climate change across the country as a whole. More specifically, there were slight

growth reductions in the warmer north but gains in the cooler south, especially at higher altitudes. When increasing CO_2 concentration was also included, responses of wood productivity were generally positive, with average increases of 19% by 2040 and 37% by 2090.

The process-based model 3-PG was parameterised for *E. fastigata* and redwoods (*S. sempervirens*) for New Zealand under current climate conditions with the spatial version of the model (3-PG2S). Using this model simulations of productivity under two management regimes (carbon and pruned) were made for both species. For *E. fastigata* there were only slight growth responses to climate change across the country as a whole under the assumption of constant CO_2, with mean increases (across management regimes) of 6% by 2040 and 12% by 2090. When increasing CO_2 concentration was also included there were average increases of 30% by 2040 and 75% by 2090. For redwoods under the assumption of constant CO_2 mean increases of 11% by 2040 and 9% by 2090 were predicted. When increasing CO_2 concentration was also included, there were mean increases of 32% by 2040 and 55% by 2090.

The physiologically-based growth model CenW 4.0 was used to simulate the response of kanuka/mānuka stands throughout New Zealand to climate change. Under constant CO_2 concentration productivity was modelled to increase by about 6% by 2040 and 9-11% by 2090. When increasing CO_2 concentration was also included productivity was modelled to increase by about 15-18% by 2040 and 24-37% by 2090.

Influence of climate change on key diseases

The two main fungal diseases affecting *P. radiata* in New Zealand are Dothistroma needle blight and Cyclaneusma needle cast. Using models developed from an extensive record set of disease observations the severity of both diseases was predicted under both current and future climate. Predictions of disease severity made to 2040 show low to moderate changes in severity for Dothistroma needle blight with severity generally declining in the North Island and increasing in the South Island. Predictions to 2040 for Cyclaneusma needle cast show little change in severity in the North Island but moderate increases in severity in the South Island. Predictions of disease severity made to 2090 show the risk from both diseases will increase significantly in parts of the South Island. In the North Island predicted disease severity to 2090 is likely to remain relatively static for Cyclaneusma needle cast and markedly decline for Dothistroma needle blight.

Influence of climate change on fire and wind risk

Fire danger ratings describing the mean number of days per year with either very high or extreme forest fire danger were predicted for 2040 and 2090 under 16 GCMs using a single mid-range A1B emissions scenario. Projections show areas of elevated fire danger under current climate in Canterbury, Gisborne, Marlborough and Central Otago/South Canterbury expand along the east coast of both islands to include coastal Otago, Wellington and Hawkes Bay by the 2040s. These elevated risks are likely to develop further in Marlborough, Hawkes Bay and Wairarapa by the 2090s. Fire dangers in Wanganui, the Bay of Plenty and Northland would also increase. Fire climate severity in Southland, south Taranaki and the Coromandel, would increase but still remain comparatively low relative to other parts of the country.

Increased fire danger has the potential to reduce forest productivity through a greater number of fires and increased area burnt. Maintaining appropriate fire management strategies, especially around fire prevention, readiness and response, will be essential to mitigating the risks associated with this increasing fire danger.

A mechanistic wind damage model (ForestGALES) was linked to various empirical growth models and a process-based growth model (CenW) to investigate potential impacts of future climate change on the risk of wind damage. For *Pinus radiata* increased tree growth rates under

the different emissions scenarios had the most significant impact on the risk of wind damage. The increases in risk were most pronounced for the high emissions A2 scenario, assuming a growth response to increases in [CO_2]. The risk was further increased by the modest increases in the extreme wind climate that are predicted to occur.

Development of a Decision Support System

The DSS was developed as a web-based tool to provide users easy access to the key results of this project. It enables users to set-up multiple scenarios to predict forest productivity under future climate change. Through the spatial user interface information is easily derived from the GIS productivity surfaces that are used by the forest process-based growth models and wind risk model. The forest process-based growth models determine the annual log yield and carbon sequestration for the selected species and silviculture regimes for a specific area. These results are converted by the forest economic model into economic values to provide the user with financial comparisons. The fire danger ratings, critical wind speed and the predicted severity for the two main fungal diseases are represented and derived from the representative GIS spatial layers. These values predict the impact future climate will have on the identified fire, diseases and wind risks. Through the DSS users are provided with sufficient information to make informed decisions on which species and silviculture regimes provides the optimal economic outcomes for a specific area under future climate change. This provides the user with the opportunity to take advantage of the economic and market opportunities arising as a result of climate change.

Introduction

Forests cover about one quarter of the Earth's land surface area. They play a major role in the present and projected future carbon budget as they contain about 80% of all above-ground and 40% of below-ground terrestrial organic carbon. They can become carbon sources when forests are harvested, degraded or damaged or carbon sinks when new forests are planted or growth rates are enhanced.

In New Zealand, the total area of forest cover is approximately 8.2 million hectares, comprising 6.4 million hectares of indigenous forests and 1.8 million hectares of planted forests. Within these planted forests, 89% of the net stocked area is comprised of radiata pine. Douglas-fir is the next most common species, making up 6%, with the remainder stocked in hardwoods, cypresses and other softwoods. As new forest planting peaked from 1992 to 1998 (average planted area of 69 000 ha $year^{-1}$) a large part of the plantation resource is now between 10 and 16 years old (New Zealand Forest Owners Association, 2007). Plantations established since 1990 on previously unforested land are potentially eligible to be counted as carbon sinks to counterbalance the emissions during the first Kyoto commitment period (2008 – 2012), and estimates of their total area range from 0.6 to 0.8 million hectares (New Zealand Forest Owners Association, 2007).

As of 2006 (New Zealand Forest Owners Association, 2007) most of the forest resource within New Zealand was located in the central North Island (550 761 ha), followed by Otago/Southland (215 662 ha), Northland (203 067 ha), Nelson/Marlborough (171 418 ha), southern North Island (168 447 ha), the East Coast of the North Island (157 009 ha), Hawkes Bay (131 768 ha), and Canterbury (113 903 ha). Relatively small areas were also located in Auckland (56 008 ha) and on the West Coast of the South Island (32 009 ha). Because of the current dominance of radiata pine within New Zealand's planted forests, coupled with its wide geographic distribution and its overall economic importance, it is important to understand the response of this species to possible changes in future environmental conditions driven by climate change. A thorough understanding of these changes will enable New Zealand's forestry sector to best adapt itself to the potential impacts of future climate change.

The Fourth Assessment Report of the IPCC (IPCC, 2007b) outlined the scope, vulnerability and the associated uncertainty of climate change on forests globally. Overall the outline drawn highlights a complex picture of positive and negative effects of climate change on forests. The overall expectation is that commercial forest productivity will rise at least modestly in the short and medium term, in response to increases in temperature and CO_2 concentration. This will be counteracted by increases in pest and pathogen outbreaks and increased risk of plantation damage from fire and wind. The IPCC also suggest that the increase in productivity will show a large regional variability and will change from low-latitude regions in the short term to high-latitude regions in the long term.

Although the IPCC provides an overview of how climate change is likely to influence forestry within Australasia, these estimates are necessarily broad, and we do not currently have detailed information describing how climate change is likely to influence plantation productivity in New Zealand at a more local level. Changes in plantation productivity which result from climate change include direct physiological responses to the changes in climate. Climate change will also influence distribution and abundance of many forest pest species (weeds, insects and pathogens) and alter the frequency and intensity of damaging abiotic factors, such as wind and fire. For this reason, a comprehensive assessment of changes in productivity has to also account for the impacts of changes in these factors as well.

The aim of this research was to determine the direct and indirect effects of climate change on plantation productivity and develop a decision support tool that can be used to optimise

forestry systems for both plantation and native systems. The research is broken down into the following steps that correspond to the chapters described below within this report :

Chapter 1. Quantify and map the area suitable for future afforestation in New Zealand. Potentially afforested areas are delineated using GIS surfaces denoting important variables influencing the afforestation potential. The productivity of these regions is described by an empirically derived GIS surface.

Chapter 2. Select the three most profitable plantation species (including radiata pine) for the case study region (East Coast of the North Island). This case study region was selected as (i) it has the greatest area that could be potentially afforested (see results from Chapter 1) and (ii) many parts of the region include highly erodible marginal land that would greatly benefit from afforestation. Further simulations investigate the productivity of these species and native species (mānuka/kānuka) under current and future climate throughout New Zealand.

Chapter 3. Process-based growth models were used to spatially estimate productivity under current and future climate for all selected exotic and native species. Future climatic inputs to the process based models were derived from a factorial combination of various Global Climate Models (GCMs) and three emissions scenarios B1 (low), A1B (mid-range) and A2 (high) as described by Meehl et al. (2007) .

Chapter 4. In this chapter we examine the indirect impacts of climate change on important biotic and abiotic factors affecting productivity of the key plantation species, radiata pine. The severity of two key diseases of radiata pine under climate change were determined. The effect of climate change on risk to radiata pine from wind and fire was also investigated.

Chapter 5. The key results described in the report have been integrated into a decision support system (DSS) that allows end-users to identify optimal end use, species, rotation length, and management for a particular site, or area, under climate change. In chapter five we describe the key components of this DSS.

A list of papers resulting from this research is given as Appendix A.

1. Spatial description of potential areas suitable for afforestation within New Zealand and quantification of their productivity under *Pinus radiata*[1]

Abstract

The demand for carbon credits to offset greenhouse gas emissions is likely to stimulate afforestation rates throughout the world. The development of maps that describe suitable new areas for plantation forestry and quantify potential productivity for these regions thus will be of considerable value to planners and growers. Using nationally available spatial datasets the objectives of this study were to (i) identify areas within New Zealand that could be afforested in the future and (ii) compare productivity between current *Pinus radiata* plantations and potential areas suitable for afforestation. Productivity for *P. radiata* was defined by 300 Index, which describes the stem volume mean annual increment at age 30 years under a reference regime of 300 stems ha^{-1}.

Within New Zealand three potential afforestation scenarios were developed in which delineated areas ranged from ca. 0.7 million ha (Scenario 1) to 1.1 M ha (Scenario 2) and 2.9 M ha (Scenario 3). All three scenarios targeted non-arable land classes for afforestation that have limitations for sustainable use under perennial vegetation. For the current plantations the mean national 300 Index was 27.4 m^3 ha^{-1} yr^{-1}. Compared to the current plantations, at the national level, 2 to 6% increases in 300 Index were predicted for areas established under these three scenarios. Such afforestation would also significantly reduce the rate of soil loss by accelerated erosion.

[1] This chapter has been published as Watt, M.S., Palmer, D. J., Höck, B. K. (2011). Spatial description of potential areas suitable for afforestation within New Zealand and quantification of their productivity under *Pinus radiata*. *New Zealand Journal of Forestry Science*, 41, 115-129.

Introduction

Plantation forestry is a major industry in the Southern Hemisphere and contributes significantly to the economy of many countries (Lewis & Ferguson, 1993; New Zealand Forest Owners Association, 2007). Although difficult to quantify, sustainably managed plantation forests also make major positive contributions to environmental and social issues. Within New Zealand the reduction of accelerated soil erosion is one of the most important and well documented auxiliary benefits of afforestation (Marden et al., 2005). The removal of natural forests in New Zealand over the last few centuries has caused rates of erosion and associated flooding and sedimentation to increase markedly, leading to detrimental environmental impacts on both affected individual land owners and communities (NWASCO, 1970). Afforestation of eroding areas has been shown to be one of the most effective ways of reducing both the size of erosion features and the volume of sediment (flow and deposition).

New opportunities for improving financial returns to tree growers are likely to provide major incentives for expansion of plantation forest in New Zealand (Hock et al., 2009). In particular, afforestation with fast-growing species is an effective means of offsetting carbon dioxide emissions to meet national commitments (Dixon et al., 1994). The volume of carbon traded has increased dramatically over the last few years and the enactment of emission trading schemes within major plantation-growing countries, such as New Zealand, is likely to markedly improve returns from forestry (Manley & Maclaren, 2009). Given the strong positive relationship between rates of return and the area annually afforested (Horgan, 2007; Manley & Maclaren, 2009), increases in returns that have been forecast to occur through carbon forestry (Manley & Maclaren, 2009) are likely to induce rapid conversion of marginal land to plantation forestry.

Developing maps that describe both suitable areas for new plantation forests and quantify potential productivity of these regions will be of considerable value to planners and growers. The objective development of these maps in New Zealand has been greatly facilitated by the recent provision of high resolution and comprehensive data sets together with increases in the capability of geographic information systems. In recent years several national extent spatial surfaces covering land-use classification (AsureQuality, 2009; Landcare Research, 2010; Newsome et al., 2000), terrain attributes (Palmer, Höck, et al., 2009) and a range of environmental variables (Leathwick et al., 2003; Leathwick & Stephens, 1998; Palmer, Watt, et al., 2009; Tait et al., 2006) have been developed.

Recent research has utilised these environmental layers to develop spatial representations of plantation productivity across broad landscape scales at a reasonably high spatial resolution (Palmer, Hock, et al., 2009; Watt, Palmer, et al., 2009). By combining productivity surfaces with maps that delineate potential regions for afforestation it should be possible to determine the productive capacity of afforestable areas on a regional basis. Comparison of productivity predictions between current and future plantations will provide some insight into the feasibility and profitability of further afforestation.

Using nationally available datasets the objective of this research was to spatially delineate the potential locations of future forests within New Zealand. Previously developed spatial surfaces of productivity for the most common plantation species, *Pinus radiata* D. Don, were then overlaid on these delineated areas. Estimates of productivity were determined for both current and future plantings at national and regional scales.

Materials and Methods

Identification of current plantations

Current *P. radiata* plantations within New Zealand were identified from Land Cover Database 2 (LCDB2) (Thompson et al., 2003) data. LCDB2 provides a snapshot of New Zealand landcover derived from satellite imagery for the summer of 2001/2002. Current plantations were identified from the following categories within the first order classification of forest; afforestation (not imaged, and also imaged, post LCDB1), forest (harvested), and pine forest (open and closed canopy). A map showing the spatial distribution of current plantations is shown as Figure 1.1.

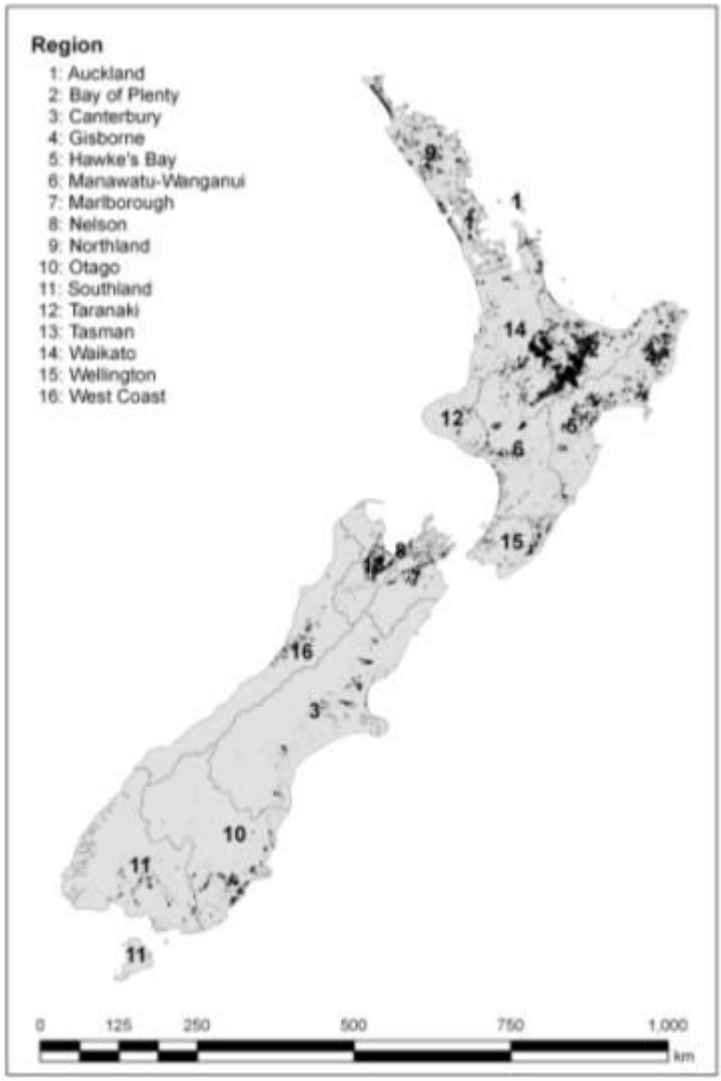

Figure 1.1. Map of New Zealand showing current plantation forests.

Delineation of future afforestation scenarios

An analysis was undertaken using the GIS platform ArcGIS™ and a variety of GIS spatial datasets to identify areas suitable for future forests. In total, three scenarios were identified from the Land Use Capability (LUC) classes. The first category included the poorest land classes with only severe erosion (Scenario 1) while the second and third categories included successively superior land use classes subject to erosion ranging from moderate to extreme (Scenario 2), and slight to extreme (Scenario 3). Depending on

the type of erosion the classes used for erosion broadly correspond to a percentage eroded area of 0.5 - 10% for slight, 2 – 20% for moderate and >20 to >60% for severe (see Lynn et al., 2009). A full description of the criteria used to select the scenarios illustrated in Figure 1.2 follows.

The AgriBaseTM-enhanced New Zealand Land Cover Database 2 (LCDB2) data (AsureQuality, 2009) was a major component in the identification of land with potential for the establishment of future forests. The New Zealand Land Cover Database (LCDB2) is a digital map of land cover created by grouping together similar classes that were identified from satellite images. There are eight 1st order classes described by LCDB2 that include the following: (1) artificial surfaces; (2) bare or lightly vegetated surfaces; (3) water bodies; (4) cropland; (5) grassland; (6) sedgeland and saltmarsh; (7) scrub and shrubland; and (8) forest. Each of the 1st order classes is divided into several categories (LCDB2 classes). For this analysis we selected categories from both grassland, and scrub and shrubland classes. These categories included depleted, low and high producing grassland (from 1st order class grassland) and gorse and broom and mixed exotic shrubland (from 1st order class scrub and shrubland).

To minimise the impact on native plant biodiversity, carbon, landscape values and areas suited to ecological protection, a number of categories within the 1st order classifications (5) grassland, and (7) scrub and shrublands were excluded from the analysis. Within the grassland class, the category of tall-tussock grassland was excluded while the categories excluded from the scrub and shrubland class included fernland, manuka and/or kanuka, matagouri, broadleaved indigenous hardwoods, sub alpine shrubland, and grey scrub. The rationale for these exclusions is that afforestation should be undertaken in a manner that minimises further native ecosystem loss.

From a carbon forestry viewpoint, the shrubland categories were excluded as they are considered native carbon sinks. The shrubland categories can be eligible for carbon credits if they are the result of natural succession on ex-pasture land since January 1990 and fulfil the definition of forests, namely having a woody cover of at least 30% and a minimum height of 5m at maturity (Ministry for the Environment, 2010).

Within the 1st order grassland category, the AgriBase™ enhanced LCDB2 that describes the type of farming at a fine scale was used to further refine the selected areas. The aim of using AgriBase™ enhanced LCDB2 was to exclude land uses with the potential for high returns - for example, dairying, horticulture, and viticulture. For the low producing and depleted grassland the classes beef (BEF), deer (DEE), grazing other peoples' stock (GRA), not farmed - idle (NOF), sheep (SHP), mixed sheep and beef (SNB), and unspecified (UNS) were selected (Figure 1.3a). For high producing exotic grassland all of these classes were selected apart from the BEF farm type class, as these areas are likely to provide higher returns.

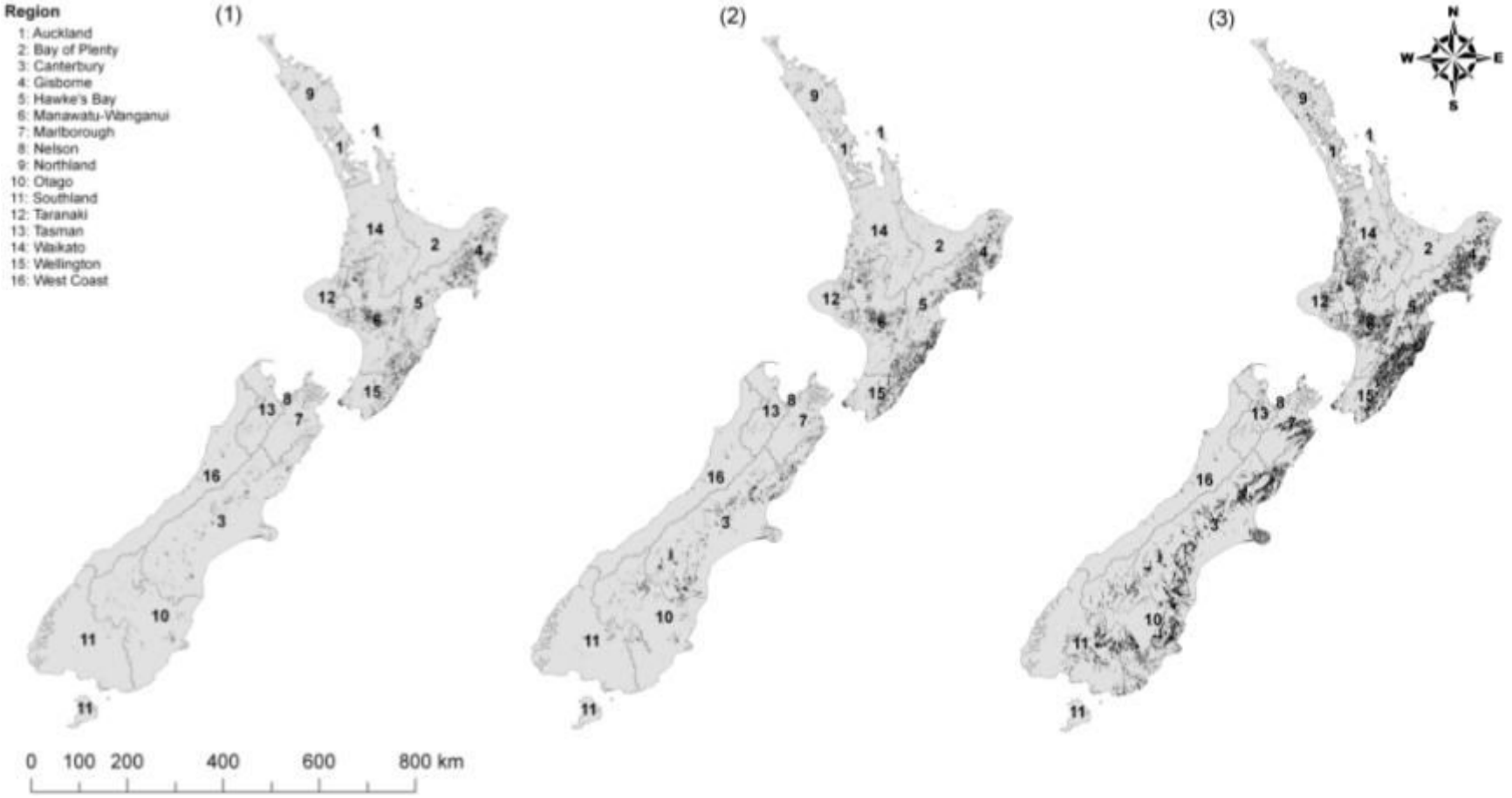

Figure 1.2. Map of New Zealand showing afforestation Scenario 1(left), 2 (centre) and 3 (right).

Land use capability (LUC) classes (Figure 1.3b, c) were used to exclude arable land and slightly limited non-arable classes and to differentiate between the three scenarios on the basis of erosion severity. Within this classification, LUC 1 to 4 denote arable land classes whereas LUC 5 to 8 are unsuitable for arable land and have slight (LUC 5), moderate (LUC 6), severe (LUC 7) and extreme (LUC 8) limitations for perennial vegetation such as pasture and forest. A full description of the LUC system is given in Lynn et al. (2009).

Based on past patterns of land use, expert opinion and classification ratings we included areas in LUC 7 and 8 (meeting other criteria outlined in Table 1.1) as potentially afforestable land. Because LUC 7 has severe limitations it is widely accepted that forestry is a more suitable sustainable use than agriculture for this class (Lynn et al., 2009). The LUC 8 lands, included as permanent carbon sinks and not harvested, may potentially provide a useful long term landuse for this class. Because erosion potential is the key limitation and differentiator of land within LUC 6, and because forestry provides the most effective solution to controlling accelerated erosion (Marden et al., 2005), we developed three scenarios based on erosion severity within LUC 6 (Figure 1.3b). The first scenario was most conservative and included only severe to extreme erosion severities; the second included moderate to extreme erosion severities; and the third was least conservative and included slight to extreme erosion severities (Figure 1.3b). All of these scenarios also included the delineated areas within LUC 7 and 8. LUC 5 was not included in our analyses because these areas are generally accepted as being more suited to agriculture than forestry (NWASCO, 1979; SCRCC, 1974). This assumption is unlikely to markedly affect results as the area of LUC 5 in New Zealand is negligible (Lynn et al., 2009).

Table 1.1. Spatial datasets and criteria used to determine potential available land.

Spatial dataset	**Criterion**
Temperature (°C)	> 7.9
Slope (degrees)	No limit
Land cover database 2 (LCDB2) in association with Agribase farm type	40: High producing grassland 42: Low producing grassland 44: Depleted grassland 51: Gorse and broom (regardless of Agribase class) 56: Mixed exotic shrubland (regardless of Agribase class)
Land use capability (LUC)	6*, 7, 8
Department of Conservation estate (DoC)	None
Potential predicted vegetation	21, 22, 23, 24, 25 (non-forest classes excluded)

* three available land scenarios were developed by subdividing LUC class 6 into three categories with the following erosion severity: (1) severe to extreme; (2) moderate to extreme; and (3) slight to extreme.

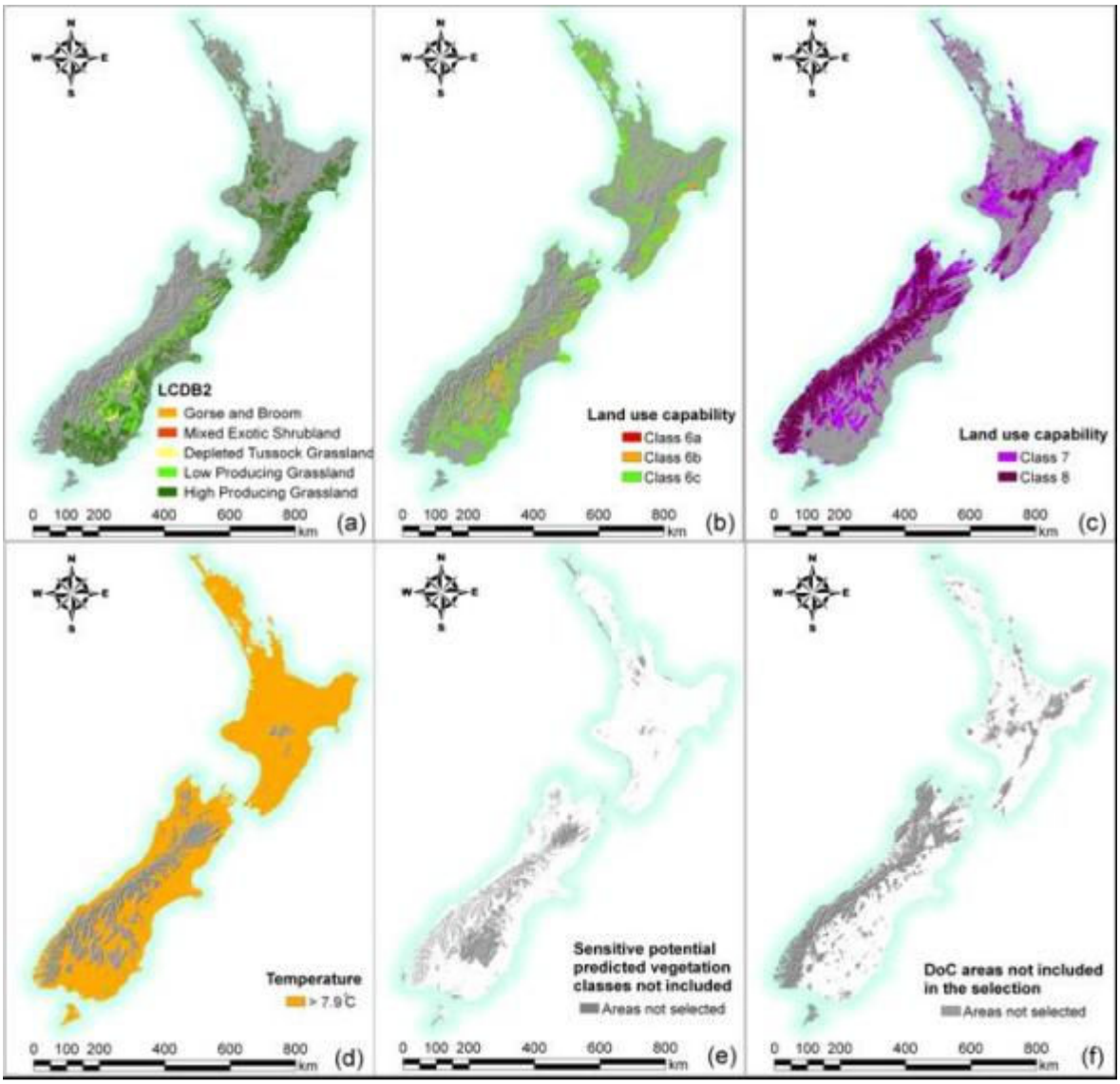

Figure 1.3. Map of New Zealand showing the distribution of: (a) Land cover database 2 (LCDB2) showing the spatial distribution of Agribase^{TM} farm types given in Table 1.1; (b) land use capability (LUC) 6, showing the three erosion classes; severe to extreme (designated as 6a), moderate to severe (designated as 6b) and slight to extreme (designated as 6c); (c) LUC 7 and 8; (d) areas above the threshold of 7.9 °C; (e) sensitive potential predicted vegetation classes; and (f) Department of Conservation (DoC) areas.

A number of other areas were excluded from the analysis. Using a 500 m resolution normalised climate surface (NIWA, 2008) (Figure 1.3d) we excluded regions with a mean annual temperature lower than 7.9 ˚C, because *P. radiata* productivity at temperatures below this threshold is very low (Palmer, Hock, et al., 2009). The areas delineated were also limited to areas exceeding a predicted 300 Index of 5 $m^3 ha^{-1} yr^{-1}$ and a Site Index of 13.5 m (for a description of this surface see (Palmer, Hock, et al., 2009)) as productivity values below these have not been recorded in New Zealand previously and are unlikely to provide a return on investment. It is more likely that natural reversion to native forest cover will be practised in these areas.

We used a number of layers to identify areas of native vegetation that should not be afforested. A number of potential predicted vegetation classes (Figure 1.3e (McGlone et al., 2004)) were used to exclude grassland and shrubland areas that have unique biodiversity value and would not naturally support trees. These regions included scrub, tussock-grassland and herbfield above the tree-line, and scrub, shrubland and tussock-grassland

classes below the tree-line, with the latter group occurring mostly in the central Otago region where they have landscape character value. These are areas that should ideally remain as shrubland and tussock type vegetation regardless of human activities.

The potential predicted vegetation also enables the identification and removal of dunelands and wetlands from the analysis because these areas are generally unsuitable for afforestation. The Department of Conservation (DoC) estate (Figure 1.3f), and current plantation areas were excluded from delineated areas. The DoC estate was defined by a vector dataset provided by DoC staff in 2009.

Determination of productivity for current and proposed plantations

Pinus radiata is a fast growing softwood that is currently the dominant production species in New Zealand, comprising 89% of the current estate (New Zealand Forest Owners Association, 2007). This study assumes that future plantings are predominantly *P. radiata.* A previously developed surface of 300 Index for *P. radiata* (Palmer, Hock, et al., 2009) was used to spatially quantify productivity for both the current estate and proposed plantings.

The 300 Index defines the stem volume mean annual increment (MAI) of *P. radiata* at age 30 years with a reference regime of 300 stems ha^{-1} (Kimberley et al., 2005). We used 300 Index in this study because standardised volume-based measurements provides a more accurate means of ascertaining site productivity for *P. radiata* than height based measurements such as Site Index (Kimberley et al., 2005). Importantly, recent research has clearly shown that accurate and unbiased values for 300 Index can be obtained using measurements taken from *P. radiata* stands differing in age or stocking from those of the 300 Index standard regime (30 years and 300 stems ha^{-1} stocking; Kimberley et al., 2005).

To calculate the 300 Index, a plot measurement consisting of the basal area, mean top height and stocking at a known age, along with stand history information (initial stocking, timing and extent of thinnings, and timing and height of prunings) are required. The 300 Index estimation procedure utilises the 300 Index model, an empirical stand level basal area growth model that expresses basal area as a function of age, stocking, Site Index and the 300 Index, effectively a local site productivity parameter (Kimberley et al. 2005). The model accounts for the effects of pruning and thinning using age-shift adjustments. For example, field trials have demonstrated that the effect of a typical pruning regime is to lose about 1.4 years' basal area growth compared with a similar unpruned regime, and this effect is incorporated into the 300 Index growth model. The model is structured so that for stands using the standard '300 Index' regime (pruned to 6 m height, and thinned at time of final pruning so that stocking density at age 30 years is 300 stems.ha^{-1}) the stem volume MAI equals the 300 Index parameter. Therefore, the 300 Index is as an index of stem volume productivity, defined as the volume MAI at age 30 years for this standard regime. Because the model is sensitive to departures from this standard regime (e.g., different stocking levels and different intensities and timing of thinning and pruning regimes), and can also adjust for the stand age, it can be used to predict the index for any plot measurement. To do this, an iterative procedure is used to determine the 300 Index parameter value compatible with the plot measurement and management history associated with the plot.

Regression kriging was used to develop a spatial surface for 300 Index (Palmer, Hock, et al., 2009). Regression kriging (or Universal Kriging, Kriging with External Drift) is one of the most widely used of the hybrid geostatistical techniques and combines ordinary kriging with regression using ancillary information. If the correlation between the dependant (300 Index in this case) and predictive variables is significant, regression kriging generally results in more accurate local predictions than generic geostatistical models such as ordinary kriging (Hengl et al., 2004; Odeh & McBratney, 2000). Regression kriging was used to develop a model from 1,764 independent values of 300 Index (n = 1,146 training observations and n = 618 validation observations) that were well dispersed throughout New Zealand. The model

accounted for 61% of the variance in the validation dataset. The underlying partial least squares model was developed from a wide range of biophysical GIS surfaces, that included primary and secondary terrain attributes (Palmer, Höck, et al., 2009), monthly and annual soil water balance (Palmer, Watt, et al., 2009), monthly and annual climate variables (Leathwick & Stephens, 1998; Mitchell, 1991), fundamental soil layers (FSL), land resource information (Newsome et al., 2000), vegetative cover (Newsome, 1987), foliar nutrition (Hunter et al., 1991), and biophysical surfaces (Leathwick et al., 2002; Leathwick et al., 2003) for New Zealand.

The previously described spatial surface of 300 Index (Palmer, Hock, et al., 2009) is reproduced as Figure 1.4. Using this developed layer, total stem volume was determined as the product of 300 Index and the average national rotation age for *P. radiata* of 28 years (New Zealand Forest Owners Association, 2007). There is typically 15% breakage in harvesting and approximately 10% of stands are unstocked so estimates of total stem volume were reduced by 25% per hectare to approximate the average merchantable volume of current and proposed plantings.

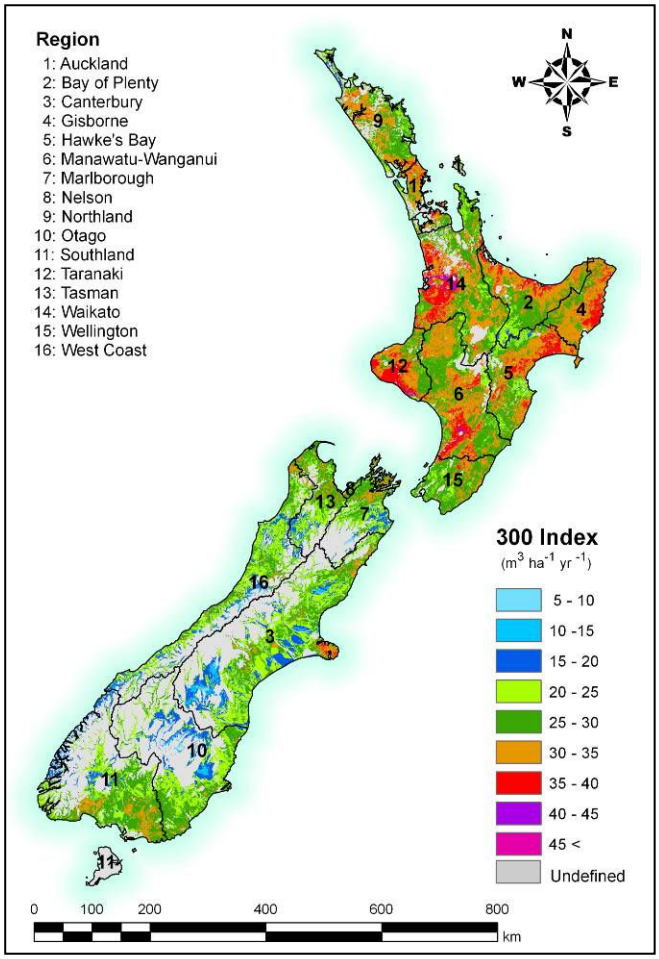

Figure 1.4. Map of New Zealand showing the spatial distribution of predicted 300 Index.

Spatial dataset resolution

Future forest scenarios were derived from five main spatial surfaces that had varying scale. All spatial surfaces were comprised of polygon vector data with the exception of air temperature which was a 500 m cell size resolution with an estimated mapping or cartographic scale of 1: 50,000. We converted these polygon vector datasets to a 25 m cell size resolution to minimise the loss of area represented in the vector during the raster conversion process. The LCDB2 dataset map accuracy was estimated at 93.9% using the

simple accuracy percentage statistic and is considered to have a scale of 1:50,000 (Ministry for the Environment, 2007). The LUC units were originally mapped at a 1:63,360 or 1 inch to 1 mile and are based on units that are considered to have uniform characteristics (NWASCO, 1979), whereas the vegetation cover map was developed at a 1:1,000,000 (Newsome, 1987). For greater detail around mapping units and classifications please refer to referenced documentation. All surfaces were available in New Zealand Map Grid (NZMG) based on the NZGD 1949 datum.

Results

Area distribution of current plantations

The 1.83 M ha currently established in *P. radiata* comprises 6.9% of the land area of New Zealand. Most of this area (73.6%) is in the North Island and the regions with the three largest areas of plantations are the Waikato, Bay of Plenty, and Northland regions. Although total forested area in the three northern South Island regions (Nelson, Marlborough and Tasman), is relatively low, these forests nevertheless comprise a moderate percentage of the total regional land area. In contrast, plantations within the remaining regions of the South Island are relatively scattered and the percentage land area in forests within these regions are far lower than that of the national average.

The majority of the current plantation estate has been established on flat to rolling land, with 61% located on land with slope < 15° (Figure 1.5a). The LUC classes on which plantations were predominantly established (Figure 1.5b) included LUC 6 (47%) and LUC 7 (30%). In total 21% of the current plantation estate is located on the arable classes LUC 1 − 4. The greatest area within each LUC class was located on slopes of 0 − 3° for LUC 1, 2, 3, 4 and 8 and 7 − 15° for LUC 6 and 7. Closer examination of the data indicated that the majority (65%) of the current plantations established on arable classes were located in the central North Island (Waikato and Bay of Plenty) and in Canterbury.

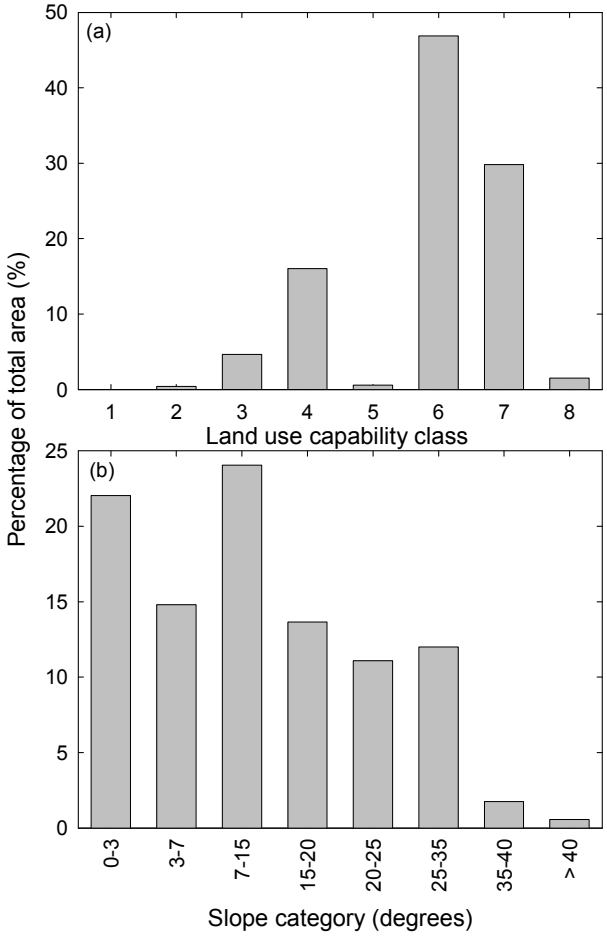

Figure 1.5. Distribution of: (a) land use classification: and (b) slope class for current plantations.

Area distribution of proposed plantations

For Scenario 1 (severe to extreme erosion severities), the delineated 698,329 ha are predominantly located in the North Island (78% of total area), and regions with greatest areas are in Gisborne and the Manawatu-Wanganui regions (Figure 1.2). Similarly, for Scenario 2 (moderate to extreme erosion severities), two-thirds of the delineated 1,134,346 ha are located in the North Island, and predominantly on the east coast (Hawkes' Bay and Gisborne) and Manawatu-Wanganui (Figure 1.2). In contrast to the moderate to extremely eroded land, most of the slightly eroded land is located in the South Island. Consequently, a far larger proportion of the 2,925,555 ha identified in Scenario 3 (slight to extreme erosion severities) is located in the South Island, with the Canterbury region having the single largest area (Figure 1.2).

For all three scenarios high producing exotic grassland was the land cover most highly represented, comprising 72, 70 and 74% of the total area for Scenarios 1, 2 and 3, respectively (Table 1.2). Low-productivity grassland was the second largest category and accounted for between 18 and 23% of the total area for all three scenarios. All other LCDB categories comprised a relatively low proportion of the area defined by the three scenarios (Table 1.2).

Table 1.2. Distribution of area (thousand hectares) by LCDB2 classes, and LUC, showing within LUC6 the area breakdown under Scenarios 1 (severe to extreme erosion), 2 (moderate to extreme erosion) and 3 (slight to extreme erosion). Also shown is the summary of total area, by scenario, which for all scenarios includes the summation of the relevant LUC 6 class with both LUC 7 and LUC 8. For the total areas by scenario the percentage breakdown is also given in parentheses.

	Area in LUC 6 for Scenario			Area in LUC7	Area in LUC8	Total area for Scenario		
	1	2	3			1	2	3
High producing grassland	6.4	289	1592	492	15.9	514 (72)	797 (70)	2100 (74)
Low producing grassland	2.2	133	551	115	6.7	124 (23)	255 (22)	672 (18)
Depleted grassland	0.6	10.2	14.3	4.8	0.4	6 (1)	15 (1)	19 (1)
Gorse and or broom	0.3	10.8	69.9	45.6	3.0	49 (4)	59 (5)	118 (7)
Mixed exotic shrubland	0.1	2.8	9.6	4.7	0.7	5 (1)	8 (1)	15 (1)
Total area	10	446	2237	662	27	698 (100)	1134 (100)	2926 (100)

Productivity of the current and proposed plantings

For the current plantations the mean national 300 Index was 27.4 m^3 ha^{-1} yr^{-1}, which equates to respective total stem and merchantable volumes of 767 and 576 m^{-3} ha^{-1}. Mean predicted productivity was greatest and markedly above the national average in Gisborne (32.2 m^3 ha^{-1} yr^{-1}), Hawke's Bay (31.3 m^3 ha^{-1} yr^{-1}) and Taranaki (31.2 m^3 ha^{-1} yr^{-1}), and close to the national average in the remainder of the North Island regions (Appendix B). In contrast, all regions within the South Island had a 300 Index lower than the national average, and by region ranged from 22.2 ha^{-1} yr^{-1} in Canterbury to 26.8 m^3 ha^{-1} yr^{-1} in Marlborough (Appendix B).

Regional variation in 300 Index for the three future afforestation scenarios showed a very consistent trend throughout New Zealand (Appendix B). There was a distinct increase in 300 Index from Northland to Gisborne, after which 300 Index declined with decreasing latitude to Otago. Values increased slightly between Otago and Southland (Appendix B).

Future proposed plantings were predicted to have a national average 300 Index that exceeded that of current forests, by between 2 and 6%, ranging from 29.1 m^3 ha^{-1} yr^{-1} for Scenario 1 to 28.3 m^3 ha^{-1} yr^{-1} for Scenario 2 and 27.9 m^3 ha^{-1} yr^{-1} for Scenario 3. Mean regional gains in 300 Index for the three scenarios, over the current estate, were evident for all regions except Southland, Taranaki, Otago and Marlborough. Mean regional gains were particularly pronounced in the northern regions of Bay of Plenty (+15.4%) and Waikato (+13.7%). The more marked increase in 300 Index for Scenario 1 over the other two scenarios was attributable to a high proportion of land for this scenario in high productivity areas, such as Gisborne and Manawatu-Wanganui, and low proportion of land located in low productivity regions, such as Canterbury (particularly compared to Scenario 3).

Discussion

Within the predominantly agricultural land classes deemed to be suitable for afforestation this analysis delineates three scenarios that are differentiated on the basis of erosion severity within LUC 6. We assumed erosion severity to be the key determinant of the potential area suitable for afforestation. Erosion is the dominant limitation for non-arable land classes (Lynn

et al., 2009) and afforestation of eroded areas provides the auxiliary benefit most likely to draw support from both landowners and government. Using this criterion, analysis suggest between 2.6 and 11% of New Zealand's land area is suitable for further afforestation. Conversion of this land to forestry is generally predicted to result in an increase in overall productivity compared with that of the current estate. These gains are likely to be more marked if areas most in need of afforestation (i.e. subject to severe to extreme erosion) are established, as these areas are predominantly located in high-productivity areas. The maps described here allow identification of high productivity areas and will reduce investor risk within new areas for which there is no prior history of plantation productivity.

Afforestation of Scenario 1, that includes the ca. 0.7 M ha in LUC classes 7 and 8, and the severe to extremely eroded class in LUC 6, is reasonably likely. Within New Zealand the analyses show that most of these high priority areas are located in the North Island and are particularly prevalent along the east coast (Gisborne) and in the Manawatu-Wanganui region. Afforestation of Scenario 2, that includes all of the aforementioned areas and the moderately eroded LUC 6 land (436,000 ha), would also be a realistic afforestation target. Nationally administered grant schemes, currently in place to support conversion of both LUC 7 and erosion-prone LUC 6 land to forest, have already facilitated afforestation of substantial areas within these classes. Given that catchment sediment loads within these regions are the highest within New Zealand (Dymond et al., 2006; Hicks, 1991; Page et al., 1999), afforestation would have considerable auxiliary benefit for not only individual landowners but also the wider community.

The probability that all of Scenario 3 could be afforested is very low because there is likely to be considerable landowner resistance to afforesting LUC 6 areas with only slight erosion. Conversion of the entire area delineated in Scenario 3 will also largely displace low intensity agriculture from the New Zealand landscape. Consequently, our analyses suggest that further afforestation is likely to range in areal extent between ~1.1 M ha (Scenario 2) and 2.9 M ha (Scenario 3). The key sensitivity around total future afforested area is likely to be the proportion of slightly eroded LUC 6 land that is converted to forestry.

The proportion of slightly eroded land that could be afforested is likely to depend largely on the rate of return for forestry, compared with other landuses, and landowner amenability to change. Historically, within New Zealand, annual rates of new afforestation exhibit a strong positive relationship with internal rate of return on the investment (IRR), with predicted new afforestation rates ranging from close to nil at IRR values ≤6.6% to approximately 100,000 ha annum^{-1} at an IRR of 11.0% (Horgan, 2007; Manley & Maclaren, 2009). Although increased returns from forestry, resulting from a value for carbon, are likely to result in greater rates of conversion, the limited amount of remaining land for agriculture may slow the afforestation rate, particularly after areas most suitable (i.e. Scenarios 1 and 2), have been converted.

The establishment of forests solely for carbon and environmental protection, in which no harvesting is planned, may be a useful land use in a number of areas. This regime is particularly well suited for LUC 8 land, in which catchment protection has been identified as a priority (Lynn et al., 2009). Areas with greater steepness also fall into this category because harvesting on steep slopes is often not feasible. Regions fitting these criteria represent a small proportion of the delineated land comprising only 2 to 5% of the total area between the three scenarios. However, there are also likely to be considerable areas that will be established solely for carbon on LUC 6 and LUC 7 land as the large distance to processing facilities or ports precludes the possibility of economic harvesting.

Spatial variation in 300 Index using the model described here has been previously shown to be primarily related to air temperature and soil water balance (Palmer, 2008). Consequently, predictions of 300 Index increased from the cooler temperate Southland region to optimum values found at mid-latitudes in the North Island, before declining further north, particularly in the warm temperate climates of Auckland and Northland. Increases in productivity also

occurred in regions with high average root-zone water storage (e.g. Southland) and were reduced in drier areas such as the Canterbury plains. Thus, the overall gains in productivity between future plantations and the current estate were mainly attributable to the delineation of land in warmer and wetter areas. For example, the marked increase in productivity of future plantings, compared with those of current plantations within the Waikato region, was predominantly due to a shift in plantation location from the cooler interior to warmer coastal areas (Figure 1.4).

The results described here could be used at a range of different scales. The productivity maps reduce investor risk particularly within new areas for which there are sparse productivity data. Maps also provide useful information for regional planning. For instance, substantial areas of highly productive land with moderate to severe erosion risk were identified in the Gisborne and Manawatu-Wanganui regions. This information could be used to develop projections of afforestation that would facilitate planning around infra-structure requirements. At the national level productivity data could be used to develop spatially explicit afforestation area targets, to offset future emissions. This type of information could be used to make informed decisions at the national level on how to develop policy to expedite afforestation.

The distribution of current plantations reinforces the future afforestation scenarios described here. The majority of forest plantations have been historically sited on LUC classes 6 and 7, which agrees well with our identified scenarios. Although arable classes have been afforested previously, such plantations were established primarily on dryland sites on the Canterbury plains and in areas with now-corrected micro-nutrient (cobalt) deficiencies in the central North Island (Will, 1985). Because of the widespread current use of irrigation and advances in our understanding of agricultural nutrition, afforestation of arable land classes is unlikely to be repeated, and we consider these forests an historical anomaly. In support of this view, many of the forests located on the Canterbury plains have been very recently converted to farm and arable land. Within New Zealand arable crops and dairy farming generally provide better financial returns than forestry (Sinclair et al., 2009) and this feature is likely to provide a disincentive to afforest high performing arable or dairy lands.

A number of assumptions have been made in the development of the maps shown in this paper. The key assumption is that *P. radiata* will be the main species used for afforestation. This assessment seems reasonable because *P. radiata* is a versatile and highly productive species that grows well across New Zealand's environmental gradient (Cown, 1997; Turner & Lambert, 1986). *Pinus radiata* is highly effective at controlling erosion and provides the greatest returns under carbon forestry among New Zealand's widely used commercial plantation species (Turner et al., 2008). This methodology could be repeated for species other than *P. radiata* should spatial surfaces for these species become available. We also assumed afforestation of the entire land in LUC 8 class under all scenarios considered. Although it is unlikely that all of LUC class 8 land will be afforested, the development of a carbon market within New Zealand is likely to make afforestation of LUC 8 for catchment protection an attractive long term option. However, as LUC 8 land represents a very small proportion of the identified scenarios (between 0.9 to 3.8%) it is worth noting our analyses are relatively insensitive to this assumption. A further assumption was that productivity surfaces could be applied to eroded land. This seems reasonable because deep-seated mass-movement erosion generally represents a very low proportion of the total land area even for severely eroded landscapes (Lynn et al., 2009).

In conclusion, our analyses in this paper has identified between ca. 0.7 M and 2.9 M ha of land that could potentially be afforested. Erosion severity was used to discriminate between scenarios because control of accelerated erosion is a major objective of afforestation in New Zealand. Compared to current plantations, all three scenarios showed an increase in productivity, at the national level.

2. The three potentially most useful exotic forest species for south eastern North Island marginal hill country[2]

Abstract

The aim of this research was to determine the most suitable plantation species for the south eastern North Island (Gisborne, Hawke's Bay, Taranaki, Manawatu/Wanganui and Wellington regions) hill country as this region includes a large area of marginal land suitable for future afforestation. Key attributes examined as part of the selection process were health, siting and productivity. Based on these criteria the species selected were *Pinus radiata*, *Sequoia sempervirens* and *Eucalyptus fastigata*.

[2] This chapter has been published as Nicholas, I., Watt, M.S. (2011) The three potentially most useful exotic forest species for south eastern North Island marginal hill country. *New Zealand Journal of Forestry* 56 (1), 15-19.

Introduction

Within the southern and eastern North Island, (Gisborne, Hawke's Bay, Taranaki, Manawatu/Wanganui and Wellington regions) there are large areas of erosion prone marginal land that are suitable for future plantations. Despite this little is known regarding the suitability of species other than *Pinus radiata* for this region. The aim of this research was to identify the three most suitable exotic forest species for afforestation within this region.

Species choice

Species choice was based on robustness and resilience. This means they must be healthy, tolerant of a range of sites and long-lived. They were also chosen for their desirable timber characteristics as well as high levels of productivity. The selected species were:

Pinus radiata
Eucalyptus fastigata
Sequoia sempervirens.

The reasons for selection of the three species are outlined below.

Species health

Sequoia sempervirens (Figure 2.1) is considered to be a relatively pest resistant tree species, with no major insect or disease problems in New Zealand or overseas (Bain & Nicholas, 2009; Gilman & Watson, 1994; Sinclair & Lyon, 2005). New Zealand disease records show there are a limited number of pathogens recorded on *S. sempervirens* and all are secondary or inconsequential (Ganley & Berndt, 2009). A few insects have been recorded damaging *S. sempervirens* in New Zealand, however these are not significant problems (Ganley & Berndt, 2009).

Figure 2.1. 29 year old *Sequoia sempervirens* (redwood), Taranaki

Eucalyptus fastigata (Figure 2.2) is one of the most healthy eucalypt species in New Zealand. Of the six insect and three pathogens that currently exist within *E. fastigata* plantations, only one insect (*Uraba lugens*, gum leaf skeletoniser) is of particular concern to this species (Ganley & Berndt, 2009). The other pests and diseases have been present in New Zealand for some time and have not made any significant impact on *E. fastigata* plantations to date.

For *P. radiata* there are several diseases that cause economic losses to the forest industry, some of which have limited control or management options. The five diseases that currently cause damage include the following pathogens/diseases; *Cyclaneusma minus* (Cyclaneusma needle cast), *Neonectria fuckeliana* (nectria flute canker), *Dothistroma septosporum* (Dothistroma needle blight), *Armillaria novaezelandiae, A. limonea* (Armillaria root rot) and *Diplodia* (syn. *Sphaeropsis*) sensu lato (Diplodia shoot blight). There are no insect pests of *P. radiata* that are currently of serious concern (Ganley & Berndt, 2009).

Siting

Pinus radiata

Pinus radiata is well suited to a very wide site range throughout New Zealand and particularly within eastern and southern regions of the North Island. Despite this broad adaptability the species does have some site limitations (Burdon & Miller, 1992). It does not tolerate very wet soils and growth can be poor on soils deficient in nitrogen or low in available phosphorus. Productivity declines markedly as annual rainfall drops below 1,000 mm and areas with less than 500 mm are generally unsuitable for commercial plantation forestry (Burdon & Miller, 1992). Frost damage does occur but can be greatly mitigated through good establishment practice. Snow damage is a widespread constraint to siting becoming a serious issue above

1,000 m in the North Island, 700 m in Canterbury and 350-500 m in the far south (Burdon & Miller, 1992).

Eucalypt

New Zealand has approximately 240 introduced eucalypt species established in the country (Nicholas, 2008). Nicholas (2008) considered that five major factors are important in matching eucalypt species to climatic conditions of a site:

- Air drainage. Frost tolerant species can be grown on sites in unsuitable areas if there is adequate air drainage.
- Out of season frosts. While some species can tolerate cold, out of season frosts can be devastating to many eucalypt species.
- Seed source. Depending on where seed is obtained from, seed source variation in climate tolerance can be as great as species variation.
- Aspect. Warm north facing aspects provide added insurance to cold damage, especially if there is adequate air drainage.
- Young seedlings are more prone to cold events than saplings. While saplings can be burnt, this is not always fatal.

While individual eucalypt species have different siting characteristics, the importance of seedlot cannot be over-emphasised, especially when it comes to frost resistance. On very cold sites, seedlot can be critical to the success of *E. fastigata* plantations. At a trial in Kaingaroa forest at 950 m, two of five seedlots tested gave acceptable survival (80-100%) while the other three seedlots ranged from 10-20% survival (C. Low pers comm). The importance of seedlot in frost resistance has also been confirmed by field and laboratory studies (Wilcox et al., 1980; Wilcox, 1982).

There are several historical publications that describe eucalypt siting. While not always accurate, as species knowledge has been improved since their publication, they do provide valid comparisons between species. Simmons (1927) allocated eucalypts into broad siting groups. He placed *E. fastigata* in Group IV which he described as “Species adapted to localities where there are light falls of snow some years, where hard frosts occur in winter and early spring, but where summer and autumn are usually warm and without extremes. Jackson (1965) identified a siting matrix for 35 species for the Hawke’s Bay region. He suggested *E. fastigata* required rainfall around 1,000 mm and a soil depth of 75 cm to 1 m.

Many authors have reported *E. fastigata* tends to grow best in well sheltered valleys of the Bay of Plenty and Taranaki regions on well-drained volcanic soils. It is intolerant of strong winds but can tolerate high rainfall and some snow. It is more tolerant of cold than *E. regnans*. In a study within the central North Island, Johnson and Wilcox (1989) concluded that *E. fastigata* was one of the best species at a low altitude (70m) site, and a possibility at the intermediate (380m) and the cold high altitude (920m) site, but at the latter site seed source was important. Of the twenty species and two hybrids tested in this series *E. fastigata* was the only species favoured as a winner or possibility across all three sites.

Weston (1957) comments that *E. fastigata* does well in Waikato and Rotorua-Bay of Plenty, but has not succeeded at lower altitudes north of Auckland, where, apparently the climate is too warm. He states it is frost tender when young, but soon becomes hardy and has tolerated up to –8°C of frost.

In the North Island the species has succeeded at altitudes up to 550m and it prefers light loamy soils, though clays are tolerated. Carter (1989) commented that *E. fastigata* was more wind firm than *P. radiata*. King (1980) considered *E. fastigata* as one of the best species in the higher rainfall areas of the Wairarapa and suggested it will grow well in slightly harder

conditions than *E. regnans.* However he stated *E. fastigata* tended to have heavy branching when open-grown.

There are several key references that broadly describe eucalypt siting (Hay et al., 2005; Nicholas, 1991; Nicholas et al., 2005). In these, *E. fastigata* and *E. globoidea* have the distinction of being the only two species that are included in two climatic categories; warm temperate and cool temperate.

Recent activity has provided a valuable data set on eucalypt siting. The Eucalypt Action Group of the New Zealand Farm Forestry Association conducted a Sustainable Farming Fund project to test siting of eucalypt species. Eucalypt research packs, comprising 15 trees × 10 species, were planted by farm foresters on 55 sites throughout New Zealand. Evaluation of survival from the national data set identified *E. fastigata* as part of a group of hardy eucalypt species (Gordon et al., 2007).

Figure 2.2: 13 year old *Eucalyptus fastigata*, Manawatu

Sequoia sempervirens

In its natural habitat, *S. sempervirens* grows from sea level to 900 metres altitude but prefers altitudes lower than 750 m. It prefers mild climates, although in many parts of its natural range it experiences winter snow and frosts of up to –10ºC. The presence of well performing stands near Winton, (Southland), North Canterbury, and Hamurana Springs, Whakarewarewa and Waiotapu near Rotorua, attest to the species' ability to do well in some cold sites in New Zealand. However, it is vulnerable to out-of-season frosts, and this is perhaps the reason for the much publicised early establishment failure of various stands in the Central North Island during the 1920s and 1930s (Nicholas, 2008).

Assessment of the performance of *S. sempervirens* on a wide range of New Zealand sites over the last ten years has shown that the species has a wider range of site tolerances than previously thought. However, redwood performs best on soils of moderate to high fertility in areas with reasonable year-round rainfall. *Sequoia sempervirens* is intolerant of strong prevailing winds, but is surprisingly resistant to toppling and breakage from periodic storms. Despite *S. sempervirens* common name, coast redwood, derived from its natural range being close to the coast, *S. sempervirens* is not tolerant of salt-laden coastal wind (Nicholas, 2008). Brown (2007) suggested *S. sempervirens* needs a temperate climate, good soils and regular rainfall. He suggested the species does not tolerate heavy frosts, salt spray or strong prevailing winds.

Recent research using a national dataset of permanent sample plots shows strong positive linear relationships between air temperature and *S. sempervirens* volume (400 Index) and height growth (Site index). Of the environmental variables considered in this study, air temperature was found to be by far the most important (Palmer, Hock, et al., 2009).

Growth data

Within the Scion Permanent Sample Plot database there is a substantial set of data for *P. radiata* across the regions of interest. Of the key species identified for marginal land in this project, there were more plots in *S. sempervirens* than *E. fastigata*, but these were concentrated in Gisborne and Hawke's Bay, a legacy of recently established silvicultural trials. These plots were supplemented with additional plots established throughout the area of interest and five plots established by other agencies.

Mean and maximum productivity for *E. fastigata* and *S. sempervirens* were derived directly from the plot data, as was the maximum regional productivity for *P. radiata*. Productivity was described by site indices determined from mean top height (height of the largest 100 diameters/ha) at respective ages of 20, 15 and 40 for *P. radiata*, *E. fastigata* and *S. sempervirens*.

For mean regional *P. radiata* productivity a national productivity model has been used to determine regional mean 300 Index (mean annual volume increment at age 30 for a stand that has a final crop stocking of 300 stems/ha) and site index (see Palmer et al, 2010 for more detail).

Variation in mean productivity

Mean site indices for *P. radiata* within Gisborne (33.2 m), Taranaki (31.2 m), and Hawke's Bay (31.3 m) exceed site indices for Manawatu (28.3 m) and Wellington (27.6 m), and it is worth noting that the site indices for Gisborne are the highest of all New Zealand regions (Palmer et al., 2010). For 300 Index regional mean values throughout New Zealand are highest in the five regions examined with values of 32.2, 31.3, 31.2, 28.3 and 27.6 m^3/ha/yr recorded, in Gisborne, Hawkes Bay, Taranaki, Manawatu/Wanganui and Wellington, respectively (Palmer et al., 2010). The mean 300 Index within New Zealand is 27.4 m^3/ha/yr, ranging from 23.3 m^3/ha/yr on the West Coast to 32.2 m^3/ha/yr in Gisborne (Palmer et al., 2010).

The mean *S. sempervirens* site index of 36 plots was 43.5 m, with a range of 27.7 to 60.1 m. From the limited data the Manawatu region plots averaged the highest site index. Productivity surfaces developed for redwood show high values of site index occur in warm coastal regions within the study area (Palmer, Hock, et al., 2009).

The mean *E. fastigata* site index from 40 plots was 25.2 m with a range of 20.5 to 30.2 m. For the regions of interest Gisborne appears to be slightly superior to the other regions.

Variation in maximum volume productivity

The data available to review species maximum productivity comes from the Scion Permanent Sample Plot database. To explore the maximum potential of the individual species, the most productive stand for each species was determined which provides an indication of potential productivity (Table 2.1). Maximum productivity will be influenced by location, stocking, management, soils and rainfall. Analyses show Gisborne to have the highest productivity for both *P. radiata* and *S. sempervirens*, while the Taranaki region had the highest productivity for *E. fastigata*. Overall, for the species represented across at least four regions, productivity was greatest for *P. radiata*, followed by *S. sempervirens*, *E. regnans*, then *E. fastigata*.

Table 2.1. Maximum productivity (m^3/ha/yr) for each species by region.

	Gisborne	**Hawke's Bay**	**Taranaki**	**Manawatu/ Wanganui**	**Wellington**
P. radiata	72	56.2	43.6	47.6	48
S. sempervirens	48	44.6	28.6	42.5	na
E. fastigata	30.1	29.8	33.8	16.9	na
E. regnans	31.5	54	46.3	26.8	na
E. nitens	na	28	na	na	na
E. globoidea	na	14.7	27.2	12.7	5.9
E. maidenii	na	13.2	na	na	na
C. lusitanica	26	30	21.3	18	23.5
P. menziesii	25	29.4	11.4	37	27.2

Additional species considered for the region

Many other species were considered in the selection process, In particular there are other species that may warrant attention on cold sites such as Douglas-fir and *E. nitens*. If there is a particular interest in durable timber *E. globoidea* is also a useful alternative because of its wide site tolerance. Other eucalypts in the same broad group as *E. fastigata*, the ash group, may also be considered where site conditions favour these species, such as *E. regnans* (mild fertile sites) and *E. obliqua* (low humidity drier sites). Cypress species of interest for solid timber production (*Cupressus lusitanica* for the regions considered) does not have the long term volume accumulation of the nominated species although it is worth noting this species does produce a durable timber with an increasing following (Nicholas, 2007).

Poplar species have a role to play on marginal hill country as through the use of poles and protective sleeves they can allow the establishment of a tree crop without significant disruption to grazing practices. However the combination of low timber density and site sensitivity has restricted the uptake of poplar as a plantation species in New Zealand despite its suitability for hill country planting.

Another deciduous species with potential is willow which is mostly used for erosion control and in a few cases fodder. There has been recent interest in establishing dedicated bioenergy plantations using willow as a multi product feed source for lignin, ethanol and sugars (Snowdon et al., 2008). Based on a 3 year rotation this requires land no steeper than 15 degrees. It has been suggested that willow is a competitive bioenergy crop to other tree options (K. Snowdon pers. comm. 2010), generally on topography that allows regular harvesting. However for best performance willow requires fertile sites with adequate rainfall.

Conclusion

The three species most suited for southern and eastern North Island regions were *P. radiata*, *S. sempervirens* and *E. fastigata*. *Pinus radiata* was selected as this species has very high productivity outperforming all other species. Furthermore productivity surfaces show the species to be well adapted to the area of interest, with the highest mean regional 300 Index values occurring within eastern and southern regions of the North Island. *Sequoia sempervirens* was selected as this species is not seriously affected by any pest species within New Zealand. As the species responds well to increasing air temperature it is very productive across eastern areas of the North Island. *E. fastigata* was selected as it is more healthy than other eucalypt species and demonstrates good growth rates and tolerance to frost. Although the data is limited for *S. sempervirens* and *E. fastigata*, neither species seems to show the wide variation in site index that would be expected from extremely site sensitive species. However, as with all tree species they can be placed on microsites where they do not grow well. On a landscape scale all three species are expected to perform well, provided they have been well established.

3. Direct impacts of climate change

3.1. Future wood productivity of *Pinus radiata* in New Zealand under expected climatic changes[3]

Abstract

The physiologically-based growth model CenW was used to simulate wood-productivity responses of *Pinus radiata* forests to climate change in New Zealand. The model was tested under current climatic conditions against a comprehensive set of observations from growth plots located throughout the country. Climate change simulations were based on monthly climate change fields of 12 GCMs forced by the SRES B1, A1B and A2 emission scenarios for 2040 and 2090. Simulations used either constant or increasing CO_2 concentrations corresponding to the different emission scenarios.

With constant CO_2, there were only slight growth responses to climate change across the country as a whole. More specifically, there were slight growth reductions in the warmer north but gains in the cooler south, especially at higher altitudes. For sites where *P. radiata* is currently grown, and across the full suite of GCMs and emission scenarios, changes in wood productivity averaged +3% for both 2040 and 2090.

When increasing CO_2 concentration was also included, responses of wood productivity were generally positive, with average increases of 19% by 2040 and 37% by 2090. These responses varied regionally, ranging from relatively minor changes in the north of the country to very significant increases in the south, where the beneficial effect of increasing CO_2 combined with the beneficial effect of increasing temperatures. These relatively large responses to CO_2 depend on maintenance of the current adequate fertility levels in most commercial plantations.

Productivity enhancements came at the expense of some soil-carbon losses. Average losses for the country were simulated to average 3.5% under constant CO_2 and 1.5% with increasing CO_2 concentration. Again, there were regional differences, with larger losses for regions with lesser growth enhancements, and lesser reductions in regions where greater productivity enhancements could partly balance the effect of faster decomposition activity.

[3] This chapter has been published in Global Change Biology as Kirschbaum, M.U.F., Watt, M.S., Tait, A., Ausseil, A.E. (2012) Future productivity of *Pinus radiata* in New Zealand under expected climatic changes. *Global Change Biology* 18, 1342-1356.

Introduction

Climate change is emerging as one of the key influences to shape the future of natural and anthropogenic systems across the world. Amongst its numerous impacts are impacts on biological systems such as on forest productivity which is strongly linked to environmental drivers (Kirschbaum & Watt, 2011). Biological productivity is a key attribute of forests both ecologically and as a determinant of the value of forests in supplying fibre for human needs.

Wood productivity has traditionally been modelled using empirical growth models (Battaglia & Sands, 1998; Fontes et al., 2010) but such models can only be parameterised using empirical datasets obtained under current growing conditions. These conditions therefore do not encompass future growing conditions expected under climate change. Process-based models are therefore considered to be more appropriate tools for future productivity projections (Medlyn et al., 2011; Schwalm & Ek, 2001) as they incorporate processes, interactions and feedbacks through which $[CO_2]$[4], water availability, and temperature affect ecosystem productivity and carbon sequestration. Consequently, these models can be used with greater confidence to estimate and undertake sensitivity analyses on how future conditions may influence productivity.

It is likely that future wood productivity will be impacted by changes in air temperature and water availability. Productivity responses to these variables can be modelled fairly confidently because model performance can be compared against differences in wood productivity under different current climatic conditions. It is more difficult to assess productivity responses to $[CO_2]$ as there is no significant current-day variability in $[CO_2]$ so that empirical testing of models is not possible. Model performance must therefore be judged against theoretical considerations and an analysis of plant responses from sites with experimentally enhanced $[CO_2]$.

However, the extent of photosynthetic response to increasing $[CO_2]$ still remains uncertain. Under well-watered conditions and in the absence of nutrient limitations, growth responses to doubling $[CO_2]$ have been reported to be of the order of 20-30% (Norby et al., 1999; Norby et al., 2005) but are likely to be less under nutrient-limited conditions (Kirschbaum, 1999a; Norby et al., 2010). There are strong theoretical reasons for expecting greater responses under water-limited conditions (Kirschbaum, 1999a), but experimental support for that notion is ambiguous (Nowak et al., 2004). Process-based models provide a mechanistic means of modelling growth sensitivity to changing $[CO_2]$ and allow simulation of the complex, but potentially important, feedbacks between $[CO_2]$, soil nutrition and water cycling (Kirschbaum, 1999a; Medlyn et al., 2011; Simioni et al., 2009).

To date, most climate-change projections have been undertaken at specific sites for a diverse range of natural or plantation forests (Medlyn et al., 2011), including alpine forests (Hasenauer et al., 1999), Mediterranean forests (Sabate et al., 2002), and pine and fir plantations (Kirschbaum, 1999a; Magnani et al., 2004; Simioni et al., 2009). However, predictions of future wood productivity are likely to be of most use to decision makers when they can be provided as spatial projections (Battaglia et al., 2009; Littell et al., 2010; Tupek et al., 2010), rather than point level estimates. Surfaces describing productivity under climate change will enable forest growers and decision makers to strategically position future forests in areas likely to be most productive in the future and to quantify future carbon inventories at national levels. This type of information would allow more robust strategic planning and formulation of policy to incentivise future plantings to offset carbon emissions through time.

Development of spatial surfaces of wood productivity from process-based models has progressed significantly over recent times as increasingly sophisticated spatial representation of the underlying input data have become available. Rapid advances in the

[4] In the following, $[CO_2]$ is used as an abbreviation for CO_2 concentration.

capability of geographic information systems (GIS) over recent years have seen the development of spatial surfaces covering a diverse range of environmental variables, including the climatic and nutrition inputs required for spatially-explicit simulations.

Pinus radiata D. Don, native to small coastal populations in California and Mexico (Burdon & Bannister, 1973), is the most widely planted species in the southern hemisphere in general (Lewis & Ferguson, 1993) and in New Zealand, in particular, where it constitutes 90% of the 1.8 M ha plantation resource. Previous research in Australia successfully used the processed-based model CenW to model the growth of *P. radiata* under current (Kirschbaum & Watt, 2011) and future (Kirschbaum, 1999a; Simioni et al., 2009) climatic conditions. Similar work with *P. radiata* was done by Battaglia et al. (2009) using the model Cabala, and Magnani et al. (2004) using HYDRALL.

In New Zealand, CenW, was recently parameterised to run and describe wood productivity under current climatic conditions based on an extensive set of plot data covering a wide environmental range within New Zealand (Kirschbaum & Watt, 2011). Here, we use the parameterised model to project future wood productivity of *P. radiata* for 2040 and 2090 within New Zealand under a comprehensive set of climate change scenarios. These simulations were run both under constant and increasing [CO_2] to cover the plausible range of possible plant responses to elevated [CO_2] to provide spatial predictions of changes in wood productivity under future climatic conditions in New Zealand. Growth responses are also analysed specifically for the regions comprising the current plantation estate.

Methods

Model description

The present work used the physiologically based CenW model vers. 4.0 that allows the incorporation of key environmental drivers that are likely to change in future (Kirschbaum, 1999b). CenW has been developed primarily for climate-change investigations and incorporates all key processes and feedbacks between plants and their environment that operate on time scales from daily (for water relations) to decadal (for soil organic matter feedbacks). It is therefore an ideal tool to model forest growth in response to multiple changes and multiple interacting factors. It was also successfully used for modelling wood productivity of *P. radiata* under current climatic conditions in New Zealand (Kirschbaum & Watt, 2011). This detailed work involved a full parameterisation that included parameterisation of the processes that governed the forest response to temperature and water availability.

The model runs on a daily time step and simulates stand characteristics, such as leaf-area development, stand height, basal area development, litter fall and exchange of water, nitrogen and carbon. Stand-level dynamics are explicitly linked to carbon and nitrogen cycling in plants and the soil. This linkage allows multiple factors to constrain estimates of growth and carbon exchange of the stand at daily and longer time scales.

Photosynthetic calculations were based on combining the photosynthesis model of Farquhar & von Caemmerer (1982) with the simple stomatal model of Ball et al. (1987). These instantaneous leaf-level equations of photosynthesis were scaled up to the canopy and to a daily time scale using the equations of Sands (1995). Daily evapotranspiration was calculated with the Penman-Monteith equation with canopy conductance explicitly linked to photosynthetic carbon gain through the Ball-Berry model. Maximum photosynthetic capacity depended on foliar nitrogen status and was further restricted by temperature limitations, water stress and constraints by water logging and excess rainfall.

The Farquhar and von Caemmerer photosynthesis model describes the dependence of photosynthesis on [CO_2], which was important for our climate change simulations. This dependence is well-calibrated against short-term photosynthetic measurements. In longer term CO_2 enrichment experiments, photosynthetic rates often decline (downward acclimation) if plants have excess carbohydrate or limited access to required nutrients. Nutrient feedback limitations are included in the model through coupled carbon and nitrogen cycles in the model. However, there are indications that downward acclimation sometimes occurs even when nutrition is not limiting (Ainsworth et al., 2004; Lewis et al., 2002). We are not aware of any well-tested quantification of this process, and our CO_2 simulations were run without this possible feedback effect. In order to bracket the likely true response, we therefore ran two simulations, one with constant [CO_2] and one with increasing [CO_2] to cover the range of possible plant responses.

Carbon allocation to different plant organs such as foliage, wood and roots, was determined by plant nutrient status, tree height and species-specific allocation factors. The allometric relationship between height and diameter has been refined in a related study so that the slope in this relationship is now expressed explicitly as a function of tree age, stand density, nutrient status and temperature, using the equations fully described in Watt & Kirschbaum (2011).

Organic matter dynamics were calculated with a version of the CENTURY model (Parton et al., 1987) that was slightly modified to better model the dynamics of forest soils and litter that have C:N ratios which are often wider than those of agricultural and grassland soils (Kirschbaum & Paul, 2002). As such, the model contains a complete and coupled nitrogen cycle, with nitrogen taken up by stands following decomposition and nitrogen mineralisation. Nitrogen was then either retained in plant pools or returned to the soil in senescence of plant organs, especially foliage and fine roots.

The functions used to describe growth processes require a large number of input parameters, many of which were based on previous *P. radiata* studies (Kirschbaum, 1999b), with additional parameters fitted to a national dataset in a related study (Kirschbaum & Watt, 2011). As external drivers, the model requires soil water holding capacity, soil texture and initial site fertility, and daily inputs of minimum and maximum temperature, precipitation, solar radiation and absolute humidity. Soil water holding capacity and soil texture were obtained as a spatial layer from the national soils data base (http://gisportal.landcareresearch.co.nz/webforms/), while a national surface for soil nitrogen concentration (W.T. Baisden, pers. comm.) was used to set initial site fertility.

Meteorological surfaces used to describe current and future climate

NIWA (National Institute of Water and Atmospheric Research Ltd.) maintains a Virtual Climate Station Network of daily weather data at a regular grid across New Zealand. Daily data are estimated for the whole of New Zealand on a 0.05° latitude/longitude grid, using a thin-plate smoothing spline to spatially interpolate daily observational data (Tait et al., 2006; Tait, 2008; Tait & Liley, 2009). The spline methodology incorporates topographic and other spatial information (depending upon the weather variable) to aid the interpolation.

For the purposes of this study, the 20-year period 1980–1999 was used to define the current climate. The 20-year weather sequence was considered to be long enough to contain a realistic representation of inter-annual variability. As our simulations ran for 30 years, we used the climate of the first decade a second time for the final 10 years of each simulation. This approach ensured that it negated any longer-term trends in the data that could have interfered and interacted with climate-change related trends in any climate variables.

Mean annual temperatures in New Zealand range from 8°C in the south to 18°C in the north (Fig. 3.1.1a). Generally, there are relatively small variations between summer and winter

temperatures, especially in coastal regions. Consequently, there are few periods with extremely hot or cold conditions in low elevation areas of New Zealand, but colder temperatures can be found at higher elevations.

Most of New Zealand receives precipitation between 500 and 2,000 mm yr^{-1} (Fig. 3.1.1b). Mountain chains extending the length of New Zealand provide a barrier to the prevailing westerly winds, dividing the country into dramatically different climatic regions. The West Coast of the South Island is the wettest area of New Zealand, whereas the area to the east of the mountains, just over 100 km away, is the driest.

New Zealand's plantation estate is distributed throughout most of the country, with large estates in the central North Island, the far north and east coast of the North Island, the upper South Island and various locations along the east coast of the South Island, especially the far south (Fig. 3.1.1c). Smaller additional estates are scattered throughout both islands in regions with moderate to good current growth potential (Fig. 3.1.1d).

Climate change projections were derived from a factorial combination of 12 Global Climate Models (GCMs) and three emissions scenarios B1 (low), A1B (mid-range) and A2 (high) as described by Meehl et al. (2007). The 12 GCMs used in this study were: CNRM, CCCma, CSIRO Mk3, GFDL CM 2.0, GFDL CM 2.1, MIROC32, ECHOG, ECHAM5, MRI, NCAR, UKMO-HadCM3, UKMO-HadGEM1.

Monthly temperature and rainfall scenarios from each GCM were statistically downscaled to a resolution of 0.05° for 2040 and 2090, using the methods of Mullan et al. (2002). For computational efficiency, the 0.05 degree estimates were averaged to a larger ¼ degree resolution, which was used for all climate-change simulations. Future weather sequences were generated through modifying the daily temperature and rainfall observations for 1980–1999 by mean changes described by the climate change surfaces. Temperature was modified by a given offset (e.g. +1°C), and precipitation was modified by a proportional change (e.g. -10%).

To adjust future atmospheric humidity, we first calculated the dew-point temperature of each day corresponding to the observed absolute humidity at 9 am. That dew-point temperature was modified by the temperature projections for specific sites and months to calculate new dew-point temperatures. New absolute humidities were then calculated from the adjusted dew point temperatures. With that procedure, relative humidity under current and future conditions remained nearly constant, which is consistent with observed global patterns (Trenberth et al., 2007) and expected trends into the future (Meehl, Stocker, et al., 2007). Solar radiation was not changed for the future climate projections.

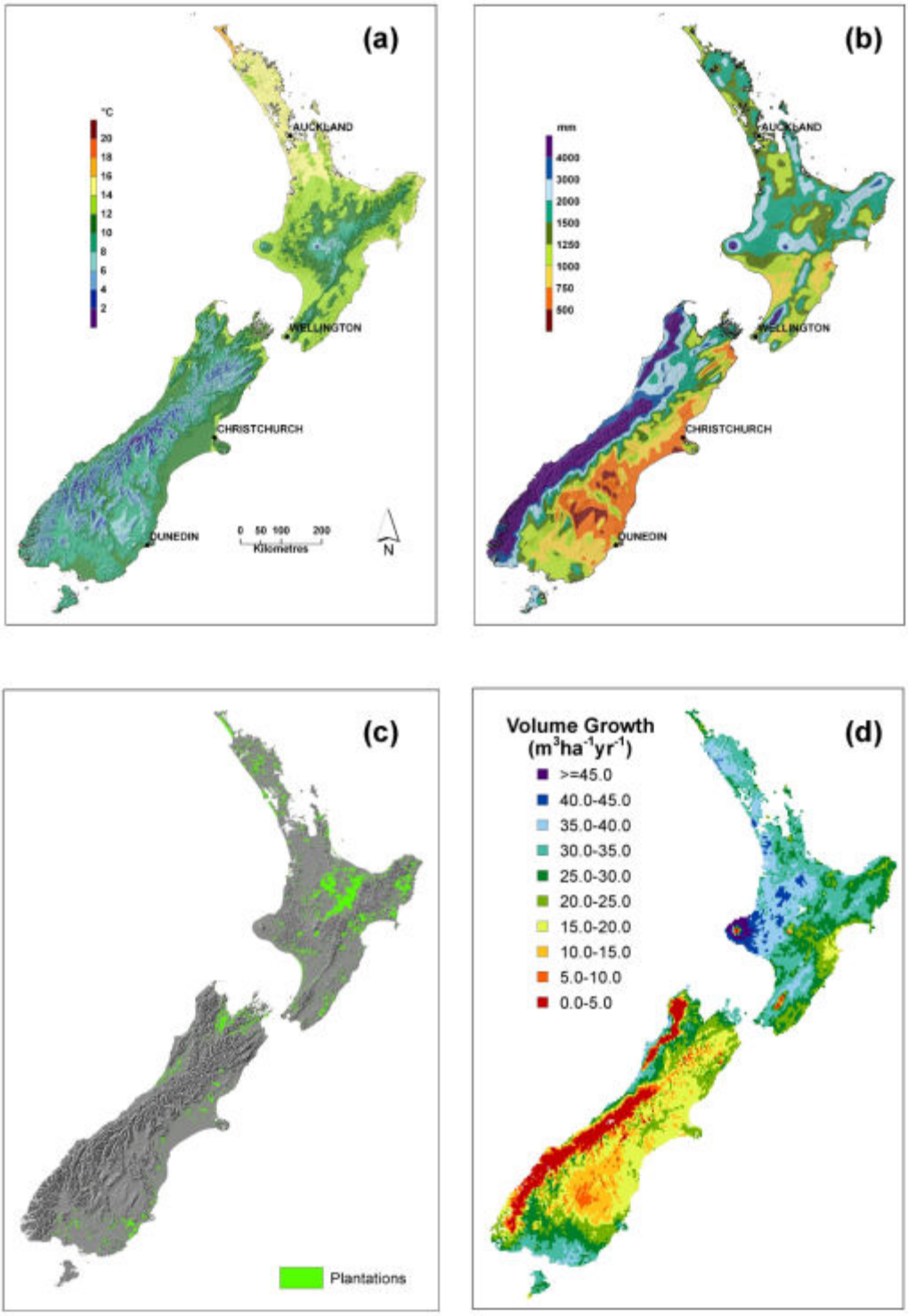

Figure 3.1.1. New Zealand map showing spatial variation in current mean annual temperature (a) and mean annual rainfall (b) (after Wratt et al., 2006), (c) the location of plantation forests in New Zealand and (d) modelled wood productivity (expressed as volume growth) of *P. radiata* under current climatic conditions (redrawn from Kirschbaum & Watt, 2011).

CO_2 concentrations

The model used either constant 1990 [CO_2] or specific [CO_2] corresponding to those expected under each of the emission scenarios. Details of the [CO_2] used under each scenario are described in Kirschbaum et al. (2012).

Model fitting to current climate

As previously described (Kirschbaum & Watt, 2011), CenW was parameterised under current climate against growth data from permanent sample plots covering almost the complete environmental range across which *P. radiata* is grown within New Zealand. This data consisted of 101 sites with 1,297 individual observations of height and/or basal area from which diameters and volumes could also be calculated. Using parameter values described in Kirschbaum & Watt (2011) there was excellent correspondence between model predictions and measurements over a wide range of sites and stand ages. Nash-Sutcliffe model efficiencies (Nash & Sutcliffe, 1970) for modelling forest growth ranged from 0.828-0.892 for height, basal area, diameter and volume.

Simulations

Using the generic parameter values determined from the model fitting, future wood productivity was simulated at ¼ degree resolution for all of New Zealand over a rotation length of 30 years for periods centred around 1990, 2040 and 2090, with weather data obtained as described above. [CO_2] was either held constant or adjusted in correspondence with specified future emissions scenarios.

Soil fertility in CenW is determined by the amount of carbon and nitrogen in different organic matter pools, and by the rate at which organic matter turns over and mineralises organic nitrogen. The model was therefore initialised by setting relative soil organic matter pool sizes proportional to soil nitrogen concentrations obtained from a national surface (W.T. Baisden, pers. comm.). The same initial values were used for current-day and future simulations. No extra fertiliser was applied during the simulations. Simulations used a standard silvicultural scenario that included planting at 1,000 stems ha^{-1}, followed by two thinnings at age 5 and 8 to respective stand densities of 500 and 300 stems ha^{-1}. Simulations continued until age 30 which is a typical rotation length over which *P. radiata* is grown in New Zealand.

Wood productivity under the current climate is shown as total stem volume increment (see below). For future climates, results are shown as the ratio of wood production under future and current climatic conditions. Simulations were run separately based on climatic inputs generated by each of the 12 GCM runs. Simulation outputs were then averaged across all runs under each of the three emission scenarios to generate regionally-specific estimates of most likely productivity changes. For assessing likely changes for the current plantation estate, we used the output from the 36 factorial combination of GCM by emissions scenarios, with changes in wood productivity expressed as probability distributions.

Soil Organic Carbon Stocks

As the model is based on fully-coupled plant and soil processes, and explicitly follows the cycling of carbon, nitrogen and water through the forest system, it also simulated changes in soil organic carbon under the different climate change scenarios. Changes in soil organic carbon resulted from modelled changes in litter production, the principal carbon input, and from changes in temperature and water status which are the primary drivers of organic matter decomposition.

Results

On average across the 12 GCMs, mean air temperature in New Zealand is projected to increase by between 0.7°C and 0.9°C by 2040 and by between 1.3°C and 2.6°C by 2090 (Table 3.1.1). These are relatively mild changes compared to those expected for other parts of the world (Meehl, Stocker, et al., 2007). When averaged across the 12 GCMs, variation in the expected temperature increases across the country was also relatively low, with projected temperature increases from 1990 to 2090 being fairly uniform with just marginally greater increases towards the north (Fig. 3.1.2a, c, e).

Table 3.1.1. Summary of climate-change responses in New Zealand under the 3 emission scenarios and 12 GCMs. Given are the mean responses under all 12 GCMs across all quarter-degree grid points within New Zealand. GCM minimum (min) and maximum (max) refer to the GCM runs with the lowest and highest changes when averaged across all grid points. Site min and max refer to the quarter-degree location in New Zealand with the highest and lowest changes, respectively, across all GCM runs.

Year	Emission scenario	Temperature change (°C)					Precipitation change (%)				
		Mean	GCM		Site		Mean	GCM		Site	
			min	max	min	max		min	max	min	max
2040	B1	0.7	0.4	1.2	0.2	1.5	1.6	–2.1	5.6	–15	+16
	A1B	0.9	0.4	1.3	0.0	1.7	2.1	0.0	5.0	–23	+22
	A2	0.9	0.3	1.3	0.0	1.7	0.9	–5.6	4.3	–17	+15
2090	B1	1.3	0.7	2.3	0.4	2.7	2.6	–4.7	7.9	–17	+25
	A1B	2.1	1.2	3.4	0.9	4.0	3.2	–1.5	12.9	–31	+44
	A2	2.6	1.6	3.6	1.4	4.2	3.0	–3.8	11.5	–21	+30

Projected changes in rainfall were also only slight, with average increases between 0.9% and 2.1% by 2040, and between 2.6% and 3.2% by 2090 (Table 3.1.1). There was more variation in possible temperature changes at the level of individual ¼ degree locations for the 36 (3 emission by 12 GCM) possible scenarios, with temperature increases by 2090 of between 0.4 and 4.2 °C and precipitation changes between -31% and +44% (Table 3.1.1).

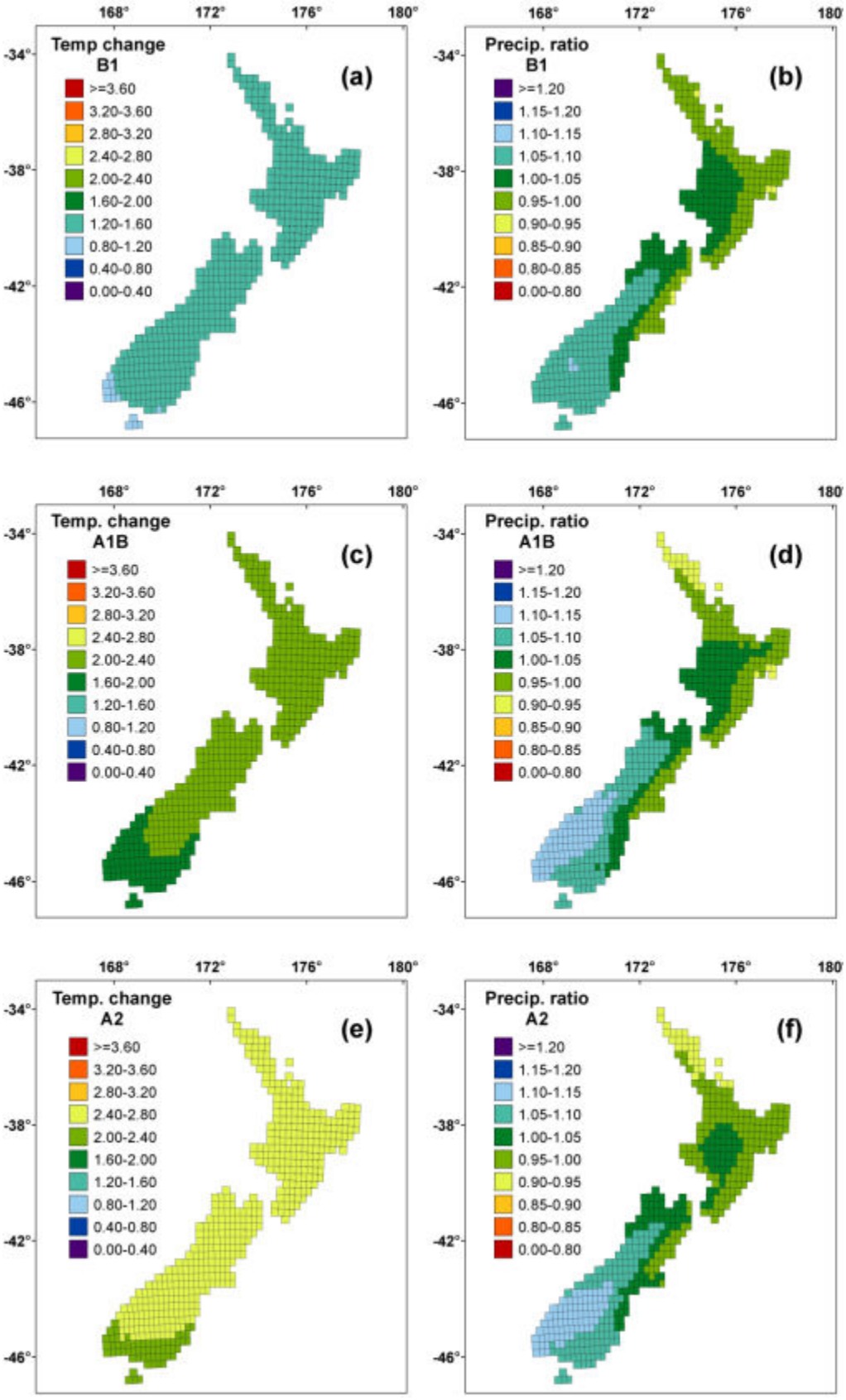

Figure 3.1.2. Climatic changes in temperature (a, c, e) and, precipitation (b, d, f) to 2090, under the B1 (a, b), A1B (c, d) and A2 (e, f) emission scenarios. The data shown here are the average responses for the 12 GCMs that were used.

Across New Zealand, there are likely to be small gains in rainfall in southern and western regions of the South Island, while there are expected to be slight reductions in rainfall in the North Island, especially over the northern and western regions (Fig. 3.1.2b). Regions with current adequate or excessive rainfall are thus expected to receive even more rainfall, whereas water-limited regions are expected to suffer some decreases in rainfall (cf. Fig. 3.1.1b). The projected changes for New Zealand were, however, fairly mild compared to climatic changes projected for other parts of the world. New Zealand is a relatively small island surrounded by a large ocean that is expected to buffer and delay more severe climatic changes.

Surfaces of wood productivity under current climatic conditions

Under current climatic conditions, there are wide regional variations in modelled volume increment across New Zealand (Fig. 3.1.1d). Wood productivity is highest in the warm and moderately wet (rainfall of 1000–3000 mm yr^{-1}) northern and western areas of the North Island, reaching maximum values of > 40 m^3 ha^{-1} yr^{-1} in the fertile Taranaki region. Wood productivity is considerably lower in the South Island. Reduced productivity west and east of the main axial ranges is attributable to very high rainfall in the west (> 3000 mm yr^{-1}) and relatively low rainfall in the east and general sub-optimal growing temperatures (Kirschbaum & Watt, 2011). Volume growth is generally low along the whole east coast and even lower in the central South Island, which is one of the driest areas in New Zealand (rainfall ~ 500 mm yr^{-1}, Fig. 3.1.1b). In contrast, in the southern more coastal regions that receive moderate rainfall (Fig. 3.1.1b) and experience no significant seasonal water deficits, wood productivity is higher (Fig. 3.1.1d).

Across New Zealand's main pine growing regions, wood productivity is often limited by sub-optimal temperatures but rainfall is mostly adequate without being excessive. Nutrient limitations were identified for only a very small number of sites (Kirschbaum & Watt, 2011). These growth limitations under current climatic conditions thus determine the response of *P. radiata* to climatic changes.

Surfaces of wood productivity under future climatic conditions with constant [CO_2]

Simulations with constant [CO_2] showed adverse effects of climate change on wood productivity in northern and low altitude regions within the North Island under most scenarios (Fig. 3.1.3). Reductions in wood productivity were especially marked for the high-emission A2 scenario and were more pronounced for projections to 2090 than for 2040 (Fig. 3.1.3). In contrast, wood productivity is likely to increase in the cooler parts of the country, including most of the South Island and in higher altitude regions of the North Island (Fig. 3.1.3).

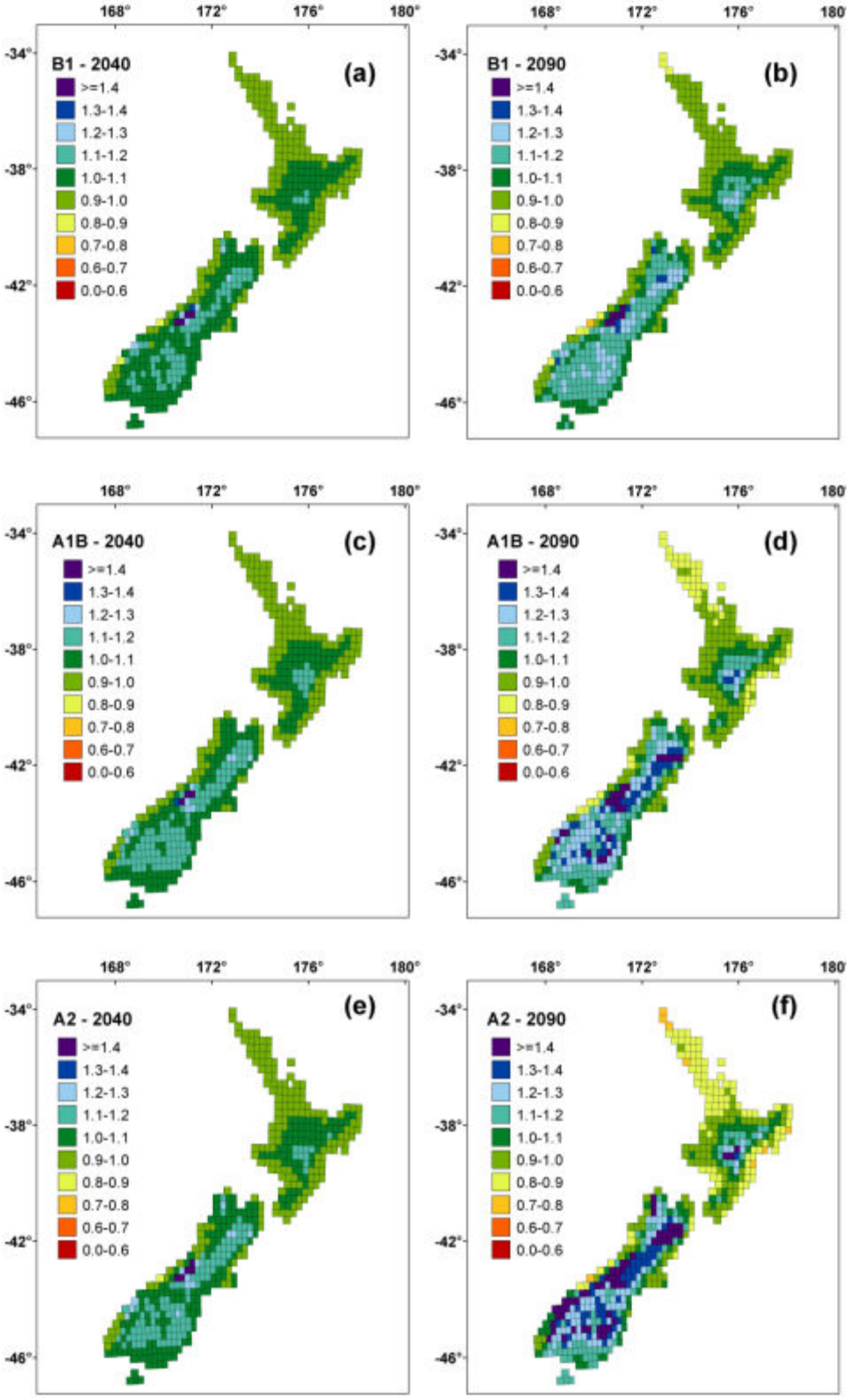

Figure 3.1.3. Climate change impacts on future wood productivity to 2040 (a, c, e) and 2090 (b, d, f) under the B1 (a, b), A1B (c, d) and A2 (e, f) emission scenarios. These climate change simulations used constant present-day [CO_2]. Results are expressed as the ratio of future wood productivity over current-day productivity. Data show the average productivity response under simulations run separately under the climatic predictions of the 12 different GCMs.

Within the current plantation estate (Fig. 3.1.4), climate change was predicted to result in gains in wood productivity in a slight majority of plantations to 2040 (62% with growth gains) and 2090 (54% with growth gains). The average productivity response was 3% in both 2040 and 2090. Even though the mean change was the same in 2040 and 2090, the range in productivity changes widened between 2040 and 2090. By 2040, more than 99% of plantations were modelled to have productivity changes between –7.5% and 17.5%, whereas by 2090 the range had widened to –22.5% to 32.5% (Fig. 3.1.4).

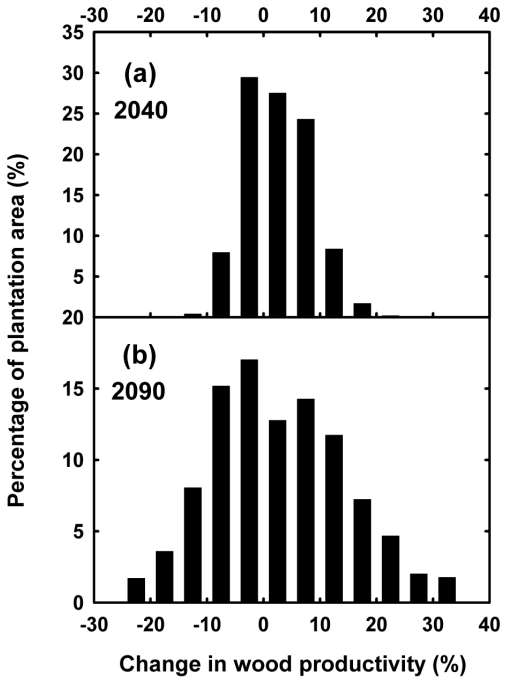

Figure 3.1.4. Frequency distribution of the current *P. radiata* estate experiencing specified wood productivity changes by 2040 (a) and 2090 (b) for runs with constant [CO_2]. The frequency distribution was obtained from relative changes for locations within the currently planted estate for all 36 future climate possibilities (12 GCMs x 3 emission scenarios).

Surfaces of wood productivity under future climatic conditions with increasing [CO_2]

Simulations that included increasing [CO_2] resulted in positive impacts on wood productivity across all emission scenarios for both 2040 and 2090 (Fig. 3.1.5). Increasing [CO_2] completely offset the losses in the North Island that had been predicted by simulations with constant [CO_2]. With increasing [CO_2], there were productivity gains throughout the North Island, especially in the higher-elevation central plateau. For the South Island, increases in wood productivity were even larger as the stimulatory effect of elevated [CO_2] added to the positive effect of warming to lead to substantial overall productivity enhancements (Fig. 3.1.5).

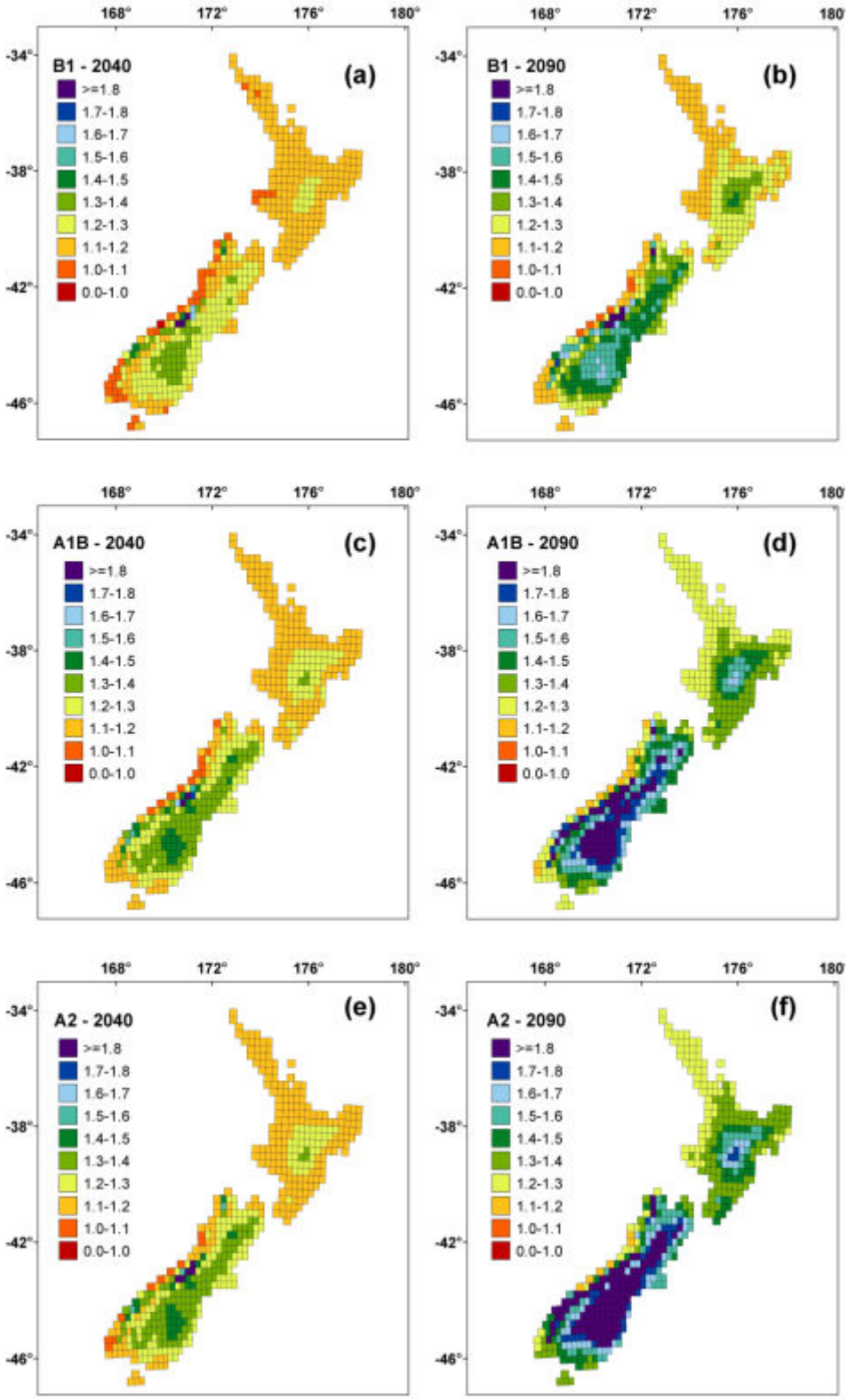

Figure 3.1.5. Climate change impacts on future wood productivity to 2040 (a, c, e) and 2090 (b, d, f), under the B1 (a, b), A1B (c, d) and A2 (e, f) emission scenarios. The simulations used increases in [CO_2] as anticipated under different scenarios. Results are expressed as the ratio of future wood productivity over current-day productivity.

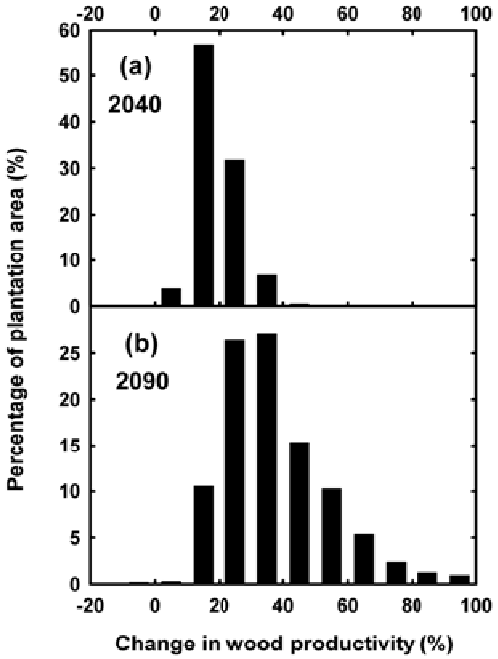

Figure 3.1.6. Frequency distribution of the current *P. radiata* estate experiencing specified wood productivity changes by 2040 (a) and 2090 (b) under simulations with increasing [CO_2]. The frequency distribution was obtained from relative changes for locations within the currently planted estate for all 36 future climate possibilities (12 GCMs x 3 emission scenarios).

The climate change response was dominated by the productivity response to increases in temperature and [CO_2] as expected changes in precipitation in New Zealand are generally only minor (Fig. 3.1.2). In areas such as the upper North Island where rainfall is expected to decrease and temperature to increase, this would lead to increasing water stress and decreased productivity if there were no changes in [CO_2]. However, increases in [CO_2] are likely to avert developing water shortages to lead to overall productivity enhancements even in areas where precipitation may decrease slightly (Fig. 3.1.5).

As a result, productivity gains were found for over 99% of all plantations in both 2040 and 2090 (Fig. 3.1.6). On average, productivity increased 19% by 2040 and 37% by 2090. Both the average and range of these gains increased markedly from 2040 (–5 to 35%) to 2090 (–5 to 95%). There were very few sites expected to experience reductions in productivity because anticipated changes in precipitation were slight and because few sites in New Zealand are likely to experience temperature increases into a range that would be detrimental for the growth of *P. radiata*.

Furthermore, marginally adverse changes in temperature or rainfall, especially where they would reduce potential water availability, were negated by the effect of increasing [CO_2]. At the same time, there were a small number of sites where beneficial changes in precipitation and temperature combined with the response to increasing [CO_2] to result in substantial productivity gains (Fig. 3.1.6).

Climate change effects on soil organic carbon stocks

Climatic changes can also affect the rates of organic matter decomposition, which, together with climate-induced changes in productivity, can lead to net changes in soil organic carbon stocks. Anticipated changes are only slight by 2040 and are therefore shown only for 2090 and only under the A2 scenario (Fig. 3.1.7).

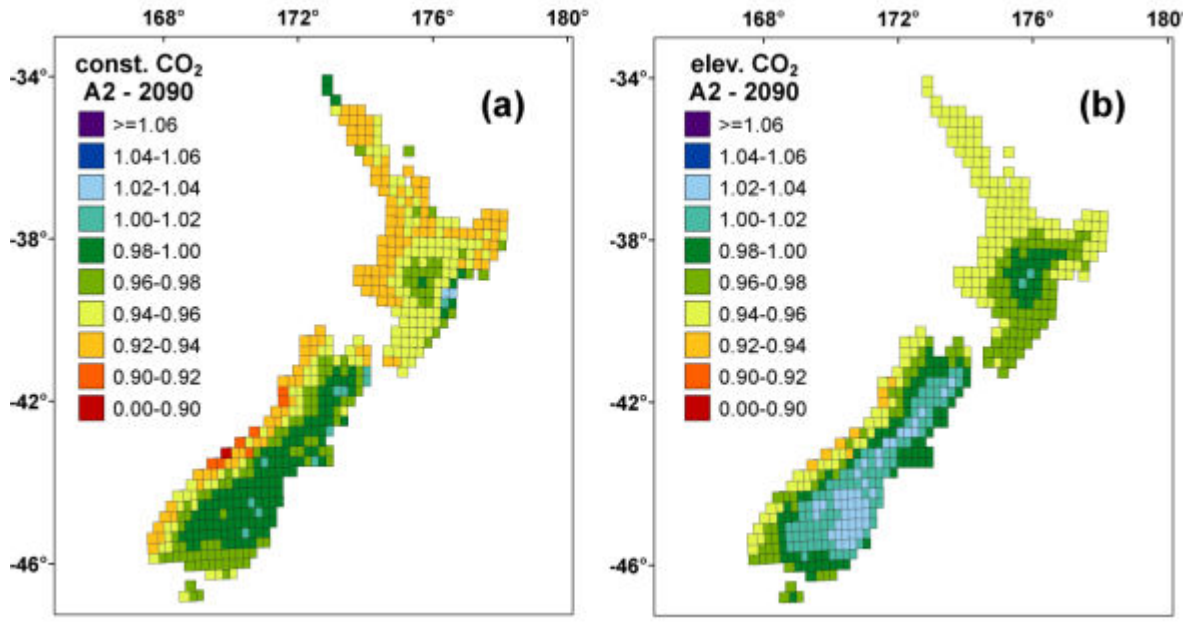

Figure 3.1.7. Climate change impacts on soil organic carbon projected to 2090 under the A2 scenario, expressed relative to 1990 values, for simulations that assume constant 1990 [CO_2] (a) or increasing [CO_2] (b). Soil organic carbon here includes the sum of all organic carbon pools, including litter, both above and below the soil surface. Data are given as the ratio of soil organic carbon in the future to that under current conditions.

The simulations showed some soil organic carbon losses for runs with both constant and increasing [CO_2], but losses were slightly higher when [CO_2] was held constant. Carbon losses were simulated for most of the North Island and the West Coast of the South Island, whereas most of the eastern regions of the South Island had relatively constant (for simulations with constant [CO_2]), or slightly increasing soil carbon levels (for simulations with increasing [CO_2]).

Discussion

Temperature, [CO_2], and water and nutrient availability are four key determinants of wood productivity that are either directly or indirectly affected by climate change, or that interact with those other drivers to determine the ultimate productivity response to climatic changes. We will discuss their respective influences in turn.

Soil water balance has long been recognised as a major determinant of *P. radiata* productivity, with productivity being sub-optimal on dryland sites where trees experience seasonal water deficits (McMurtrie et al., 1990; Richardson et al., 2002; Watt et al., 2003; Watt, Palmer, et al., 2010). This research is consistent with CenW simulations that showed productivity to increase with precipitation up to ~2,000 mm, with productivity reductions at supra-optimal precipitation (Kirschbaum & Watt, 2011).

Future water balances could be affected by changes in precipitation as the principal input, or by evapotranspiration, the most substantial component of water loss from the system. Within New Zealand, the low to moderate changes in rainfall predicted under climate change are likely to have little impact on water balances. The currently dry and water-limited east coast regions could potentially respond the most to reductions in precipitation, but anticipated changes were generally limited to ± 5% (Fig. 3.1.2), with consequently limited effects on stand water balances.

Water loss from stands by evapotranspiration is strongly affected by stomatal conductance, foliage area and vapour pressure deficits. Assuming a constant diurnal temperature range, VPD will increase with warming by about 5-6% $°C^{-1}$ (Kirschbaum, 2000) and drive increases in evapotranspiration. However, under New Zealand conditions, with relatively small anticipated increases in temperature (Fig. 3.1.2), temperature-driven increases in evapotranspiration rates are likely to be more than offset through stomatal closure in response to increasing [CO_2] (data not shown). This is likely to result in an overall reduction in evapotranspiration that is greater than anticipated reductions in precipitation for any part of New Zealand. Hence, even regions that are currently water limited could see slight improvements in their water status in future.

A large amount of empirical research has found air temperature to be an important determinant of P*. radiata* growth in New Zealand (Hunter & Gibson, 1984; Jackson & Gifford, 1974; Watt, Palmer, et al., 2010), with conditions in most locations in New Zealand currently being sub-optimal for growth (Kirschbaum & Watt, 2011). With small anticipated precipitation changes in New Zealand (Fig. 3.1.2), simulations showed increases in productivity in response to increasing temperature for most of New Zealand even without factoring in responses to increasing [CO_2] (Fig. 3.1.3). Negative responses were confined to regions in the North Island, especially the far north as expected air temperatures in these areas surpass optimum growth temperatures for *P. radiata*. Adverse changes to stand water balances in these warm regions further added to the negative direct-temperature effects on productivity. However, increases in [CO_2] completely negated these losses, and gains were simulated throughout the country (Fig. 3.1.5), reflecting the substantial increases in photosynthesis and water use efficiency that can result from increasing [CO_2].

Nutrition is also a key determinant of productivity, with nitrogen and phosphorus being the elements most closely linked to productivity. In the decomposition of soil organic matter, CO_2 is released to the atmosphere and any excess nitrogen and phosphorus is mineralised and becomes available for plant uptake. If plants are able to fix more carbon through increased [CO_2], but nutrient uptake is limited, the plant internal nutrient status declines, as is usually observed experimentally (Drake et al., 1997; Nowak et al., 2004).

This provides a first negative feed-back effect on plant responses to increasing [CO_2]. Plants that fix more carbon also produce more litter which adds to soil organic carbon and can immobilise nutrients. This reduces the nutrients available for plant uptake and provides a second negative feed-back effect (Comins & McMurtrie, 1993; Kirschbaum et al., 1998; Rastetter et al., 1992), a process more recently termed ‘progressive nitrogen limitation’ (Luo et al., 2004). This process is likely to be offset under climate change by increasing temperatures which can lead to a loss of organic matter (Fig. 3.1.7) and stimulate the mineralisation of nitrogen (Kirschbaum, 1999a). With increasing temperature, more nutrients can become available for plant uptake and can stimulate plant productivity independent of any direct physiological plant responses to increasing temperature (Schimel et al., 1990).

Simulations of the growth of *P. radiata* in New Zealand have shown nutrition to be generally adequate for the growth of stands (Kirschbaum & Watt, 2011). Commercial pine forests in New Zealand are regularly analysed for their foliar nutrient levels (Payn et al., 2000) which often indicate some degree of nutrient deficiencies (Davis et al., 2007; Smith et al., 2000). When stands are identified with deficient or marginal nutrient levels, supplemental fertilisers

are usually supplied to rectify any deficiencies (Will, 1985). The predicted growth enhancements shown in the present simulations can only be achieved if the current favourable nutritional levels can be maintained into the future. Growth enhancements through climatic changes could not be sustained if they would lead to uncorrected nutritional limitations.

The findings reported here are basically consistent with those found in other studies that modelled the effect of climate change on biological productivity of forests. Responses to temperature and rainfall depend on the current climatic conditions relative to the species optimal temperature response. For our simulations, moderate increases in temperature were generally positive for productivity because conditions in New Zealand are currently sub-optimal for the productivity of *P. radiata* (Kirschbaum & Watt, 2011). Booth & McMurtrie (1988) predicted contraction in the area of *P. radiata* with climate change in Australia, where the species is currently grown at higher temperatures than in New Zealand. Similarly, Battaglia et al. (2009) presented a divergent picture of climate-change effects on *P. radiata* productivity in Australia, depending mainly on the current growth conditions, with plantations in warmer regions generally adversely affected by climate change, but with beneficial effects for plantations currently grown in cooler regions.

Interactions with water availability are particularly interesting, with increasing [CO_2] conferring higher water use efficiency (Magnani et al., 2004). For New Zealand simulations that included increasing [CO_2] led to higher modelled productivity even for regions where moderate reductions in rainfall are expected, and where evaporative demand could increase with higher temperatures. Similarly, Simioni et al. (2009) found that modelled productivity in Western Australia could be maintained at or above current levels despite reductions in rainfall, but productivity began to decline under more extreme climate change scenarios under which reductions in rainfall exceeded achievable increases in water use efficiency.

The simulations presented here highlight increases in [CO_2] as a key determinant of future productivity of *P. radiata* within New Zealand. Despite a large amount of experimental work, there is still uncertainty surrounding the response of plants to these increases in [CO_2] (Körner, 2006; Körner et al., 2007). In the present work, we have dealt with this uncertainty through presenting simulations that bracket likely extremes. When we kept [CO_2] constant, mean climate change responses were varied, with moderately negative responses in the north and moderately positive responses in the south (Fig. 3.1.3). When [CO_2] was increased, there were substantial gains throughout the country (Fig. 3.1.5).

Hence, the critical question is whether the actual CO_2 response will be as strong as predicted in the model runs. The well-characterised effects of [CO_2] on photosynthesis (Farquhar & von Caemmerer, 1982; Long et al., 2006) suggest the potential for substantial growth responses. Growth responses in response to increasing [CO_2] have also been observed in both small-scale experimental studies (Curtis & Wang, 1998; Luxmoore et al., 1993; Poorter & Navas, 2003) and larger-scale field studies using 'free air CO_2 enrichment' (Ainsworth & Long, 2005; McCarthy et al., 2010; Norby et al., 2005; Nowak et al., 2004).

Nonetheless, despite this large amount of experimental work, there is still considerable controversy around the magnitude of growth responses to increasing [CO_2] (Körner et al., 2007; Nowak et al., 2004), which makes it difficult to forecast productivity changes with a high level of confidence. Complicating factors include downward regulation of photosynthesis that has been observed in many small-scale trials (Gunderson & Wullschleger, 1994; Long et al., 1996) but has been shown to be largely attributable to low sink strength, especially with plants being grown in very small pots (Arp, 1991). Conversely, apparent growth responses can be accentuated through positive feedback during the early exponential growth phase of plants so that enhancements of relative growth rate (Poorter & Navas, 2003) provide a better measure of plant responses to [CO_2] than the more typically reported biomass enhancement ratios.

In the field, responses to [CO_2] will be limited if increased photosynthetic carbon gain cannot be matched by similarly increased nutrient supply. Under these circumstances, lower foliar nutrient concentrations are likely to reduce inherent photosynthetic rates (Kirschbaum et al., 1998; Nowak et al., 2004; Rastetter et al., 1992). This feedback is included in the CenW simulations but was found to be of little consequence in New Zealand's *P. radiata* forests, where fertility levels are kept high. However, to fully sustain possible growth enhancements in future may require increased fertiliser application rates.

The magnitude of growth gains under increased [CO_2] clearly interacts with other environmental conditions. Greatest growth gains are likely to be found on warm sites with adequate nutrition, but where water is limiting so that the growth response to CO_2 can shift from a direct photosynthetic response to a dependence on the numerically more substantial increase in water-use efficiency (Kirschbaum, 1999a; Körner et al., 2007) related to stomatal closure under elevated [CO_2] (Medlyn et al., 2001). As most of New Zealand has relatively fertile soils and moderate to good water availability, the effects of increasing [CO_2] are ubiquitous but generally only moderate. Greatest gains are likely on dryland sites, located in eastern regions of both islands (Fig. 3.1.5).

Future wood productivity will also depend on the effect of climate change on abiotic and biotic factors, and their consequent impacts on tree growth. They may be mediated through changes in the distribution and abundance of weeds, pathogens and insects, and through the severity of abiotic factors such as wind throw and fire.

Potential gains in productivity are of little benefit if stands are killed by fire or novel pest species. Fire severity is linked to temperature and fuel load, both of which may increase with climate change either directly with warmer conditions, or indirectly as a consequence of greater biological productivity. Changes in wind speed and relative humidity are even more important in determining fire severity and any adverse changes in these variables could greatly increase fire risks (Dowdy et al., 2010). This has been predicted as a likely impact of climate change in fire prone regions such as Australia (King et al., 2011) and Canada (Flannigan, Logan, Amiro, et al., 2005). Similarly, changed distributions of pest species can potentially cause significant future problems (Sutherst et al., 2007), and mountain pine beetle outbreaks linked to climate change have already been observed in Canada and the Western United States (Cullingham et al., 2011; Hicke et al., 2006; Stinson et al., 2011). Such factors can potentially negate any potential productivity gains. Dead trees do not respond to elevated [CO_2].

The improvements in biological productivity reported here constitutes one reassuring aspect of climate change, but it does not allay other concerns related to climate change. An optimal response to the prospect of climate change, including both adaptation and mitigation, needs to be based on the best overall understanding of the combined impacts of all relevant aspects, and some of those can include changes for the better. It is imperative to know of all changes so that society can take advantage of any positive changes as well as minimise the adverse consequences of negative impacts.

3.2 Influence of climate change on productivity of *Eucalyptus fastigata*

Abstract

Eucalyptus fastigata is a fast growing species that is disease resistant, has high wood density, and can tolerate a wide range of New Zealand environments. It has high potential as a plantation species for large scale afforestation on marginal agricultural land. However, it is unknown how the species will perform with climate change. The process-based model 3-PG (physiological processes for predicting growth), has previously been parameterised for *E. fastigata* for New Zealand under current climate conditions with the spatial version of the model (3-PG2S). This model was used to test the potential productivity of *E. fastigata* under three IPCC SRES climate change scenarios for 2040 and 2090; low emission B1 scenario, emission stabilisation scenario A1B, and high emission scenario A2. Each scenario was tested without and with an increase in net primary productivity from higher atmospheric CO_2 concentrations (CO_2 fertiliser effect) with climate change. Productivity increased with each scenario with the highest level of productivity in 2090. Climate change also increased the potential range of the species in New Zealand, especially in the inland areas of the South Island and the Central North Island. The increase in temperature and decrease in frost days with climate change had the biggest impact on productivity. The decline in precipitation in some areas of New Zealand with some scenarios was not large enough to have a negative impact on productivity. In conclusion, a global $2^{o}C$ rise in temperature is unlikely to adversely impact *E. fastigata* productivity in New Zealand. In fact, climate change is likely to be quite beneficial in terms of productivity and the expansion of favourable sites for the species.

Introduction

In the last 10 years, *Eucalyptus fastigata* (Deane and Maiden) has been identified as a promising species with high commercial potential, thus providing an alternative to *Pinus radiata* (D. Don) plantations. *Eucalyptus fastigata* is a fast growing disease resistant eucalypt that can tolerate a number of New Zealand environments. It can be grown as a timber crop or for pulp and paper (Meason et al., 2011). It is highly suitable for carbon forestry. Research on *E. fastigata* was neglected until the establishment of the Future Forests Research program in 2008. Under the Diverse Forests Theme, knowledge on genetics, site productivity, growth dynamics, and management was dramatically improved (Meason et al., 2011). This research provided the foundation for this study.

Global warming and its impact on the climate is likely to impact many natural and human induced ecosystems. It can impact on forest ecosystems directly or indirectly, and it can impact gradually or abruptly. Climate change may impact tree growth and mortality from gradual changes in temperature, rainfall patterns, and solar radiation (Coops & Waring, 2011). More abrupt impact may occur from increased frequency in wildfires, droughts, out of season frosts, and outbreaks of insects and diseases (Chapin et al., 2010). The complexity of climate change and its direct and indirect effect on forest ecosystems means that forest models must be dynamic enough to simulate these effects.

Mathematical models used in forestry are typically statistically-derived and known as empirical-based models (Campion et al., 2005; Clutter et al., 1992). Data for empirical-based models for a species are collected from permanent sample plots (PSPs) located over the range of sites and stand ages. The accuracy of empirical-based models are limited to the species and site conditions for which they were originally developed (Landsberg et al., 2003). Such models cannot simulate the growth and yield under changing environmental or management conditions (Battaglia & Sands, 1997; Battaglia & Sands, 1998). This is a particular issue for simulating the impact of climate change on forests as climate change may modify ecosystem processes in a number of direct and indirect ways. Empirical-based models are inflexible and unable to predict forest growth under these non-linear changes. An alternative modelling approach is process-based modelling, which is based on a species physiological limitation's to growth. Process-based modelling is dynamic and is able to incorporate climate changes multitude of direct, indirect, gradual, and abrupt effects to the forest ecosystem to robustly predict future growth under a range of scenarios.

3-PG (physiological processes for predicting growth), is a process-based model developed by Landsberg and Waring (1997). It was designed to be more practical than other process-based models by using a combination of physiological principles and empirical data to simplify model parameterisation. Although 3-PG is most commonly used for eucalypts, it is neither species- nor site-specific for even-age species and has been successfully parameterised for a number of ecosystems throughout the world (Sands, 2004). Several researchers have successfully used 3-PG to assess the potential impacts of climate change and vulnerability of a number of forest species (including *Pseudotsuga menziesii*) in Pacific North-West Region of North America (Coops & Waring, 2010; Coops & Waring, 2011; Waring et al., 2005) and *Eucalyptus* in Brazil (Almeida et al., 2009).

The objectives of this study are 1) modify 3-PG to simulate the effects of climate change in New Zealand, 2) develop potential productivity surfaces for *E. fastigata* under a range of climate change scenarios.

Materials and Methods

The model

The forest growth model 3-PG2S uses subroutines to predict net primary productivity (NPP), transpiration, respiration, and growth. It also computes a water and carbon balance at monthly intervals (Landsberg & Waring, 1997). Absorbed photosynthetically active radiation (APAR) is calculated as a function of photosynthetic active radiation (PAR) and LAI. The utilised portion of APAR (APARu) is established by a series of modifiers with values ranging from zero (total constraint) to 1 (no constraint) (Coops et al., 2009; Landsberg & Waring, 1997). 3-PG2S simulates the forest's water balance; that is water entering, leaving and being stored in the system. Water movement in soil discriminates between water in the "root zone" and "non-root zone" of the soil profile. Suboptimal temperatures, high vapour pressure deficits, infertile soils, and soil available water combine to limit photosynthesis and affect growth and allocation of dry mass. Because leaves are shed at predicted rates, the mass of leaves and their area vary seasonally, increasing when conditions are favourable, and decreasing when they are not. Undulations in LAI affect the amount of NPP and transpiration. 3-PG2S predicts the variables of interest to foresters like stem numbers, mean diameters, standing volume, carbon sequestered, and growth over short or very long rotations. The model was parameterised for *E. fastigata* grown in New Zealand in an earlier study (Meason et al., 2011). The parameterised model performed well in predicting stand volume for both the calibration dataset (R^2 = 0.84) and the validation dataset (R^2 = 0.99) (Meason et al., 2011).

3-PG2S includes an option to simulate a potential CO_2 fertilisation effect with climate change. The "fertilisation effect" is a term that describes the increase in a species net primary productivity with the increase in atmospheric CO_2 concentration. The increase in net primary productivity can be caused by a number of factors including increased water use efficiency and photosynthesis upregulation (Ainsworth and Long, 2005). The potential CO_2 fertilisation effect was simulated in 3-PG2S by methods described by Almeida et al. (2009). Briefly, the canopy quantum efficiency and canopy conductance are normally fixed in the model. These parameters were given modifiers to simulate higher leaf intercellular CO_2 concentration and higher water use efficiency with higher atmospheric CO_2 concentration and lower stomatal conductance (Almeida et al., 2009). The values of the modifications were based on simulations performed in the detailed growth model CABALA (Battaglia et al., 2004).

Model input data

Three types of spatial datasets were required to run the spatial model. The first data set contained the latitude of each spatial location. The second data set was the soil textural classification and plant available soil water, modified from Newsome and colleagues (2008). The third set contained the climate change scenarios provided by National Institute of Water and Atmospheric Research (NIWA) and Landcare Research. All grid layers were at a 5,000 m resolution. The soil and climatic layers are discussed in more detail below. All layers were masked for areas with a mean annual temperature layer of less than 8^{o}C. This removed most mountainous areas of New Zealand that would be too cold to grow most commercial tree species.

Climatic data layers

The monthly climate data surfaces required by the model are mean daily maximum and minimum temperature (^{o}C), rainfall (mm), number of rain days (days mnth^{-1}), solar radiation (MJ m^{-2} dy^{-1}), and number of frost days (days mnth^{-1}). All current and future climate data, except frost days, were provided by NIWA.

New Zealand climate change scenario projections are based on the Canadian Centre for Climate Modelling and Analysis (CCCma) CGCM3 global circulation model (GCM) using the emission scenarios from the United Nations Intergovernmental Panel on Climate Change (IPCC) Fourth Assessment Report (AR4) (IPCC, 2007a). The CCCma GCM was selected from the 12 GCM's available from NIWA as it best represented "middle of the road" temperature rises for New Zealand. The CCCma GCM produced a series of emission scenarios based on the IPCC Special Report on Emission Scenarios (SRES); low emission B1 scenario, a balancing of emission sources that leads to a stabilisation of atmospheric CO_2 after 2080 - A1B scenario, and high emission A2 scenario (IPCC, 2000). These scenarios were generated for two future periods, 2030-2049 (2040 for short) and 2080-2099 (2090 for short). Each NZ SRES scenario produced a percentage difference to current climatology (averaged for years 1980 to 1999) for monthly mean maximum daily temperature, mean minimum daily temperature, and total rainfall. These percentages were converted into monthly values based on current climate values.

As there were no NZ SRES projections for solar radiation and rain days, current climate values were used. Frost day projections were based on Landcare Research's frost day layers for the current climate. For each NZ SRES scenario for 2040 and 2090, the percentage change in mean annual temperature was calculated. This percentage was applied evenly to adjust the number of frost days per month under climate change.

Soil layers

Soil textural data was from Landcare Research's fundamental soil layer textural classification map with a 100 m resolution (Newsome et al., 2008). The classification is based on the interpretation of soil surveys from the 1:63,360/1:50,000 scale New Zealand Land Resource Inventory with reference to analytical results stored in the Nation Soils Database or as professional estimates by pedologists acknowledged as authorities in the soils of the region in question (Newsome et al., 2008). Soils were classified into 27 soil units and seven non-soil units. This was used to classify soil into 33 different categories of soil water characteristics - drainage, storage, and availability to plants. This information was required for the 3-PG2S soil water sub-model. Soil textural classes and plant available soil water for each soil unit were developed by Landcare based on earlier research (Webb & Wilson, 1995). The plant available soil water classification is based on profile total available water to a depth of 0.9 m or to the potential rooting depth based on research by Gradwell and Birrell (1979), Wilson and Giltrap (1982), and Griffiths (1985). Soil depth information currently available was too limited for modelling purposes, so the depth value was set to 1 m throughout the country. The soil fertility spatial layer was not developed due to a lack of information. The soil fertility modifier was set to 0.6 for *E. fastigata* for all soil types.

Model simulations

Following parameterisation, we simulated climate change scenarios for two management regimes, carbon and prune log. Under the carbon regime the stand is established at 1,250 stems per hectare (SPH) for carbon sequestration. It is grown for 30 years with no thinning or pruning. As the stand ages, tree mortality naturally thins the stand. The carbon regime is also suitable for growing a stand for pulp. The prune log regime is established at 1,000 SPH and it is thinned and pruned at ages seven, 10, and 15. At age 7, it is thinned to 500 SPH and pruned to 2.5m. At age 10, the stand is thinned to 250 SPH and pruned to 4m. At age 15, the stand is thinned to final stocking of 200 SPH and pruned to 6m. The model outputs included accumulated stand volume ($m^3\ ha^{-1}$), mean tree diameter at 1.4m height (cm), total stand basal area (BA, $m^2\ ha^{-1}$), and mean annual volume increment (MAI, $m^3\ ha^{-1}\ yr^{-1}$). The CO_2 fertiliser effect with increasing atmospheric CO_2 concentration may increase net primary productivity. However, the experimental evidence that the CO_2 fertiliser effect increases NPP

long term is uncertain due to a number of physiological and environmental factors (Karnosky, 2003). Thus, two values were produced for each scenario, with and without the CO_2 fertiliser effect. This provided a range of predicted productivity with the CO_2 fertiliser effect representing the high end of future productivity using projected atmospheric CO_2 concentrations (IPCC, 2000). Values used in this study are listed in table 3.2.1. The low end of future productivity was provided by simulations without a CO_2 fertilisation effect (using current ambient atmospheric CO_2). Ambient atmospheric CO_2 concentration for the current climate simulation was assumed at 350 ppm. The results from the climate change scenarios were compared to simulated productivity using current climate data.

Table 3.2.1: Assumed atmospheric CO_2 concentration by climate change scenario and year

SRES Climate change scenario	Atmospheric CO_2 concentration (ppm) Year 2040	Year 2090
B1	450	550
A1B	470	720
A2	470	820

Results

Eucalyptus fastigata productivity varied throughout New Zealand under current climate conditions (Figures 3.2.1and 3.2.2). Average productivity for New Zealand was 20.1 and 10.5 m^3 ha^{-1} yr^{-1} for the carbon and prune regimes, respectively (Tables 3.2.2 and 3.2.3). Productivity increased for all climate change scenarios for both the carbon and prune management regimes (Tables 3.2.2 and 3.2.3). Productivity increases were most evident for the carbon regime due to the higher stocking (tree density) at age 30 due to the management regime (not shown). Productivity in 2090 was higher than 2040 for each climate change scenario and management scenario, with and without the CO_2 effect (Tables 3.2.2 and 3.2.3). The B1 scenario had the smallest increase in productivity with 2040 values similar to current climate conditions (Tables 3.2.2 and 3.2.3). Productivity for the A1B scenarios was higher than B1, and the productivity of the A2 scenarios were higher than the other two scenarios (Tables 3.2.2 and 3.2.3). For the carbon regime A2 2090 scenario, the changes in climate (no fertiliser effect) increased productivity by 17% (Table 3.2.2). When a CO_2 fertiliser effect was assumed, productivity increased by 91% (Table 3.2.2). The A2 2090 scenario assuming a fertiliser effect increased productivity by 112% for the prune regime (Table 3.2.3). No climate change scenario had a negative impact on productivity.

Table 3.2.2: Summary table of *Eucalyptus fastigata* mean annual volume increment (m^3 ha^{-1} yr^{-1}) for the carbon forest/pulp management regime by climate scenario with and without the CO_2 fertiliser effect

Climate Scenario	CO_2 fertilisation effect	Minimum (m^3 ha^{-1} yr^{-1})	Mean (m^3 ha^{-1} yr^{-1})	Maximum (m^3 ha^{-1} yr^{-1})
Current	n/a	0.09	20.1	59.4
B1 2040	No	0.09	20.2	62.4
	Yes	0.09	24.0	72.7
B1 2090	No	0.09	20.8	62.1
	Yes	0.09	27.9	80.1
A1B 2040	No	0.09	21.2	58.5
	Yes	0.09	25.9	69.9
A1B 2090	No	0.09	22.7	57.6
	Yes	0.09	34.8	84.9
A2 2040	No	0.09	21.9	62.7
	Yes	0.09	26.8	74.5
A2 2090	No	0.09	23.5	61.3
	Yes	0.09	38.3	94.2

Productivity varied by region, with some regions having higher productivity than others. This was more evident for the climate change scenarios that assumed a CO_2 fertiliser effect (Figures 3.2.3 to 3.2.8). Overall, the North Island had higher productivity than the South Island and areas near the coast had higher productivity than inland areas (Figures 3.2.3 to 3.2.8). Each area had proportionally the same productivity for each climate change scenario. That is, highly productive areas remained highly productive for each climate change scenario and vice versa for the lowly productive areas. The Northland, Auckland, Manawatu – Wanganui, and Gisborne regions, as well as coastal areas in the North Island, had the highest productivity for all scenarios (Figures 3.2.3 to 3.2.8).

Table 3.2.3: Summary table of *Eucalyptus fastigata* mean annual volume increment (m^3 ha^{-1} yr^{-1}) for the prune management regime by climate scenario with and without the CO_2 fertiliser effect

Climate Scenario	CO_2 fertilisation effect	Minimum (m^3 ha^{-1} yr^{-1})	Mean (m^3 ha^{-1} yr^{-1})	Maximum (m^3 ha^{-1} yr^{-1})
Current	n/a	0.03	10.5	53.3
b1 2040	No	0.03	10.6	53.0
	Yes	0.03	13.1	60.8
b1 2090	No	0.03	11.0	52.4
	Yes	0.03	15.5	66.3
a1b 2040	No	0.03	11.2	52.8
	Yes	0.03	14.1	61.9
a1b 2090	No	0.03	12.0	51.4
	Yes	0.03	20.0	73.2
a2 2040	No	0.03	11.6	52.8
	Yes	0.03	14.7	62.0
a2 2090	No	0.03	12.4	50.6
	Yes	0.03	22.3	75.7

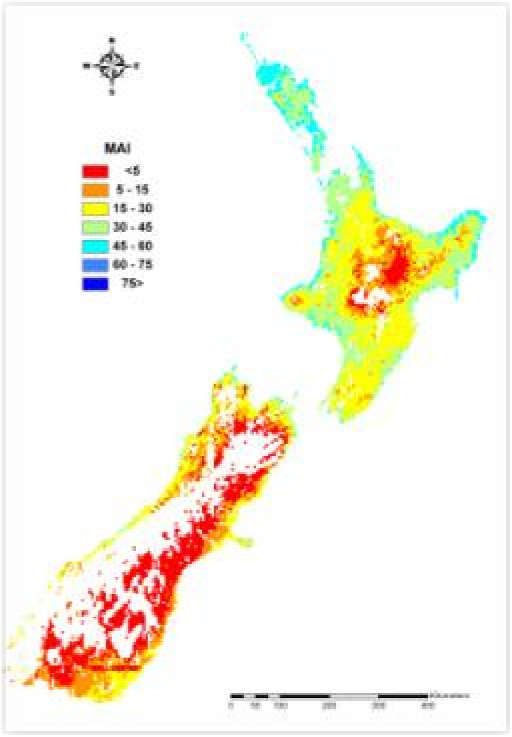

Figure 3.2.1: *Eucalyptus fastigata* productivity, as measured with mean annual volume increment (MAI m^3 ha^{-1} yr^{-1}), for a 30 year carbon forest regime under current climatology

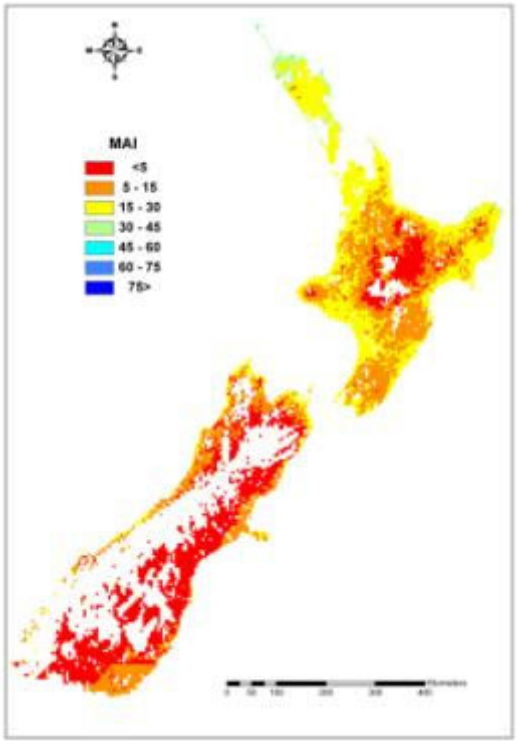

Figure 3.2.2: *Eucalyptus fastigata* productivity, as measured with mean annual volume increment (MAI m^3 ha^{-1} yr^{-1}), for a 30 year carbon prune log regime under current climatology

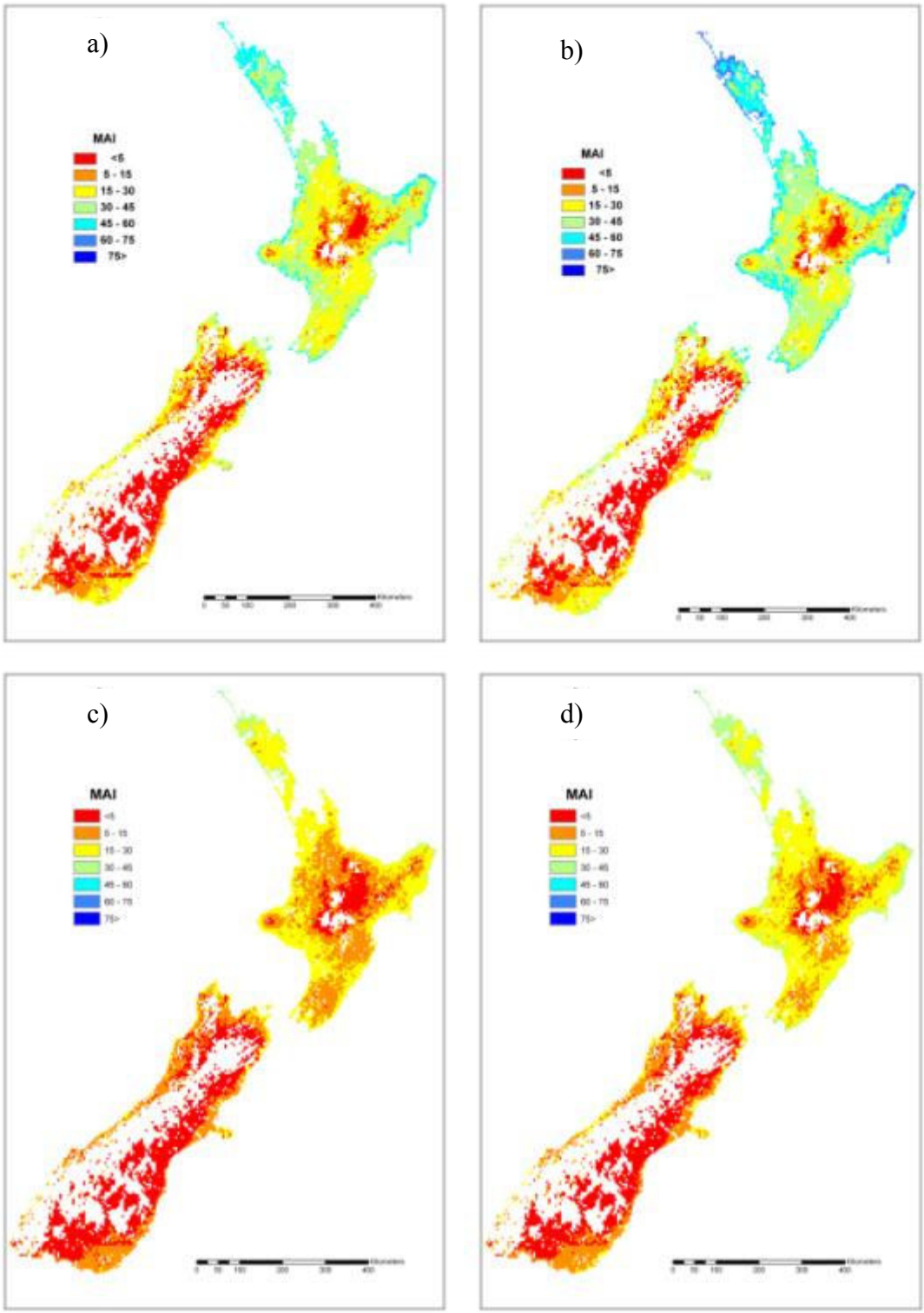

Figure 3.2.3: *Eucalyptus fastigata* productivity, as measured with mean annual volume increment (MAI m^3 ha^{-1} yr^{-1}), under climate change scenario B1 in 2040 for a carbon regime without (a) and with (b) a CO_2 fertiliser effect and a prune log regime without (c) and with (d) a CO_2 fertiliser effect

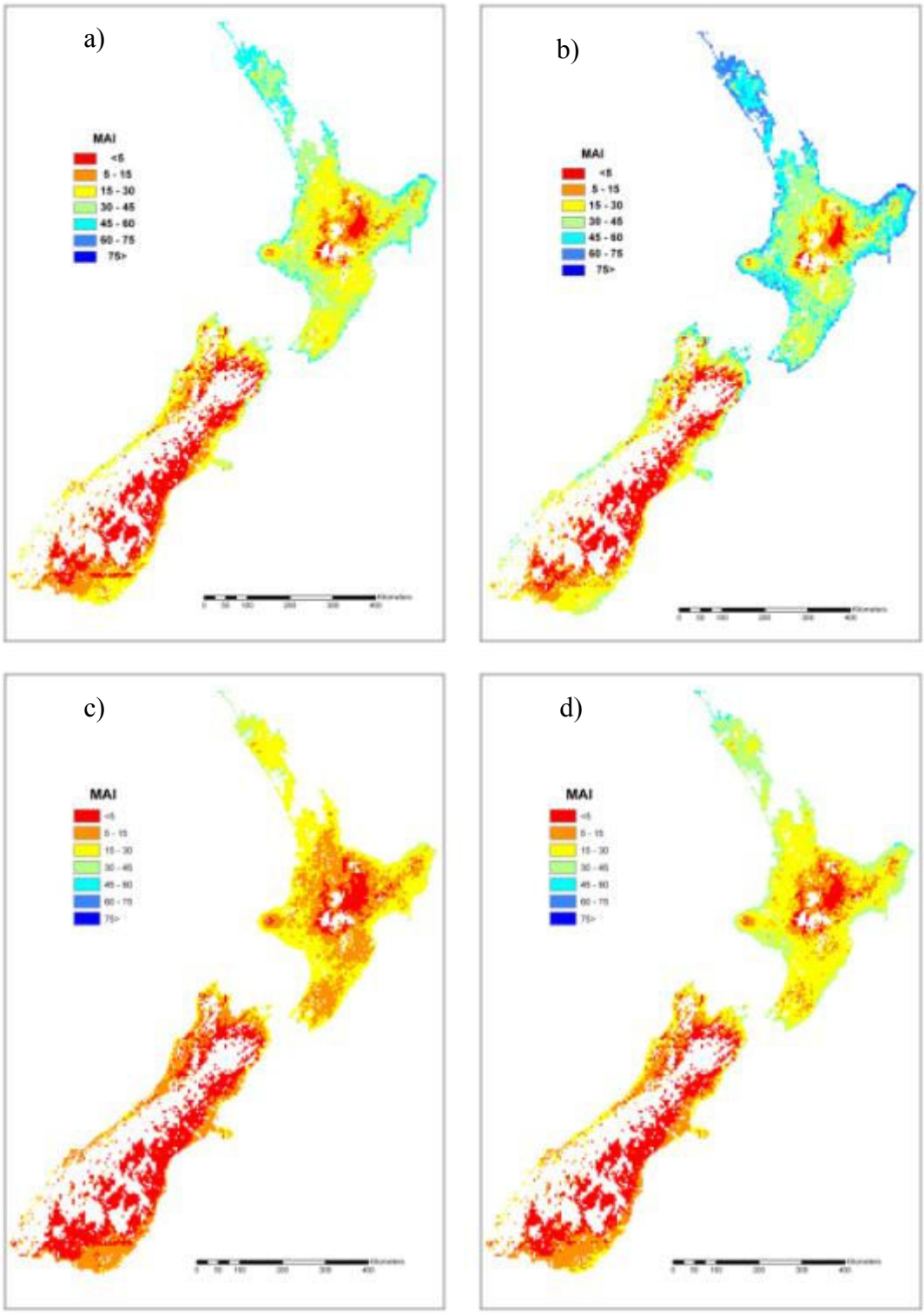

Figure 3.2.4: *Eucalyptus fastigata* productivity, as measured with mean annual volume increment (MAI m^3 ha^{-1} yr^{-1}), under climate change scenario B1 in 2090 for a carbon regime without (a) and with (b) a CO_2 fertiliser effect and a prune log regime without (c) and with (d) a CO_2 fertiliser effect

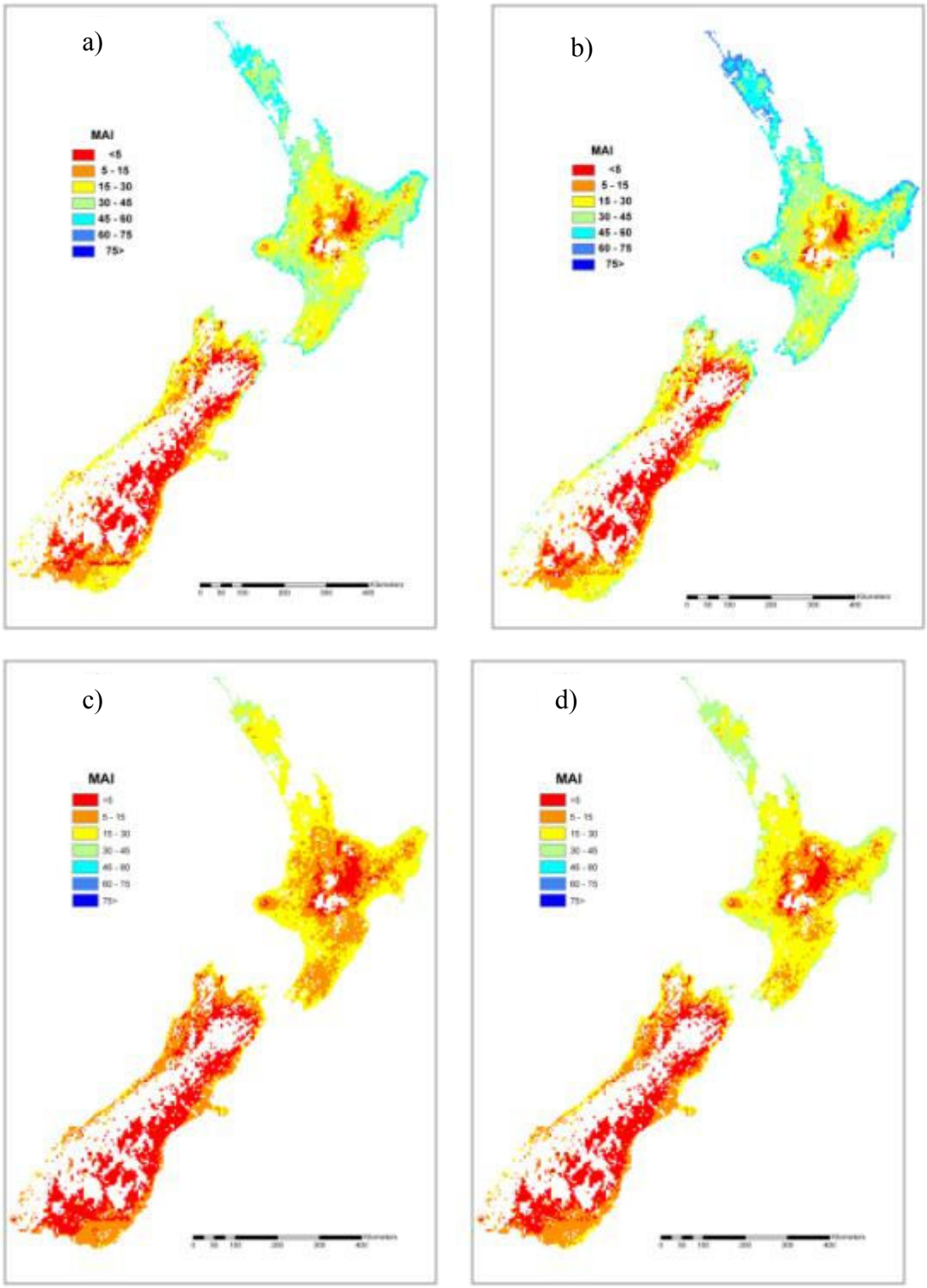

Figure 3.2.5: *Eucalyptus fastigata* productivity, as measured with mean annual volume increment (MAI m^3 ha^{-1} yr^{-1}), under climate change scenario A1B in 2040 for a carbon regime without (a) and with (b) a CO_2 fertiliser effect and a prune log regime without (c) and with (d) a CO_2 fertiliser effect

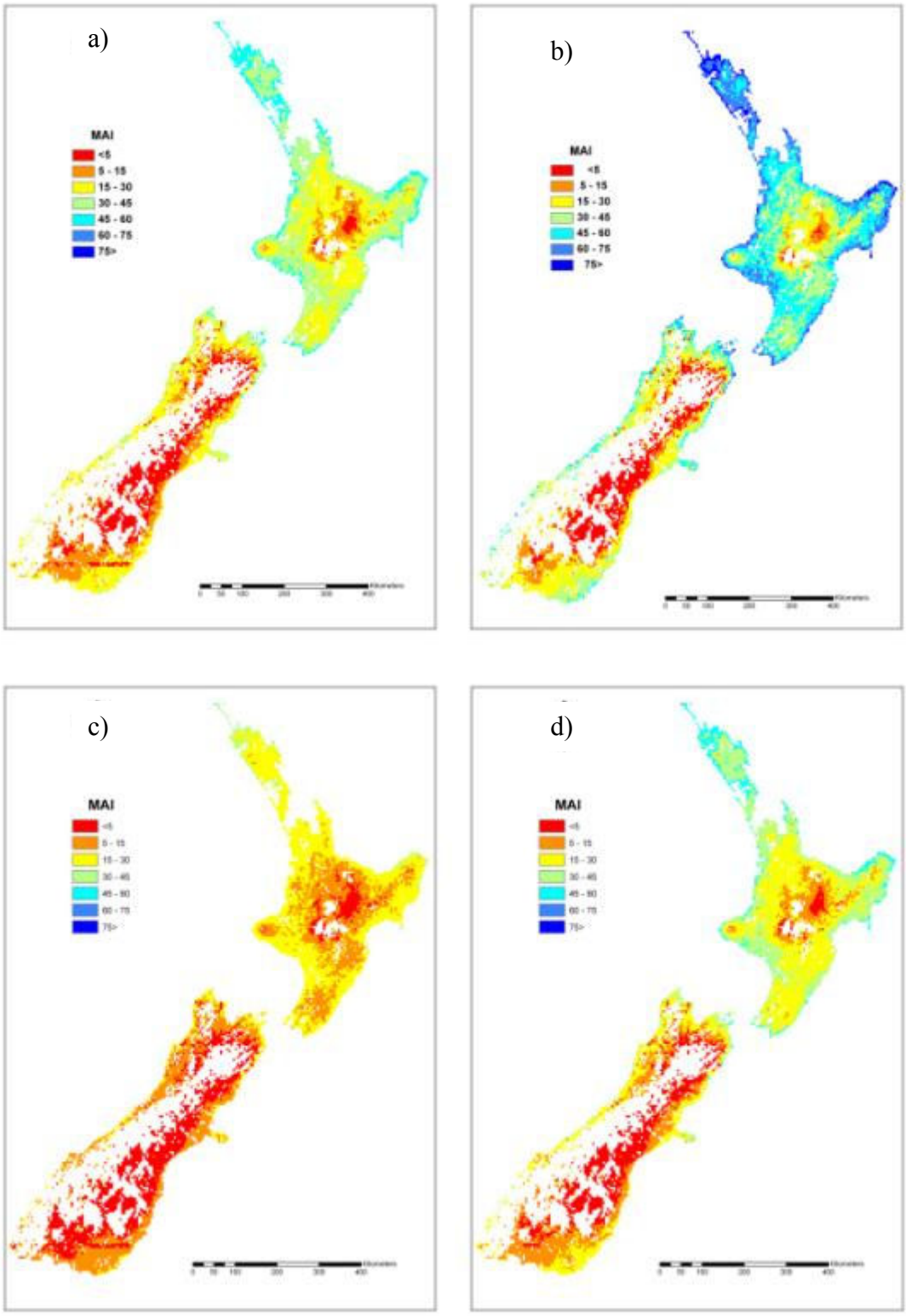

Figure 3.2.6: *Eucalyptus fastigata* productivity, as measured with mean annual volume increment (MAI m^3 ha^{-1} yr^{-1}), under climate change scenario A1B in 2090 for a carbon regime without (a) and with (b) a CO_2 fertiliser effect and a prune log regime without (c) and with (d) a CO_2 fertiliser effect

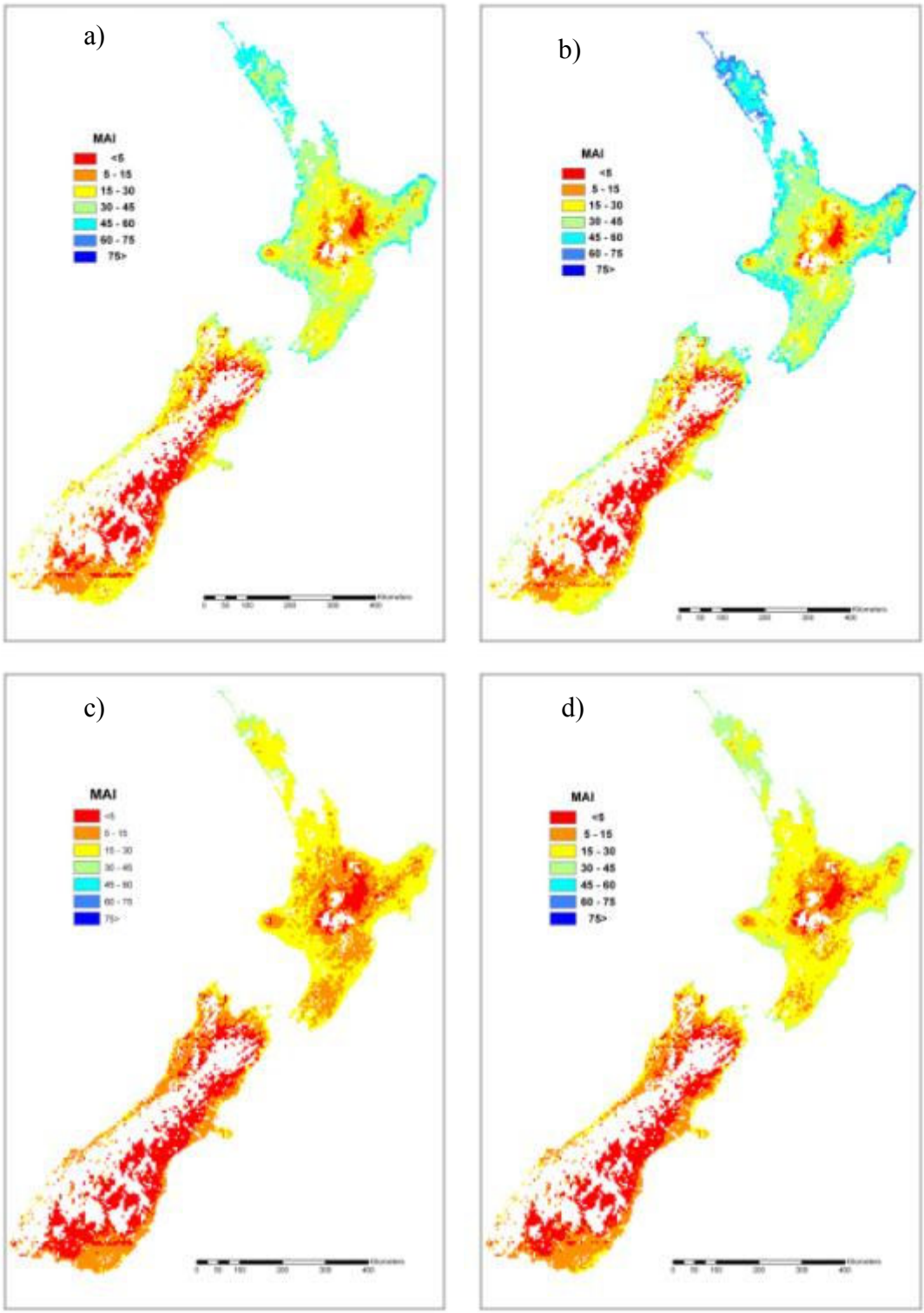

Figure 3.2.7: *Eucalyptus fastigata* productivity, as measured with mean annual volume increment (MAI m^3 ha^{-1} yr^{-1}), under climate change scenario A2 in 2040 for a carbon regime without (a) and with (b) a CO_2 fertiliser effect and a prune log regime without (c) and with (d) a CO_2 fertiliser effect

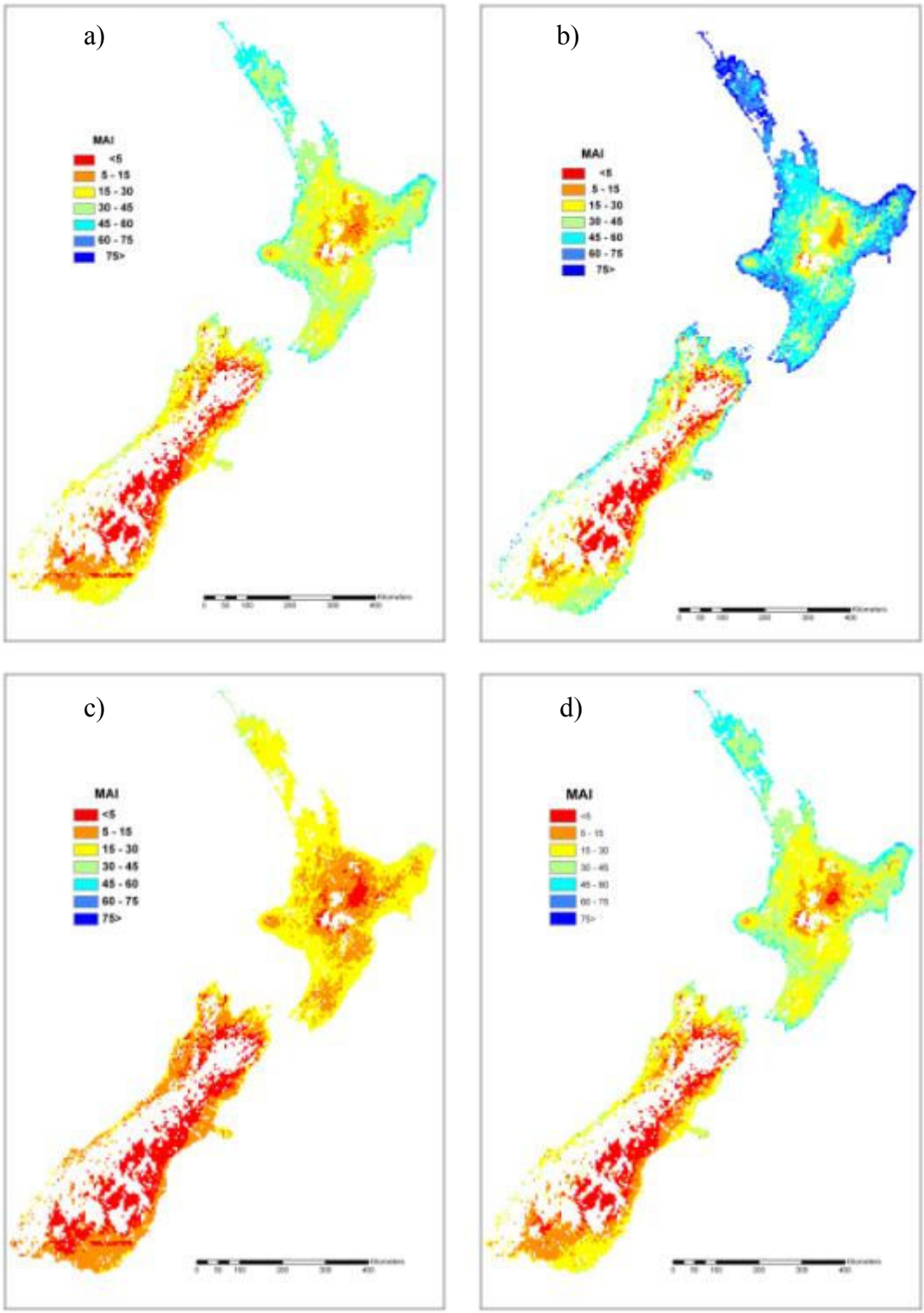

Figure 3.2.8: *Eucalyptus fastigata* productivity, as measured with mean annual volume increment (MAI m^3 ha^{-1} yr^{-1}), under climate change scenario A2 in 2090 for a carbon regime without (a) and with (b) a CO_2 fertiliser effect and a prune log regime without (c) and with (d) a CO_2 fertiliser effect

Discussion

Eucalyptus fastigata benefited from the net increase in temperature while changes in precipitation had minimal effect. However, the climatic factor that had the biggest impact on productivity was the reduction in frost days. *As E. fastigata* is a frost sensitive species, a reduction of frost days increased current productivity in frost prone areas. Climate change also increased the potential range of the species in New Zealand, especially in the inland areas of the South Island and the Central North Island. Relative productivity at each location did not change with each climate change scenario. Areas with high productivity under current conditions were also highly productive with climate change, and vice versa for areas with low productivity. This was due to three reasons; first, the temperature increases occurred uniformly throughout New Zealand. Second, the forecasted increase in temperature was not high enough to negatively impact photosynthesis through stomatal closure. Third, the changes in precipitation with climate change were too small to negatively impact growth. With average precipitation in forestry areas over 1,000 mm yr^{-1}, a 5-15% decline in rainfall is not large enough to have any impact. Current climate change scenarios are based on changes in long term averages from scaled down global circulation models with no extreme climatic events. If climate change alters precipitation frequency and duration, or causes periods of drought, this would have a significant impact on growth. If such climate modelling becomes available in the future, it is recommended that the climate change scenarios in this report be reassessed.

The CO_2 fertiliser effect had a large impact on productivity in 2090, but not 2040. This was due to the atmospheric CO_2 concentration used in the scenarios. In 2040, the CO_2 concentration was 100 – 120 ppm higher than ambient. This resulted in a small increase in NPP. For the 2090 scenarios, the CO_2 concentrations were a lot higher (200-470 ppm) than ambient, which resulted in a large increase in NPP. It is unclear from current research that increased atmospheric CO_2 will cause a sustainable, long term increase in NPP for forests (Karnosky, 2003). This study showed that the increases in temperature and reduction in frost days with climate change can increase *E. fastigata* productivity. If a CO_2 fertiliser effect did occur, then productivity could be enhanced even further. Reporting productivity with and without the CO_2 fertiliser effect produced a large productivity range for each scenario. Due to the uncertainties' with the CO_2 fertiliser effect, it is recommended that the simulations without the effect be used as conservative prediction of *E. fastigata* productivity with climate change. Productivity from simulations with the CO_2 fertiliser effect should be used only as a best case scenario.

The model had some limitations due to the current knowledge on the spatial variability of soil depth and soil fertility. The depth of soil in forests and ex-pasture land is at best crude, thus a uniform depth of 1m was used for the model. Areas with shallow soils and decreasing precipitation are most likely to have longer periods of soil water deficit that may decrease productivity. More research is required on shallow soils so that the effects of reductions in soil water can be more accurately simulated. Current methods to measure soil fertility for *P. radiata* includes the C:N ratio and 300 index. Species other than radiata pine can be more sensitive to soil nutrients other than the C:N ratio (Ledgard et al., 2005). In a 2010 study of the eight environmental site factors influencing *E. fastigata* productivity, soil extractable phosphorus was the only significant measure of soil fertility (Meason et al., 2010). Maps of plant available phosphorus and other nutrients throughout New Zealand have been developed by researchers. However, these maps are too coarse to predict soil fertility for *E. fastigata* for existing stands or be used in process-based modelling. The development of a new index of soil fertility for Eucalyptus and other alternative (to radiata pine) tree species is under development at Scion. Until it is developed, a constant soil fertility factor was used. It is unlikely that the climate change scenarios would have a negative impact on soil fertility for most regions in New Zealand. There is no known destructive pest for *E. fastigata* in New Zealand or Australia. Indeed, one of the reasons why *E. fastigata* is the focus of current research and management is because it is resistant to pathogens that afflict other Eucalyptus

species in New Zealand. Thus, this study assumed that no new pathogen will impact its growth under the climate change scenarios.

Recommendations and Conclusions

Increasing temperature and less frost days were the most important climatic factors impacting growth with the climate change scenarios. The decrease in precipitation in some regions reduced the size of productivity gains. However, the reduction in precipitation was not large enough to adversely affect productivity in most areas in New Zealand. In conclusion, a global 2^{o}C rise in temperature is unlikely to adversely impact *E. fastigata* productivity in New Zealand. In fact, climate change is likely to be quite beneficial in terms of productivity and the expansion of favourable sites for the species.

The climate change simulations in this report is one of the first climate change modelling studies for alternative (to radiata pine) exotic forestry species in New Zealand. Improving the process-based model 3PG will help provide more precise simulations of the potential impacts on climate change. This includes accurate spatial representation of soil depth and soil fertility. Improvements with climatology, for example modelling variation in rainfall frequency and intensity, would lead to better modelling of potential climate change impacts. Comparing the impact of climate change on different landuses requires the comparison of productivity between very different models with differing inputs, assumptions, and time scales. Further work is required to understand the differences and similarities of various models so landuse analysis can be made in a more dynamic way.

3.3 Influence of climate change on productivity of coast redwood

Abstract

Sequoia sempervirens is a timber species that is highly valued in the Western United States. The species ability to sequester carbon over hundreds of years makes it an ideal species for carbon forestry. It has high potential as a plantation species for large scale afforestation on marginal agricultural land. However, there are not enough permanent sample plots (PSP's) to develop a robust growth model under current or future climatic conditions. The process-based model 3-PG (physiological processes for predicting growth), was parameterised for *S. sempervirens* for New Zealand conditions, and then validated with the spatial version of the model (3-PG2S). The model performed adequately in predicting stand basal area (BA) for the calibration dataset (R^2 = 0.78). The model over-predicted BA for stands with less than 50 m^2 ha^{-1} and over predicted BA for stands with greater than 150 m^2 ha^{-1}. The parameterised model was used to test the potential productivity of *S. sempervirens* under three IPCC SRES climate change scenarios for 2040 and 2090; low emission B1 scenario, emission stabilisation scenario A1B, and high emission scenario A2. Each scenario was tested without and with an increase in net primary productivity from higher atmospheric CO_2 concentrations (CO_2 fertiliser effect) with climate change. Productivity increased with each scenario with the highest level of productivity in 2090. Climate change also increased the potential range of the species in the North Island, while productivity of inland areas of the South Island and the Central North Island remained low. The increase in temperature and decrease in frost days with climate change had the biggest impact on productivity. The decline in precipitation in some areas of New Zealand with some scenarios was small, but not enough to adversely productivity. *Sequoia sempervirens* appeared to be sensitive to soil site conditions like available soil water for tree uptake and soil fertility. The species frost tolerance is not understood. How these environmental factors affect productivity need to be fully understood before *S. sempervirens* productivity can be predicted robustly for current and future conditions. More accurate information on soil depth and soil fertility is also required. The current parameterised model did clearly show that that a global 2^oC rise in temperature is unlikely to adversely impact *S. sempervirens* productivity in New Zealand.

Introduction

Sequoia sempervirens (coast redwood (D.Don) Endl.) is an alternative commercial species to *Pinus radiata* (radiata pine) (Anon., 2009; Brown, 2007; Cornell, 2002; Knowles & Miller, 1993; Libby, 1999; Nicholas et al., 2007). Although coast redwood timber is not used on a large scale domestically, there is a well-established market in the United States. The timber, highly desired for its heartwood colour and rot resistant properties, has multiple outdoor and indoor uses (Webb, 2007). Uses include house sidings, fences, outdoor decking and furnishings, interior trim and moulding, and interior shelving (Webb, 2007).

Research in the last 15 years has identified the potential for redwood as a fast growing plantation species in New Zealand (Brown et al., 2008). With logging in California of redwood forests becoming increasingly restricted, there is an opportunity for New Zealand to become an important supplier of the timber. Further, its ability to sequester carbon long after canopy closure means that redwood is highly suitable for long-term carbon forestry in New Zealand.

Global warming and its impact on the climate is likely to impact many natural and human induced ecosystems. It can impact on forest ecosystems directly or indirectly, and it can impact gradually or abruptly. Climate change may impact tree growth and mortality from gradual changes in temperature, rainfall patterns, and solar radiation (Coops & Waring, 2011). More abrupt impact may occur from increased frequency in wildfires, droughts, out of season frosts, and outbreaks of insects and diseases (Chapin et al., 2010). The complexity of climate change and its direct and indirect on forest ecosystems means that forest models must be dynamic enough to simulate these effects.

Mathematical models used in forestry are typically statistically-derived and known as empirical-based models (Campion et al., 2005; Clutter et al., 1992). Data for empirical-based models for a species are collected from permanent sample plots (PSPs) located over the range of sites and stand ages. The accuracy of empirical-based models are limited to the species and site conditions for which they were originally developed (Landsberg et al., 2003). Such models cannot simulate the growth and yield under changing environmental or management conditions (Battaglia & Sands, 1997; Battaglia & Sands, 1998). This is a particular issue for simulating the impact of climate change on forests as climate change may modify ecosystem processes in a number of direct and indirect ways. Empirically-based models are inflexible and unable to predict forest growth under these non-linear changes. An alternative modelling approach is process-based modelling, which is based on a species physiological limitation's to growth. Process-based modelling is dynamic and is able to incorporate climate changes multitude of direct, indirect, gradual, and abrupt effects to the forest ecosystem to robustly predict future growth under a range of scenarios.

3-PG (physiological processes for predicting growth), is a process-based model developed by Landsberg and Waring (1997). It was designed to be more practical than other process-based models by using a combination of physiological principles and empirical data to simplify model parameterisation. Although 3-PG is most commonly used for eucalypts, it is neither species- nor site-specific for even-age species and has been successfully parameterised for a number of ecosystems throughout the world (Sands, 2004). Several researchers have successfully used 3-PG to assess the potential impacts of climate change and vulnerability of a number of forest species (including *Pseudotsuga menziesii*) in Pacific North-West Region of North America (Coops & Waring, 2010; Coops & Waring, 2011; Waring et al., 2005) and *Eucalyptus* in Brazil (Almeida et al., 2009).

The objectives of this study are 1) parameterise 3-PG to simulate *S. sempervirens* productivity under current climate conditions in New Zealand, 2) develop potential productivity surfaces for *S. sempervirens* under a range of climate change scenarios.

Materials and Methods

The model

The forest growth model 3-PG2S uses subroutines to predict net primary productivity (NPP), transpiration, respiration, and growth. It also computes a water and carbon balance at monthly intervals (Landsberg & Waring, 1997). Absorbed photosynthetically active radiation (APAR) is calculated as a function of photosynthetic active radiation (PAR) and LAI. The utilised portion of APAR (APARu) is established by a series of modifiers with values carrying form zero (total constraint) to 1 (no constraint) (Coops et al., 2009; Landsberg & Waring, 1997). 3-PG2S simulates the forest's water balance; that is water entering, leaving and being stored in the system. Water movement in soil discriminates between water in the "root zone" and "non-root zone" of the soil profile. Suboptimal temperatures, high vapour pressure deficits, infertile soils, and soil available water combine to limit photosynthesis and affect growth and allocation of dry mass. Because leaves are shed at predicted rates, the mass of leaves and their area vary seasonally, increasing when conditions are favourable, and decreasing when they are not. Undulations in LAI affect the amount of NPP and transpiration. 3-PG2S predicts the variables of interest to foresters like stem numbers, mean diameters, standing volume, carbon sequestered, and growth over short or very long rotations.

3-PG2S includes an option to simulate a potential CO_2 fertilisation effect with climate change. The "fertilisation effect" is a term that describes the increase in a species net primary productivity with the increase in atmospheric CO_2 concentration. The increase in net primary productivity can be caused by a number of factors including increased water use efficiency and photosynthesis upregulation (Ainsworth and Long, 2005). The potential CO_2 fertilisation effect was simulated in 3-PG2S by methods described by Almeida et al. (2009). Briefly, the canopy quantum efficiency and canopy conductance are normally fixed in the model. These parameters were given modifiers to simulate higher leaf intercellular CO_2 concentration and higher water use efficiency with higher atmospheric CO_2 concentration and lower stomatal conductance (Almeida et al., 2009). The values of the modifications were based on simulations performed in the detailed growth model CABALA (Battaglia et al., 2004).

Model parameterisation

Data for model parameterisation was collected from 59 plots from 12 sites (Table 3.3.1).The sites were selected for their representation of the range of environments that coast redwood is currently grown in New Zealand (Figure 3.3.1). Further adjustments were made to the model with the calibration dataset. Data from TEWE, KANG, MANT, TUTI, and OTCO were used to develop thinning and mortality functions. There is not enough information available on biomass partitioning for coast redwood grown in New Zealand. Thus, a *P. radiata* biomass allocation function that was previously developed for 3-PG was used.

Table 3.3.1: Summary table of sites used for the calibration dataset

Site	Region	Year planted	Stand ages when measured	Number of plots	Current stocking (stems per hectare)
RAKA	Northland	1994	16-18	2	356-650
TAUD	Waikato	1922	80-86	1	460
TEWE	Taranaki	1957	46-50	2	133-500
BROW	Waikato	1995	12-14	2	850
BRAN	Bay of Plenty	1969, 1997, 2000	3-37	3 (1 plot per age)	363-883
KANG	Bay of Plenty	1982	22-28	8	350-859
RUAT	Gisborne	1976	28-31	2	617-1000
WAEK	Gisborne	1998	7-11	4	500-750
TUTI	Napier	1998	6-13	21	850-350
MANT	Gisborne	1978	26-32	6	317-633
HUND	Canterbury	2002	6	1	620
OTCO	Otago	1988	18-25	7	360-1660

Leaf litter, specific leaf area, canopy leaf area measurements were collected from RAKA, TUTI, and KANG. These measurements were used to calibrate the model's simulation of stand leaf area and canopy turnover as the stand aged. Photosynthesis measurements were taken from KANG to determine changes of the photosynthetic rate between seasons. These measurements were entered into CABALA to simulate the variation of photosynthesis and carbon assimilation with changing temperature, precipitation, and atmospheric vapour pressure deficit. These simulations were used to help calibrate 3-PG2S for changes in coast redwood NPP with the climate change scenarios.

Temperature modifiers to growth were based on earlier studies with *E. fastigata* and other Eucalyptus species. Frost and fertility modifiers to growth were based on adjusting these variables to fit the calibration data set.

Figure 3.3.1: Location of coast redwood calibration sites

Model input data

Three types of spatial datasets were required to run the spatial model. The first data set contained the latitude of each spatial location. The second data set was the soil textural classification and plant available soil water, modified from Newsome and colleagues (2008). The third set contained the climate change scenarios provided by National Institute of Water and Atmospheric Research (NIWA) and Landcare Research. All grid layers were at a 5,000m resolution. The soil and climatic layers are discussed in more detail below. All layers were masked for areas with a mean annual temperature layer of less than 8^{o}C. This removed most mountainous areas of New Zealand that would be too cold to grow most commercial tree species.

Climatic data layers

The monthly climate data surfaces required by the model are mean daily maximum and minimum temperature (^{o}C), rainfall (mm), number of rain days (days mnth^{-1}), solar radiation (MJ m^{-2} dy^{-1}), and number of frost days (days mnth^{-1}). All current and future climate data, except frost days, were provided by NIWA.

New Zealand climate change scenario projections are based on the Canadian Centre for Climate Modelling and Analysis (CCCma) CGCM3 global circulation model (GCM) using the emission scenarios from the United Nations Intergovernmental Panel on Climate Change (IPCC) Fourth Assessment Report (AR4) (IPCC, 2007a). The CCCma GCM was selected from the 12 GCM's available from NIWA as it best represented "middle of the road" temperature rises for New Zealand. The CCCma GCM produced a series of emission scenarios based on the IPCC Special Report on Emission Scenarios (SRES); low emission B1 scenario, a balancing of emission sources that leads to a stabilisation of atmospheric CO_2 after 2080 - A1B scenario, and high emission A2 scenario (IPCC, 2000). These scenarios were generated for two future periods, 2030-2049 (2040 for short) and 2080-2099 (2090 for short). Each NZ SRES scenario produced a percentage difference to current climatology (averaged for years 1980 to 1999) for monthly mean maximum daily temperature, mean minimum daily temperature, and total rainfall. These percentages were converted into monthly values based on current climate values.

As there were no NZ SRES projections for solar radiation and rain days, current climate values were used. Frost day projections were based on Landcare Research's frost day layers for the current climate. For each NZ SRES scenario for 2040 and 2090, the percentage change in mean annual temperature was calculated. This percentage was applied evenly to adjust the number of frost days per month under climate change.

Soil layers

Soil textural data was from Landcare Research's fundamental soil layer textural classification map with a 100 m resolution (Newsome et al., 2008). The classification is based on the interpretation of soil surveys from the 1:63,360/1:50,000 scale New Zealand Land Resource Inventory with reference to analytical results stored in the Nation Soils Database or as professional estimates by pedologists acknowledged as authorities in the soils of the region in question (Newsome et al., 2008). Soils were classified into 27 soil units and seven non-soil units. This was used to classify soil into 33 different categories of soil water characteristics - drainage, storage, and availability to plants. This information was required for the 3-PG2S soil water sub-model. Soil textural classes and plant available soil water for each soil unit were developed by Landcare based on earlier research (Webb and Wilson, 1995). The plant available soil water classification is based on profile total available water to a depth of 0.9 m or to the potential rooting depth based on research by Gradwell and Birrell (1979), Wilson and Giltrap (1982), and Griffiths (1985). Soil depth information currently available was too

limited for modelling purposes, so the depth value was set to 1 m throughout the country. The soil fertility spatial layer was not developed due to a lack of information. The soil fertility modifier was set to 0.7 for *S. sempervirens* for all soil types.

Model simulations

Following parameterisation, we simulated climate change scenarios for two management regimes, carbon and prune log. Under the carbon regime the stand is established at 1,250 stems per hectare (SPH) for carbon sequestration. It is grown for 43 years with no thinning or pruning. As the stand ages, tree mortality naturally thins the stand. The prune log regime is established at 400 SPH and it is pruned at ages five, eight, and 12. At age five, it is pruned to 2.5m. At age eight, the stand is pruned to 4m. At age 12, the stand is pruned to 6m. The model outputs included accumulated stand volume (m^3 ha^{-1}), mean tree diameter at 1.4m height (cm), total stand basal area (BA, m^2 ha^{-1}), and mean annual volume increment (MAI, m^3 ha^{-1} yr^{-1}). The CO_2 fertiliser effect with increasing atmospheric CO_2 concentration may increase net primary productivity. However, the experimental evidence that the CO_2 fertiliser effect increases NPP long term is uncertain due to a number of physiological and environmental factors (Karnosky, 2003). Thus, two values were produced for each scenario, with and without the CO_2 fertiliser effect. This provided a range of predicted productivity with the CO_2 fertiliser effect representing the high end of future productivity using projected atmospheric CO_2 concentrations (IPCC, 2000). Values used in this study are listed in table 3.3.2. The low end of future productivity was provided by simulations without a CO_2 fertilisation effect (using current ambient atmospheric CO_2). Ambient atmospheric CO_2 concentration for the current climate simulation was assumed at 350 ppm. The results from the climate change scenarios were compared to simulated productivity using current climate data.

Table 3.3.2: Assumed atmospheric CO_2 concentration by climate change scenario and year

SRES Climate change scenario	Atmospheric CO_2 concentration (ppm) Year 2040	Year 2090
B1	450	550
A1B	470	720
A2	470	820

Results

Model calibration

Overall, the calibrated model provided a good prediction of stand growth for a majority of calibration sites with an R^2 of 0.78 (Figure 3.3.2). However, the model generally over-predicted stand growth for sites with low basal area (generally younger sites) and it under-predicted growth for sites that had a basal area greater than 150 m^2 ha^{-1} (Figure 3.3.2). The large under-prediction was due to the TAUD site that is one plot that wasn't measured until 80 years-old. As the data is from one plot and the stand history is unknown, data from this site cannot be seen as typical for the Waikato region. However, it is likely that the under-prediction is partly due to the model as 3-PG has difficulty simulating stands greater than 50 years. If the TAUD site was removed from the calibration graph, the actual verse predicted regression line would be closer to the 1:1 line.

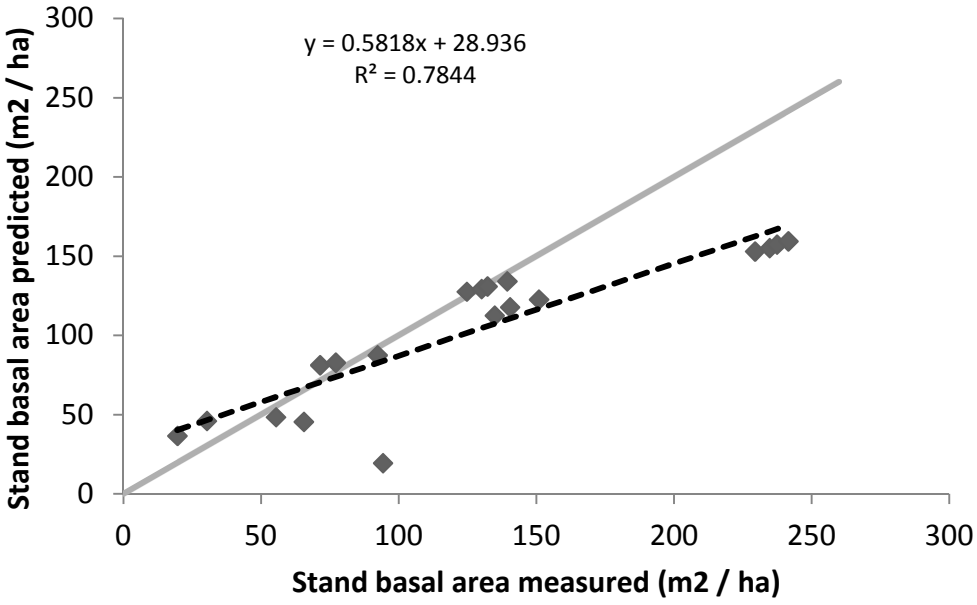

Figure 3.3.2: Model predictions of stand basal area compared with measured values from eight sites of the calibration dataset

Sequoia sempervirens is more sensitive to frost than other alternative forestry species. Thus, simulating the effect of frost days on growth is especially important to predict productivity throughout New Zealand. The model's frost day's modifier is a linear function of the number of growth days lost every time a ground frost occurs. The frost modifier was set to 0.4 for the entire country. Although this modifier is not an accurate reflection of the physiological effects of frost on *S. sempervirens* growth, it provided a growth penalty for growing *S. sempervirens* in frost prone areas. The higher the number of frost days, the greater the cumulative number of growth days lost for the tree for each year. Thus, if two sites have similar temperature and precipitation, the site with more frost days would be less productive. The frost modifier does not take into account the severity of frosts, or the impact of out-of-season frosts. The frost modifier did provide an appropriate growth penalty of growing *S. sempervirens* for coastal and upland areas near the coast. However, the frost modifier created a growth penalty too severe for areas in the Central North Island and inland areas of the South Island (Figures 3.3.3 and 3.3.4). This was partly due to the fact that existing stands are planted in areas that do not receive many frost days. More information is required on the limits of *S. sempervirens* frost tolerance to accurately simulate the effects of frost on growth for inland, frost prone, areas.

Climate change simulations

Sequoia sempervirens productivity varied throughout New Zealand under current climate conditions (Figures 3.3.3 and 3.3.4). Average productivity for New Zealand was 18.4 and 23.9 m^3 ha^{-1} yr^{-1} for the carbon and prune regimes, respectively (Tables 3.3.3 and 3.3.4). Productivity increased for all climate change scenarios for both the carbon and prune management regimes (Tables 3.3.3 and 3.3.4). Productivity in 2090 was higher than 2040 for each climate change scenario and management scenario, with and without the CO_2 effect (Tables 3.3.3 and 3.3.4). The B1 scenario had the smallest increase in productivity with 2040 values similar to current climate conditions (Tables 3.3.3 and 3.3.4). Productivity for the A1B scenarios was higher than B1, and the productivity of the A2 scenarios were higher than the other two scenarios (Tables 3.3.3 and 3.3.4).

For the carbon regime A2 2090 scenario, the changes in climate (no fertiliser effect) increased productivity by 20% (Table 3.3.3). When a CO_2 fertiliser effect was assumed, productivity increased by 86% (Table 3.3.4). The A2 2090 scenario assuming a fertiliser

effect increased productivity by 60% for the prune regime (Table 3.3.4). No climate change scenario had a negative impact on productivity.

Table 3.3.3: Summary table of *Sequoia sempervirens* mean annual volume increment (m^3 ha^{-1} yr^{-1}) for the carbon forest management regime by climate scenario with and without the CO_2 fertiliser effect

Climate Scenario	CO_2 fertilisation effect	Minimum (m^3 ha^{-1} yr^{-1})	Mean (m^3 ha^{-1} yr^{-1})	Maximum (m^3 ha^{-1} yr^{-1})
Current	n/a	0.07	18.4	53.9
b1 2040	no	0.07	21.4	53.9
	yes	0.07	24.9	61.9
b1 2090	no	0.07	21.2	53.1
	yes	0.07	27.6	67.6
a1b 2040	no	0.07	22.1	53.8
	yes	0.07	26.5	63.2
a1b 2090	no	0.07	22.0	52.3
	yes	0.07	32.5	74.6
a2 2040	no	0.07	22.9	53.9
	yes	0.07	27.4	63.3
a2 2090	no	0.07	22.0	51.6
	yes	0.07	34.3	77.1

Productivity varied by region, with some regions having higher productivity than others. This was more evident for the climate change scenarios that assumed a CO_2 fertiliser effect (Figures 3.3.5 to 3.3.10). Overall, the North Island had higher productivity than the South Island and areas near the coast had higher productivity than inland areas (Figures 3.3.5 to 3.3.10). Each area had the proportionally the same productivity for each climate change scenario. That is, highly productive areas remained highly productive for each climate change scenario and vice versa for the lowly productive areas. The coastal areas of the North Island had the highest productivity for all scenarios (Figures 3.3.5 to 3.3.10). The South Island had low productivity for most climate change scenarios. Only the A2 2090 scenario with the CO_2 fertiliser effect significantly increased the productivity in large areas of the South Island above 40 m^3 ha^{-1} yr^{-1} (Figure 3.3.10).

Table 3.3.4: Summary table of *Sequoia sempervirens* mean annual volume increment (m^3 ha^{-1} yr^{-1}) for the prune management regime by climate scenario with and without the CO_2 fertiliser effect

Climate Scenario	CO_2 fertilisation effect	Minimum (m^3 ha^{-1} yr^{-1})	Mean (m^3 ha^{-1} yr^{-1})	Maximum (m^3 ha^{-1} yr^{-1})
Current	n/a	0.07	23.9	65.1
b1 2040	no	0.07	23.9	60.6
	yes	0.07	27.4	69.3
b1 2090	no	0.07	23.2	60.6
	yes	0.07	25	70.9
a1b 2040	no	0.07	24.1	60.5
	yes	0.07	29.1	70.6
a1b 2090	no	0.07	23.9	58.8
	yes	0.07	36	82.0
a2 2040	no	0.07	24.9	60.4
	yes	0.07	30.1	70.7
a2 2090	no	0.07	23.8	58.0
	yes	0.07	38.1	84.8

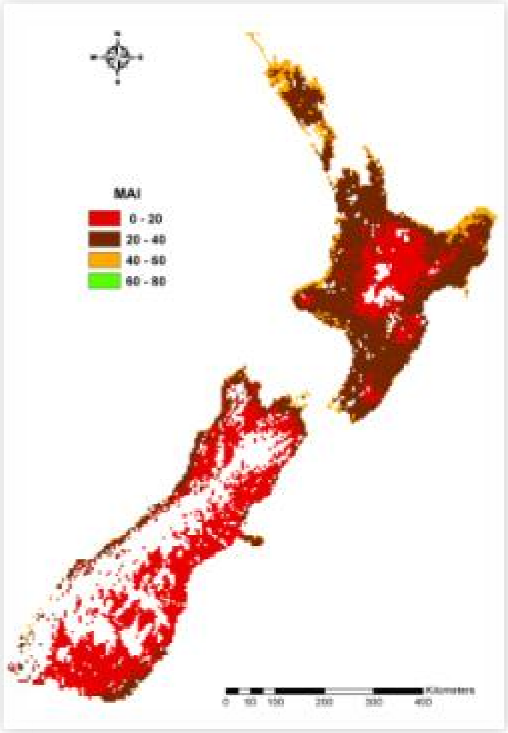

Figure 3.3.3: *Sequoia sempervirens* productivity, as measured with mean annual volume increment (MAI m^3 ha^{-1} yr^{-1}), for a 43 year carbon forest regime under current climatology

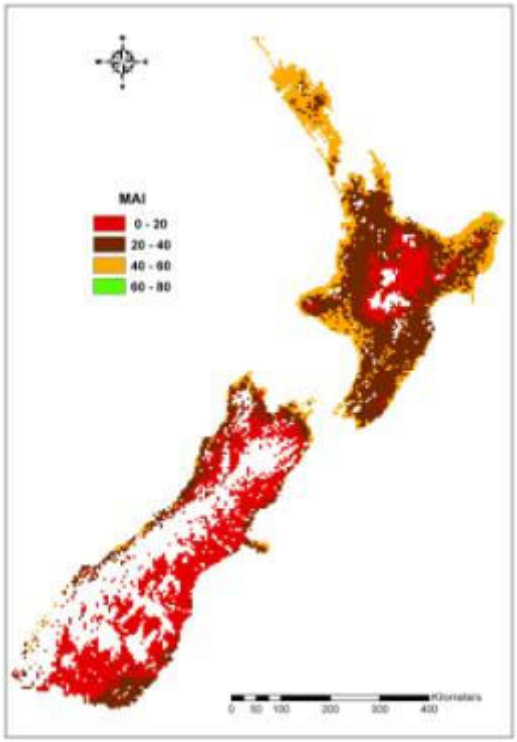

Figure 3.3.4: *Sequoia sempervirens* productivity, as measured with mean annual volume increment (MAI m^3 ha^{-1} yr^{-1}), for a 43 year carbon prune log regime under current climatology

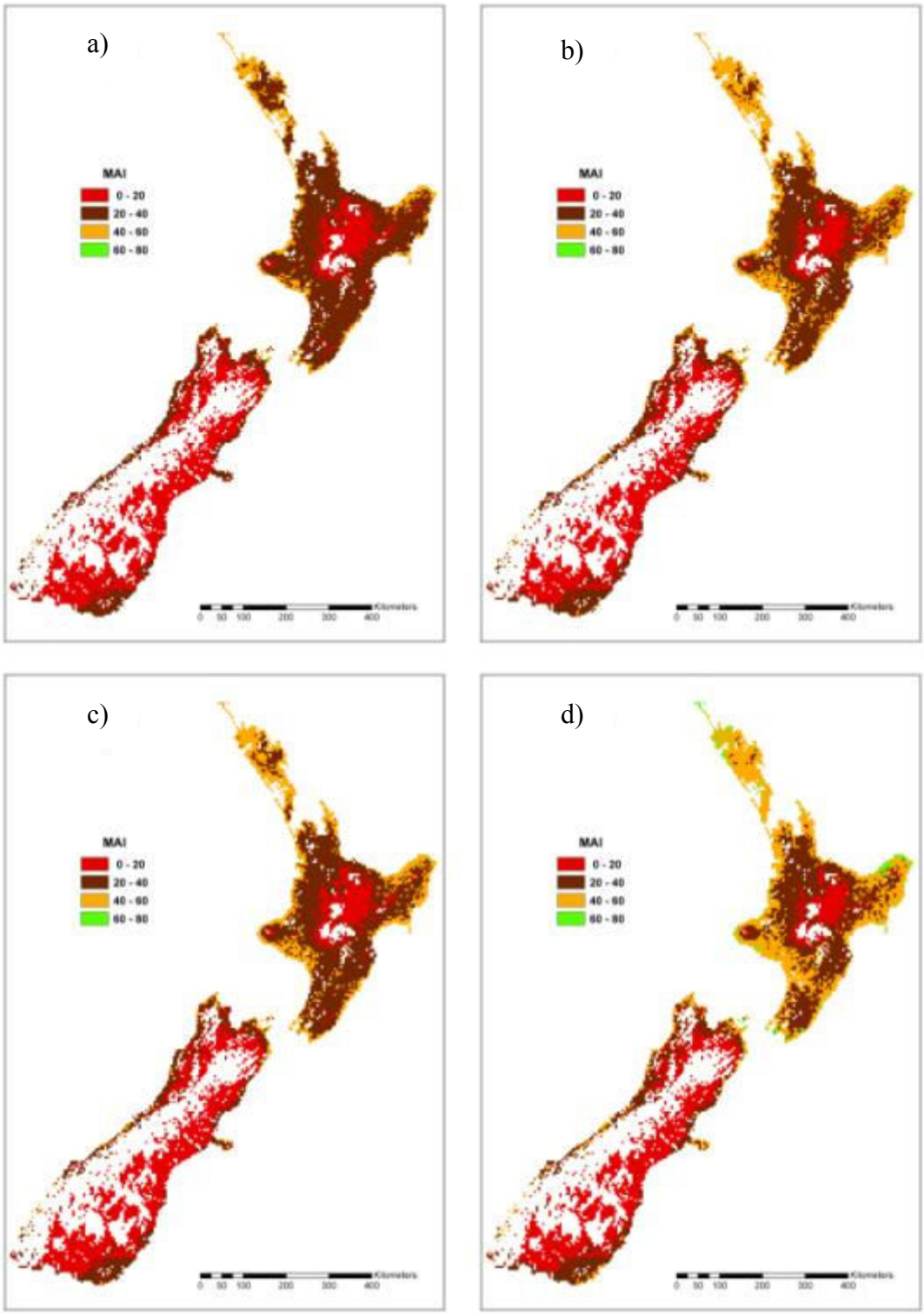

Figure 3.3.5: *Sequoia sempervirens* productivity, as measured with mean annual volume increment (MAI m^3 ha^{-1} yr^{-1}), under climate change scenario B1 in 2040 for a carbon regime without (a) and with (b) a CO_2 fertiliser effect and a prune log regime without (c) and with (d) a CO_2 fertiliser effect

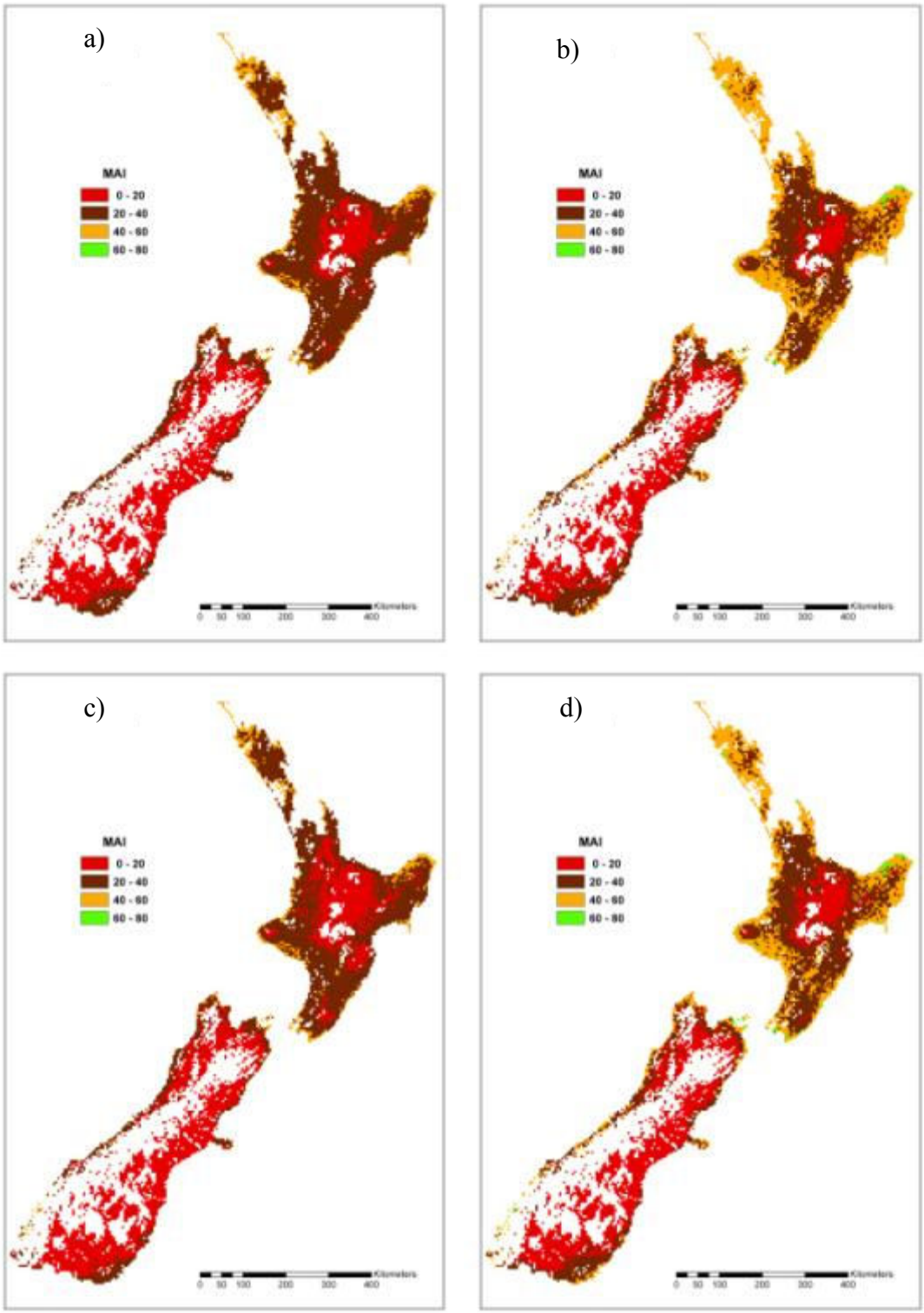

Figure 3.3.6: *Sequoia sempervirens* productivity, as measured with mean annual volume increment (MAI m^3 ha^{-1} yr^{-1}), under climate change scenario B1 in 2090 for a carbon regime without (a) and with (b) a CO_2 fertiliser effect and a prune log regime without (c) and with (d) a CO_2 fertiliser effect

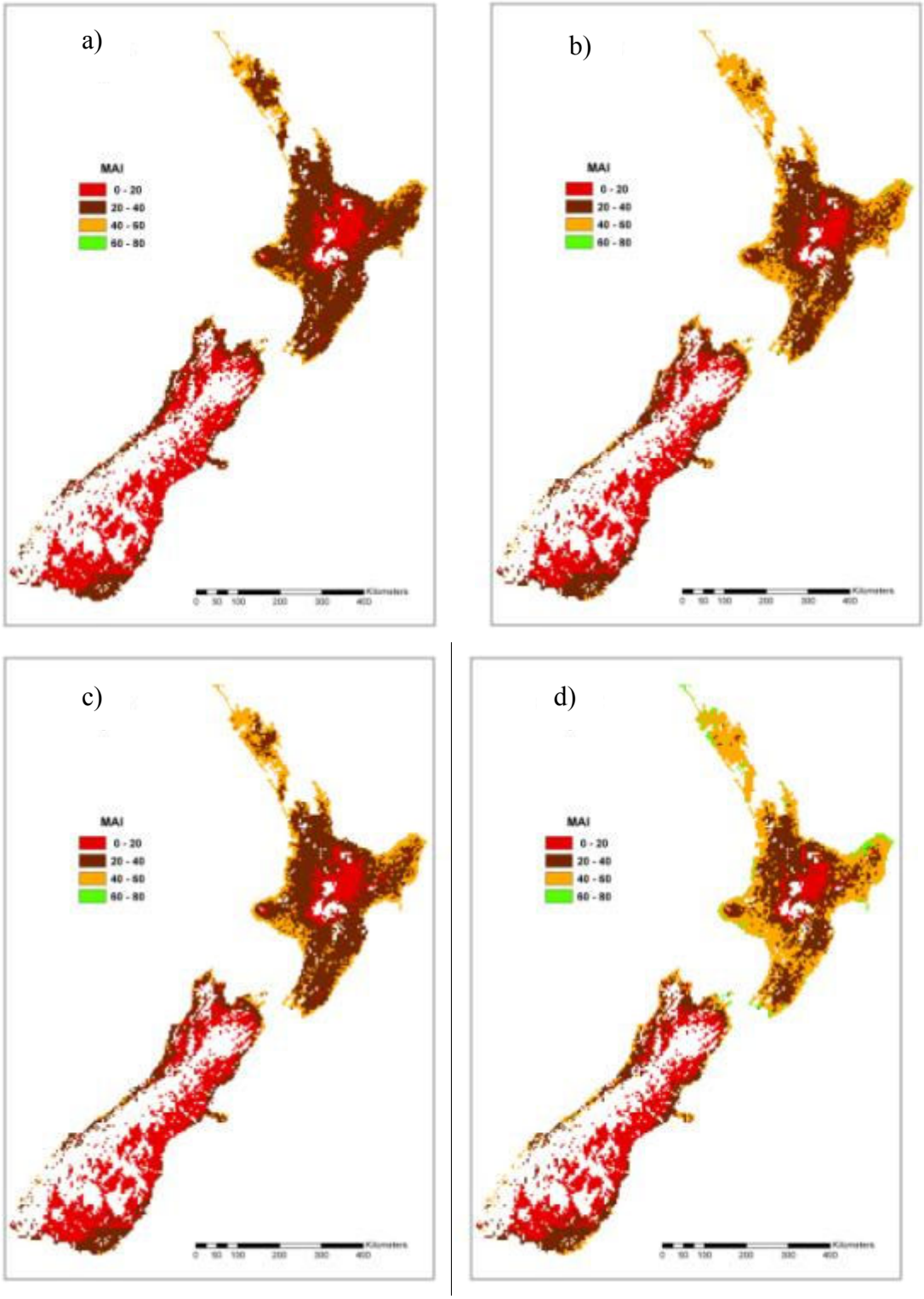

Figure 3.3.7: *Sequoia sempervirens* productivity, as measured with mean annual volume increment (MAI m^3 ha^{-1} yr^{-1}), under climate change scenario A1B in 2040 for a carbon regime without (a) and with (b) a CO_2 fertiliser effect and a prune log regime without (c) and with (d) a CO_2 fertiliser effect

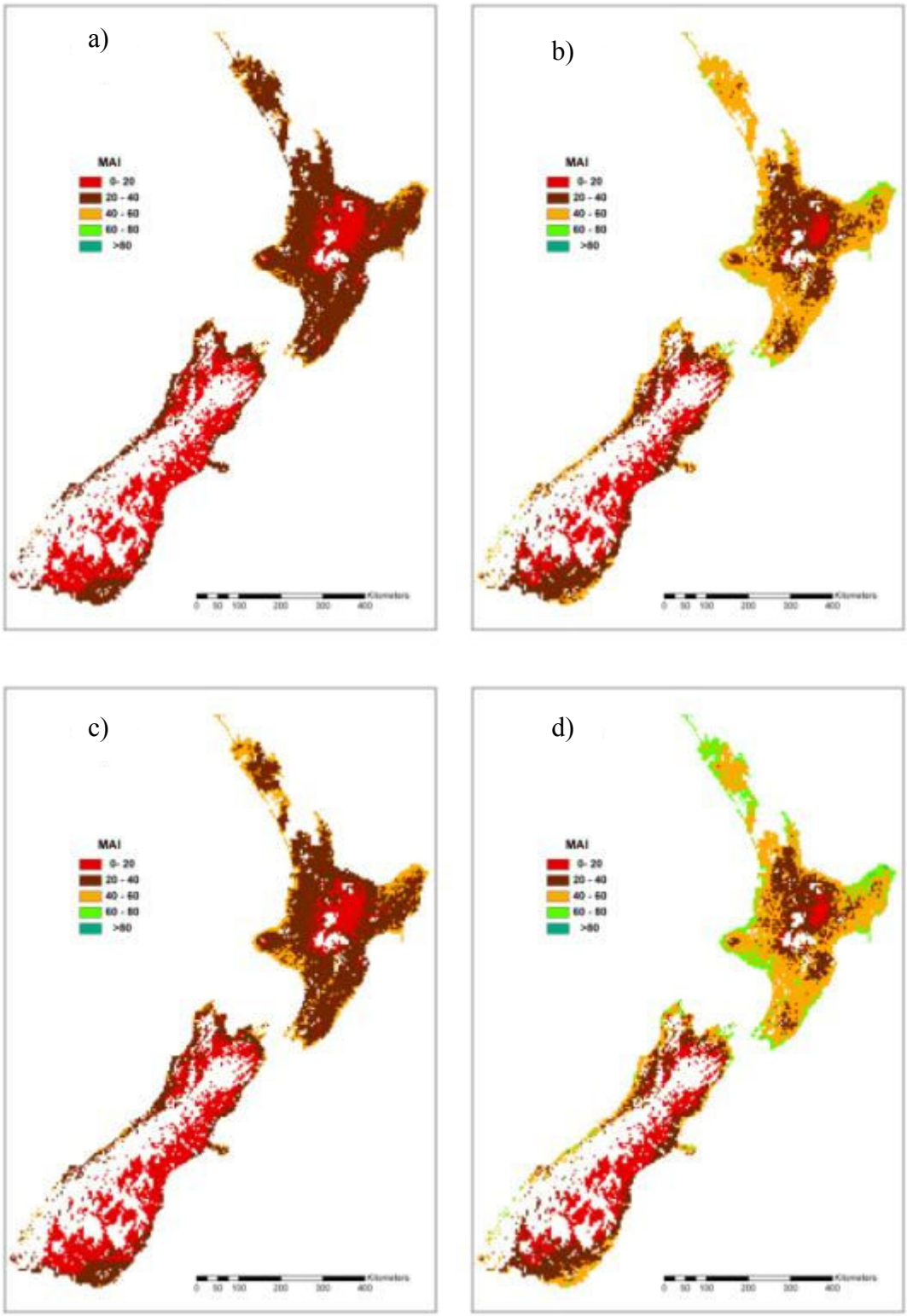

Figure 3.3.8: *Sequoia sempervirens* productivity, as measured with mean annual volume increment (MAI m^3 ha^{-1} yr^{-1}), under climate change scenario A1B in 2090 for a carbon regime without (a) and with (b) a CO_2 fertiliser effect and a prune log regime without (c) and with (d) a CO_2 fertiliser effect

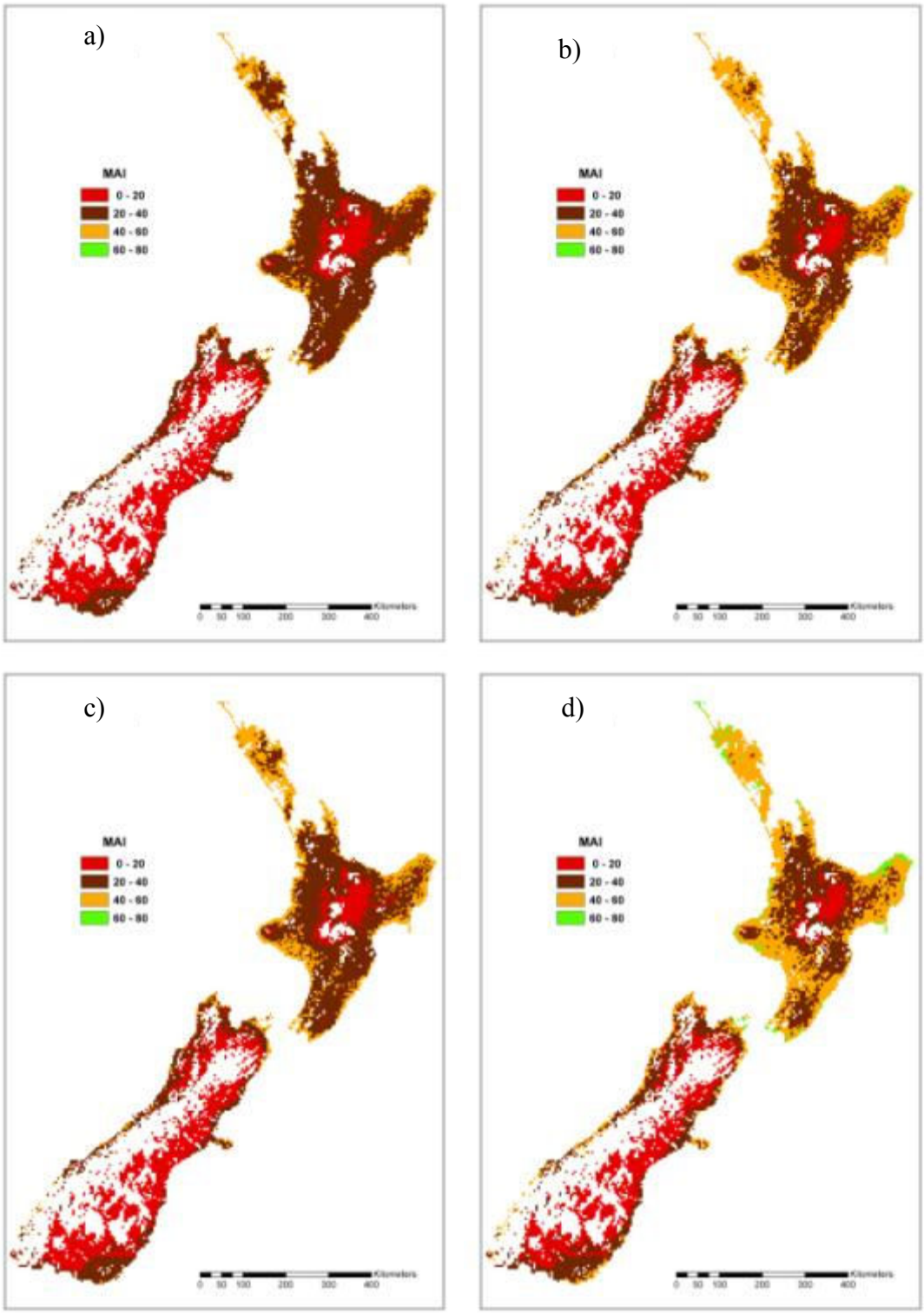

Figure 3.3.9: *Sequoia sempervirens* productivity, as measured with mean annual volume increment (MAI m^3 ha^{-1} yr^{-1}), under climate change scenario A2 in 2040 for a carbon regime without (a) and with (b) a CO_2 fertiliser effect and a prune log regime without (c) and with (d) a CO_2 fertiliser effect

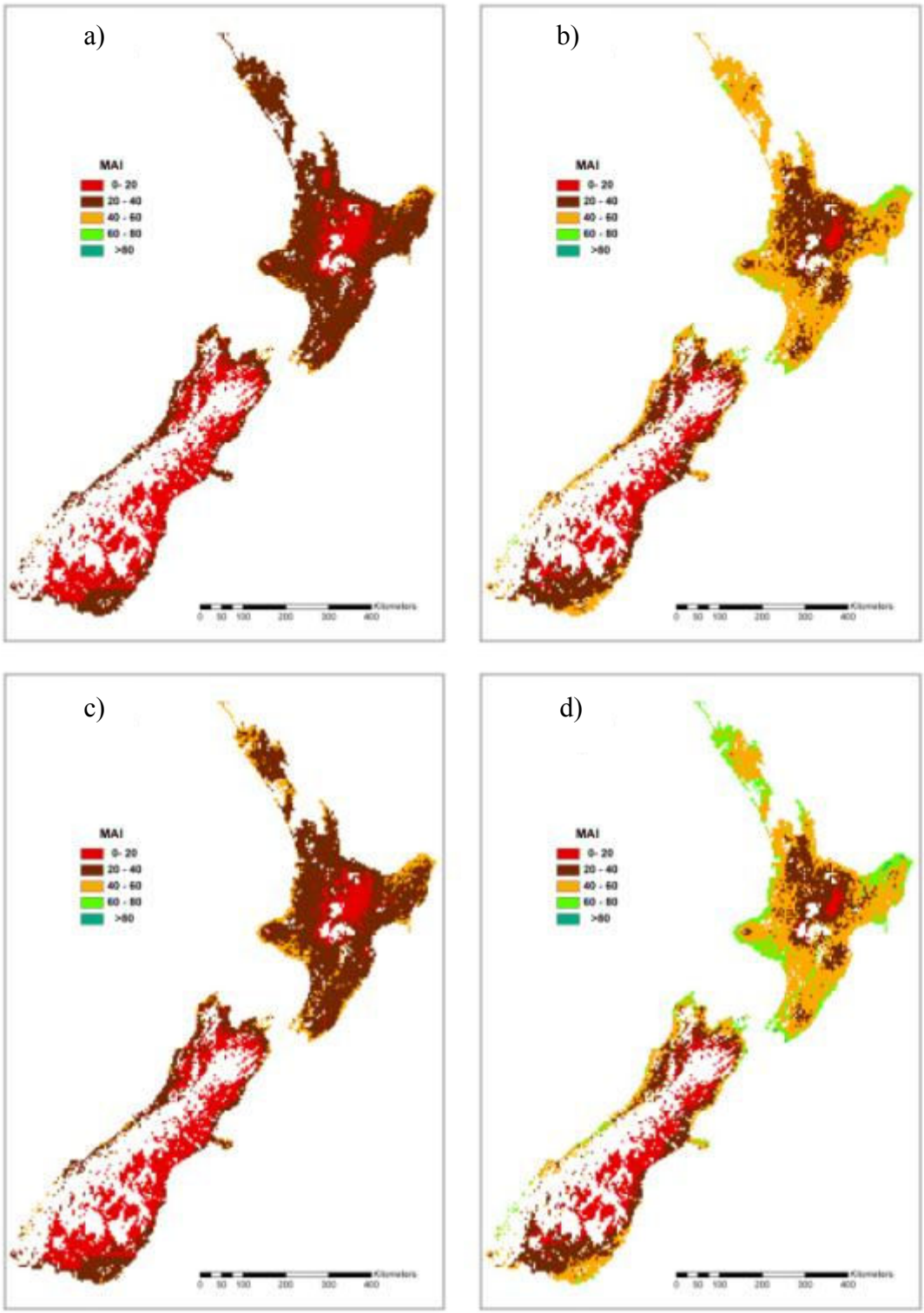

Figure 3.3.10: *Sequoia sempervirens* productivity, as measured with mean annual volume increment (MAI m^3 ha^{-1} yr^{-1}), under climate change scenario A2 in 2090 for a carbon regime without (a) and with (b) a CO_2 fertiliser effect and a prune log regime without (c) and with (d) a CO_2 fertiliser effect

Discussion

Sequoia sempervirens benefited from the net increase in temperature while changes in precipitation had minimal effect. However, the climatic factor that had the biggest impact on productivity was the reduction in frost days. *As S. sempervirens* is a frost sensitive species, a reduction of frost days increased current productivity in frost prone areas. The parameterised model underestimated *S. sempervirens* productivity in inland areas that have a high number of frost days, which was represented on the maps as areas that had productivity less than 20 m^3 ha^{-1} yr^{-1}. These areas had the largest increase in productivity with climate change. The B1 scenario had the smallest change in temperature and frost days, followed by the A1B scenario and the A2 scenario, which had the largest decrease in frost days. The number of frost days in 2090 was a lot less than under the current climate or at 2040. Although areas with less than 20 m^3 ha^{-1} yr^{-1} benefitted the most with the reduction in frost days with climate change, this is not evident on the productivity maps because even doubling or tripling a low growth rate still classified growth in these inland areas in the lowest category of 20 m^3 ha^{-1} yr^{-1}. It was clear from the productivity maps that upland areas near the coast that had moderate frost days benefited from the reduction of frost days. Coast redwood productivity in these areas increased by one productivity class for the A1B and A2 2090 scenarios.

Relative productivity at each location did not change with each climate change scenario. Areas with high productivity under current conditions were also highly productive with climate change, and vice versa for areas with low productivity. This was due to three reasons; first, the temperature increases occurred uniformly throughout New Zealand. Second, the forecasted increase in temperature was not high enough to negatively impact photosynthesis through stomatal closure. Third, the changes in precipitation with climate change were too small to negatively impact growth. With average precipitation in forestry areas over 1,000 mm yr^{-1}, a 5-15% decline in rainfall is not large enough to have any adverse impact. Current climate change scenarios are based on changes in long term averages from scaled down global circulation models with no extreme climatic events. If climate change alters precipitation frequency and duration, or cause periods of drought, this would have a significant impact on growth. If such climate modelling becomes available in the future, it is recommended that the climate change scenarios in this report be reassessed.

The CO_2 fertiliser effect had a large impact on productivity in 2090, but not 2040. This was due to the atmospheric CO_2 concentration used in the scenarios. In 2040, the CO_2 concentration was 100 – 120 ppm higher than ambient. This resulted in a small increase in NPP. For the 2090 scenarios, the CO_2 concentrations were a lot higher (200-470 ppm) than ambient, which resulted in a large increase in NPP. It is unclear from current research that increased atmospheric CO_2 will cause a sustainable, long term increase in NPP for forests (Karnosky, 2003). This study showed that the increases in temperature and reduction in frost days with climate change can increase *S. sempervirens* productivity. If a CO_2 fertiliser effect did occur, then productivity could be enhanced even further. Reporting productivity with and without the CO_2 fertiliser effect produced a large productivity range for each scenario. Due to the uncertainties' with the CO_2 fertiliser effect, it is recommended that the simulations without the effect be used as conservative prediction of *S. sempervirens* productivity with climate change. Productivity from simulations with the CO_2 fertiliser effect should be used only as a best case scenario.

The model had some limitations due to the current knowledge on the spatial variability of soil depth and soil fertility. The depth of soil in forests and ex-pasture land is at best crude, thus a uniform depth of 1m was used for the model. Areas with shallow soils and decreasing precipitation are most likely to have longer periods of soil water deficit that may reduce productivity. More research is required on shallow soils before reductions in soil water can be accurately simulated. Current methods to measure soil fertility for *P. radiata* includes the C:N ratio and 300 index. Alternative species (to radiata pine) can be more sensitive to soil nutrients other than the C:N ratio (Ledgard et al., 2005). A recent study with *Eucalyptus*

fastigata found eight environmental site factors were influencing productivity (Meason et al., 2010). Soil extractable phosphorus was the only measure of soil fertility significantly influencing *E. fastigata* productivity (Meason et al., 2010).

One of difficulties in parameterising 3-PG was the variability of productivity between individual plots for a number of sites. The variability of productivity within a site would suggest that *S. sempervirens* is sensitive to soil site conditions like soil available water for tree uptake and soil fertility. In fact, *S. sempervirens* appears more sensitive than *E. fastigata*, Douglas-fir, and other alternative (to radiata pine) forestry species. To ensure more accurate modelling, accurate spatial information is needed for soil depth and measures of soil fertility that *S. sempervirens* is particularly sensitive to. Maps of plant available phosphorus and other nutrients throughout New Zealand have been previously developed by researchers. However, these maps are too coarse to predict soil fertility for *S. sempervirens* for existing stands or to be used in process-based modelling. The development of a new index of soil fertility for eucalypts and other alternative tree species is under development at Scion. Until it is developed, a constant soil fertility factor was used. It is unlikely that the climate change scenarios would have a negative impact on soil fertility for most regions in New Zealand.

There is no known destructive pest for *S. sempervirens* in New Zealand. Thus, this study assumed that no new pathogen will impact its growth under the climate change scenarios.

Recommendations and Conclusions

Increasing temperature and less frost days were the most important climatic factors impacting growth with the climate change scenarios. The decrease in precipitation in some regions reduced the size of productivity gains. The reduction in precipitation was not large enough to adversely affect productivity in many areas in New Zealand. However, there were indications that the productivity increase was not at its maximum potential in some areas. This was likely due to the reduction in precipitation. More research is required to understand the degree of sensitivity *S. sempervirens* has to soil water and changes in precipitation. In conclusion, a global 2^{o}C rise in temperature is unlikely to adversely impact *S. sempervirens* productivity in New Zealand.

The climate change simulations in this report represent one of the first climate change modelling studies for alternative (to radiata pine) exotic forestry species in New Zealand. Improving the process-based model 3PG will help provide more precise simulations of the potential impacts on climate change. The current parameterised model needs to be improved by fully investigating the current limitation of growth in New Zealand including frost tolerance, soil fertility, and soil water. In addition, accurate spatial representation of soil depth and soil fertility is required. Improvements with climatology, for example modelling variation in rainfall frequency and intensity, would lead to better modelling of potential climate change impacts. Comparing the impact of climate change on different landuses requires the comparison of productivity between very different models with differing inputs, assumptions, and time scales. Further work is required to understand the differences and similarities of various models so landuse analysis can be made in a more dynamic way.

3.4 Modelling the growth of kanuka-manuka stands in New Zealand

Abstract

The physiologically-based growth model CenW 4.0 was used to model the growth of kanuka/mānuka stands throughout New Zealand. Key modelling attributes for this stand type were the physiological responses to environmental conditions, species-specific height-diameter relationships, self-thinning when trees reached critical sizes for given stand densities, competition from weeds during initial stand establishment and early growth, and gradual stand collapse and replacement by other tree species for stands beyond 50 years of age.

The model parameterisation relied mainly on stand-level observations of biomass and total-stand carbon for stands from 2-96 years in age located throughout New Zealand and on analysis of the observed distribution of kanuka/mānuka stands as a function of environmental conditions from throughout New Zealand. These observations were supplemented by findings from past modelling work and specific measurements of a number of stand attributes from a small number of more intensively studied sites.

Overall, average biomass productivity in New Zealand was modelled to be 2.2 tC ha^{-1} yr^{-1} for stand growth over the first 25 years of growth, with highest growth rates of about 3.5 tC ha^{-1} yr^{-1} at the most productive sites. When accumulation of dead biomass was also included, this equated to total stand carbon accumulation rates of more than 4.5 tC ha^{-1} yr^{-1} at the most productive sites.

Stands also showed a strong dependence on temperature and precipitation, with kanuka/manuka being totally absent from sites with mean annual temperatures below 5°C. The probability of occurrence was linearly dependent on temperature for the range of temperatures found in New Zealand. For precipitation, its occurrence increased linearly up until about 1400 mm yr^{-1}, but showed a decreasing probability of occurrence for precipitation exceeding about 2000 mm yr^{-1}.

The model parameterisation allowed construction of productivity maps for New Zealand, showing highest productivity in the high rainfall regions of the North Island, reduced productivity in lower-rainfall east coast regions of both islands and cooler sites at high elevation and for most of the South Island, and unsuitable conditions for the upper mountain spine of the South Island.

In response to climate change, but with constant CO_2 concentration, little change was modelled for most of the North Island, except in the warmest and driest regions, where the model indicated slight reductions in productivity. For the South Island, productivity was generally modelled to increase owing to the beneficial effect of increasing temperature. Across the country and for different emissions scenarios, productivity was modelled to be increase by about 6% by 2040 and 9-11% by 2090.

When increasing CO_2 was also included, productivity was modelled to be enhanced across the whole country, with slight productivity increases for most of the North Island and more substantial increases for the South Island where the beneficial effects of increasing temperature combined with the beneficial effect of increasing CO_2 yielded the greatest productivity gains. On average across the country, productivity was modelled to increase by about 15-18% by 2040 and 24-37% by 2090.

Introduction

When agricultural land is abandoned in New Zealand, or when natural vegetation is disturbed by storms or landslides, it is often colonised by shrubland (Rogers & Leathwick, 1994; Stephens et al., 2005; Wilson, 1994) consisting of mānuka (*Leptospermum scoparium*) and/ or kanuka (*Kunzea ericoides*).

Shrubland growth rates were previously estimated by Trotter et al. (2005), but Trotter et al. (2005) provided only generic rates without any differentiation by environmental factors. Other growth rates for specific sites were reported by Scott et al. (2000), but provided no broad national coverage. Nor did these estimates allow any assessment of the interaction with stand age, weed competition or a breakdown between carbon accumulation in long-lived carbon pools like woody structures or in pools, like foliage that accumulate for only a few years before reaching a new equilibrium.

A key compilation of carbon accumulation in stands situated across New Zealand was provided by Payton et al. (2010). They provided detailed information from a large number of sites and attempted to model the environmental dependence of growth rate. However, because of limited coverage of sites with different environmental conditions, they were able to identify only precipitation as an important environmental constraint. In the present work, we aimed to build on the work that had been done in these papers and use a physiologically-based model to model the growth and carbon accumulation in kanuka/mānuka stands growing under different environmental conditions in New Zealand.

We considered three primary data sources:

1) Data compiled in a report by Payton et al. (2010) which summarised the growth of 40 stands of ages from 2 to 96 years. The stands were located throughout New Zealand at 35 distinct locations. This gave detailed information of site carbon storage, stand properties, such as stocking and sizes of individual trees. A weakness of the data set was its primary distribution within the main growing areas of kanuka/mānuka. It did not provide very good information on the extreme performance of kanuka/ mānuka at the margins of its distribution.
2) Data from 15 sites in three broad regions from the National Vegetation Survey. This information covered a wide range of temperatures and precipitation, but the sites were clustered in only four regions of the country. Information consisted of diameter increments of individually-tagged stems measured some years apart. A weakness of that data set is that it is not readily comparable to stand-level biomass increment, which is heavily affected by carbon losses from tree mortality.
3) Data on the observed distribution of kanuka/mānuka within New Zealand. That information was most valuable for defining parameters at the limits of the distribution of kanuka/mānuka.

The modelling in the end used data from the comprehensive data sets 1) and 3). NVS data were not used because of uncertainty about relating stem diameter increments to whole-stand biomass increments.

After completion of the description of kanuka/mānuka growth under current climatic conditions, we also aimed to assess the likely climate-change response of growth under three different emissions scenarios and for 2040 and 2090. These simulations were done with either constant CO_2, or with CO_2 concentrations increasing in line with that provided under different emissions scenarios.

Methods

Kanuka/mānuka distribution

To analyse the current distribution of kanuka/mānuka in New Zealand, we obtained the observed area of kanuka/mānuka in New Zealand at 0.05 degree resolution. For each location, the observed area was expressed as percentage cover (0-100%). As the actual distribution of kanuka/manuka would also be strongly affected by non-biophysical factors, such as agricultural land use, we recorded actual land use only up to a maximum fraction, such as 1%, and recorded any distribution at or above the defined threshold as the value of the threshold. That mainly turned the data of actual distribution into data that more resembled a data set of absence vs presence in a given area. For the data reported below, an occurrence threshold of 1% was used.

Data were then binned by temperature or precipitation intervals, with temperature intervals of 1°C. For precipitation, intervals of 100 mm yr^{-1} were used for precipitation up to 2000 mm yr^{-1} with the intervals gradually being increased for increasing precipitation amounts as the number of data points gradually diminished with increasing precipitation.

For each temperature and precipitation range, the data were then averaged to give the average distribution over the range of sites within given temperature and precipitation domains. That information is then reported as the probability of occurrence of kanuka/ mānuka within given environmental domains.

Model description

We used the process-based model CenW to model the productivity of kanuka/ mānuka stands in New Zealand. CenW has been used extensively to predict the growth of pine stands (Kirschbaum, 1999b; Kirschbaum & Watt, 2011) and native eucalypt forests in Australia (Kirschbaum et al., 2007). The model has also been used to derive a productivity surface for a generic forest cover for all of Australia (Roxburgh et al., 2004).

The simulations used version 4.0. The model and its source code are available at: http://www.kirschbaum.id.au/Welcome_Page.htm, with a full list of relevant equations available at http://www.kirschbaum.id.au/CenW_equations.pdf.

The model runs on a daily time step and simulates stand characteristics, such as leaf-area development, stand height, basal area development, litter fall and exchange of both water and CO_2. Stand-level dynamics are explicitly linked to carbon and nitrogen cycling in the soil and plants (Kirschbaum & Paul, 2002). This linkage allows multiple factors to constrain estimates of growth and carbon exchange of the stand at daily and longer time scales.

The model can be run over periods of many decades, which was necessary for the simulation of productivity of kanuka/mānuka stands with relevant growth periods of about 50 years and more. The model required a small set of daily climatic inputs as described below. The model also required an estimate of site fertility, soil water-holding capacity, silt and sand fraction as a measure of soil texture, initial stand stocking and a measure of the intensity of weed competition.

Model fitting

Predictions of different measures of growth were fitted to independent observations from 69 stands located at 52 distinct locations throughout New Zealand (Fig. 3.4.1). Different measures of growth were available from the different sites. Data set 1 (Payton et al., 2010)

consisted of measures of total stand biomass (including below-ground) at respective ages inferred from growth ring counts.

Data set 2 consisted of measured diameter increments of individually-tagged stems from the national vegetation survey (NVS). For the present work, it had been attempted to convert these individual-tree measures to a relative diameter increment to infer growth estimates under different environmental conditions throughout the country. However, it is not clear whether such a connection can readily be made, and after some initial attempts to include those observations, they were ultimately omitted.

Data set 3 gave the observational distribution of kanuka/ mānuka as a function of mean climatic conditions, which showed a strong and clear dependence of the probability of occurrence as a function of temperature and precipitation (see below). That information was used primarily to constrain the performance of kanuka/ mānuka at the extremes of its distribution for which there were few other data available.

Observations were available from sites with mean annual temperatures ranging from 8 to 15°C and with mean annual precipitation ranging from 700 to 3600 mm yr^{-1}, with the NVS data covering a wider range of environmental conditions than the Payton et al. (2010) data set. Overall, there were few observations available at the margins of apparent growth suitability which caused a strong reliance on the observed distribution for constraining parameters.

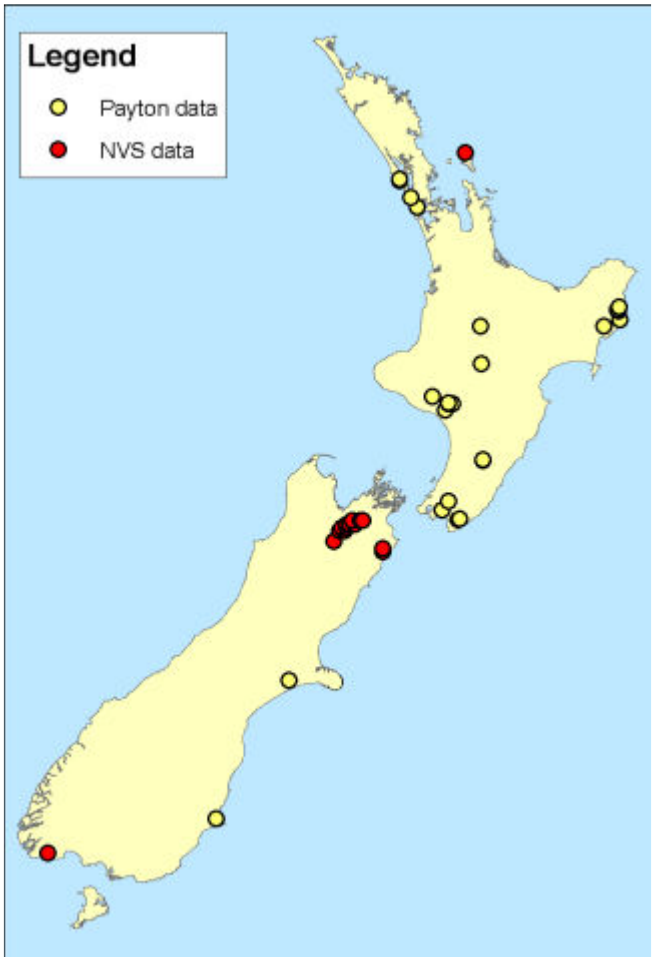

Figure 3.4.1. Location of the data in our observational data set.

The data set of Payton et al. (2010) covered a wide range of measurement ages (2–96 years) which provided useful information about the down-turn in growth rates as stands grew older.

It was assumed that all stands began with a high initial stand density that was greatly reduced through natural mortality. Growth was apparently inhibited by variable, but at some locations intense, weed competition in the early stages of growth, and by inherent age related growth reductions at later ages. Kanuka/ mānuka is an early succession stand type but given enough time, stands are typically replaced and outcompeted by other species, such as beech in wetter locations, and totara and matai forests at drier locations.

Initial parameter estimates were based on specific measurements where possible, and the earlier modelling work of Whitehead et al. (2004*b*) and Whitehead and Walcroft (2005). Wood density for kanuka was measured as 774.7 ± 11.7 kgDW m^{-3} by Burrows (2010) and 843 ± 41 kgDW m^{-3} by Burrows et al. (2009). We used an average wood density of 800 kgDW m^{-3}, with no dependence on age, stocking, fertility or temperature as no information was available about those factors.

We used a specific leaf area index of 9.1 ± 0.2 m^2 $kgDW^{-1}$ as measured by Burrows (2010). Other specific information on stand allometric properties was sourced from Scott et al. (2000) and leaf nitrogen concentrations from Ross et al. (2009). Parameter estimates were further modified in the present work to minimise the residual sums of squares between modelled and observed data. The range of parameter values was further constrained to remain within physiologically plausible bounds to retain the physiological integrity of the simulations.

Twenty years of daily weather input data was obtained from the Virtual Climate Station Network (VCSN) from NIWA (National Institute of Water and Atmospheric Research Ltd.). Daily VCSN data were estimated for the whole of New Zealand on a 0.05° latitude/longitude grid (Tait et al., 2006; Tait, 2008; Tait & Liley, 2009) as described by Kirschbaum & Watt (2011). For the present modelling work we used daily precipitation, maximum and minimum air temperatures, solar radiation and absolute vapour pressure (measured at 9 a.m.). Climate change simulations used the average temperature and rainfall anomalies from 12 Global Circulation Models forced with greenhouse gas emissions from three emissions scenarios (A1B, A2, B1). Further details are given by Kirschbaum et al. (2012).

The model was run with prescribed constant foliar nitrogen concentrations at each site. Nitrogen concentrations were set from a correlation with a national surface of soil nitrogen concentration (W.T. Baisden, pers. comm.), but best model parameterisation was achieved with a very weak dependence on that national data set. Soil water-holding capacity and the percentage of silt plus clay were obtained from the National Soils Database (Wilde et al., 2000). The model was run from seeding to the age at which the last observations were available from individual stands.

The key parameter values used in the model are given in Appendix C.

Statistical analysis

The accuracy and bias of the final fitted model was determined by calculating model efficiency. This statistic assesses not only the strength of the correlation between model and data, but also whether there is any consistent bias in the relationship. High model efficiency can only be achieved when model and data are strongly correlated and when there is little systematic bias in the model. Model efficiency, EF, was determined as (Nash & Sutcliffe, 1970):

$$\mathrm{EF} = 1 - \frac{\sum (y_o - y_m)^2}{\sum (y_o - \bar{y})^2} \qquad [3.4.1]$$

where y_o are the individual observations, y_m the corresponding modelled values and $\bar{y}$ the mean of all observations.

Sensitivity to climatic conditions

For each site within our data set, we undertook a climatic sensitivity analysis by simulating changes in total biomass accumulation across a wide range of air temperatures and precipitation. Temperature was varied by increasing or decreasing daily minimum and maximum temperatures by up to 10 °C. Absolute humidity was also adjusted to increase the dew point temperature by the same amount as the change in minimum and maximum temperatures. This alteration resulted in relative humidity remaining virtually constant. Precipitation was changed by varying daily total precipitation by between 10% and 300% of observed values, without changing the number of rain days. For investigating the effect of

both air temperature and precipitation, foliar nitrogen concentration was maintained at base values.

Results

The observational data set contained detailed stocking numbers and heights and diameters from a number of sites across the country. From that, it was possible to develop some general allometrics for kanuka/ mānuka stands (Figs. 3.4.2, 3.4.3).

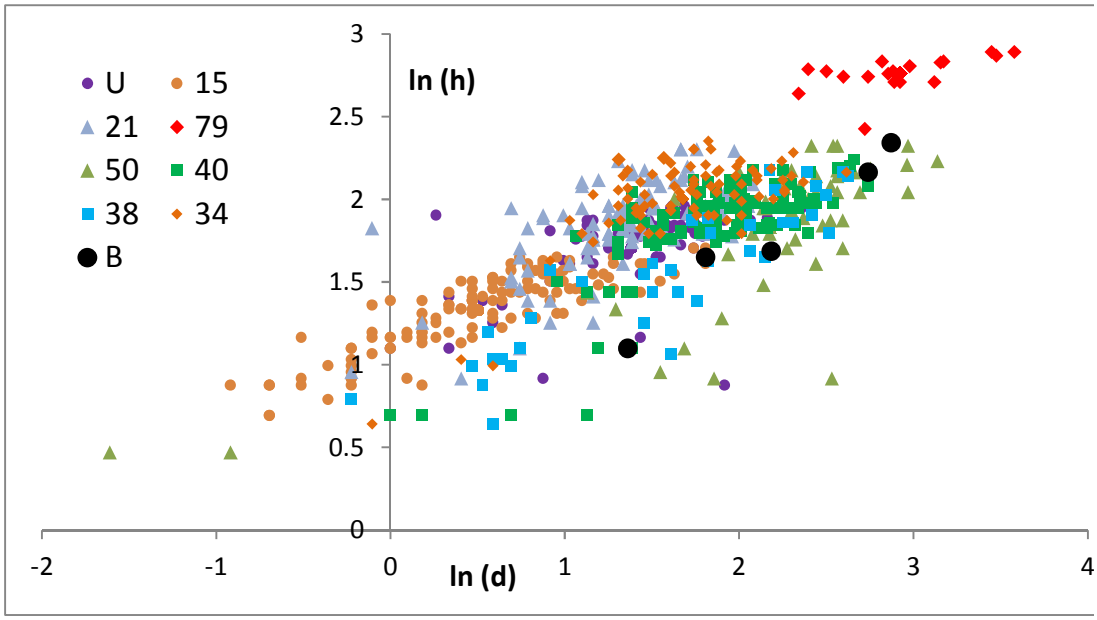

Figure 3.4.2. Plotting observed log-transformed height vs diameters. Different symbols refer to stands of different ages as indicated in the legend. Data marked 'U' are of unknown age and data marked 'B' are from data observed by Burrows et al. (2009) from stands at Hinewai station.

There is no obvious separation in the data apart from the 79-year old stand for which the observed range in diameters was accompanied by little change in height. However, in that stand, even the smallest diameter trees were much taller than the average of similarly-sized trees from the younger stands. It is therefore not clear whether the apparently different relationship between height and diameter in the oldest stand was related to its age or a function of some other peculiar property of that stand.

Comparing the national data set with the specific data from Hinewai as measured by Burrows et al. (2009) (marked "B") show quite a different slope, with the Hinewai data apparently starting at greater diameter for a given height, but obtaining greater height increment with further diameter increment than apparent in the national data set (Fig. 3.4.2). In order to obtain a national height-diameter relationship, we developed a relationship based on the national data set (Fig. 3.4.3).

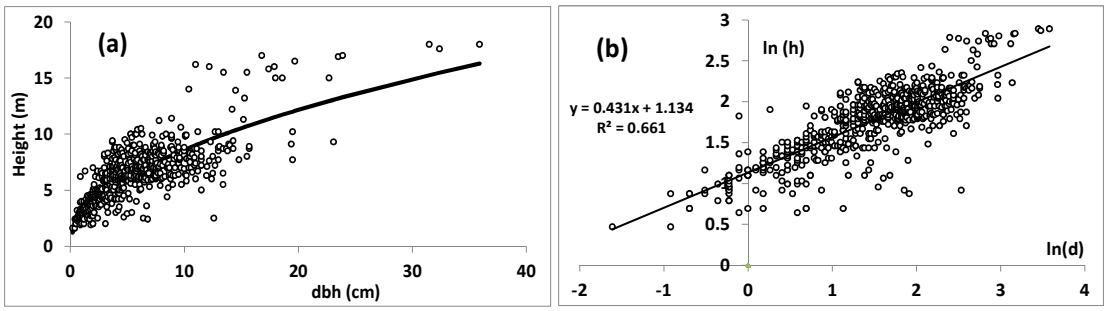

Figure 3.4.3. Observed height vs corresponding diameter for data from the national data set in normal units (a) and in log-transformed form (b). A linear relationship was fitted to all the data and is also shown in both graphs.

There was no obvious difference in the height-diameter relationship with differences in tree size and the same linear relationship fitted well across the range of tree sizes. The slope was, however, only 0.43, which is remarkably low, and led to tree sizes that did not exceed 18 metres even for trees with diameters that exceeded 35 cm. This relationship was then used for modelling all available data.

For 33 stands from the national data base (Payton et al., 2010), there was also available information on stocking and mean diameters (Fig. 3.4.4).

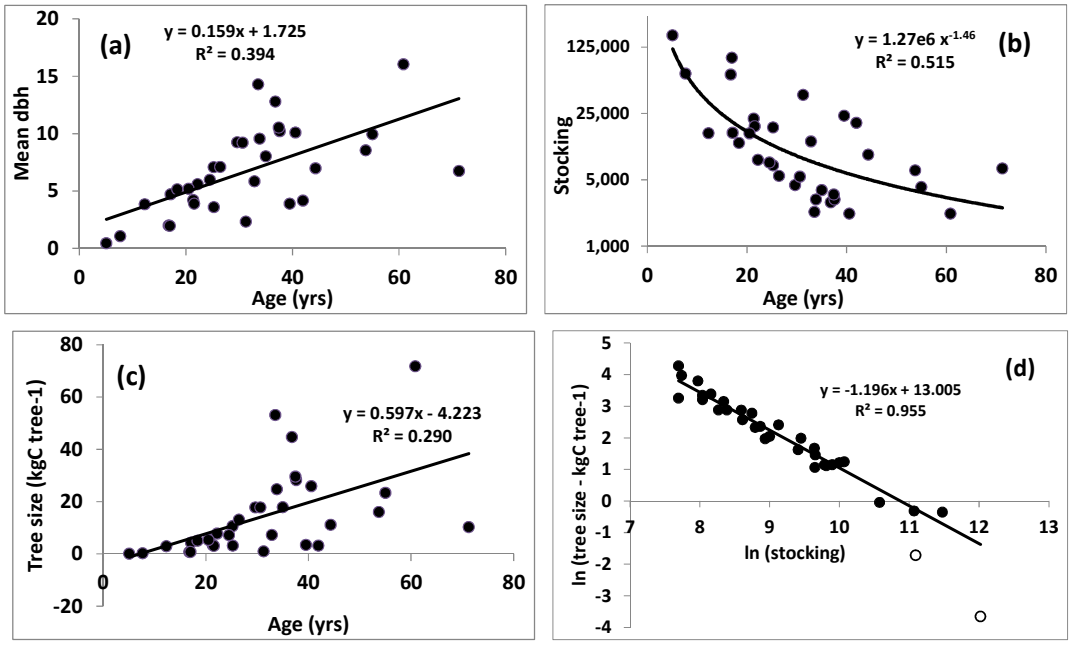

Figure 3.4.4. Stand properties from the national data base, showing dbh (a), stocking (b) and average tree sizes (c) as a function of the age of individual stands and the log of average tree size plotted against the log of stocking together with a linear relationship fitted to the data (d). The two stands indicated with open symbols were excluded from the fitting.

The national data base contained information on stands with a wide range of properties. Mean dbh ranged from 0.4 to 16 cm, generally increasing with age (Fig. 3.4.4a). Similarly, the average size of individual trees increased with age from 25 gC tree^{-1} in the youngest stand to 70 kgC tree^{-1} in one of the oldest stands (Fig. 3.4.4c). At the same time, stocking decreased from 166,000 individuals per hectare in the youngest stand to 2,200 individuals per hectare in some of the older stands (Fig. 3.4.4b).

These data coalesced into a very tight relationship of log-transformed size of individual trees vs stocking, giving a high R^2 = 0.955. Based on the two-halves self-thinning law, the slope of the relationship was expected to be -1.5 (Kirschbaum et al., 2007; Osawa & Allen, 1993). The much lower slope of -1.2 in the present data set probably reflects the very low slope of the height-diameter relationship (Fig. 3.4.3). The theoretical slope of -1.5 is predicated on a height-diameter relationship of 1.

Carbon gain in these stands is strongly affected by stand geometry together with stand mortality due to self-thinning to reduce stocking from more than 100,000 stems ha^{-1} during initial stand development to less than 2,500 stems ha^{-1} in mature stands. In some instances, initial stocking appears to be insufficient to achieve the potential stand carrying capacity for individuals (see the two open symbols in Fig. 3.4.4d). This could be due to the nearest stand being some distances away so that the available seed bank provides limiting conditions for initial seedling establishment.

In that case, seedlings could be expected to grow for some time without significant mortality until the size of individual trees corresponds to that given by the straight line in Fig. 3.4.4d. Mortality would then commence with some loss of living biomass and further stand development in terms of number of individuals and their average size would be expected to follow the straight line in Fig. 3.4.4d.

The comprehensive data set compiled by Payton et al. (2010), consists of estimated stand biomass from 52 stands from across the country and for ages from 2 to 96 years. The wide geographic spread of the observations and over the range of ages provided model constraints of both environmental factors and stand development with age. Data were also expressed as both live biomass and total carbon stocks (including dead trees and the developing litter layer).

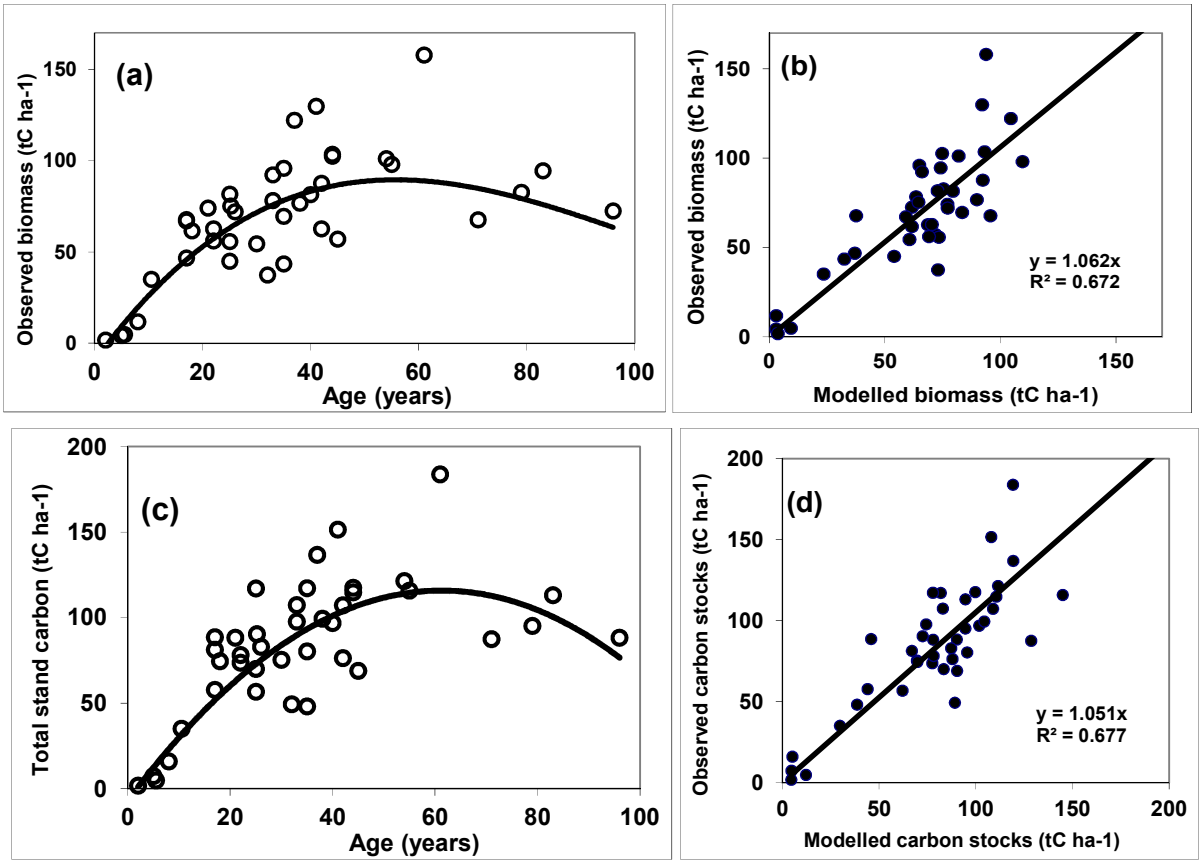

Figure 3.4.5. Observed and modelled total live biomass (a) and total stand carbon stocks (c) vs age for the national data set and observed vs modelled live biomass (b) and total stand carbon (d). The symbols in (a) and (c) show the observed data, and the lines in (a) and (c) are polynomials fitted to the modelled data. They are included to show how the modelled age pattern compares with the observed one. Data of observed vs modelled biomass are also shown with a line of best fit, forced through the origin. Model efficiencies were 0.654 and 0.664 for live biomass and total stand carbon, respectively. Data after Payton et al. (2010).

Figures 3.4.5a and 3.4.5c show that stands increase in size only for about the first 50 years, but growth then slowed and standing biomass appeared to even decrease. Kanuka/mānuka are generally pioneer species that invade abandoned grassland or sites otherwise devoid of tree vegetation. Once a closed canopy develops, kanuka growth can proceed rapidly for several decades (Fig. 3.4.5a), but stands then begin to senesce and longer-lived trees emerge from the canopy and eventually form a different stand of mature trees (Allen et al., 1992; Sullivan et al., 2007) capable of supporting a larger ultimate biomass.

That period of transition from a well-developed 50-year old kanuka/ mānuka stand to later-succession species can be characterised by several decades with no growth. The present simulations are essentially restricted to describing the early growth phase and are thus essentially limited to growth over the first 50 years, but for model parameterisation, the older stands from the Payton et al. (2010) data set were included as well.

The data in Figure 3.4.5 also make it possible to calculate rate of biomass and total stand carbon accumulation as a function of stand age (Fig. 3.4.6). Growth rate increases for the first few years of stand development, peaks for stand of about 15 years of age, and then gradually decreases for older stands. Average biomass growth rates (for the average of the sites for which data were available) reached a peak of about 2.7 tC ha^{-1} yr^{-1} at age 15, and the declined to a value of about 1.8 tC ha^{-1} yr^{-1} at age 50 (Fig. 3.4.6a).

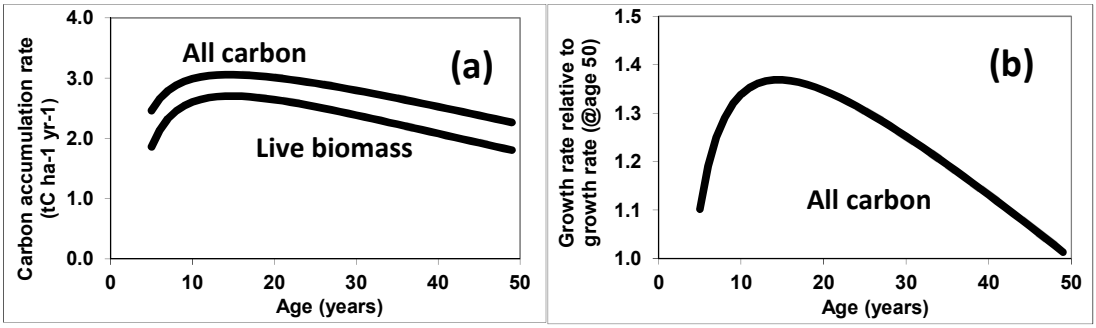

Figure 3.4.6. Derived carbon accumulation rates (a) based on the data in Figs. 3.4.5a and 3.4.5c, and the ratio of carbon accumulation rates relative to that of a 50-year old stand. The curves are given by:
$B = -9.86/a + 4.080 – 0.0504a + 165e\text{-}6a^2$
$C = -6.94/a + 4.014 – 0.0329a + 1.96e\text{-}6a^2$
where B is live biomass, C is total stand carbon, including litter and dead wood, and a is stand age in years.

Total carbon accumulation followed a similar time course, with a peak of about 3.1 tC ha^{-1} yr^{-1} at age 15 and a rate of 2.2 tC ha^{-1} yr^{-1} measured for 50-year old stands (Fig. 3.4.6a). That means that compared to the average carbon accumulation rate of 50-year old stands, growth rates are higher by about 25% for the first 30 years, and 37% for the first 15 years of growth (Fig. 3.4.6b). Growth and carbon accumulation rates shown in some the simulations presented below were obtained for 50-year old stands. They can be converted to the carbon accumulation rates of younger stands by applying the relationships given in Figure 3.4.6.

Model simulations included not only biomass growth and total carbon accumulation, but also stand properties such as the development of average stem diameters (Fig. 3.4.7). Overall, there was good agreement between observed and modelled data across the wide range of stand ages, sizes, stocking densities and environmental growth conditions.

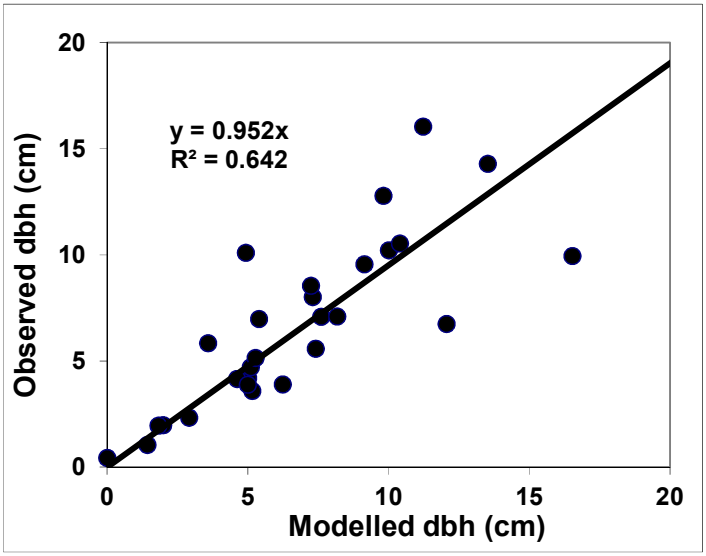

Figure 3.4.7. Observed vs modelled dbh from the national data set. Model efficiency was 0.632. Data after Payton et al. (2010).

Figure 3.4.8 shows growth rates for the stands depicted in Fig. 3.4.5 to more directly assess the effect of environmental conditions on growth and biomass accumulation. Very young stands were omitted in determining model efficiencies because the effect of weed competition could be of significant importance in those early years of stand development, and since no site-specific data on the extent of weed competition was available, growth rates for very young stands could not be obtained with high confidence.

Conversely, old stands were also excluded because the draw-down in the growth of old stands is not a fixed and unique stand property, but it involves interactions with the other plant communities that will eventually take over and start to dominate the stand in the longer term (Sullivan et al., 2007). These interactions are therefore likely to be site-specific and generic relationships could not be determined with high confidence. For stands of intermediate age, however, productivity is principally determined

by biophysical factors, with early weed competition fading into lesser significance, and later competitive interactions with emergent species not yet playing a major role.

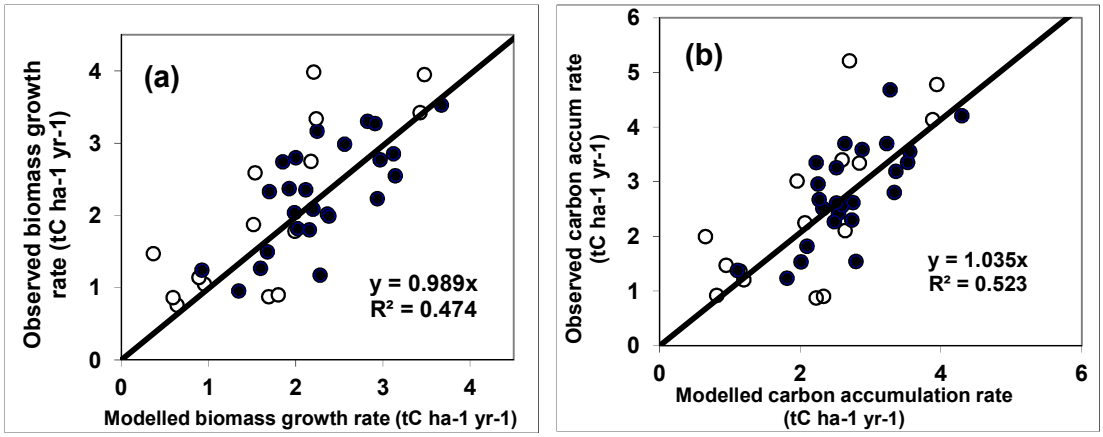

Figure 3.4.8. Observed vs modelled biomass growth and carbon accumulation rates. Data for stands between 20 and 50 years are shown as solid symbols and data from younger and older stands are shown as open symbols. The fitted line was fitted to the data from the restricted data set. Model efficiencies were 0.473 and 0.511 for rates of biomass and total carbon stocks, respectively. Data from Payton et al. (2010).

These data restricted to intermediate ages (solid symbols in Fig. 3.4.8) gave good agreement between modelled and observed data which indicated that most of the influence of environmental factors was captured by the model. It gave a range of productivities ranging from about 1 tC ha^{-1} yr^{-1} for the least to about 3.5 tC ha^{-1} yr^{-1} for the most productive sites (Fig. 3.4.8a). When the accumulation of dead plant material, especially dead stems, was also included, total carbon accumulation rates could be as high as 4.5 tC ha^{-1} yr^{-1} (Fig. 3.4.8b). Overall, the simulations show little systematic bias with lines of best fit having slopes close to 1.

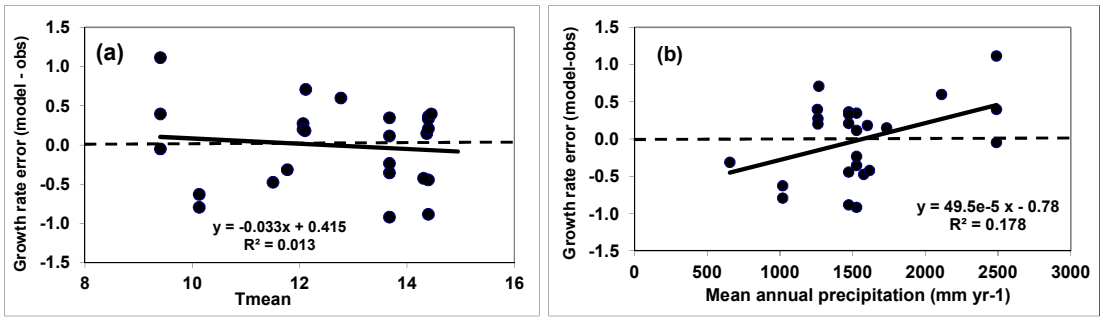

Figure 3.4.9. Differences between modelled and observed data plotted as a function of mean annual temperature (a) and mean annual precipitation (b) for the Payton et al. (2010) data set. Positive values mean that the model over-estimates rates.

The extent of remaining bias in the simulations is shown more explicitly in Figure 3.4.9, which shows the remaining difference between modelled and observed data expressed against mean annual temperatures (a) and mean annual precipitation (b).

With the fitted final fitted parameters, growth appeared to be overestimated for the coolest sites, but underestimated for the second-coolest sites (Fig. 3.4.9a). Overall, there was only a negligible trend of prediction bias as a function of temperature.

With respect to precipitation, growth at the high-rainfall site was significantly overestimated and underestimated for the site with lowest precipitation (Fig. 3.4.9b). Overall, the line of best fit suggested that there could be remaining scope for further improvement in parameter estimates, but specific work with any of the relevant parameters showed that it was not possible to further improve the response to temperature or precipitation without significantly compromising other aspects of the model fits. So, the existing parameter fits had to be accepted as the best set despite some remaining systematic biases.

The Payton et al. (2010) data set, however, had only observation between 9.5-14.5°C mean annual temperature and from 650 mm (one site) to 2500 mm yr^{-1} which was not sufficient to adequately describe the environmental response especially at the extremes of its distribution.

We addressed the problem of limited information about the performance at more extreme conditions by analysing the current distribution of kanuka/ mānuka in New Zealand which revealed the limits of its distribution in relation to extremes of temperature (Fig. 3.4.10) and precipitation (Fig. 3.4.11).

A 1% occurrence threshold was used for this analysis. This was done because for larger proportional coverage of an area anthropogenic factors play an increasingly important role. For a small threshold, physiological factors primarily determine whether the conditions are suitable for kanuka/mānuka or whether they are not.

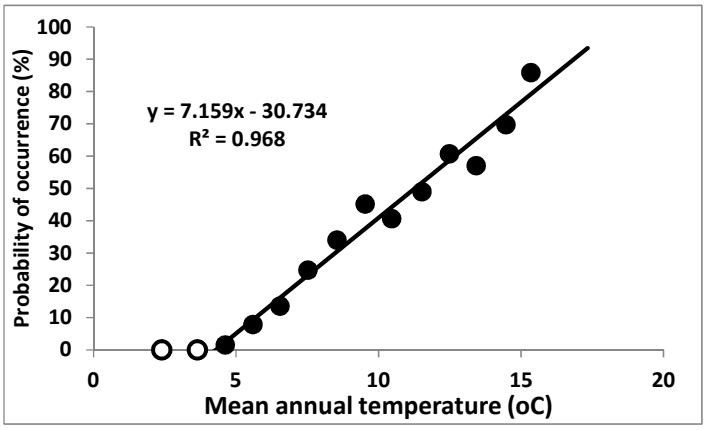

Figure 3.4.10. Observed probability of occurrence of kanuka/ mānuka in New Zealand as a function of mean annual temperature. These data have been calculated with an occurrence threshold of 1% which means that for any 0.05° location, any prevalence by greater than 1% of the actual area was recorded as 1%.

This analysis provided unexpectedly clear and consistent relationships, with R^2 of 97% of the dependence of distribution on temperature (Fig. 3.4.10). The data showed with remarkable consistency that kanuka/mānuka does not occur at all on sites with mean annual temperatures of 4°C or less (Fig. 3.4.10), and its probability of occurrence increases linearly from 4.5°C to 15.5°C, corresponding to the highest temperatures found in New Zealand (Fig. 3.4.10).

Similarly, kanuka/ mānuka is virtually absent on the few sites in New Zealand that receive less than 400 mm yr^{-1}, and its probability of occurrence increases linearly with increasing rainfall of up to about 1400 mm yr^{-1} , then has a slight plateau with high probability of occurrence from 1400-1800 mm yr^{-1}, and then its occurrence decreases again for further increases in precipitation, with a probability of occurrence of only about 10-20% for precipitation of 4000 mm yr^{-1} or more (Fig. 3.4.11). This relationship was also very tight in the low-precipitation range with R^2 = 0.96, while the dependence was less tight in the high-precipitation range, but still accounted for 88% of observed variation (Fig. 3.4.11)

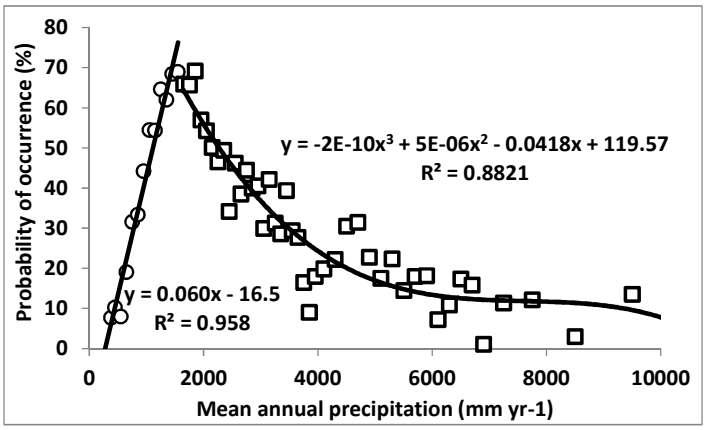

Figure 3.4.11. Observed probability of occurrence of kanuka/ mānuka in New Zealand as a function of mean annual precipitation. Different curves are drawn for the data up to 1550 mm yr^{-1}, and from 1650 mm yr^{-1} onwards.

Interpretation of the data in terms of growth responses is more difficult. Clearly, at temperatures below 5°C, kanuka/ mānuka does not occur at all, and its total absence from those environments can be equated with physiological unsuitability. Kanuka/mānuka clearly cannot tolerate conditions that correspond to annual mean temperatures below 5°C.

It is more difficult to relate the probability of occurrence with physiological parameters at temperatures and precipitation higher than these threshold values. The near-linear dependence of occurrence on environmental drivers is mediated through competitive interactions with other possibly competing vegetation types, and since competing vegetation would have a variety of responses to environmental conditions, the increasing occurrence of kanuka/mānuka with increasing temperature and precipitation (up to 1400 mm) must be indicative of improving stand-physiological performance over that range of conditions, but it would be too simplistic to infer a linear dependence of growth rates from the observation of a linear dependence of occurrence. The absolute thresholds of occurrence were therefore used as the primary constraining information that could be used for stand-level models of productivity.

With the set of best parameters, modelled stand growth over 50 years is then shown in response to variations in temperature, precipitation, soil fertility and weed competition in Figures 3.4.12-3.4.15.

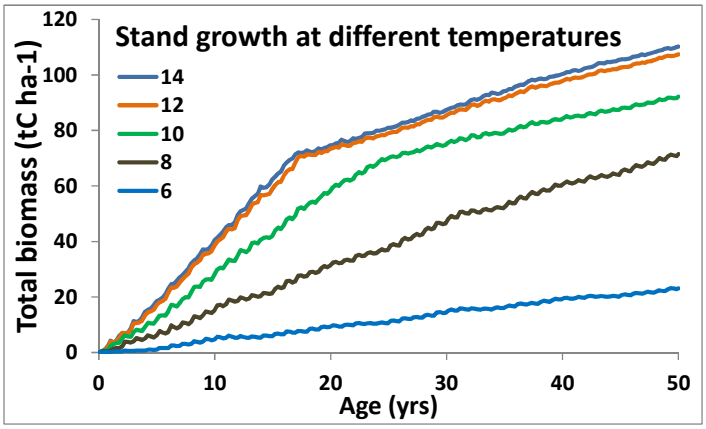

Figure 3.4.12. Modelled stand growth over 50 years for stands at different temperatures. The base conditions are those for a site in Manawatu, mean annual precipitation of 1318 mm yr-1, foliar nitrogen concentration of 10 g $kgDW^{-1}$ (cf. Fig. 13) and run with minimum initial weed competition (50 kgDW ha^{-1}). The numbers in The Figure give mean annual temperatures (°C).

Figure 3.4.12 shows modelled stand growth over 50 years, and the way that this is modified by temperature. At mean annual temperatures above 10°C, and with no weed competition, growth is relatively rapid over the first 10-15 years. Stand growth then slows down as individual trees reach critical sizes for the stand density at that time, and self-thinning commences (see Fig. 3.4.4d). The ensuing tree mortality greatly reduces subsequent net stand productivity. While stands continue to

fix similar amounts of carbon as before the commencement of mortality, the biomass of dying trees must be subtracted from live stand biomass as a whole, and with those on-going negative contributions, net stand increment is much reduced compared to stand dynamics before the commencement of self-thinning.

Dead stems still contribute to total stand carbon stocks with stand-level carbon stocks being substantially higher than carbon stocks in live biomass (Figs. 3.4.5). Self-thinning rather than photosynthetic carbon gain is probably the principal reason for stand increment of kanuka/mānuka to be substantially lower than that of pine forests in New Zealand (Kirschbaum & Watt, 2011). Self-thinning clearly plays an important role in kanuka/mānuka stands as observed stand density tends to decrease strongly with increasing age (Fig. 3.4.4b), with the self-thinning relationship described consistently and well with the self-thinning law, albeit with modified parameters (Fig. 3.4.4d).

The only uncertainty with respect to carbon losses during self-thinning relates to the average size of dying trees relative to the size of surviving ones. The available data set provided only indirect information with respect to that question. If the average size of dying trees is less than assumed in the present parameterisation, then associated carbon losses would also be reduced, or, conversely, carbon losses could be even greater if dying trees are even bigger than was assumed.

The ultimate parameterisation also suggests that growth is likely to be sensitive to low temperatures, hence the absence of kanuka/ mānuka in cold mountainous regions and the much greater abundance at warmer sites (Fig. 3.4.10). Growth differences are likely to be most pronounced over the early growth phase before self-thinning commences as self-thinning produces a self-correction, with faster-growing stands likely to lose a larger proportion of their biomass than those with slower growth for which the on-set of self-thinning is delayed so that stand differences diminish.

The parameterisation also suggests that the growth of kanuka/ mānuka would be sensitive to water stress, with growth reductions likely as precipitation falls below 1000 mm yr^{-1} (Fig. 3.4.13). This is consistent with the compilation of Payton et al. (2010), who highlighted water limitations as the principal identified limitation for kanuka/mānuka productivity in New Zealand.

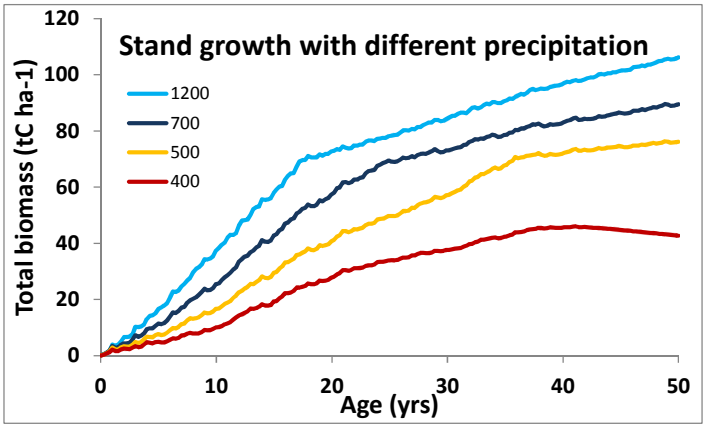

Figure 3.4.13. Modelled stand growth over 50 years for stands with different precipitation as indicated in the Figure (mm yr^{-1}). Other than precipitation, growth conditions were the same as listed in the Legend of Fig. 3.4.11, with annual mean temperature of 12.1°C.

It is also consistent with the virtual absence of kanuka/mānuka from New Zealand's driest sites (Fig. 3.4.11) that receive annual rainfall of just under 400 mm yr^{-1}. Water limitations are further amplified by low soil water holding capacity, weed competition (as alternative user of scarce water resources) and higher temperatures as evaporative losses increase with increasing temperature.

The response to site fertility is shown in Figure 3.4.14. Fertility for all sites was estimated from a national surface of soil nitrogen concentrations, but the best parameterisation tended towards negligible discrimination of fertility levels based on that national surface, which probably indicates that existing nutrient limitations are poorly described by the available nitrogen surface. A national surface is also available only for nitrogen, but it is likely that many sites will be limited by phosphorus rather than nitrogen.

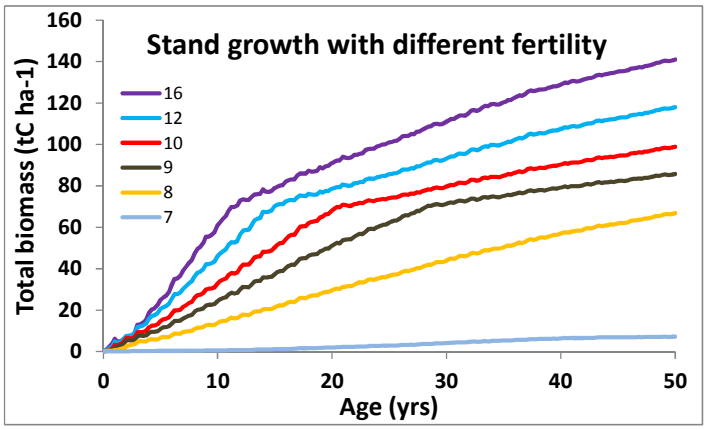

Figure 3.4.14. Modelled stand growth over 50 years for stands with different fertility in g kgDW^{-1} as indicated in the Figure. Other than fertility, growth conditions were the same as stated in the Legends of Figs. 3.4.12 and 3.4.13.

It is likely, however, that most sites were moderately nutrient limited, and that growth of most stands could be enhanced if fertility were higher. There are other possible limitations not included in the present simulations, such as growth in water-logged soils, sandy, rocky or ultramafic (toxic) soils identified by Payton et al. (2010).

The other important biotic factor reducing early productivity is weed competition (Allen et al., 1992), which could be identified at some sites as a likely cause of early growth inhibition. The national data base could be modelled with only a minor weed contribution (initial weed dry weight of 75 kgDW ha^{-1}). As no site-specific measurements of weed competition were available, it was not possible to distinguish between low growth in particular young stands being due to intense weed competition or due to unidentified adverse environmental conditions.

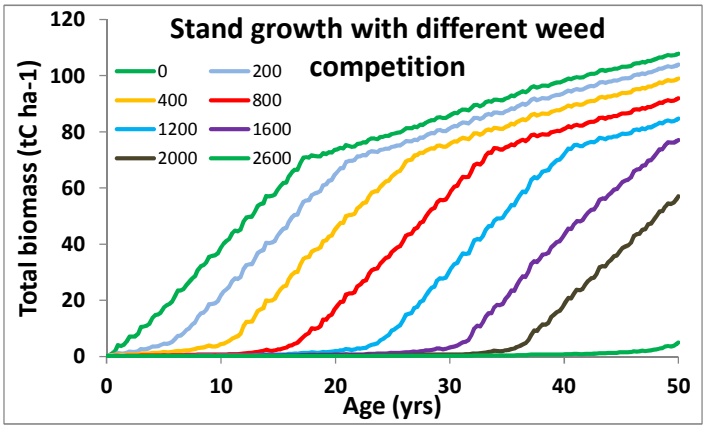

Figure 3.4.15. Modelled stand growth over 50 years for stands with different initial weed competition. Numbers in the Figure refer to the amounts of weeds initially present in kg ha^{-1} at stand establishment. Other than for weed competition, growth conditions are the same as stated in the Legends of Figs. 12 and 13.

Weed competition is also parameterised through a number of factors, such as maximum weed height and initial weed leaf area and others. All these are likely to differ between sites, with low-stature grass being the dominant competitive species at one site and taller gorse or broom being more important at another. Again, in the absence of site specific information, the same parameters had to be used throughout the country.

The effect of weed competition is seen in Figure 3.4.15 as a delay in initial establishment of kanuka/mānuka. When kanuka/ mānuka finally breaks through the weed layer and can establish its own dominant canopy to overtop and out-shade weeds, growth proceeds at a similar rate (near parallel lines in Fig. 3.4.15). Weed competition, therefore, becomes progressively less important as one considers longer time periods, but it provides a critical growth control over the first few years, or for up to several decades for intense weed competition (Fig. 3.4.15). Very intense and vigorous weed growth can even prevent the establishment of kanuka/mānuka indefinitely.

The response to environmental variables is more directly shown in Figure 3.4.16, which shows normalised modelled growth rates in response to variations in temperature by up to 10°C.

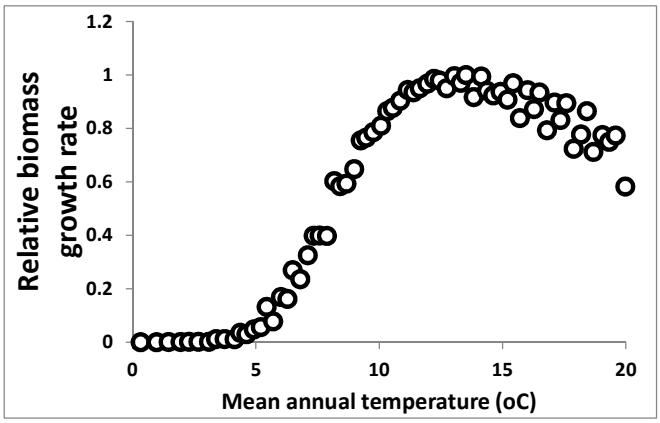

Figure 3.4.16. Average modelled biomass growth rates as a function of temperature. Simulations were done for each distinct location from the Payton et al. (2010) and NVS data sets. For each location, simulations were done at the observed climatic conditions, and with temperature increased or decreased by up to 10°C. Data were then expressed for each site relative to the highest modelled growth rate at optimal temperature, and all data were then combined and sorted by temperature. They are expressed here as average values for ten consecutive observations.

The simulations indicate that temperature is close to optimal at most of the observational sites from the Payton et al. (2010) data set, which had observations ranging from about 9-14.5°C (cf. Figs. 3.4.10, 3.4.16). The inferred temperature response function therefore relied heavily on the observed distribution of kanuka/ mānuka (Fig. 3.4.10) which indicated that kanuka/mānuka cannot grow at annual mean temperatures below about 4 degrees, and its likelihood of occurrence as an indicator of its growth performance increases strongly with temperature. The modelled growth rates closely mirror the observed distribution of kanuka/mānuka (cf. Fig. 3.4.10, 3.4.16).

CenW has two principal controls on the temperature response of stands, one that directly relates growth to mean daytime temperature, and one that scales back growth as a function of frost damage, and is thus more closely related to minimum temperatures. The final combination of parameters that gave the best fit to the observational data indicated a relatively strong importance of frost damage, but that particular controlling factor setting the temperature response was poorly constrained by the available observations.

The work of Greer et al. (1991) and Greer & Robinson (1995) suggests that the extent of frost damage might have possibly been overestimated in the present study. On the other hand, the measure of frost damage used by Greer et al. (1991) and Greer & Robinson (1995) might also have been too insensitive to fully account for the full extent of subtler frost damage that might have reduced photosynthetic rates without leaving lasting visual marks so that the question of the exact factors responsible for low-temperature growth reductions is still unresolved. If more information on the temperature response of specific stands, or more growth information from stands at lower temperature became available, it would become possible to better confirm whether the strong temperature response was indeed driven primarily by frost sensitivity or a daytime response to temperature.

As it was modelled, optimum temperatures were in the range from 12-15°C, with no observational sites that would have constrained the temperature range at its upper temperature range. The distributional data (Fig. 3.4.10) indicate maximum distribution at 15°, the highest mean annual temperature observed in New Zealand, but it is uncertain how well kanuka/mānuka would perform at even higher temperatures. Kanuka (Kirschbaum & Williams, 1991) and mānuka stands (Stephens et al., 2005) occur in Australia as well, including at higher temperatures than its natural occurrence in New Zealand, but there is not enough available information about its performance at those higher temperatures in Australia to have included that in the parameterisation for New Zealand.

The model runs indicate a broad precipitation optimum from about 1000-2500 mm annual precipitation (Fig. 3.4.17), but only a single site within the observational data set clearly fell into the low-precipitation range (Fig. 3.4.10b) and could be used to constrain the

parameterisation of stand responses to water limitations. The observed probability of occurrence (Fig. 3.4.11) was therefore used to add further important constraints to the parameterisation under driest conditions, and the modelled productivity (Fig. 3.4.17) approximately corresponds to the observed probability of occurrence (Fig. 3.4.11).

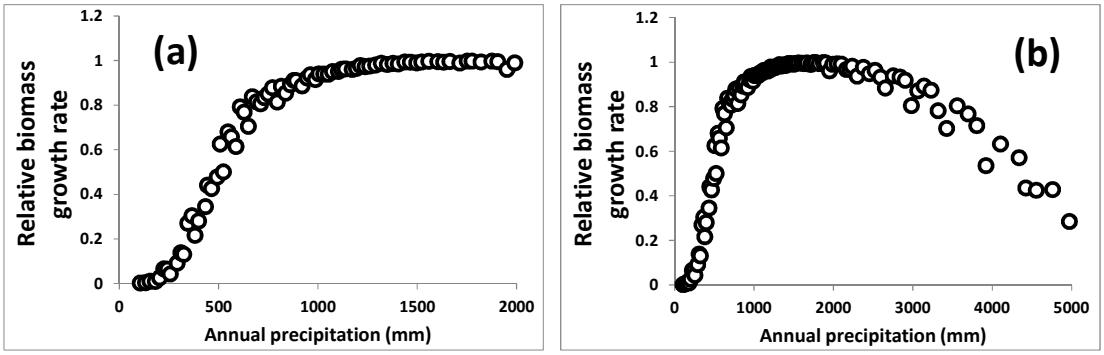

Figure 3.4.17. Average modelled biomass growth rates as a function of annual precipitation, shown for 0-2000 mm annual precipitation in (a) and over a wider range of up to 5000 mm in (b). Data and modelling conditions as for Fig. 3.4.16, except that precipitation rather than temperature was the variable being modified.

The simulations indicated additional growth inhibition at sites with excessive rainfall, beginning at about 2000-2500 mm yr^{-1}. This was consistent with observations of reduced productivity at some high-rainfall sites, by reports of water-logging sensitivity of mānuka, and by the reduced probability of occurrence at higher precipitation (Fig. 3.4.11). The probability of occurrence (Fig. 3.4.11) falls off more sharply at higher precipitation than modelled productivity (Fig. 3.4.17), which is likely to be related to additional competitive pressure from high-rainfall adapted species and due to a paucity of disturbed sites. Much of the high-rainfall region in New Zealand is contained within largely undisturbed national parks that provide limited opportunities for kanuka/mānuka to establish as it is primarily a pioneer community that establishes on newly disturbed sites, following fire, landslides or land abandonment.

Combining the final data parameter set with soils and climatic information for New Zealand, it became possible to model the growth of kanuka/mānuka for the country as a whole (Fig. 3.4.18). This is shown both a live biomass growth, averaged over the first 25 years of stands, and as total carbon accumulation of stands. Total carbon accumulation includes the accumulation of dead stems, in particular, that constitute an important carbon pools in stands subject to significant tree mortality as a result of self-thinning.

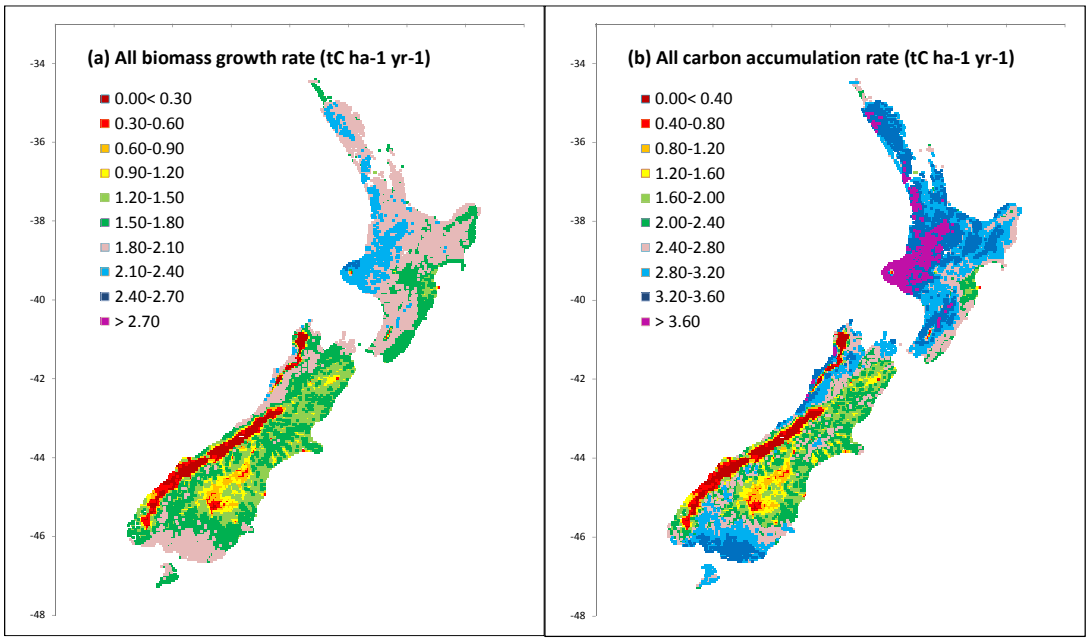

Figure 3.4.18. Modelled growth rates of kanuka/ mānuka stands over 50 years for New Zealand, shown as total biomass growth rate (a) and the rate of total stand carbon accumulations (b).

Across New Zealand, growth was modelled to be high across the western half of the North Island, with live-biomass productivity of about 3 tC ha^{-1} yr^{-1}, or 4.5 tC ha^{-1} yr^{-1} when carbon accumulation in dead biomass was also included (Fig. 3.4.18). Growth potential is much reduced in drier regions, especially Canterbury and Otago and, to a lesser extent, in Hawke's Bay. The growth potential is also much reduced in cooler locations, like most of the South Island, especially in the higher mountainous regions. Southland also has a reasonable growth potential of about 2.5-3.0 tC ha^{-1} yr^{-1} for living biomass and 3.5-4.5 tC ha^{-1} yr^{-1} with the inclusion of litter and dead plant material.

With the full parameterisation of the model and its mechanistic basis, it was then also possible to simulate the effect of climate change on productivity. These simulations were done first with keeping CO_2 concentrations constant at 1990 values to assess the effect of climatic changes other than CO_2 concentration. This was followed by simulations with the same climatic changes as before, but also changing CO_2 concentrations in line with concentrations expected under different emission scenarios.

In principle, it is possible to have reasonably high confidence in modelled climate-change responses to temperature and precipitation because the model has been parameterised against observations across a similar range of conditions as those anticipated in future. In the present work, our confidence in the reliability of this parameterisation was somewhat limited, however, by the rather narrow range of climatic conditions over which detailed observations were available.

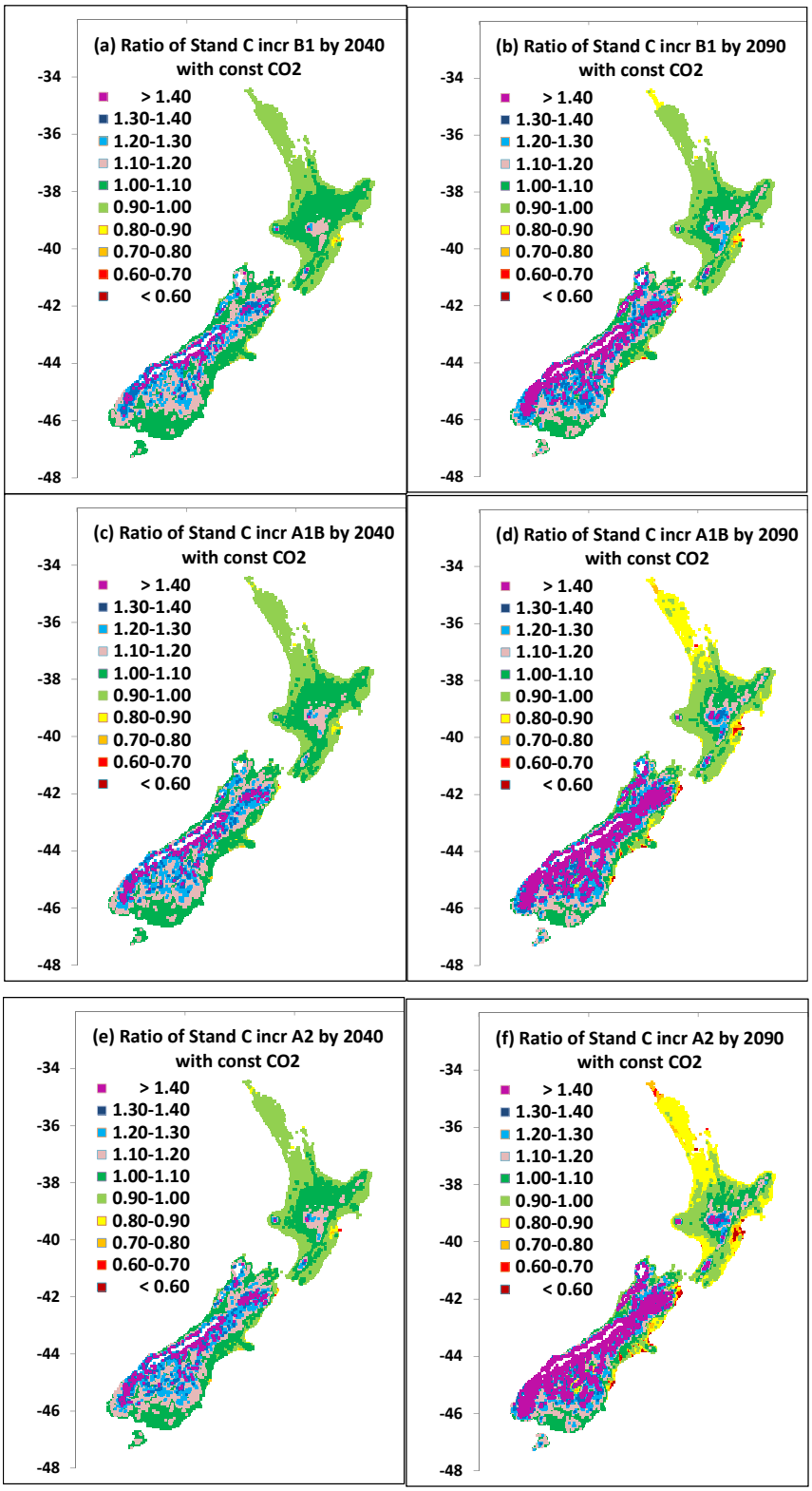

Figure 3.4.19. Modelled climate change response of carbon accumulation rates of kanuka/mānuka stands under constant CO_2 for 2040 and 2090 under three representative emission scenarios. Sites shown in white had current biomass production rates of less than 0.2 tC ha^{-1} yr^{-1} so that productivity ratios are not very meaningful.

This was supplemented by using information about the observed distribution of kanuka/mānuka, but even that information was limited to the range of climatic conditions observed within New Zealand, and the distribution of kanuka/mānuka was highest at the highest temperatures found in New Zealand. It is, therefore not known whether those highest

temperatures correspond to the temperature optimum, or whether even higher temperatures might be even more beneficial for kanuka/mānuka.

Figure 3.4.19 shows anticipated productivity changes for 2040 (left panels) and 2090 (right panels) under three different emission scenarios as shown in the Figure. All productivity estimates are expressed relative to simulated productivity in 1990.

Overall, productivity is expected to increase slightly for most of the North Island except the far north, where temperatures are expected to become supra-optimal, and where water stress may become more prevalent with greater evaporative demand under higher temperature. This will reduce productivity unless increased evaporative demand can be matched by increased precipitation.

		1990	**2040**			**2090**		
			B1	**A1B**	**A2**	**B1**	**A1B**	**A2**
Const. CO_2	Biomass growth rate (tC ha^{-1} yr^{-1})	1.53	1.59	1.61	1.60	1.62	1.63	1.63
	Change (%)		4.0	4.7	4.6	5.8	6.4	6.3
Incr. CO_2	Biomass growth rate (tC ha^{-1} yr^{-1})	n/a	1.74	1.78	1.78	1.83	1.96	2.04
	Change (%)		13.2	16.0	15.9	19.3	27.9	32.8
Const. CO_2	Carbon accumul. rate (tC ha^{-1} yr^{-1})	2.37	2.47	2.49	2.48	2.51	2.50	2.48
	Change (%)		4.1	4.8	4.6	5.7	5.4	4.4
Incr. CO_2	Carbon accumul. rate (tC ha^{-1} yr^{-1})	n/a	2.79	2.88	2.87	2.97	3.21	3.34
	Change (%)		17.6	21.4	21.1	25.1	35.5	40.9

Table 3.4.1. Modelled climate change response of biomass growth rates and total stand carbon accumulation of kanuka/ mānuka stands for 2040 and 2090 under three representative emission scenarios and with either constant or increasing CO_2 concentration. Shown are mean productivity over 50 years for New Zealand as a whole as the mean over all 0.05° locations being modelled. This was simulated for 1990 and for 2040 and 2090 under three different emissions scenarios. Each simulated mean future productivity is also expressed as the percentage change from 1990. Percentage changes were based on productivity estimates given with higher resolution than is shown in the Table.

Productivity is expected to increase more in cooler regions, such as for most of the South Island and sites at higher-elevation regions of both islands. These patterns are likely to intensify somewhat between 2040 and 2090. For New Zealand as a whole, productivity is expected to increase by about 6% by 2040 and 9-11% by 2090, with little difference between the different emission scenarios (Table 3.4.1)

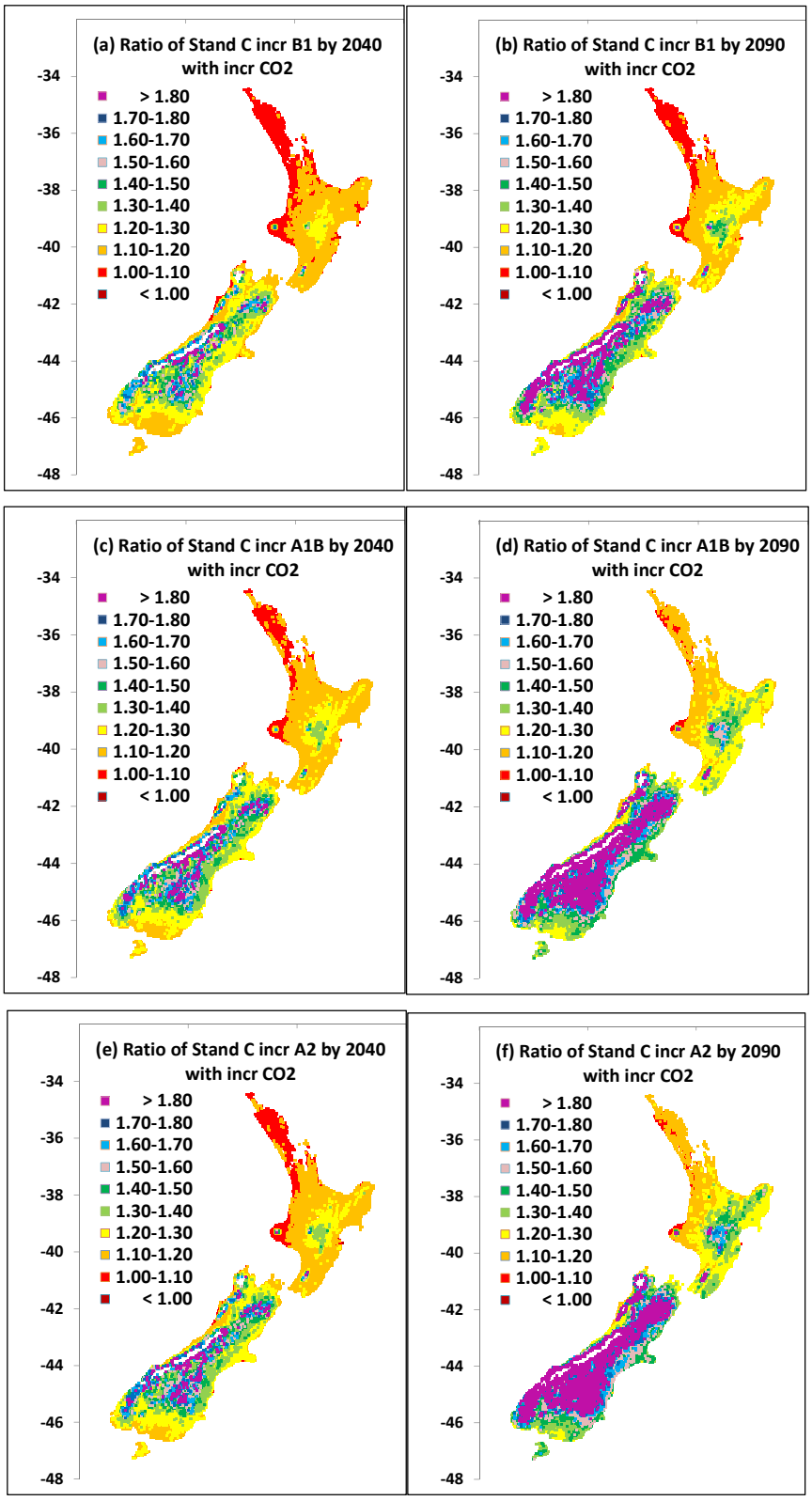

Figure 3.4.20. Modelled climate change response of carbon accumulation rates of kanuka/ mānuka stands with increasing CO_2 for 2040 and 2090 under three representative emission scenarios. Sites shown in white had current biomass production rates of less than 0.2 tC ha^{-1} yr^{-1} so that productivity ratios are not very meaningful.

Figure 3.4.20 shows simulations run with increasing CO_2 concentration in line with concentration estimates under the different emissions scenarios. Other than the changing CO_2 concentration, simulation details and the lay-out of the Figures is the same as for Figure 3.4.19.

With the inclusion of increasing CO_2, productivity, changes become positive for all of New Zealand, even for Northland and the drier east coast, where the beneficial effect of increasing CO_2 negated the negative effect of supra-optimal temperatures. For the North Island, beneficial effects were, however, largely restricted to increases in productivity by less than 10% by 2040, and between 10-20% by 2090.

For the South Island, there are likely to be more substantial positive productivity changes, with the effect of elevated CO_2 adding to the beneficial effect of temperature increases that are expected to over-come the low-temperature limitations that currently restricts productivity for most of the South Island. Southland stands out somewhat as benefitting less from climatic changes because growth conditions in Southland are already quite favourable (cf. Fig. 3.4.18).

For New Zealand as a whole, productivity is expected to increase under the influence of climatic changes (Table 3.4.1), which is expected to be enhanced further if increasing CO_2 is also included. With all factors included, productivity was modelled to increase under the different scenarios by 15-18% by 2040, and by 24-37% by 2090 (Table 3.4.1).

Discussion

The modelling of the growth and carbon balance of kanuka/mānuka presented unique modelling challenges. Stand growth of kanuka/mānuka appeared to be controlled by a combination of plant physiological factors, to a variable extent by weed competition (Smale, 1994; Smale et al., 1997), and the on-set of maturity-related slow-down in stand growth and replacement of pioneer stands of kanuka/ mānuka with later-succession species.

None of these factors are fully understood nor tightly constrained through the available observational data. Kanuka/mānuka grows as a pioneer community that typically gets established after some kind of disturbance, either natural, such as fire or land-slide, or anthropogenic, such as abandonment of marginal grazing land (Sullivan et al., 2007; Wilson, 1994). Patterns of establishment are therefore likely to vary widely with the type of disturbance, nature of previous vegetation, if any, and the density of kanuka/mānuka seed availability that determines the density of early establishment (Allen et al., 1992).

Details of early establishment, and the extent of weed competition, are not generally known for specific sites. Poor growth at a time of observation, for example, could, therefore, in principle, be due to intense early weed competition or a growth response to unfavourable environmental conditions. As the simulations showed (Fig. 3.4.15), different intensities of weed competition can greatly affect the early establishment of kanuka/mānuka and affect the growth of stands for up to several decades.

The bulk of available observations also covered only a narrow environmental range, with most observations derived from the central distribution of kanuka/mānuka with favourable growing conditions (Figs. 3.4.16, 3.4.17) so that these observations provided little information about the effects of temperature and precipitation at the more extreme ends of the distribution of kanuka/manuka. The NVS data provided observations across a wider range of environmental conditions, but uncertainties about interpretation of the measurements of individual-stem increments (as recorded in the NVS data set) to whole stand biomass increments, precluded use of this data set.

We therefore used information on the observed distribution of kanuka/mānuka as a function of temperature and precipitation (Figs. 3.4.10, 3.4.11) as additional constraints defining the

physiological limits of the growth of kanuka/mānuka. This analysis provided unexpectedly clear and consistent relationships, with R^2 of 0.97 for the dependence of distribution on temperature (Fig. 3.4.10) and R^2 = 0.96 for the dependence on precipitation in the low-precipitation range and R^2 = 0.88 in the high-precipitation range (Fig. 3.4.11). Leathwick and Rogers (1996) had also identified temperature and precipitations as key drivers of succession and added distance from intact forest, topography, slope and aspect as additional important drivers at local scales.

It is remarkable that such high R^2 values could be found given that there must be unaccounted other factors that also affect the distribution, with land-use patterns the most important amongst them. However, probability of occurrence cannot be directly related to physiological performance of stands other than in determining the absolute margins of physiological tolerance. Nonetheless, while the physiological characteristics of potentially competing population types is likely to follow different patterns, the only consistent factors driving the success of kanuka/mānuka stands across different environmental domains are its own physiological characteristics, and to explain a steep linear dependence on temperature and precipitation has to require some strong dependence of physiologically determined growth rate across the same range of conditions. This inferred dependence was, therefore, included as an additional constraint in the parameter fitting.

Detailed analysis of the original growth observations also revealed some unusual growth patterns in kanuka/mānuka stands, with little height growth as stands developed, but large on-going diameter increments (Figs 3.4.2, 3.4.3). This also led to an unusually shallow slope in the self-thinning relationship (-1.2 instead of the more typically observed -1.5), but all stands despite their enormous variability (Figs. 3.4.4a-4c) conformed tightly to the developed self-thinning relationship (Fig. 3.4.4d).

The intense self-thinning also has an important corollary for stand productivity. Stands typically start with high stand densities of tens of thousands or even more than 100,000 stems per hectare (Fig. 3.4.4a), which progressively diminishes as stands grow older and taller. But dying stands inevitably cause a loss of standing live biomass, thus create an important drain on site carbon balances. The number of trees dying is tightly controlled by the average growth of trees in the stand and the parameters of the self-thinning relationship, but for assessing the effects on carbon balances, it is also important to know how large dying trees are compared to the average size of trees in the stand. Limited information (data not shown) suggests that dying trees are typically of similar size as surviving trees, which would lead to large on-going carbon losses, but insufficient information has been available to tightly constrain that relationship. However, that would be an important facet for quantifying the effect of self-thinning on carbon balances.

Overall, despite a range of problems and some uncertain key relationships, it was possible to adequately describe the growth of stands from the Payton et al. (2010) national data base (Figs. 3.4.5-3.4.8). Mean growth rates derived for optimal growth conditions are slightly higher than values reported by Trotter et al. (2005), who reported carbon accumulation rates of 1.9-2.5 tC ha^{-1} yr^{-1}, whereas we found growth to be more variable, with rates of 1.0 to 3.5 tC ha^{-1} yr^{-1} across a range of different sites (Fig. 3.4.8a), although the national average growth rate of 2.2 tC ha^{-1} yr^{-1} is similar to that reported by Trotter et al. (2005).

The findings of the present work are similar to those of Payton et al. (2010), who derived similar growth estimates and a similar slow-down in growth rate with stand age. Our findings differ from those of Payton et al. (2010) in that our findings assign greater importance to temperature as a rate limiting factor. Those two aspects were very poorly constrained through the existing growth observations in the Payton et al. (2010) data set as that data set contained too few observations in that critical range of environmental conditions. Instead, our parameter estimation relied heavily on the distributional data of kanuka/mānuka throughout New Zealand. These data provided some clear and consistent trends with temperature, in

particular, but the nature of the underlying measurements needs to be borne in mind in interpreting the certainty of these findings.

Applying these constraints to New Zealand as a whole showed high growth rates in warm regions with regular precipitation (eastern North Island), and lower growth rates where either temperatures are too low (South Island), or where water availability limits productivity (east coast of both islands and central South Island). Comparing overall growth rates and regional patterns with those found for *P. radiata* (Kirschbaum & Watt, 2011) showed similar regional patterns for both stand types, but growth rates for *P. radiata* that were about three times those for kanuka/mānuka.

The lower growth rate of kanuka/mānuka reflected nutrient limitations and the carbon drain from self-thinning. In *P. radiata*, self-thinning is prevented by silvicultural thinning that maintain stand density below those critical thresholds when spontaneous mortality would commence. Productivity in kanuka/mānuka could probably be enhanced if stands were thinned to optimal spacings, but that management option is restricted by also having to maintain sufficient plant densities to maintain a closed canopy and suppress weed competition. The absence of economic returns from wood sales further prevent the economic viability of costly silvicultural intervention unless carbon credits can create sufficient economic returns in future.

Considering the growth potential of kanuka/mānuka stands into the future, the simulations showed little cause for concern (Table 3.4.1). Kanuka/mānuka appears to be strongly limited by temperature at present, with a positive response to temperature across the range of temperatures currently found in New Zealand (Fig. 3.4.10). It is, therefore, likely that stands will also respond positively to any temperature increases from climate change. Responses to precipitation are more complicated as plants are unlikely to respond to rainfall itself, but to water availability, instead. While precipitation is the principal determinant of water availability, the relationship between precipitation and water availability is also affected by temperature, with more precipitation needed at higher temperatures to maintain the same level of water limitation. With climate change, it is, therefore, possible for water limitations to develop due to warming even if precipitation does not change.

Simulations that included all these factors (but maintained constant CO_2) suggested slight decreases in productivity across most of the North Island and slightly greater increases in productivity for most of the South Island, especially at higher elevation (Fig. 3.4.19), with a slight increase in average productivity for the country as a whole (Table 3.4.1). These patterns intensified from 2040 to 2090, with relatively little difference between the different emissions scenarios. The most positive changes were observed for the coldest sites in New Zealand, and the most negative changes for the water-limited regions in far parts of Northland and for the drier east coast (Fig. 3.4.19).

When increasing CO_2 was also included, responses became positive for nearly all sites, in particular, turning the negative changes for warm and dry regions into gains as well (Fig. 3.4.20) because of the strong effect of increasing CO_2 in increasing water use efficiency. In other regions, the positive effect of increasing CO_2 combined with the beneficial effect of increasing temperature to lead to significant overall growth responses of 24-37% for 2090 compared to 1990 growth rates (Table 3.4.1).

Similar as for the simulations of the climate-change response of *P. radiata* (Kirschbaum et al., 2012), the simulations for kanuka/mānuka highlight plant responses to increases in CO_2 concentration as a key determinant of future productivity changes. Hence, the critical question is whether the actual CO_2 response will be as strong as that provided through the algorithms that underly the model runs. The model is based on the well-characterised short-term effects of CO_2 concentration on photosynthesis. To calculate ultimate impacts on growth, the model includes several feedback processes that either enhance or reduce the

magnitude of the initial response. Resultant plant responses are broadly consistent with both small-scale glasshouse-based experiments and larger-scale field studies using 'free air CO_2 enrichment' technologies (see discussion in Kirschbaum et al., 2012).

Nonetheless, despite the large amount of experimental work, and the broad agreement between modelled and observed patterns, there is still remaining controversy around the magnitude of growth responses to increasing CO_2 concentration. This makes it difficult to forecast productivity changes with a high level of confidence.

However, the work reported here provides a reassuring aspect for carbon stores that might be established through carbon credits in native kanuka/mānuka stands. The present simulations give no cause to assume that these existing stores might be vulnerable through climatic changes. Temperature increases are generally positive for stand productivity, and while water availability may change adversely if increased evaporative demand under warmer conditions cannot be matched by increased precipitation, the simulations showed no particular sensitivity or thresholds in relation to water availability so that catastrophic system collapses are unlikely even under adverse changes. Increasing CO_2 concentrations should further enhance productivity.

At the same time, further work to obtain more information on growth rates, especially under less than optimal growing conditions, would strengthen the confidence in the current findings. An issue of particular importance is the extent of carbon losses associated with self-thinning. While it is clear that there must be substantial self-thinning and loss of individual trees, the magnitude of associated carbon losses is less clear. Establishing the average size of dying trees would be valuable information to provide on that key question.

4. Indirect effects

4.1 Predicting the severity of Dothistroma needle blight on *Pinus radiata* under future climate in New Zealand[5]

Abstract

Dothistroma needle blight is a very damaging foliar disease of *Pinus* species. An existing model for predicting spatial variation in Dothistroma needle blight severity was used to predict disease severity (S_{sev}) under current and future climate.

Spatial predictions of S_{sev} under current climate varied widely throughout New Zealand. Values of S_{sev} were highest in moderately warm wet environments in the North Island and on the west coast of the South Island. In contrast, relatively low values of S_{sev} were predicted in drier eastern and southern regions of New Zealand.

Changes in S_{sev} from current climate were predicted to be low to moderate under climates projected for 2040. However, over the longer term, to 2090, projected changes in S_{sev}, resulting from climate change, ranged from moderate to high. Over both projection periods S_{sev} was predicted to decline in the North Island and increase within the South Island. Surfaces such as those presented here are a critical element for decision support systems that provide information on site suitability for plantation species under increasing rates of global warming.

[5] This chapter has been published as Watt, M.S., Palmer, D. J., Bulman, L.S. (2011) Predicting the severity of Dothistroma needle blight on *Pinus radiata* under future climate in New Zealand. *New Zealand Journal of Forestry Science*, 41, 207-215.

Introduction

Climate has long been recognised as an important environmental determinant in the distribution of pathogens and development of disease (De Wolf & Isard, 2007; Hepting, 1963; Wallin & Waggoner, 1950). This is particularly the case for plant pathogens, where air temperature has been shown to influence their growth and cold season survival, while rainfall can strongly affect their ability to disperse and infect their hosts (Coakley et al., 1999; De Wolf & Isard, 2007). Process-based niche models, such as CLIMEX^{TM}, have utilized the relationship between climate and disease presence to project potential distribution of a wide range of invasive plant pathogens and disease (Desprez-Loustau et al., 2007; Ganley et al., 2009; Paul et al., 2005; Venette & Cohen, 2006; Watt, Kriticos, et al., 2009). These projected disease distributions have predicted the likelihood that a disease could become established in a region but have not predicted disease severity. Despite the responsiveness of many diseases to climate, disease severity has been less widely predicted across broad spatial scales than potential distribution, although there are some notable exceptions (Watt, Stone, et al., 2010; Watt, Palmer, et al., 2011).

Dothistroma needle blight, also known as red band needle blight, is one of the most important foliar diseases of *Pinus* spp in the world (Barnes et al., 2004). According to the current phylogenetic understanding, the disease is caused by two divergent lineages of fungi, *D. septosporum* (Dorog.) Morelet and *D. pini* Hulbary (Barnes et al., 2004). *Dothistroma* spp. are known to infect over 70 pine species (Bednárová et al., 2006) and under high infection pressure and favourable conditions also infects *Pseudotsuga menziesii* (Mirb.) Franco (Dubin & Walper, 1967), *Larix decidua* Mill (Bassett, 1969) and five species of *Picea* (Gadgil, 1984a; Jankovský et al., 2004; Lang, 1987; Neves et al., 1986).

Although Dothistroma needle blight occurs widely on host species in their native range, it is generally most damaging as an invasive disease in exotic pine plantations (Gibson, 1974), where it is capable of causing substantial growth loss (Bulman, 2006; Hocking & Etheridge, 1967; van der Pas, 1981). In the early 1960s, outbreaks of Dothistroma needle blight in *Pinus radiata* D. Don plantations were particularly severe in East Africa, New Zealand, and Chile and led to abandonment of planting *P. radiata* in East Africa (Gibson, 1974) and India (Mehrotra, 1997), and other susceptible pine species in North America (Gibson, 1974) and central USA (Peterson, 1967). In the late 1990s and early 2000s outbreaks were recorded in British Columbia (Woods, 2003; Woods et al., 2005) and parts of Europe (Brown, 2005; Villebonne & Maugard, 1999).

Pinus radiata, a highly susceptible *Pinus* species (Bulman et al. 2004), comprises 90% of an economically important plantation forest resource (1.8 million ha) in New Zealand (New Zealand Forest Owners Association, 2010). Dothistroma needle blight was first observed in New Zealand during 1962 and spread through the majority of the country over the following decades (Bulman et al. 2004; Gilmour 1967). Currently Dothistroma needle blight is controlled by spraying of copper oxides and silvicultural practices that promote airflow and remove susceptible individuals (e.g. thinning (Gadgil, 1970; Marks & Smith, 1987)), and reduce inoculum (e.g. pruning (Gadgil, 1970; van der Pas, Bulman, et al., 1984)).

Although *Dothistroma pini* does not occur in New Zealand the causal pathogen *Dothistroma septosporum* is present throughout New Zealand (Bulman *et al.* 2004). Projections of future distribution show almost the entire country remains suitable for *D. septosporum* under climate change to 2090 (Watt, Ganley, et al., 2011). Despite this, marked variation in disease severity has been reported under current climate (Bulman et al., 2004; Watt, Palmer, et al., 2011) as climate has a strong influence on disease infection rates and severity. Experimental research shows that rates of infection increase markedly as the environment becomes more warm and wet reaching a reported optimum at constant temperatures of between 16 and 20°C when needles are continuously moist for 10 hours (Gadgil, 1974; Gilmour, 1981). Field observations concur with these observations. Disease severity has been found to be

positively linked with summer rainfall in British Columbia (Woods et al., 2005) and New Zealand (Bulman, 2006).

A recently developed model of Dothistroma needle blight severity for New Zealand confirms these findings and integrates the effect of different climatic variables on severity into a single model (Watt, Palmer, et al., 2011). This model was developed from an extensive national dataset and showed disease severity to be sensitive to rainfall, relative humidity, air temperature and stand age. Analyses showed that optimum environmental conditions for Dothistroma needle blight were high late spring rainfall (> 150 mm month^{-1}), high relative humidity and a mean daily air temperature of 15.5 °C over late spring to mid autumn. Projections of disease severity from this model agree with the observed severity pattern. Within New Zealand highest severity is reached in wet regions with moderate to warm air temperatures while lowest severity occurs in dry areas or sub-tropical regions in the far north (Bulman et al., 2004) where air temperature exceeds the disease optimum.

Given the responsiveness of the pathogen to variation in air temperature, climate change is likely to have a marked effect on disease severity and host productivity. Pathogens have shorter generation times than trees and so their populations can be expected to respond more rapidly to climate change. Consequently, over the rotation interval of a forest, Dothistroma needle blight has the potential to cause significant growth reduction in a plantation that may have been only marginally at risk at the time of establishment. The development of models that account for this variation in impact over the course of a crop life is critical for making informed decisions on where to site *P. radiata* under increasingly rapid rates of global warming.

Using the previously developed model to spatially predict disease severity the objective of this study was to compare disease severity under current and future climate within New Zealand. Projections of disease under future climate within New Zealand were developed using a comprehensive set of 36 climate change scenarios for both 2040 and 2090.

Methods

Severity dataset

Dothistroma needle blight incidence and severity data collected over a 36 year period from 1965 to 2010 (mean of 2000) were used in analyses. The percentage of the stand (scale = 0 to 100) affected by the disease (S_{inc}), and for those affected trees the severity (scale of 0 – 1) of the disease (A_{sev}) was estimated using the 5% step method (Bulman et al., 2004). This method was used throughout the assessment period. The stand level product of these measurements (S_{inc} x A_{sev}) was used to determine the severity of Dothistroma needle blight within the stand ($S_{sev,}$ scale = 0 –100). For each estimate, location (easting, northing) was recorded and the stand age at which the assessment was made. The 10,648 stand level observations of S_{sev} were averaged to a 25 km^2 resolution, resulting in a 169 mean estimates of S_{sev}. These data covered a wide environmental range and were located within almost all localities of the current *P. radiata* plantation resource (see Watt, Palmer et al., 2011 Figure 1 for distribution).

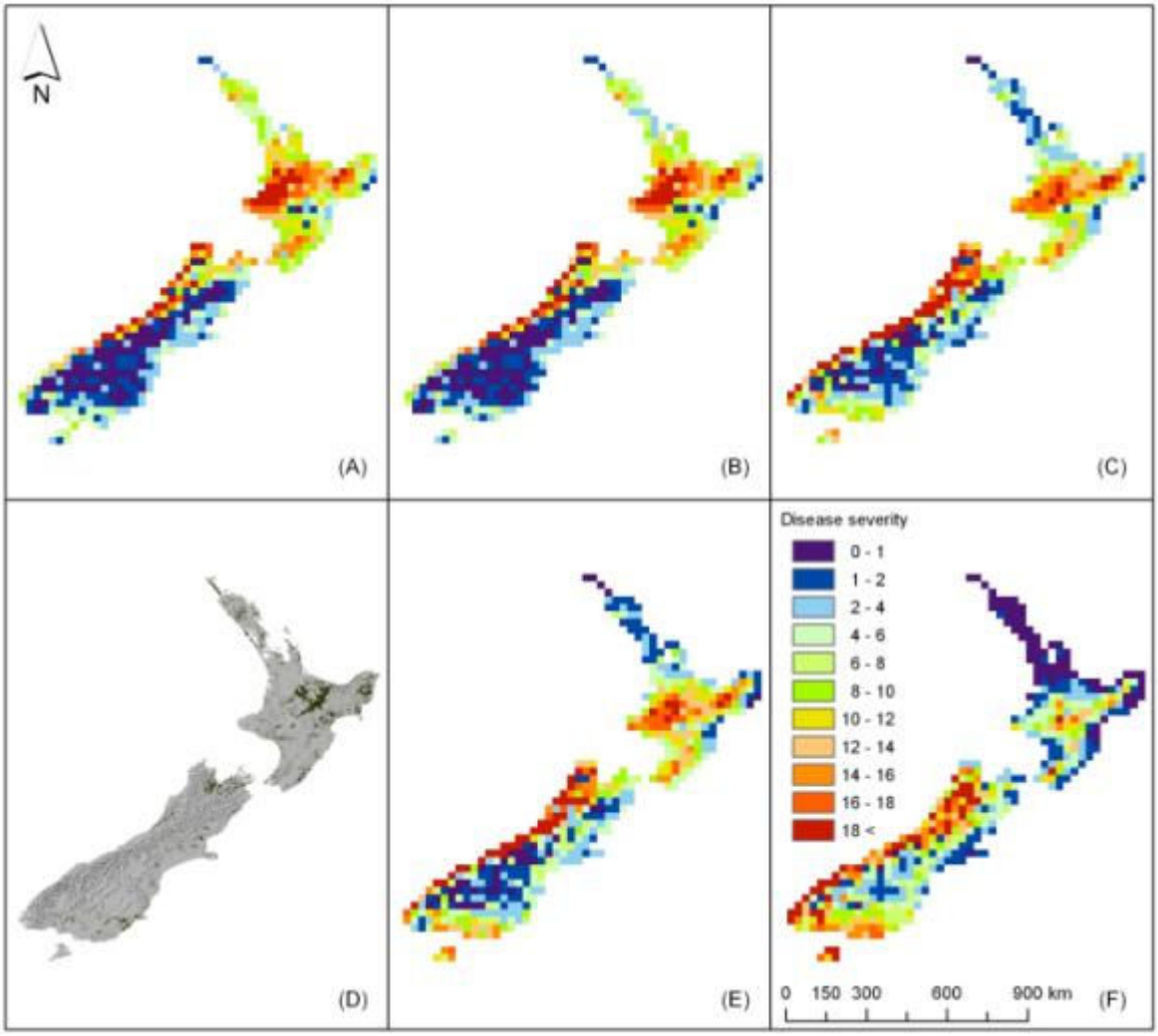

Figure 4.1.1. Variation in disease severity under current climate (A), and future climate during 2040 projected by scenarios representing extreme changes in stand severity, S_{sev}. These are (B) ECHAM5 (least change in S_{sev}), and (C) NCAR (greatest change in S_{sev}), and during 2090 projected by (E) UKMO-HadCM3 (least change in S_{sev}), and (F) MIROC 32 (greatest change in S_{sev}). All GCMs presented use the moderate emission scenario, A1B. Also shown are the location of New Zealand *Pinus radiata* plantations in panel (D).

Meteorological data

Mean monthly meteorological data from NIWA (National Institute of Water and Atmospheric Research Ltd.) were used in this study. Data were interpolated for the whole of New Zealand on a 500 m^2 grid, using a thin-plate smoothing spline to spatially interpolate the data. This surface was derived from data collected over a 30-year period from 1971–2000 (mean time of 1985). Meteorological data include mean monthly total rainfall; mean wind speed; mean, minimum and maximum air temperature; and relative humidity. Following the procedure outlined in Watt, Palmer et al., 2011, these surfaces were updated to reflect current climate (defined as 2010).

Climate change projections used in this study were derived from the factorial combination of 12 Global Climate Models (GCMs) and the B1 (low), A1B (mid-range) and A2 (high) emission scenarios, that have been fully described, previously (Ministry for the Environment, 2008). The 12 GCMs used in this study, which cover the expected range in climate change for New Zealand, are abbreviated to: CNRM, CCCma, CSIRO Mk3, GFDL CM 2.0, GFDL CM 2.1, MIROC32, ECHOG, ECHAM5, MRI, NCAR, UKMO-HadCM3, UKMO-HadGEM1.

Temperature and rainfall were statistically downscaled for each GCM to a resolution of 0.05 degree (~5 km) for two future periods 2030-2049 (midpoint reference year is 2040) and 2080-2099 (midpoint reference year is 2090). Because climate change projections are referenced to 1990, we subtracted the temperature change between 1990 and the current time (2010), from climate change surfaces before applying the climate change projections. Using a previously described rate of change in temperature over the last century of 0.009 °C year^{-1} (NIWA, 2010; Salinger, 1981) this scales to a temperature difference between 2010 and 1990 of 0.18 °C. Summary statistics describing projected future changes in air temperature and rainfall, relative to the baseline (2010), are shown in Table 4.1.1.

Table 4.1.1. Summary of changes in air temperature and rainfall under the climate change scenarios, in relation to current climate.

Year	Emission scenario	Temperature change (°C)			Rainfall change (%)		
		Mean	Min.	Max.	Mean	Min.	Max.
2040	B1	0.53	0.24	0.91	2.2	-9.3	11.7
	A1B	0.69	0.27	1.09	-0.3	7.5	11.6
	A2	0.69	-0.08	0.96	-0.7	-5.7	7.6
2090	B1	1.21	0.44	2.16	0.1	-9.7	11.5
	A1B	1.89	0.84	2.97	-2.6	-18.1	14.1
	A2	2.46	1.31	3.14	1.0	-17.0	14.9

Values shown give the mean New Zealand change pooled across the 12 Global Climate Models (GCMs), within each emission scenario. The lowest and highest mean New Zealand change (in rainfall and temperature) from the 12 GCMs are represented by the Min. and Max.

Analyses

All analyses were undertaken using SAS (SAS-Institute-Inc., 2000). Current climate and stand age was linked to S_{sev} at the resolution of these surfaces and these data were then averaged to a 25 km^2 resolution for analyses. As described in Watt, Palmer et al., 2011, 20% of the 169 measurements available for modelling were randomly selected and withheld from the model fitting for later validation. S_{sev} was log transformed for the modelling [ln (S_{sev} + 1)] which corrected the non-normal distribution of residuals evident in later analyses.

The multiple regression model of S_{sev} outlined in Table 4.1.2 was developed from the fitting dataset by using the methods described fully in Watt, Palmer et al. (2011). We chose not to use a model with spatial covariance as it is unknown whether this spatial covariance will remain constant under climate change. Consequently the precision of the multiple regression model used here (R^2=0.68) was slightly lower than that of the final model cited in Watt, Palmer et al., 2011 (R^2=0.72) that included spatial covariance for projections under current climate. The final regression model included stand age (A), mean total November rainfall (P_{Nov}), mean relative humidity from October to April ($RH_{Oct-Apr}$) and mean air temperature from November to April ($T_{Nov-Apr}$). All four variables were highly significant (Table 4.1.2). Diagnostics describing the model fit and partial response functions between all four variables and S_{sev} are described in detail in Watt, Palmer et al.(2011).

Table 4.1.2. Summary of statistics for the final predictive model of Dothistroma needle blight severity. Parameter values and variable partial R^2 (in brackets) and cumulative R^2 values are shown, describing model fit to the fitting dataset. For the significance category (Signif), the *F* values and *P* categories from an *F*-test, are shown, with asterisks *** representing significance at $P < 0.001$. Reproduced from Watt, Palmer, (2011).

Equation: $\ln(S_{sev}+1) = \alpha_1 + \alpha_2 A + \alpha_3 A^2 + \alpha_4(1-\exp(-\alpha_5 P)) + \alpha_6 T + \alpha_7 T^2 + \alpha_8(1-\exp(-\alpha_9 RH))$

Para.	Value	Variable	Units	R^2	Signif.
α_1	-14876.0				
α_2	0.22480	Stand age (A)	years	0.14 (0.14)	10.5***
α_3	-0.00940				
α_4	5.03981	November rainfall (*P*)	m	0.47 (0.33)	39.8***
α_5	0.03176				
α_6	3.36750	Mean air temp. Nov. - April (*T*)	°C	0.55(0.08)	11.7***
α_7	-0.10847				
α_8	14846.9	Mean relative humidity at 9am Oct. - April (*RH*)	%	0.60 (0.05)	16.2***
α_9	0.13136				

Model projections

Spatial projections of S_{sev} were developed from the described model under current and future climate using the 36 described climate change scenarios for both 2040 and 2090. For these projections the stand age used in the model was held at a constant value of 9 years which was the mean value in the fitting dataset. As mean S_{sev} responds differentially between the North and South Island under climate change, mean values of S_{sev} for the 36 climate change scenarios were determined by island. The two GCMs representing the extremes were determined as those with the lowest and highest average absolute changes in S_{sev} from current climate, for New Zealand. Projections of S_{sev} for these extreme climate change scenarios under the A1B emission scenario are displayed with current climate, for both projection periods.

Results

Model projections under current climate

As previously reported (Watt, Palmer, et al., 2011) spatial projections, developed using the regression model at a constant age of 9 years (mean age in the fitting dataset) clearly highlight the importance of environment on S_{sev} in the North Island. Values of S_{sev} were highest in moderately warm and relatively wet regions in the central North Island (Fig. 4.1.1a). Reductions in S_{sev} occurred with decreasing latitudes in warm temperate northern regions of the North Island as air temperature increased and rainfall declined. S_{sev} was relatively low in moderately warm but drier eastern regions and in cooler dry southern areas of the North Island (Fig. 4.1.1a). Average S_{sev} within the North Island was 10.9.

Compared to the North Island, the mean S_{sev} within the South Island of 4.3 was markedly lower (Fig. 4.1.1a). However, there was wide spatial variation that was particularly marked from west to east as the main axial ranges have a substantial influence on rainfall distribution. In regions west of the main axial ranges, where rainfall exceeds 2,000 mm, and temperatures are moderate, values of S_{sev} ranged from 14 to 20. In contrast, east of the main divide, where rainfall ranges from 500 to 1,250 mm, S_{sev} was lower than 8 (Fig. 4.1.1a). On the South Island east coast there was a gradual decline in S_{sev} from east to west, caused by reductions in air temperature that occurred with increasing altitude and proximity to the main axial ranges (Fig. 4.1.1a).

Projections under climate change

Changes in S_{sev} from current climate were predicted to be low to moderate under projections during 2040 (Figs. 4.1.2a, b), with S_{sev} values in the North Island declining on average by 10 % (10.9 *vs*. 9.8) and increasing by an average of 31% in the South Island (5.6 *vs*. 4.3). Variation in S_{sev} was relatively low between emission scenarios (Figs. 4.1.2a, b). Changes in S_{sev} from current climate for GCMs representing extremes, ranged widely from –1.8% (for MRI) to –25% (for MIROC 32) for the North Island and from 2% (for ECHAM 5) to 55% (NCAR) for the South Island (see Fig. 4.1.1 b, c for projections from contrasting GCMs under the AIB scenario).

Over the longer term, to 2090, projected changes in S_{sev} resulting from climate change, ranged from moderate to high (Fig. 4.1.2 c, d). Compared to current climate, mean S_{sev} were reduced by 18%, 31%, and 48%, respectively, under the B1, A1B and A2 emission scenarios for the North Island (Fig. 4.1.2c). Conversely, S_{sev} increased, on average, by 50%, 67%, and 92%, respectively, under the B1, A1B and A2 emission scenarios for the South Island (Fig. 4.1.2d). Similarly, there was wide variation in changes in S_{sev} between the 12 GCMs. Changes in S_{sev} ranged from –17% (for CNRM) to –61% (for MIROC 32) for the North Island and from 46% (for UKMO-HadCM3) to 108% (MIROC32) for the South Island (see Fig. 4.1.1e, f for contrasting GCMs under the AIB scenario). Compared to current climate, reductions in S_{sev} occurred throughout most of the North Island in the future, with the most marked reductions occurring in coastal and northern regions (Fig. 4.1.1e,f). In contrast, with the exception of the northern areas, increases in S_{sev} were projected within most South Island regions, with gains most pronounced in southern regions (Fig. 4.1.1e,f).

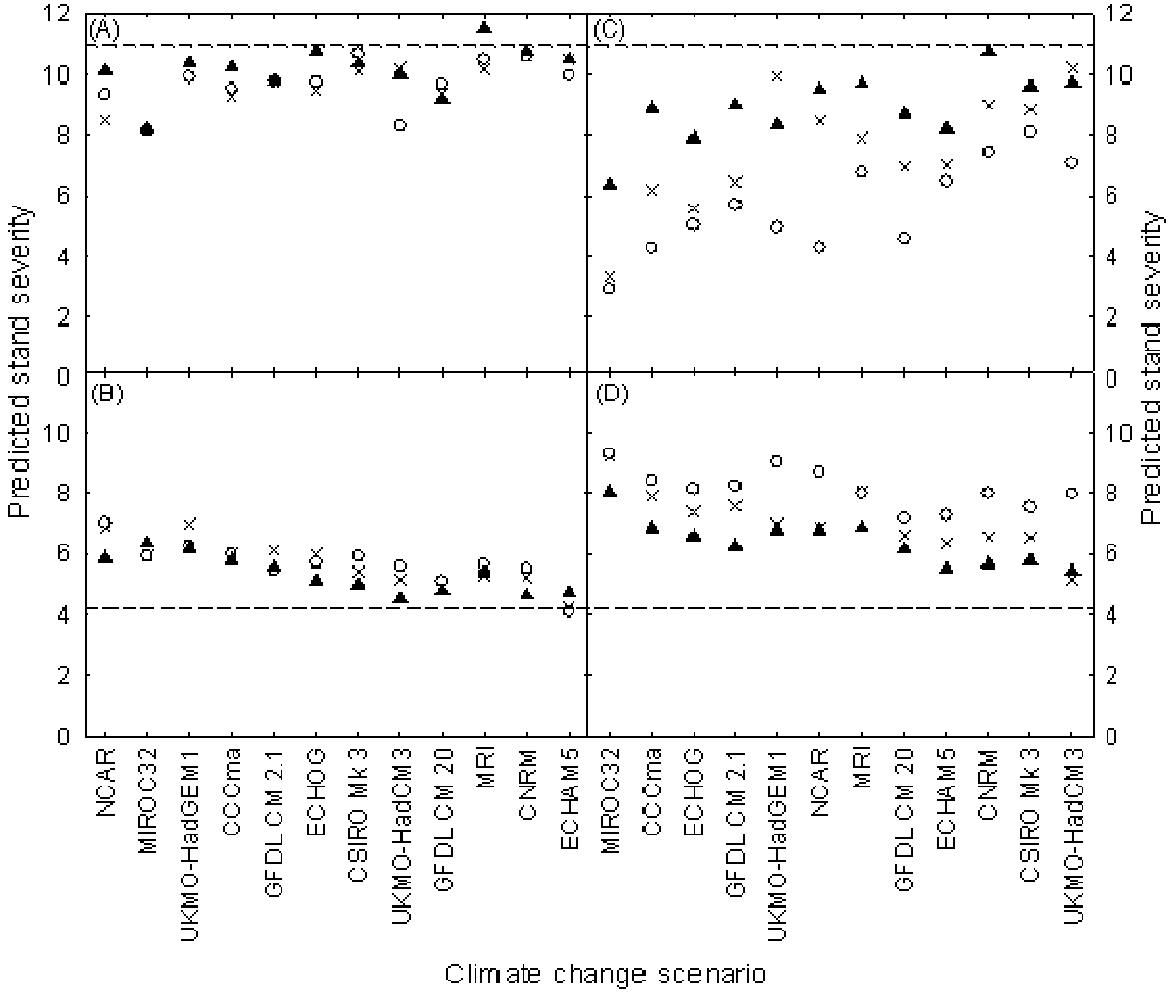

Figure 4.1.2. Variation in mean predicted S_{sev} for New Zealand under 12 models using the B1 (triangles), A1B (crosses) and A2 (open circles) emission scenarios, projected to 2040 within the (A) North Island and (B) South Island and to 2090 within the (C) North Island and (D) South Island. The mean predicted S_{sev} under current climate is shown on both figures as a dashed line. Scenarios are sorted in descending order of mean stand severity, averaged across New Zealand for both 2040 and 2090.

Discussion

Dothistroma needle blight is one of the most damaging diseases of *Pinus radiata* within New Zealand. Volume loss has been shown to scale linearly with average disease level. For instance, over a seven-year period trees with a 50% infection rate had a 50% volume growth loss, compared to trees with little infection (van der Pas, 1981). In many east coast and southern regions that have low disease severity no treatment is required, while repeated treatments are required in areas with high disease severity. From 2005 to 2010, over 90% of the area sprayed for Dothistroma needle blight control was located in the central North Island (see Fig. 4.1.1d for location of these forests) with the remainder being treated within the northern and western regions of the South Island (Nelson and Westland). Forests located on the west and east coasts of the North Island are treated occasionally (Bulman, L., unpub. data).

Spatial projections of regional variation in disease severity under current climate presented both here and in Watt, Palmer et al. (2011) are consistent with previous empirical observations describing regional variation in severity (Bulman et al., 2004). For example, in

the North Island, infection levels tend to be low in Northland and along the east coast (Hawke's Bay and Wairarapa), whereas the central North Island, Waikato and Taranaki are the most severely affected regions. In the South Island, both modelled and empirical data indicate that infection is most severe west of the main axial ranges, with low infection levels generally found throughout the remainder of the South Island. Currently, the disease is particularly problematic to the forest industry as a large proportion (ca. 30 %) of the *P. radiata* estate is located in the severely affected central North Island region (Fig 4.1.1d), where rainfall is high and air temperature is close to optimum for the pathogen.

Spatial projections of future disease severity to 2090 were found to vary widely between both the GCMs and emission scenarios. When interpreting the results, it is also worthwhile considering the findings of Rahmstorf et al.(2007) who showed that recent trends in recorded climate change and sea level rise are effectively beyond the upper end of the emission scenarios considered by the IPCC. Therefore, the GCMs that project moderate to high temperature increases (e.g.MIROC32), and scenarios that project moderate (A1B) to high (A2) emissions should be given more weight as indicators of future climatic conditions.

Our results suggest that climate change is likely to have a significant effect on severity of Dothistroma needle blight over the long term. Projections of disease severity to 2040 show low to moderate change from projections under current climate, as air temperature is not forecast to increase substantially within New Zealand over the medium term. However, by 2090 reductions in disease severity are relatively marked within the North Island, particularly under the AIB and A2 emission scenarios, as air temperature surpasses the disease optimum in most regions. These reductions are particularly pronounced in the far north where increases in temperature make the environment largely unsuitable for the expression of the disease. In contrast, there are relatively substantial increases in disease severity within most of the South Island, particularly within relatively wet southern regions under the more extreme A2 scenarios. Under the most extreme climate change scenarios disease severity in the lower South Island is predicted to be broadly similar to that of the worst affected central North Island regions under current climate.

It is worth noting that within northern areas of the North Island projections of severity under climate change are extrapolated above the air temperature range used to construct the model. However, as both the raw data (not shown) and model show markedly lower disease severity within these regions under current climate we have a reasonable level of confidence in these low extrapolated values. In addition, the degree of extrapolation is relatively small (maximum of 2.46 °C), compared to the total range of mean annual air temperatures over which the model was developed (ca. 8°C).

Although *P. radiata* has the highest general growth rate of plantation species cultivated in New Zealand, there are a number of potential alternative species with relatively good growth rates that are not currently subject to serious diseases (e.g. *Sequoia sempervirens* (D. Don) Endl.). Decisions around species selection are usually based on a relatively broad set of criteria that, in addition to susceptibility to biotic and abiotic risk factors, include factors affecting profitability (e.g. growth rates, product value, and rotation length). Accounting for direct growth responses of plantation species to climate change is likely to be at least as important as defining how biotic risk changes. For instance, in the central North Island disease severity of Dothistroma needle blight is projected to markedly reduce over the long term. However, as the temperature optimum for *P. radiata* growth closely matches that of disease severity these reductions in disease severity are likely to be accompanied by growth responses that are far lower than the substantial growth gains predicted throughout the South Island (Kirschbaum et al., 2010). Spatial models and decision support systems that integrate these complexities and appropriately weight risk factors should be developed to determine how climate change is likely to influence the future distribution of New Zealand plantation species.

4.2. Impact of climate change on Cyclanuesma needle cast[6]

Abstract

Cyclaneusma needle cast is a very damaging foliar disease of *Pinus* species. It is particularly widespread and detrimental to the growth of planted forests in New Zealand. The influence of climate change on the spatial distribution of disease severity (S_{sev}) would provide forest managers with insight into where to deploy disease resistance planting stock in the future. Here we use an existing model of Cyclaneusma needle cast severity, developed from an extensive dataset, to spatially predict disease severity under current and future climate to 2040 and 2090.

Spatial predictions of S_{sev} under current climate varied widely throughout New Zealand. Values of S_{sev} were highest in moderately warm, wet and humid high elevation environments located in the central North Island. In contrast, relatively low values of S_{sev} were predicted in drier eastern and southern regions of New Zealand.

Projections within the North Island show relatively little change in S_{sev} from current climate over the short term and low to moderate reductions in S_{sev} within most areas over the long term. In contrast, within the South Island, S_{sev} was predicted to markedly increase over both projection periods, with more pronounced increases in S_{sev} projected by 2090. Surfaces presented here are a critical element of decision support systems that describe how climate change is likely to influence plantation productivity and vulnerability to abiotic and biotic risk factors.

[6] This chapter is in press with the New Zealand Journal of Forestry Science as Watt, M.S., Palmer, D.J., Bulman, L.S. and Harrison, D. Predicting the severity of Cyclanuesma needle cast on *Pinus radiata* under future climate in New Zealand.

Introduction

Cyclaneusma needle cast is a damaging disease of *Pinus* species (Millar & Minter, 1980) caused by the pathogens *Cyclaneusma minus* (Butin) DiCosmo, Peredo & Minter and *Cyclaneusma niveum* (Pers.) DiCosmo, Peredo & Minter. The disease is present on all continents where *Pinus* spp. are grown and is characterised by yellow and brown mottling of needles that are prematurely cast (Gadgil, 1984b; Stahl, 1966).

Cyclaneusma needle cast is particularly problematic within planted pine forests where significant economic losses have been recorded. The highly susceptible species *Pinus radiata* (Gadgil, 1984b) is the most commonly planted species in the southern hemisphere (Lewis & Ferguson, 1993) and also comprises 90% of an economically-important planted forest resource (1.7 million ha) in New Zealand (NZFOA, 2010).

A recently developed model of Cyclaneusma needle cast for New Zealand has shown that air temperature has a strong influence on the spatial distribution of the disease (Watt et al., 2012). This model was developed from an extensive national dataset and showed disease severity to be sensitive to mean air temperature, elevation, mean relative humidity and stand age. Analyses showed disease severity increased to a maximum at mean winter air temperatures of between 7 and 9°C before declining. Relationships between disease severity and all other variables were linear and positive.

Given the responsiveness of the pathogen to variation in air temperature, climate change is likely to have a marked effect on disease severity and host productivity. Pathogens have shorter generation times than trees and so their populations can be expected to respond more rapidly to climate change. Consequently, over the rotation interval of a forest Cyclaneusma needle cast has the potential to cause significant growth reduction in a plantation that may have been only marginally at risk at the time of establishment. The development of models that account for this variation in impact over the course of a crop life is critical for making informed decisions on where to deploy disease resistant *P. radiata* under increasingly rapid rates of climate change.

Using the previously developed model to spatially predict disease severity the objective of this study was to compare disease severity under current and future climate within New Zealand. Projections of disease under future climate within New Zealand were developed using a comprehensive set of 36 (12 Global Climate Models x 3 emission scenarios) climate change scenarios for both 2040 and 2090.

Methods

Severity dataset

Data from aerial and ground surveys of disease severity carried out between 1972 and 2006 were included in the analyses. In total, there were 9,855 records included in the database of disease from plantations across New Zealand. For each record the fraction of the stand (scale 0 to 1) affected by the disease (S_{inc}), and the severity of the infection (A_{sev}) (0 to 1) was estimated. The product of these measurements (S_{inc} x A_{sev}) was used to determine the severity of Cyclaneusma needle cast for each record (S_{sev}, scale 0 to 1). For each observation, location was recorded as well as the age of the stand on which the estimate was being made. To spatially consolidate the data, the 9,855 records were averaged to a 5 km^2 resolution. This averaging was undertaken so that measurements of S_{sev} included a number of temporally dispersed observations representative of the long term average meteorological data used to model disease severity. After undertaking this averaging a total of 387 estimates of S_{sev} were available for the modelling. These data covered a wide

environmental range and were located within almost all areas in which the current *P. radiata* plantation resource occurs (see Watt et al., 2012, Figure 1 for distribution).

Meteorological data

Mean monthly meteorological data from the National Institute of Water and Atmospheric Research Ltd. (NIWA) were used in this study to develop a predictive model of S_{sev}. Data were interpolated for the whole of New Zealand on a 500 m^2 grid, using a thin-plate smoothing spline to spatially interpolate the data. This surface was derived from data collected over a 30-year period from 1971 – 2000 (mean time of 1985).

Analyses

A previously described model (Watt et al., 2012) was used to describe S_{sev} under future climate. A brief summary of this model follows. In total 80% of the 387 available observations were used for model development while the remaining 20% (n = 77 randomly selected observations) were withheld for model validation. The final model of disease severity was developed from transformed values of stand severity [$tS_{sev} = \ln (S_{sev} + 1)$] using the regression kriging approach, that is fully described in Watt et al. (2012). The predictive variables included mean winter air temperature (T_{win}), relative humidity (RH_{win}) in winter (July), elevation (E) and stand age (A) in the following formulation,

$$tS_{sev} = \beta_0 + \beta_1 T_{win} + \beta_2 T_{win}^2 + \beta_3 E + \beta_4 RH_{win} + \beta_5 A \qquad [4.2.1]$$

where β_0 to β_5 represent empirically fitted parameters. Parameter values and summary statistics for the model are described in Table 4.2.1. Spatial covariance in the dataset was found to be highly significant ($P < 0.001$). After testing a wide range of structures this covariance was found to be best represented using an isotropic spatial covariance structure. Estimated covariance parameters within this structure for the partial sill, range and nugget were 0.0014, 29 km and 6.7×10^{-4}. The sill, which represents the sum of the partial sill and nugget was 0.002. The effective range, the distance at which the spatial auto-correlation in the dataset declined to less than 0.05, was determined as 3 x range = 87 km. For distances greater than or equal to the range (87 km), spatial correlation between observations was effectively zero. The final model with spatial covariance accounted for 72.8 % of the variance in the validation data.

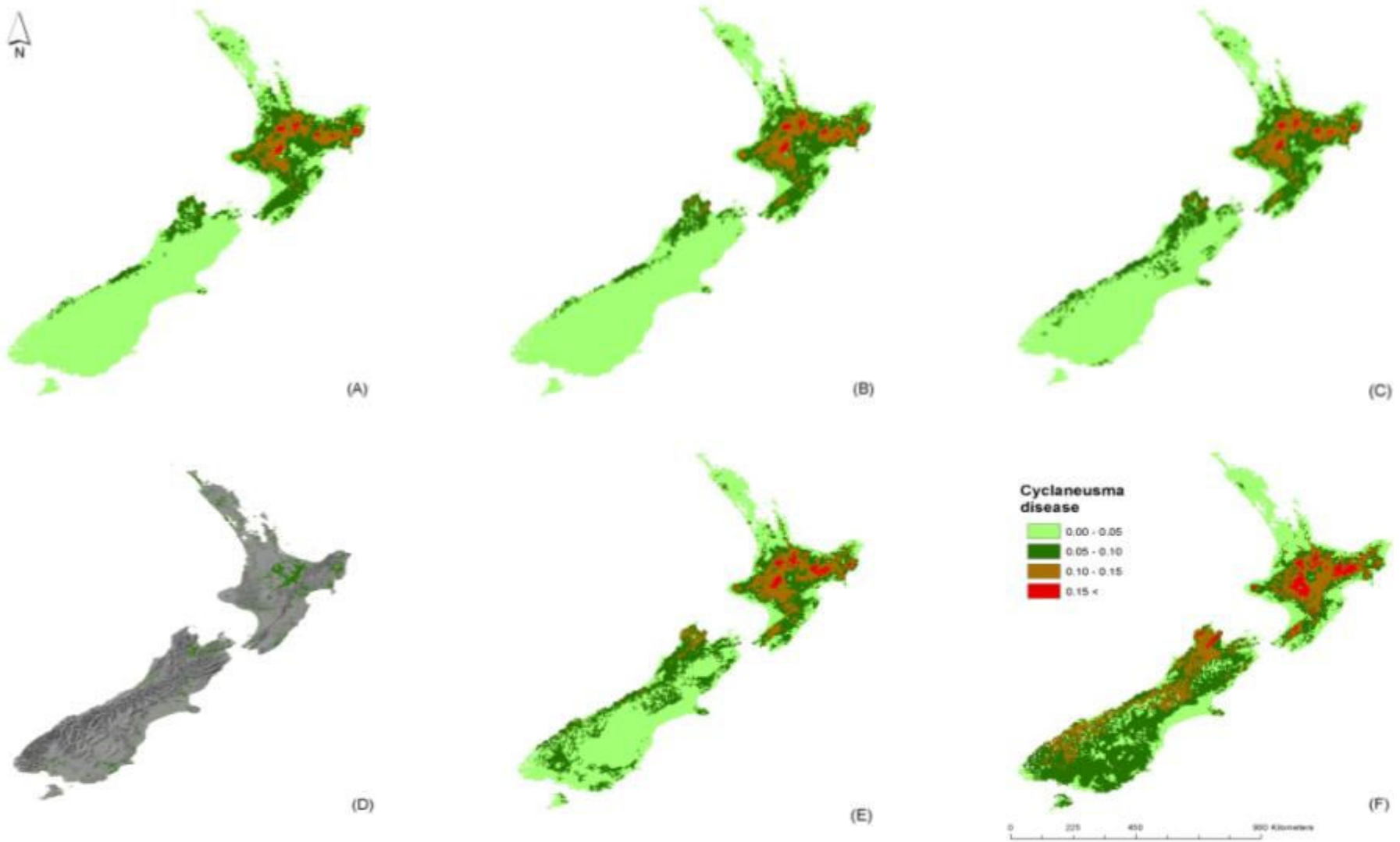

Figure 4.2.1. Variation in disease severity under current climate (A), and future climate during 2040 projected by scenarios representing extreme changes in stand severity, S_{sev}. These are for 2040 (B) ECHAM5 under A2 (least change in S_{sev}) and (C) UKMO HADGEM1 under A1B (greatest change in S_{sev}), and during 2090 projected by (E) CSIRO Mk3 under B1 (least change in S_{sev}), and (F) UKMO HADGEM1 under A1B (greatest change in S_{sev}). Also shown are the location of New Zealand *Pinus radiata* plantations in panel (D).

Table 4.2.1. Summary of statistics for the regression model of Cyclanuesma needle cast severity. All statistics relate to the log transformed dependent variable (i.e. tS_{sev}), which represents a natural log transformation of S_{sev} determined as $tS_{sev} = \ln (tS_{sev}+1)$. For the significance category the *F* values and *P* categories from an *F*-test, are shown, with asterisks *** representing significance at $P < 0.001$.

Parameter	Value	Variable	Units	Significance
β_0	-0.7306	Intercept		
β_1	0.08144	Mean winter air temperature (T_{win})	^oC	30.9***
β_2	-0.00481	T_{win}^2		24.2***
β_3	1.60×10^{-4}	Elevation	m	42.8***
β_4	4.259×10^{-3}	Mean relative humidity during July	%	9.1***
β_5	3.326×10^{-3}	Stand age	years	30.5***

Model projections

Spatial projections of S_{sev} were developed from the described model under current and future climate using 36 described climate change scenarios for both 2040 and 2090. Climate change projections used in this study were derived from the factorial combination of 12 Global Climate Models (GCMs) and the B1 (low), A1B (mid-range) and A2 (high) emission scenarios, that have been fully described, previously (Ministry for the Environment, 2008). The 12 GCMs used in this study, which cover the expected range in climate change for New Zealand, are abbreviated to: CNRM, CCCma, CSIRO Mk3, GFDL CM 2.0, GFDL CM 2.1, MIROC32, ECHOG, ECHAM5, MRI, NCAR, UKMO-HadCM3, UKMO-HadGEM1. Temperature and rainfall were statistically downscaled for each GCM to a resolution of 0.05 degree (~5 km) for two future periods 2030-2049 (midpoint reference year = 2040) and 2080-2099 (midpoint reference year is 2090). Summary statistics describing projected future changes in air temperature and rainfall are shown in Table 4.2.2.

Table 4.2.2. Summary of changes in air temperature and rainfall under the climate change scenarios, in relation to current climate.

Year	Emission scenario	Temperature change (°C)			Rainfall change (%)		
		Mean	Min.	Max.	Mean	Min.	Max.
2040	B1	0.53	0.24	0.91	2.2	-9.3	11.7
	A1B	0.69	0.27	1.09	-0.3	7.5	11.6
	A2	0.69	-0.08	0.96	-0.7	-5.7	7.6
2090	B1	1.21	0.44	2.16	0.1	-9.7	11.5
	A1B	1.89	0.84	2.97	-2.6	-18.1	14.1
	A2	2.46	1.31	3.14	1.0	-17.0	14.9

Values shown give the mean New Zealand change pooled across the 12 Global Climate Models (GCMs), within each emission scenario. The lowest and highest mean New Zealand change (in rainfall and temperature) from the 12 GCMs are represented by the Min. and Max.

Compared to current climate predicted changes in mean S_{sev} under climate change were very different between the North and South Island. Consequently, mean values of S_{sev} for the 36 climate change scenarios are displayed by island. The two GCMs representing the extremes were determined as those with the lowest and highest average absolute changes in S_{sev} from current climate, for New Zealand. Projections of S_{sev} for these extreme climate change scenarios are displayed with current climate, for both projection periods.

Results

Model projections under current climate

As previously reported (Watt et al., 2012), spatial projections developed using the regression model at a constant age of 16 years (mean age in the fitting dataset) clearly highlight the importance of environment on S_{sev}. Values of S_{sev} were highest in moderately warm and relatively wet regions, with high relative humidity, in the central North Island (Fig. 4.1.1a). Reductions in S_{sev} occurred in warm temperate northern regions of the North Island as air temperature increased beyond the optimum. S_{sev} was relatively low in moderately warm but drier eastern regions and in cooler dry southern areas of the North Island (Fig. 4.1.1a). Average S_{sev} within the North Island was 0.064.

Compared to the North Island, the mean S_{sev} within the South Island of 0.021 was markedly lower (Fig. 4.2.1a). However, there was wide spatial variation that was particularly marked from west to east as the main axial ranges (Southern Alps) have a substantial influence on rainfall distribution and relative humidity. In regions west of the Southern Alps, where relative humidity is high, and temperatures are moderate, values of S_{sev} ranged from 0.05 to 0.1. In contrast, east of the main divide, where conditions are drier and relative humidity is low, S_{sev} was lower than 0.05 (Fig. 4.2.1a).

Projections under climate change

Changes in S_{sev} from current climate projected to 2040 ranged widely between the North and South Island. Within the North Island there was a slight increase in S_{sev} but this was limited to a maximum gain of 2.5% (S_{sev} = 0.0651 *vs*. 0.0635) across the 36 scenarios (Fig. 4.2.2a). In contrast, increases in the South Island averaged 75% (S_{sev} = 0.0380 *vs*. 0.0217) (Fig. 4.2.2b), with the greatest increases of 121% (S_{sev} = 0.0480 *vs*. 0.0217) occurring under the UKMO HadGEM1 model coupled with the A1B emission scenario (see Fig. 4.2.1c for spatial variation in S_{sev} under this scenario).

Compared to current climate, changes in S_{sev} were more marked by 2090. Within the North Island there were in general slight reductions in S_{sev} that averaged 7% (S_{sev} = 0.0592 *vs*. 0.0635) (Fig. 4.2.2c). Despite these overall reductions, there was a reasonably significant increase in S_{sev} within the central North Island (Fig. 4.2.1e, f). More marked overall changes were noted within the South Island, with S_{sev} increasing by on average 162% (S_{sev} = 0.0569 *vs*. 0.0217) (Fig. 4.2.2d), with maximum increases of 214% (S_{sev} = 0.0681 *vs*. 0.0217) noted for the UKMO HadGEM1 model using the A2 emission scenario. Predicted gains in severity were similar for the UKMO HadGEM1 model when combined with the A1B emission scenario. Under this scenario increases in S_{sev} occurred in almost all regions of the South Island and were particularly marked in high elevation regions (Fig 4.2.1f).

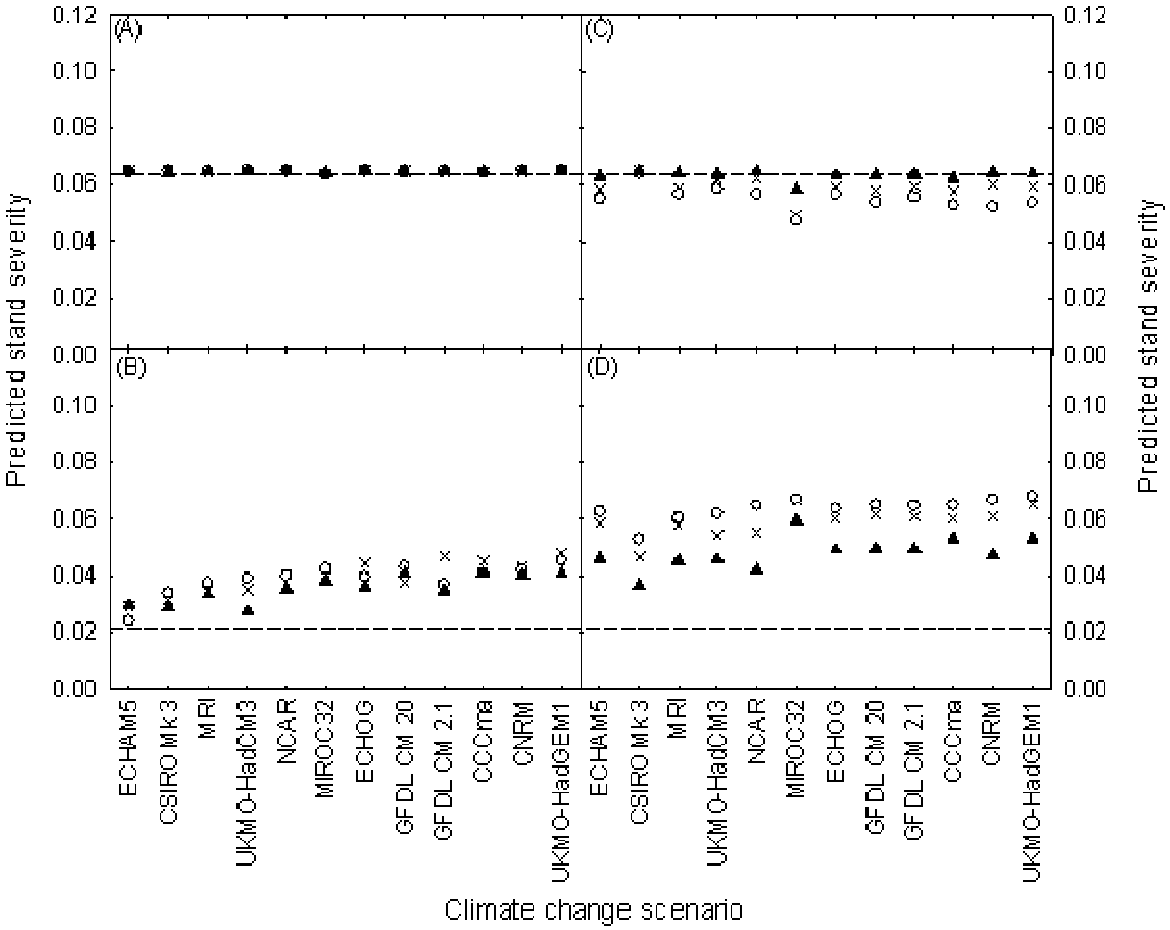

Figure 4.2.2. Variation in mean predicted stand severity for New Zealand under 12 models using the B1 (triangles), A1B (crosses) and A2 (open circles) emission scenarios, projected to 2040 within the (A) North Island and (B) South Island and to 2090 within the (C) North Island and (D) South Island. The mean predicted stand severity under current climate, by island, is shown on both figures as a dashed line. Scenarios are sorted in ascending order of mean stand severity, after averaging across New Zealand for both time periods.

Discussion

Cyclaneusma needle cast is a very damaging disease of *Pinus radiata* within New Zealand, where it is widely distributed. Volume losses have been shown to scale linearly with disease severity, reaching mean volume increment reductions of ca. 60% at disease severities of 80% (van der Pas, Slater-Hayes, et al., 1984). Although fungicides do provide some control of the disease it is currently not economic to use these chemicals to treat the disease on a commercial basis (Vanner, 1986). Tree breeding has resulted in improvements in disease resistance in younger stands through development of a *P. radiata* breed with high needle retention. Given the difficulty in controlling the disease it is important to understand how climate change is likely to influence spatial variation in disease severity. Such knowledge could influence the deployment of resistant tree breeds in the future.

Spatial projections of future disease severity to 2090 were found to vary widely between both the GCMs and emission scenarios. When interpreting the results, it is worthwhile considering the findings of Rahmstorf et al. (2007) who showed that recent trends in recorded climate change and sea level rise are effectively beyond the upper end of the emission scenarios considered by the IPCC. Therefore, the GCMs that project moderate to high temperature

increases, and scenarios that project moderate (A1B) to high (A2) emissions should be given more weight as indicators of future climatic conditions.

Results suggest changes in disease severity, from those noted under current climate, are likely to be far more marked within the South Island than the North Island. Over the short term little change in S_{sev} is noted within the North Island while only minor reductions occur over the long term to 2090. In contrast increases in S_{sev}, from values noted under current climate, are quite pronounced within the South Island reaching mean S_{sev} for the most extreme scenario of 0.0681. To place this in context the mean predicted S_{sev} during 2090 in the South Island is broadly equivalent to mean S_{sev} within the North Island under current climate (S_{sev} = 0.0569 vs. 0.0635).

Areas currently most affected by the disease are located in central (central North Island) and northeastern regions (East Cape) of the North Island. Although changes in S_{sev} within the North Island are not overall as marked as the South Island it is worth noting that S_{sev} does increase within the central North Island over the long term (2090), particularly under the most extreme scenario (Fig. 4.1.2F). Within northeastern regions, little change in S_{sev} from current climate is noted under climate change (Fig. 4.1.2F).

Although *P. radiata* has the highest general growth rate of plantation species cultivated in New Zealand, there are a number of potential alternative species with relatively good growth rates that are not currently subject to serious diseases (e.g. *Sequoia sempervirens* (D. Don) Endl.). Decisions around species selection should be based on a broad set of criteria that, in addition to susceptibility to biotic and abiotic risk factors, include factors affecting profitability (e.g. growth rates, product value, and rotation length). Making a species selection decision based purely on susceptibility to a disease may result in negative economic consequences. For instance, in East Africa during the early 1960s outbreaks of Dothistroma needle blight in *P. radiata* resulted in the replacement of this species by *P. patula* Schiede ex Schltdl.and *Cupressus lusitanica* Mill. While the replacement species were unaffected by the disease their growth was only two-thirds to three-quarters of that of *P. radiata* (Gibson, 1974). Furthermore, the replacement of *P. radiata* jeopardised the establishment of a pulp industry in Kenya (Gibson et al., 1964). Accounting for direct growth responses of plantation species to climate change is therefore likely to be at least as important as defining how biotic risk changes. Spatial models and decision support systems that integrate these complexities and appropriately weight risk factors should be developed to determine how climate change is likely to influence the future distribution of New Zealand plantation species.

4.3 Impact of climate change on fire risk

Abstract

Recent study results using the latest global climate model projections indicate that fire climate severity in New Zealand is likely to rise significantly with climate change in many parts of the country. A doubling or even trebling of fire danger is possible in some areas as a result of decreases in rainfall and increases in temperature, with higher wind speeds and lower humidity also contributing to higher future fire dangers.

Most Global Climate Model scenarios show dramatic potential increases in the likelihood of days of VH+E fire danger on which any fires would be difficult, if not impossible to control. The greatest relative (%) changes are likely in areas of the country where current fire dangers are comparatively benign (e.g. coastal Southland, Wanganui). Significant increases are also predicted for coastal Otago and Wellington despite their moderate current fire climate. Smaller percentage changes will also result in significant increases in absolute fire danger in other areas, including several of those where fire dangers are currently highest (e.g. Gisborne, Christchurch).

Increased fire danger as a result of warmer, drier and windier weather conditions has the potential to impact significantly on forest productivity in many areas of the country. Higher future fire danger is likely to result in longer fire seasons, and increased incidence of fires and plantation area burned. However, current fire occurrence statistics do not allow for prediction of the magnitude of these increases. This is an issue that warrants improving as a matter of urgency. Despite this, the mapping of likely changes in future fire danger provides an indication of potential impacts of climate change on fire risk and, in turn, forest productivity. Maintaining appropriate fire management strategies, especially around fire prevention, readiness and response, will be essential to mitigating the risks associated with this increasing fire danger.

Introduction

As in many other parts of world, analyses of the effects of climate change on fire risk in New Zealand have shown the potential for significant increases in future fire climate severity. The first New Zealand study, by Pearce et al. (2005) (also see Pearce & Clifford, 2008), highlighted the potential for increases in fire danger in many parts of the country due to increases in temperature and changes in rainfall patterns. This was reiterated in the more recent study by Pearce et al. (2011), which utilised more up-to-date projections of changes in fire climate for a wider range of Global Climate Model (GCM) scenarios to provide improved estimates of potential impacts on fire danger (Scion, 2011b).

At the outset of this project, it was proposed to use the results from the Pearce et al. (2011) analysis, together with relationships derived between present fire climate (Pearce, Kerr, Clifford, et al., 2011; Scion, 2011a) and fire occurrence statistics, to predict the impact of projected changes in future fire danger on future fire incidence and area burned. These types of studies have proven invaluable in other parts of the world (Carvalho et al., 2011; Flannigan, Logan, Stocks, et al., 2005; Tian et al., 2011), and such an analysis in New Zealand would provide a much better indication of the impact of climate change on future fire risk and forest productivity.

However, initial investigations into the development of fire occurrence relationships under current fire climate proved problematic (Pearce, 2012). National fire occurrence data is incomplete, and only available on a regional basis through the combined data obtained from the National Rural Fire Authorities annual return of fires (Anderson et al., 2008; Doherty et al., 2008). The lack of accurate, detailed data by location or even fire authority area meant it was practically impossible to derive useful predictive relationships for fire occurrence against current fire climate at point weather station locations that could then be used to predict potential future fire occurrence. This is an area that warrants significant effort in future to improve fire occurrence statistics to the point where relationships with fire climate can be derived.

The failure to derive these fire occurrence relationships with climate change meant that this analysis has had to rely solely on the results for future fire danger from the Pearce et al. (2011) study, and qualitative discussion of the potential impacts of climate change on future fire risk and forest productivity.

Methods

Improved estimates of the effects of climate change on fire risk were provided by Pearce et al. (2011). This study addressed a number of short-comings identified during the previous analysis of climate change effects on fire danger (Pearce et al., 2005). This included consideration of projected changes for all the key weather elements affecting fire danger (that is, wind speed and relative humidity, as well as temperature and rainfall), and improved estimates of these changes and potential future fire climate variability. This level of information was not available when the 2005 study was carried out, but has since become available through a broader range of possible climate change scenarios and improved Global Circulation Models (GCMs).

Fire danger ratings for 50 years (the 2040s, 2030-2049) and 100 years (the 2090s, 2080-2099) into the future were estimated using changes in climate inputs from current climate (based on the 1980s baseline, 1970-1999). These changes in temperature, humidity, wind speed and rainfall were obtained from statistical downscaling of 16 of the IPCC's 4th Assessment GCMs to the New Zealand region for the single mid-range A1B emissions scenario. Changes were applied to daily weather station observations from 20 sites across New Zealand. The number of stations that could be used was limited to those with climate

records for the full 20 year baseline period. Further details of the methods used in this study, including the 16 GCMs investigated, are contained in Pearce et al. (2011).

Fire climate severity for current and future fire climates at each location was compared using the estimates from the different GCMs, including both individual model estimates as well as the average across all 16 models investigated. Use of the multi-model average is a recognised way of describing the "best estimate" from consensus of the widely varying models being compared (Meehl, Stocker, et al., 2007; MfE, 2008). However, to help illustrate the range of possible outcomes, the model averages were also contrasted with examples of individual models producing low, mid and high-range changes (see Pearce et al., 2011).

Fire climate severity under current and future climate was compared using two measures of severity derived from the Fire Weather Index (FWI) System – the Daily Severity Rating (DSR), and the frequency of days of Very High and Extreme (VH+E) Forest fire danger. Both these measures capture the influences of higher temperatures, decreased rainfall and humidity, and increased wind speeds on drying out fuels and increasing likely fire behaviour, and therefore potential fire occurrence and impacts under climate change.

Results

In terms of future changes in fire climate severity, the impacts on the potential number of days of Very High and Extreme (VH+E) fire danger are arguably more intuitive than those for Seasonal Severity Rating (SSR), so are used here. Both relative (%) and absolute changes in fire danger were investigated, but caution needs to be applied when interpreting relative changes. The greatest percentage increases were predicted at stations where the current fire danger is negligible (e.g. West Coast – Westport (WSA) & Hokitika (HKA)), so that any increase proved highly significant. As a result, only absolute changes (in the number of days of VH+E fire danger) are discussed here[7]. These are summarised for fire season months for both the 2040s and 2090s in Table 4.3.1.

Results from the Pearce et al. (2011) study indicate that fire climate severity is likely to increase significantly with climate change in many parts of the country. This is primarily the result of increases in temperature and decreases in rainfall, although higher wind speed and lower humidity will also contribute to higher future fire danger.

The areas where fire dangers are most likely to increase from current levels, as indicated by the 16-model average (Table 4.3.1), were the east and south of the South Island, especially coastal Otago, Marlborough and south-eastern Southland, and the west of the North Island (particularly around Wanganui). There is also potential for increased fire danger under the most extreme model scenarios across the lower North Island and into the Bay of Plenty.

Fire dangers in other areas may remain unchanged, or in fact decrease by the 2090s, due mainly to increased rainfall. These areas include the West Coast of the South Island and western areas of the North Island such as Taranaki where fire dangers are already low, and East Cape and the Coromandel. Potential also exists for decreased fire danger in Northland, Southland and parts of Canterbury under some models.

Unlike the previous study (Pearce et al., 2005), eastern areas such as Canterbury and East Coast/Hawkes Bay did not show significantly increased fire potential. However, the low relative (%) increases at Gisborne Aero (GSA) and Christchurch Aero (CHA) corresponded to what is still a significant number of additional days of VH+E fire danger, due to their comparatively high current fire danger levels.

[7] see Pearce et al. (2011) for description of percentage changes in fire danger to both 2040 and 2090.

For example, Christchurch Aero (CHA) showed potential based on the 16-model average for an additional 5.4 and 8.6 days/season for the 2040s and 2090 respectively (up from the current 39.7 days, to 45.1 and 48.3 days/season), and maximum possible increases of 8.7 and 20.8 days (to 48.4 and 60.5 days/season). Similarly, 16-model average increases projected for Gisborne Aero (GSA) would correspond to an additional 6.6 and 9.8 days/season for the 2040s and 2090s (up from 34.1 days, to 40.7 and 43.9 days/season), with maximum increases of 9.9 and 20.5 days (to 44.0 and 54.6 days/season). So while demonstrating smaller potential percentage increases than many other locations, these projected changes would still see these areas continue to have some of the more severe fire climates in the country (see Figure 4.3.1).

Greater potential increases were projected for Wellington Aero (WNA), where the 16-model average indicated an extra 16.2 and 17.3 days/season for the 2040s and 2090s (up from the current 16.8 days, to 32.9 and 34.1 days/season), and maximum possible increases of 34.7 and 47.8 days/season (to 51.5 and 64.6 days season, respectively). In the latter case, this would result in WNA having one of the, if not the, most severe fire climates in the country (and higher than Christchurch Aero's 60.5 days/season of VH+E for the 2090s).

Table 4.3.1. Changes in the number of days of Very High and Extreme (VH+E) Forest fire danger for the 2040s (2030-2049) and 2090s (2080-2099) from current levels (1980-1999) projected from 16 GCMs at 20 station locations across New Zealand.

Station Code	Number of days/fire season of VH+E Fire Danger												
	Current VH+E (days/ season)	Models for 2040s						Models for 2090s					
		Model average (days/season)	Model range (days/season)	Average change (no. days)	Model range (no. days)	Average change (%)	Model range (%)	Model average (days/season)	Model range (days/season)	Average change (no. days)	Model range (no. days)	Average change (%)	Model range (%)
KX	**5.9**	**8.3**	(6.6 – 10.4)	2.5	(0.7 – 4.5)	42	(12 – 77)	**8.3**	(5.2 – 13.9)	2.5	(-0.6 – 8.0)	43	(-11 – 137)
DAR	**2.7**	**4.0**	(2.9 – 4.9)	1.4	(0.3 – 2.3)	51	(9 – 85)	**4.2**	(2.5 – 6.6)	1.6	(-0.2 – 4.0)	59	(-6 – 149)
COR	**1.5**	**2.1**	(1.6 – 2.6)	0.6	(0.1 – 1.1)	42	(7 – 73)	**2.2**	(1.5 – 3.3)	0.7	(-0.1 – 1.8)	44	(-3 – 120)
AKL	**8.3**	**12.2**	(9.6 – 14.9)	3.9	(1.4 – 6.6)	47	(16 – 80)	**12.4**	(7.7 – 22.0)	4.1	(-0.6 – 13.7)	50	(-7 – 166)
TGA	**7.7**	**9.8**	(8.6 – 12.1)	2.1	(0.9 – 4.4)	27	(12 – 56)	**10.1**	(8.0 – 14.1)	2.4	(0.3 – 6.4)	32	(3 – 83)
ROA	**1.5**	**2.6**	(1.8 – 3.5)	1.1	(0.3 – 2.0)	76	(17 – 133)	**2.6**	(1.7 – 4.9)	1.1	(0.2 – 3.4)	76	(10 – 223)
GSA	**34.1**	**40.7**	(35.7 – 44.0)	6.6	(1.6 – 9.9)	19	(5 – 29)	**43.9**	(34.2 – 54.6)	9.8	(0.0 – 20.5)	29	(0 – 60)
APA	**2.2**	**3.5**	(2.9 – 4.3)	1.3	(0.7 – 2.1)	60	(32 – 93)	**3.5**	(1.8 – 6.1)	1.3	(-0.4 – 3.9)	59	(-18 – 175)
NPA	**1.1**	**1.4**	(0.9 – 2.2)	0.4	(-0.2 – 1.1)	35	(-19 – 105)	**1.5**	(0.8 – 2.8)	0.5	(-0.3 – 1.7)	47	(-24 – 162)
WUA	**2.6**	**5.5**	(4.1 – 8.0)	3.0	(1.6 – 5.5)	117	(61 – 214)	**5.8**	(3.0 – 12.2)	3.3	(0.4 – 9.6)	129	(16 – 376)
PPA	**2.0**	**3.8**	(2.6 – 6.5)	1.9	(0.6 – 4.5)	97	(31 – 231)	**4.7**	(2.4 – 12.3)	2.8	(0.4 – 10.4)	142	(21 – 531)
WNA	**16.8**	**32.9**	(23.9 – 51.5)	16.2	(7.1 – 34.7)	97	(42 – 207)	**34.1**	(16.2 – 64.6)	17.3	(-0.6 – 47.8)	103	(-4 – 285)
NSA	**8.9**	**12.4**	(11.0 – 14.8)	3.5	(2.1 – 6.0)	40	(24 – 67)	**12.8**	(9.0 – 18.4)	3.9	(0.1 – 9.6)	44	(1 – 108)
WSA	**0**	**0.01**	(0 – 0.1)	0.01	(0 – 0.1)	0	(0 – 1000+)	**0.03**	(0 – 0.2)	0.03	(0 – 0.2)	0	(0 – 2000+)
HKA	**0**	**0**	0	0	0	0	0	**0**	0	0	0	0	0
KIX	**6.3**	**14.7**	(9.1 – 23.4)	8.4	(2.8 – 17.1)	134	(44 – 271)	**15.2**	(6.8 – 30.7)	8.9	(0.5 – 24.4)	142	(7 – 387)
CHA	**39.7**	**45.1**	(38.4 -48.4)	5.4	(-1.4 – 8.7)	13	(-3 – 22)	**48.3**	(41.8 – 60.5)	8.6	(2.1 – 20.8)	22	(5 – 52)
QNA	**5.7**	**7.0**	(5.2 – 8.7)	1.3	(-0.5 – 3.0)	23	(-9 – 53)	**8.0**	(5.8 – 11.2)	2.3	(0.1 – 5.5)	41	(3 – 97)
DNA	**5.7**	**18.3**	(13.3 – 29.7)	12.6	(7.6 – 24.0)	220	(133 – 421)	**22.2**	(13.8 – 44.3)	16.5	(8.1 – 38.6)	290	(142 – 676)
NVA	**0.4**	**0.9**	(0.5 – 1.7)	0.5	(0.1 – 1.3)	129	(25 – 325)	**1.3**	(0.6 – 3.1)	0.9	(0.2 – 2.7)	222	(38 – 663)
Avg.	**7.6**	**11.3**	**(0 – 51.5)**	**3.6**	**(-1.4 – 34.7)**	**64**	**(-19 – 1000)**	**12.1**	**(0 – 64.6)**	**4.4**	**(-0.6 – 47.8)**	**79**	**(-24 – 2000)**

Despite a more benign current fire climate, Dunedin Aero (DNA) also showed the potential for significant increases. In fact, it demonstrated the greatest potential relative increases (of over 200%), representing a likely trebling of its current fire danger level. The increases projected by the 16-model average corresponded to potential for an additional 12.6 and 16.5 days/season of VH+E fire danger for the 2040s and 2090s (up from the current 5.7 days, to 18.3 and 22.2 days/season). Even greater possible increases were indicated under the most extreme models, with an additional 24.0 and 38.6 days (up to 29.7 and 44.3 days/season). These are very dramatic potential increases for this region in the likelihood of days of VH+E fire danger on which any fires would be difficult, if not impossible to control.

The projected changes found in the Pearce et al. (2011) study were generally greater than those found previously (Pearce et al., 2005; Pearce & Clifford, 2008). However, they also varied more widely between GCMs due to greater ranges in projected changes, especially seasonal differences in rainfall and temperature.

While many of the GCMs used by Pearce et al. (2011) showed continuing increases through to the 2090s, a feature of several models was for fire danger to increase more rapidly to the 2040s, and then to stabilise or decrease by the 2090s. This levelling off was due to greater predicted increases in rainfall (especially during fire season months) in these models for the latter part of this longer projection period.

Projected regional changes were also mapped to illustrate potential changes across the country for the 2040s and 2090s, again using the 16 model averages (Figure 4.3.1). While results were also calculated for the full calendar year, those presented here are based on changes predicted for the recognised fire season period (October to April), when higher fire dangers and the majority of fires are likely to occur.

Maps of projected changes in fire danger were produced by interpolating the changes predicted at each of the 20 station locations. Final maps were produced through cokriging, using station location (latitude/longitude) and elevation as surface prediction variables, as well as the fitted surface for current fire climate severity (for days of VH+E fire danger) derived from data for 77 station locations by Pearce et al. (Pearce, Kerr, Clifford, et al., 2011). The inclusion of the latter significantly improved the prediction of potential changes at locations remote from the sampled station sites, although caution should still be applied when interpreting the maps for these locations due to the interpolation being based on such a relatively small number of data points (only 20 stations).

The changes found by Pearce et al. (2011) would see areas of elevated fire danger under current climate in Canterbury, Gisborne, Marlborough and Central Otago/South Canterbury (Figure 4.3.1, left) expand along the east coast of both islands to include coastal Otago, Wellington and Hawkes Bay by the 2040s (Figure 4.3.1, centre). These elevated risks are likely to develop further in Marlborough, Hawkes Bay and Wairarapa by the 2090s (Figure 4.3.1, right). Fire dangers in Wanganui, the Bay of Plenty and Northland would also increase. However, despite significant relative (%) increases in Southland, south Taranaki and the Coromandel, fire climate severity in these areas would increase but still remain comparatively low relative to other parts of the country (Scion, 2011b).

Discussion

Results from Pearce et al. (2011) indicate that changes in overall fire climate severity are also associated with significant changes in the contributing fire danger ratings (FWI System values). These indicate that fire managers can expect increased drought frequency, as well as potential for longer fire seasons in some parts of the country. These in turn could contribute to an increased number of fires or greater areas burned, and

(a) Current

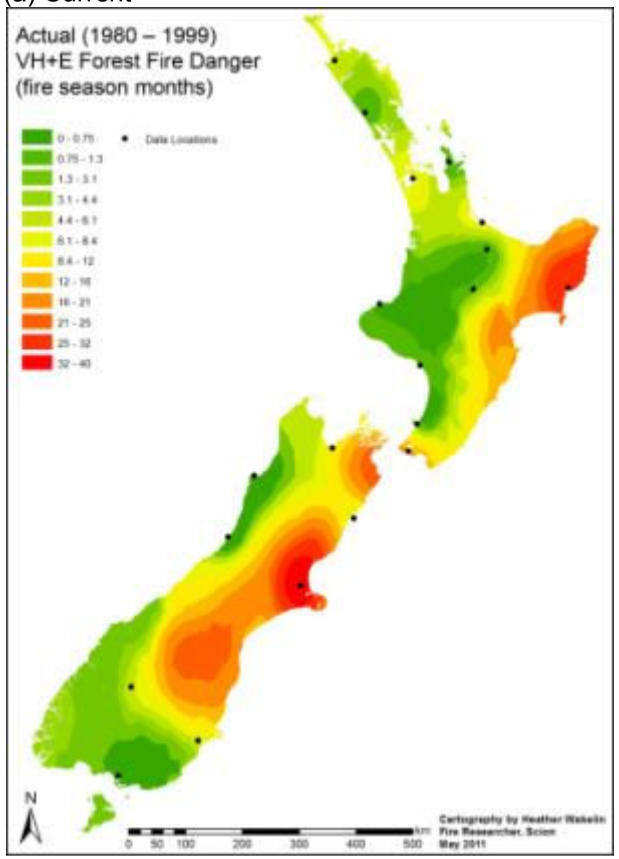

(b) 2040s

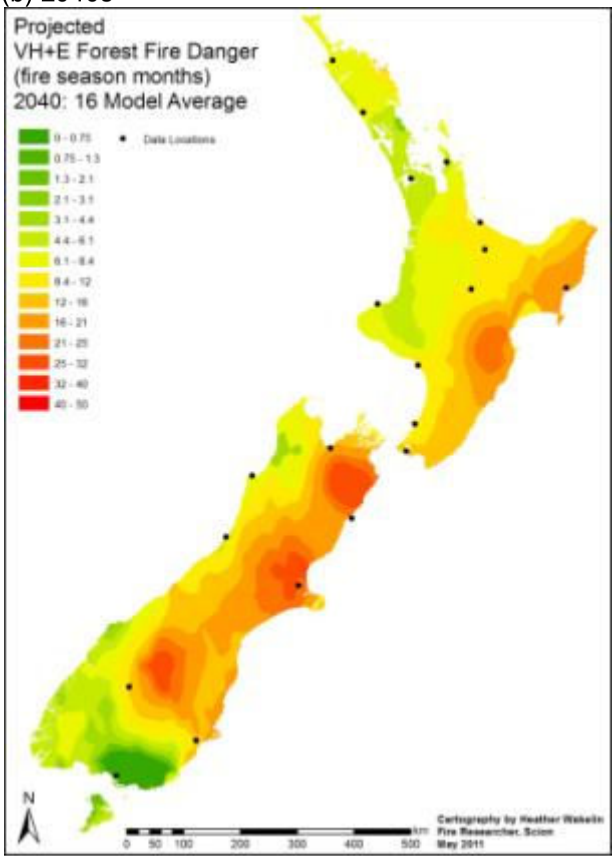

(c) 2090s

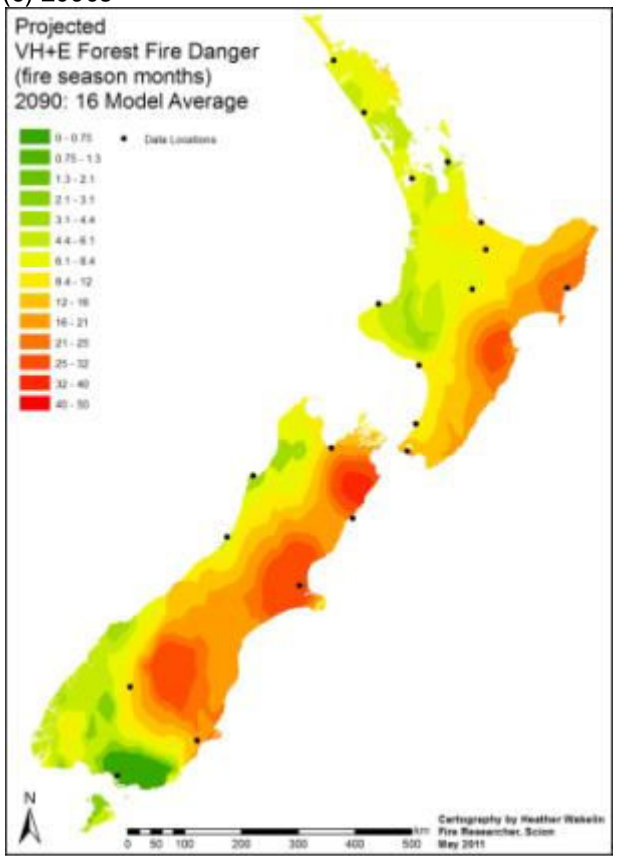

Figure 4.3.1. Pattern of projected changes in the average number of days/year of Very High and Extreme (VH+E) Forest Fire Danger over fire season months (Oct-Apr) from (a) current climate, to (b) the 2040s (2030-2049), to (c) the 2090s (2080-2099), based on the overall average of the 16 GCMs investigated.

increased fire suppression costs and damages. However, further research is required to more clearly define the relationships between fire danger ratings and fire occurrence potential. Planned research to address this issue was not possible here due to problems with the quality, completeness, and regional and seasonal accumulation of fire occurrence data. These issues need to be rectified at the national level as a matter of urgency if better information on current and future fire impacts is to be obtained. This includes enabling analyses of relationships between fire occurrence and current and future fire climate to be undertaken (Anderson et al., 2008; Watt et al., 2008).

In the interim, the mapping of likely changes in future fire danger provides an indication of potential impacts of climate change on fire risk and, in turn, forest productivity. Comparison of the levels of fire danger for current (1990s) climate with that for the 2040s and/or 2090s provides a forest owner with an idea of the level of fire risk for their location. In terms of the number of days/fire season of Very High and Extreme (VH+E) forest fire danger, the following general classification applies:

Risk Class	No. days/fire season of VH+E fire danger
Low	0 – 5
Moderate	6 – 10
High	11 – 20
Very High	21 – 30
Extreme	>30

The frequency of days of VH+E fire danger indicates the number of days on which fire outbreaks would be difficult, if not impossible, to control based on their likely fire intensity. Thus, an indication that the number of days of VH+E fire danger at a site has the potential to increase from about 6 days/season currently, to around 18 days by the 2040s and more than 22 days/season by the 2090s (as in the case of Dunedin Aero, DNA; see Table 4.3.1), shows the potential for a significant increase in fire risk and associated fire impacts on forest productivity. In comparison, an indicated increase from 34 days/season currently to 41 days by the 2040s and 44 days/season by the 2090s (as for Gisborne Aero, GSA), may not be as significant but still indicates continuing potential for high forest productivity losses due to extreme fire risk.

It should be noted that this assessment only includes the effects of climate on fire behaviour potential in a mature pine stand, and does not capture any additional effects of topography (i.e. slope) or fuel type differences which could increase fire behaviour further. Similarly, the fire danger class frequencies indicated represent the average number of days of VH+E fire danger/season. There will be considerable variability from year to year at most sites as a result of normal seasonal climate patterns (e.g. La Nina & El Nino), producing higher numbers of days of VH+E fire danger in some years than indicated by the average, and less in others. There is also some evidence that the frequency of extremes may increase with climate change (Hasson et al., 2008; Plummer et al., 1999), suggesting extreme years with higher frequencies than the average may become even more common.

Potential damage to or loss of plantations from fire is a major risk facing forest owners and, due to the value of the asset being protected, fire has been an important consideration for New Zealand forestry since plantations were first established in the mid-1890s (Pearce et al., 2008). Radiata pine, which makes up the majority of New Zealand's plantation forests, has very low tolerance to fire. Any heating of the cambium through the relatively thin bark or of roots through shallow soil, or damage to live foliage from crown fire or heat scorch, is normally sufficient to kill trees. Other plantation species such as Douglas-fir and eucalypts are more fire-adapted (e.g., thicker bark, self-pruning), and will survive all but the most severe fires (Watt et al., 2008).

During the last 60-70 years, fires have resulted in over 40 000 ha of exotic plantation forest being burned (with a conservative value in excess of $300M), at an annual loss of around 570 ha (0.12% of the planted estate). The average annual loss over the past decade (to 2007) is somewhat lower (about 380 ha/annum or 0.02% of the plantation estate), largely due to improvements in fire management and a reduction in forestry prescribed burning (and associated risk of escapes) (Cameron et al., 2007). However, current plantation fire statistics are unreliable due to poor reporting and confidentiality issues (Cameron et al., 2007; Doherty et al., 2008).

The physical and economic effects of a forest fire depend on the fire intensity and areal extent, as well as other factors such as the species, silvicultural management and forest purpose. The most obvious costs are those associated with crop loss, fire suppression, and re-establishment, although these may be offset in some cases through insurance or salvage. However, fires can also have indirect costs that may be even more significant than these direct losses. These can include effects on infrastructure (road, rail or powerline damage or closures), tourism and recreation (aesthetics and access), environmental impacts (erosion, water supply contamination, nutrient loss) and effects on human health (smoke pollution, mental and emotional effects). Downstream impacts on the local, regional, and even national economies can also be significant, including potential for mill closures, job losses, reduced export revenue, and all of the consequent effects on support industries and affected communities. The greater variety of reasons for growing forests, for bioenergy, carbon, protection and recreation, as well as traditional forestry and wood products, is also an increasingly important consideration, as these can incur additional costs (e.g. associated with loss of carbon).

Typically, forest fires are therefore considered to negatively impact on forest productivity by damaging or killing trees and reducing recoverable wood volume. Fire can also play a significant role in reducing the productivity of forest ecosystems through the loss of nutrients contained in vegetation and upper soil layers to the atmosphere through volatilisation, in run-off or wind dispersion of ash (Harwood & Jackson, 1975; Raison, 1979). Intense fires can also result in loss of organic matter and microbial activity (Covington & Sackett, 1984; Goh & Phillips, 1991), and produce significant changes in soil structure leading to increased erosion (DeBano et al., 1998; Leitch et al., 1983). An increase in fire frequency and associated area burned with climate change could therefore result in reduction in forest soil productivity, and an increased need for fertiliser application for forest re-establishment following fire (Watt et al., 2008).

Increased fire risk through drier and warmer conditions does not however necessarily imply an overall loss in forest productivity. In a case study for Swiss forests examining climate change and forest growth using the European Forest Information Scenario Model (EFISCEN) (Sallnäs, 1990), Schelhaas et al. (2002) found the net effect, which accounted for losses due to fire and other disturbances and gains due to growth, to be positive. Meyer (2005) also used EFISCEN to examine the effects of fire, both current and future, in the French Mediterranean area. The EFISCEN model is suited to slow-growing, even-aged managed forest in the European region. Management options are limited to thinning and felling, but mortality due to natural mortality, insects, disease, windthrow and fire can also be included in the simulations. Fire hazard is taken as a proxy for warm and dry years. Within the model, actual damage in a certain time step depends on the hazard type, vulnerability and area of exposure, and is modelled using Monte Carlo simulations.

Increased fire frequency with climate change could however result in a need for greater areas of productive forest land to be set aside for fire protection works, such as firebreaks, waterpoints, or fuel breaks/buffer zones of less flammable (and less productive) species. This, combined with the likelihood of increased expenditures on fire prevention activities, provision of firefighting resources and fire suppression, could have a significant impact on the economics of forestry.

The effects of fire on forest productivity are also likely to be exacerbated through interactions with other factors that are likely to be modified as a result of climate change. There are obvious links between drought and fire risk, and increased drought risk with climate change (Mullan et al., 2005) would result in drier and more available and continuous fuels, and therefore potentially more frequent and severe fires and larger areas burned. Changes in the extent and distribution of weeds with climate change could lead to more flammable fuel types, especially woody scrub (e.g., gorse, broom) and grass weeds, that are more flammable and carry higher/more available fuel loads (Watt et al., 2008). These ignite more readily, burn more intensely and are harder to extinguish, potentially resulting in larger areas burned.

There are also links between fire damage and insect attack, whereby fire-damaged forest areas can be favourable to some insect species (e.g., bark beetles; (Bradbury, 1998; Suckling et al., 2001)). Increased fire risk with climate change could therefore lead to more widespread insect outbreaks and greater damage to forest areas adjacent to burnt areas. Conversely, insect attack can also lead to increased fire hazard by producing higher fuel loads and greater availability of dead fuels (e.g., spruce budworm and mountain pine beetle-killed forest in Canada). New insect invasions through climate change could therefore result in increased forest damage and fire-susceptibility. An increase in the frequency of extreme climatic events with climate change, such as tropical cyclones and wind storms, could also result in greater wind damage and therefore increased fuel hazard in forest areas. More dead, downed woody fuels would potentially lead to higher risk of ignitions, more intense fires and greater areas burned (Watt et al., 2008).

Adaptation and mitigation of increasing fire risk with climate change therefore requires an awareness of how fire risk is changing over time, and development of appropriate fire management strategies to deal with these changes. This includes fire prevention activities such as education, fire danger rating burning and access controls aimed at reducing fire occurrence, as well as fuel reduction (including via silviculture, such as pruning and thinning), and use of firebreaks and less flammable species aimed at reducing fire consequences. Fire readiness actions, including training and equipment, fire weather monitoring and prediction of fire behaviour potential, should also be used as the basis for being able to respond more quickly and effectively when fires occur. Increased fire suppression capability is also likely to be required to cope with a greater number of fires and area burned, including fostering relationships with neighbouring forest owners and fire authorities, and use of the Coordinated Incident Management System (CIMS) to more effectively and efficiently manage large fire events. Maintaining appropriate fire management strategies, especially around fire prevention, readiness and response, will therefore be essential to mitigating the risks associated with increasing fire danger.

4.4 Impact of climate change on wind risk

Abstract

Wind is the major abiotic factor responsible for damage to New Zealand's planted forests. A mechanistic wind damage model (ForestGALES) was linked to various empirical growth models and a process-based growth model (CenW) to investigate potential impacts of future climate change on the risk of wind damage. Hourly wind speed data from the National Climate Database and the National Rural Fire Authority's fire weather network were analysed and used to develop a surface showing the spatial variation in extreme wind speed.

The spatial variation in extreme wind speed was related to vapour pressure deficit, TOPEX (an index of local topographic exposure) and November rainfall. The regression model developed in this study explained approximately 58% of the variation in extreme wind speed and can be used to compare the relative risk of damage at different locations throughout New Zealand. Literature on the predicted impacts of future climate change on the extreme wind climate were reviewed and these indicate that there will be an increase in extreme wind speeds, but that these increases will be modest (only a few per cent).

Increased tree growth rates under the different emissions scenarios had the most significant impact on the risk of wind damage. The increases in risk were most pronounced for the A2 scenario with increased CO_2 concentration in the atmosphere. The risk was further increased by the modest increases in the extreme wind climate that are predicted to occur.

Introduction

Wind is a significant disturbance agent in New Zealand's forests, with most damage resulting from extra-tropical depressions or from topographically-enhanced westerly air flows (Martin & Ogden, 2006). In planted forests, records of wind damage events date back as far as 1940 (Somerville, 1995; Thompson, 1976), with many of these events resulting in considerable financial loss. Prior to the late 1970s, wind damage was generally viewed as a problem that was confined to Canterbury and other parts of the South Island, such as Nelson and Otago/Southland. However, this view changed as a result of storms that occurred in the central and upper North Island in 1979, 1982 and 1988. In particular, south-easterly winds during Cyclones Bernie (1982) and Bola (1988) caused severe damage to 5 000 ha and 26 000 ha of planted forests, respectively (Carter, 1989; Moore et al., in review; New, 1989) . Most recently, significant amounts of damage have occurred in forests located in the southern part of the North Island. Available records document approximately 63,000 ha of damage, while significant amounts of less severe damage (ranging from isolated trees to small groups of trees) has not been recorded (Moore et al., in review; Somerville, 1995).

There is considerable uncertainty around the potential impacts of future climate change on the risk of wind damage to planted forests in New Zealand. This arises from uncertainty around the future extreme wind climate and how the forest will respond. In recent years there has been a considerable amount of work undertaken to investigate what the impacts of future climate change will be on the extreme wind climate in New Zealand (Ministry for the Environment, 2008; Mullan et al., 2011; Wratt et al., 2004). In this most recent report (Mullan et al., 2011) conclude that "*the frequency of extreme winds over this century is likely to increase in almost all regions of New Zealand in winter and decrease in summer especially for the Wellington region and the South Island. However, the magnitude of the increase in extreme wind speed is not large – only a few per cent by the end of the century under the middle-of-the-range A1B emission scenario*". In the earlier report into the impacts of future climate change on New Zealand's planted forests (Watt et al., 2008), we used the approach taken by Quine and Gardiner (2002) to undertake a sensitivity analysis showing the impacts of a 1, 5 and 10% increase in extreme wind speed on the risk of damage for radiata pine stands growing in the Central North Island and Canterbury. This analysis showed that for stable stands with a low risk of damage, small to moderate changes in the future extreme wind climate increases may only have a negligible impact on the risk of damage. However, for those stands which are more vulnerable, even relatively small changes in the future extreme wind climate could have large impact on the risk of damage.

This earlier analysis did not consider what impact increased tree growth might have on the risk of wind damage. This effect has been shown to be highly significant for Swedish forests (Blennow & Olofsson, 2008; Blennow, Andersson, Bergh, et al., 2010; Blennow, Andersson, Sallnas, et al., 2010). Until recently, we lacked a means to quantify changes in forest productivity under future emissions scenarios. However, spatially explicit estimates of radiata pine productivity now exist for the different future emissions scenarios (see Section 3.1) and these can now be used in conjunction with a mechanistic wind damage model (Moore & Somerville, 1998) to investigate the impacts of tree growth and the extreme wind climate on the risk of wind damage.

In this study a mechanistic wind damage model and a stand growth and yield model was used to assess the relative risk of wind damage to radiata pine.

Wind firmness of radiata pine

Biomechanical characteristics that affect the wind firmness of a tree include stem form, wood strength, root anchorage strength, crown frontal area, crown mass and crown drag coefficient. The ForestGALES model developed by Gardiner et al. (2000) uses this information to calculate the critical wind speed necessary to uproot or break a tree. The model has been parameterised for radiata pine growing in New Zealand (Moore and Somerville, 1998) and has also been used to compare the relative wind firmness of radiata pine and Douglas-fir (Moore and Gardiner, 2001). Information on root anchorage strength has been collected for a number of tree species around the world through tree winching studies (Moore, 2000; Nicoll et al., 2006; Peltola et al., 2000). These studies have shown that root anchorage strength (as measured by the maximum bending moment that a tree can resist) is strongly related to stem mass (or volume). Nicoll et al. (2006) have also shown that the anchorage strength of UK-grown conifer species was strongly dependent on soil type, but that species differences did exist. In New Zealand, Moore (2000) found that the anchorage strength of radiata pine differed across soil types, but for a given soil type (in this case pumice soils) Moore and Gardiner (2001) found that there was no difference in the anchorage strength of radiata pine and Douglas-fir trees of the same size.

Impacts of future climate change on the risk of wind damage to radiata pine stands

Previous simulations of the impacts of future climate change on the risk of wind damage to planted forests only considered the effects of a changing wind climate (Watt et al., 2008). However, increasing tree growth under a warmer climate could make trees more vulnerable to wind damage at a younger age, and could increase the amount of time that trees have a higher risk of wind damage unless the rotation length is reduced (Blennow and Olofsson, 2008; Blennow et al., 2010a,b). These authors used a process-based biomass model to estimate the change in net primary production (NPP) under different future emissions scenarios and were able to relate the relative change in NPP to a relative change in site productivity as measured by site index. From this, they used a forest growth simulator to predict the state of the forest at different points into the future and then calculated the risk of wind damage using a mechanistic wind damage model. Finally, the future extreme wind climate and hence the probability that the critical wind speed for damage was exceeded was determined from regionally downscaled runs from a global circulation model. For their case study area in southern Sweden, Blennow et al (2010a) found that a greater proportion of the predicted change in the risk of wind damage was due to changes in wind climate than to changes in the sensitivity of the forest to wind.

A similar approach was applied to radiata pine growing in New Zealand (Figure 4.4.1). Changes in future radiata pine productivity have been determined for the different emissions scenarios using the process based model CenW. These changes have been related to changes in the 300 index and site index, which are used to parameterise a growth model. Predictions of future stand structure and wind climate are then passed to ForestGALES, which predicts the future risk of wind damage.

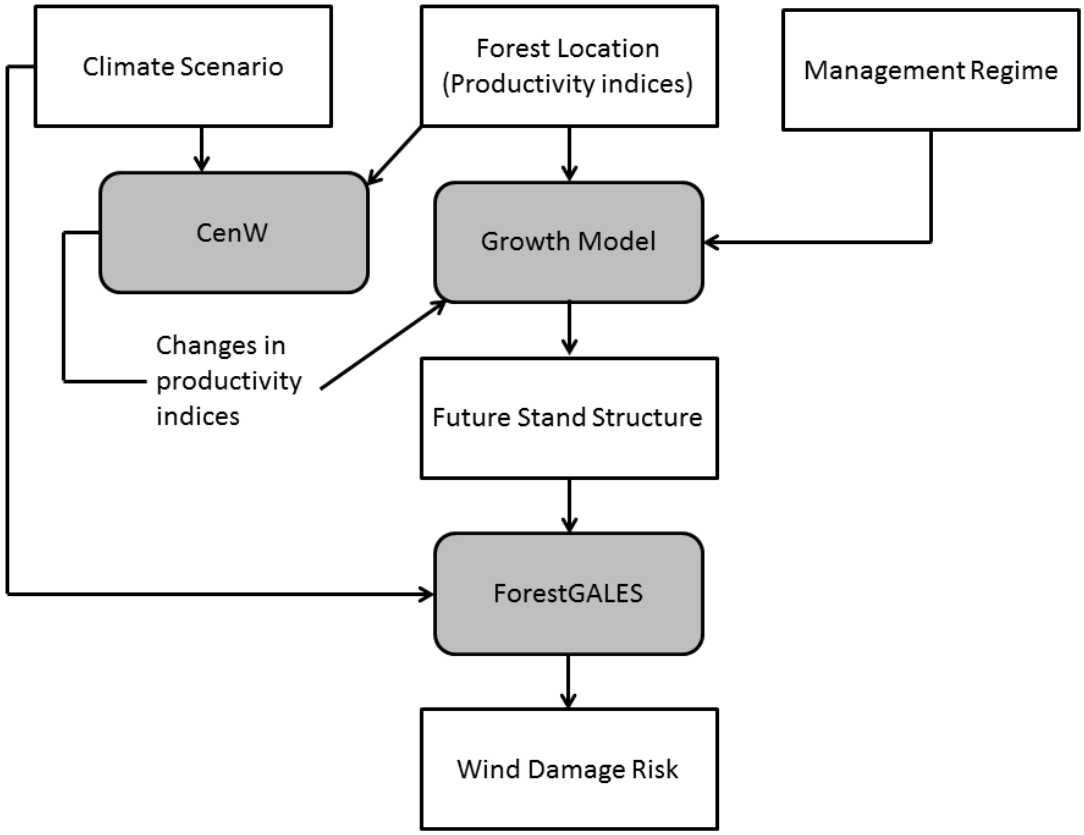

Figure 4.4.1. Flow chart showing how the impacts of future climate on the risk of wind damage were modelled.

Spatial variability in extreme wind speeds

One of the challenges when attempting to predict the risk of wind damage to forests is to predict the spatial variability in the wind climate. A number of approaches have been used in different parts of the world, ranging from numerical airflow models (Ruel et al., 1997), topographic indices (Quine & White, 1994) through to spatial interpolation from meteorological stations (Mullan et al., 2011). In New Zealand, NIWA has developed a Virtual Climate Station Network (VCSN), which covers the country on a 0.05° latitude by 0.05° longitude grid. Wind speed values are available from 1 January 1997 and the spatial variation in the top 1% of daily wind speed values is shown in Figure 4.4.2.

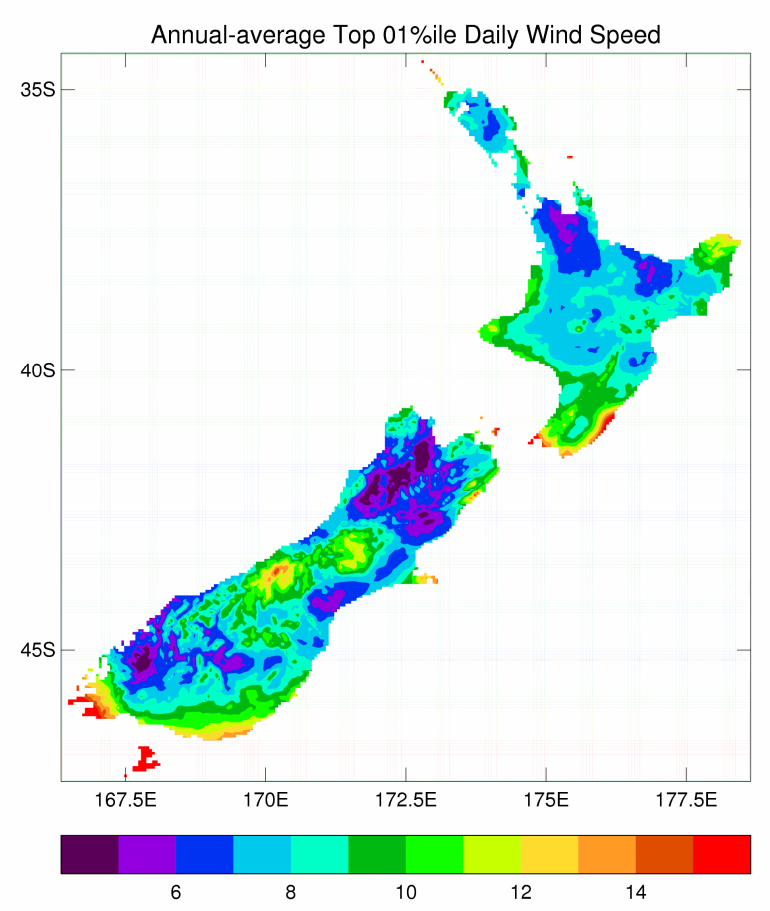

Figure 4.4.2. Spatial distribution of the top 1% of daily wind speeds (m/s) in NIWA's Virtual Climate Station Network gridded wind dataset (from Mullan et al., 2011).

While this information is useful for showing the spatial variation in strong winds, quantitative predictions of future wind damage risk require information on the return periods of extreme hourly wind speeds. This can be determined for meteorological stations with long-term continuous records using standard extreme value analysis techniques. Unfortunately, many (if not most) of the meteorological stations which have a suitably long length of record are located at airports and away from forested areas. There are also very few stations with sufficiently long length of record (>20 years) for this type of analysis. Another option is to use the relationship between the parameters describing the distribution of mean hourly wind speeds (typically these data follow a 2-parameter Weibull distribution, which has location and scale parameter) and those of the Gumbel distribution for the annual maximum wind speeds.

The annual probability of a critical wind speed (u) for damage to occur being exceeded is given by the following equation:

$$AEP = 1 - exp\left(-exp\left(-\left(\frac{u-V}{\frac{1}{a}}\right)\right)\right) \qquad [4.4.1]$$

where V and 1/a are the mode and dispersion parameters respectively of the extreme value distribution for annual maximum hourly wind speed. It has been shown that a slightly better fit occurs when using u^2 rather than simply u, such that:

$$AEP = 1 - exp\left(-exp\left(-\left(\frac{u^2-U}{\frac{U}{Ua}}\right)\right)\right) \qquad [4.4.2]$$

where:

$$U = (A\,U_c)^2 \quad [4.4.3]$$

$$U_c = 13.5690 - 11.8633k + 4.4345k^2 - 0.590k^3 \quad [4.4.4]$$

$$U_a = 5 \quad [4.4.5]$$

In these equations A and k correspond to the location and scale parameters, respectively, of a 2-parameter Weibull distribution fitted to data on hourly mean wind speed (Quine, 2000).

In order to develop a spatially explicit model for the *U* parameter in Eq. [4.4.3], hourly wind speed data were obtained for all stations in NIWA's National Climate Database that contained at least five years' worth of data; in total this was 148 stations. Data were also obtained from a further 149 stations that were part of the National Rural Fire Authority's (NRFA) network (Table 4.4.1). The location of these stations is shown in Figure 4.4.3.

Table 4.4.1. Summary information for the data used to develop the spatial surfaces of extreme wind speed. Mean values of the Weibull *A* and *k* parameters are given along with the range of values.

Network	Number of stations	Weibull *A*	Weibull *k*
NIWA	148	4.75 (1.46, 14.16)	1.65 (1.10, 2.36)
NRFA	149	3.79 (0.73, 10.49)	1.46 (0.94, 2.08)
Overall	297	4.27 (0.73, 14.16)	1.55 (0.94, 2.36)

For each of the 297 stations, a 2-parameter Weibull distribution was fitted to the time series of hourly mean wind speed values. The value of *U* was calculated from these Weibull *A* and *k* parameters using Eq. [4.4.3] and [4.4.4]. A number of different variables were tested for their ability to explain the spatial variability in *U*. The final model included vapour pressure deficit (VPD), TOPEX (an index of local topographic sheltering) and mean November rainfall (NovRain) as described in the following equation,

$$\sqrt{U} = 61.52 - 143.21VPD + 105.4VPD^2 - 0.0028TOPEX - 0.021NovRain \quad [4.4.6]$$

The two climatic variables appear to explain differences between the wet, less windy areas such as the West Coast of the South Island and the drier windier parts of the country. The significance of TOPEX reflects the fact that higher wind speeds are found on the tops of hills compared with more sheltered valleys. The model was able to account for 58% of the variation in *U*; 54% from the multiple linear regression model and an additional 4% through kriging of the residuals. The spatial surface showing the variation in extreme wind speed is shown in Figure 4.4.3. For ease of presentation and interpretation we have shown the square root of *U* (i.e. $U^{0.5}$) in this figure. This can loosely be interpreted as the modal value of the extreme wind speed distribution.

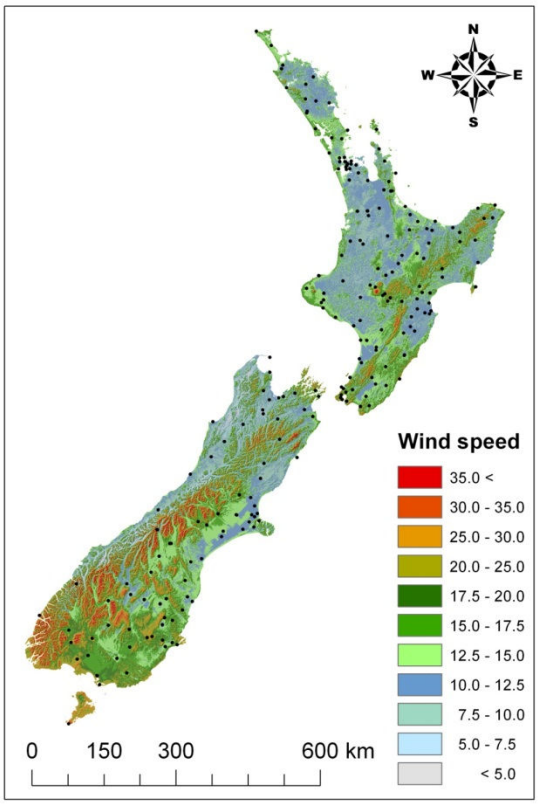

Figure 4.4.3. Spatially interpolated surface showing the distribution of extreme wind speeds ($U^{0.5}$). The location of the meteorological stations used to develop this surface are indicated with black dots.

Changes in extreme wind speeds under climate change

Future trends in extreme wind speeds for New Zealand have been investigated by Wratt et al. (2004), Ministry for the Environment (2008) and Mullan et al. (2011). All of these studies suggested that future changes in extreme wind speeds are likely to be small and will vary in magnitude across different regions of New Zealand. In order to determine whether there are likely to be any significant changes in the parameters describing the distribution of extreme wind speeds, data from the Regional Climate Model (RCM) runs were analysed. These data consisted of the annual maximum mean hourly wind speed and the annual maximum wind speed for the periods 1971-2000 and 2071-2100 (assuming the A2 emission scenario). The Regional Climate Model was run for a 0.27° latitude by 0.27° longitude grid, which is a much coarser resolution than the VCSN.

For each grid point in the simulation, a Gumbel distribution was fitted to the time series of annual maximum mean hourly wind speeds. This was done separately for the two 30-year periods and yielded a value of the mode and dispersion parameter for each grid point. These values were then used to predict the annual probability of a wind speed in excess of 25 m/s for the period 1971-2000 and 2071-2100. From these simulations, it is apparent that the highest wind speeds occur through Cook Strait and off the coast of south Westland (Figure 4.4.4). The probability of a wind speed in excess of 25 m/s is considerably lower on land than it is over the ocean, with the exception of the land near Cook Strait, Foveaux Strait and the top of the Southern Alps. There was very little difference in the probabilities between two time periods, with only a few areas predicted to have an increase in the exceedance probability of up to 5-10%. Because of the relatively low resolution of the simulations, the earlier analysis based on actual observations will be used to calculate the probability of a wind speed being exceeded at particular location. This approach has been incorporated into the decision support tool.

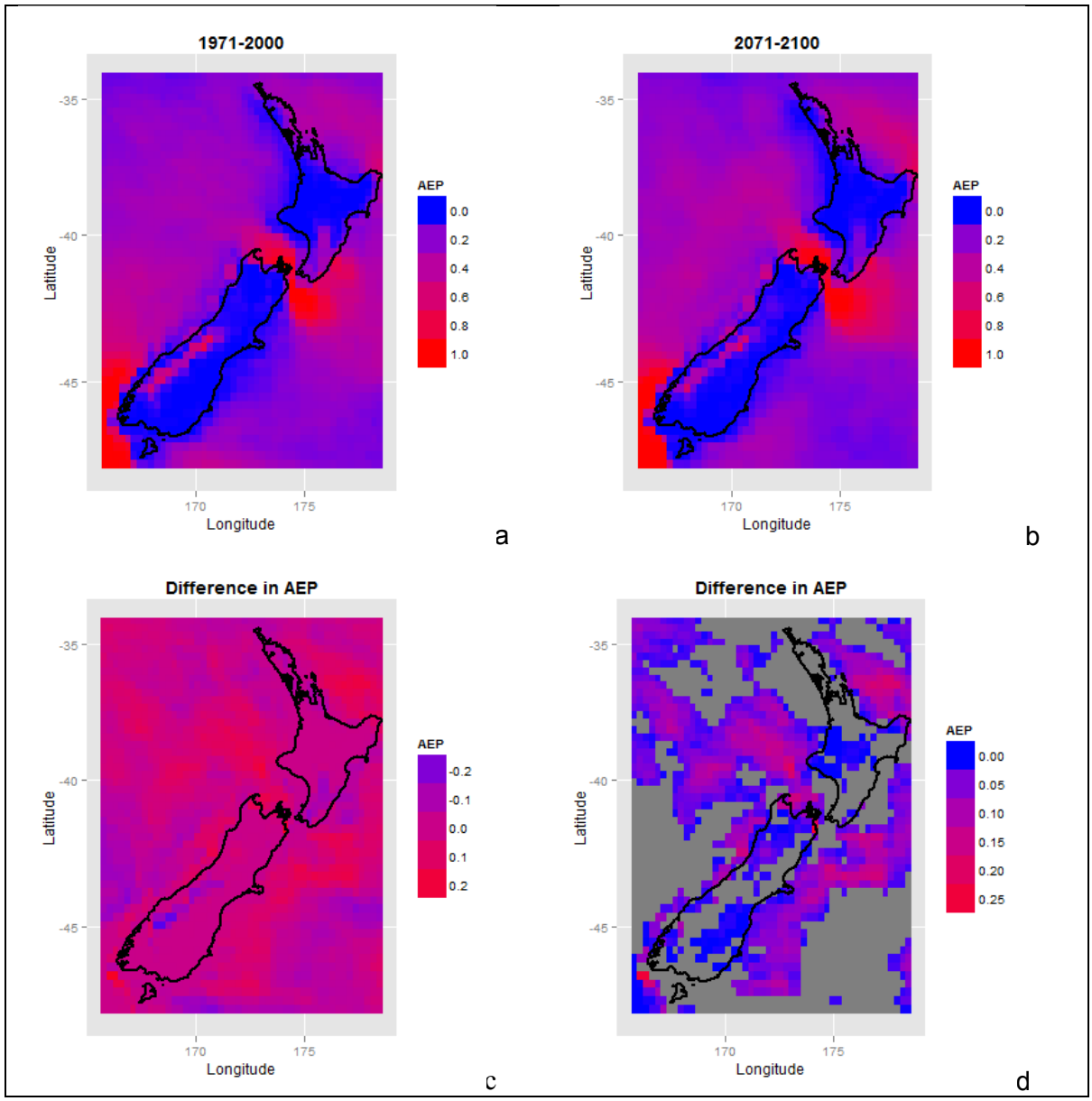

Figure 4.4.4. Regional Climate Model simulations of the extreme wind speeds for the periods1971-2000 and 2071-2100. The annual probability of an extreme wind speed in excess of 25 m/s was calculated for the two periods (a,b), along with the difference in this annual probability (c). Those areas where the probability is predicted to increase are highlighted (d).

Comparison of different silvicultural regimes

The risk of wind damage was predicted for three contrasting radiata pine regimes under current and future climate scenarios. These regimes are briefly described in Table 4.4.2 and are the standard regimes used in other areas of this report as well as in the decision support system that has been developed (see Section 5). Each regime was modelled using a growth simulator, which was developed from meta-modelling the output from the Forecaster growth model for a range of sites across New Zealand. The geographic location chosen for the simulations had values of site index and 300 index, respectively, that were close to the national mean values of 29.8 m and 25.2 m^3/ha/year (Mark Kimberley, unpublished data). The changes in these productivity indices were taken from the CenW simulations reported in Section 3.1 (Table 4.4.3). The annual probability of damage was calculated using Eqs. [4.4.2] – [4.4.5], with national average values of the Weibull *A* and k parameters taken from Table 4.4.1.

Table 4.4.2. Characteristics of the three radiata pine silvicultural regimes.

Event	Regime		
	Pruned	Unpruned	Carbon
Initial stocking (stems/ha)	720	900	1020
First thinning	500 stems/ha @ age 7	600 stems/ha @ age 8	-
Second thinning	380 stems/ha @ age 9	-	-

Table 4.4.3. Values of 300 index and site index used to initiate the model runs for the current climate and for the different future emission scenarios, with (Y) and without (N) the effects of increased CO_2 concentration considered.

Year	Scenario	Increased CO_2 conc.	300 Index	Site Index
1990			24.74	33.4
2040	B1	N	26.60	35.2
2040	A1B	N	26.82	35.5
2040	A2	N	26.68	35.4
2040	B1	Y	30.75	37.0
2040	A1B	Y	32.00	37.8
2040	A2	Y	31.81	37.7
2090	B1	N	27.65	36.3
2090	A1B	N	28.05	37.5
2090	A2	N	28.40	38.2
2090	B1	Y	34.50	39.3
2090	A1B	Y	39.18	42.3
2090	A2	Y	41.88	44.0

Under current climatic conditions, all three regimes had very similar critical wind speed values from approximately 30 years of age onwards, although stands grown on pruned and un-pruned regimes were less wind-firm than the stand grown on a carbon regime prior to age 20 years (Figure 4.4.5). The annual probability of damage was relatively low for all regimes, reflecting the relatively benign extreme wind climate at the site. On sites with a more severe wind climate the relative wind risk for the difference regimes would be more pronounced.

Under the future climate scenarios the critical wind speed for damage decreased (Figure 4.4.6). This was most pronounced under the A2 scenario with increased CO_2 concentration. These differences in the critical wind speed translated into large differences in the risk of damage. For example, the risk of damage to the carbon regime was very low under 1990 conditions, but increased substantially under the 2040 and 2090 A2 emissions scenarios (Figure 4.4.7). The risk increased further if a 5% increase in the extreme wind climate was

also assumed, but this increase was less than that due to the increase in forest productivity. The increased growth rate of the trees means that they reach a larger size more rapidly and the onset of mortality also occurs at a younger age (Figure 4.4.8). This may help to explain why the stands are predicted to be more wind-firm initially under this scenario but then to be more vulnerable later on. Under the most extreme A2 scenario, both the pruned and un-pruned stands have reached the zone of imminent mortality by the time of first thinning. Under these conditions the trees would be relatively slender and there would be a relatively high risk of wind damage following thinning. With increased growth rates it is likely that thinning operations would be carried out earlier and rotation lengths would also be shortened as trees would have a reached a merchantable size earlier.

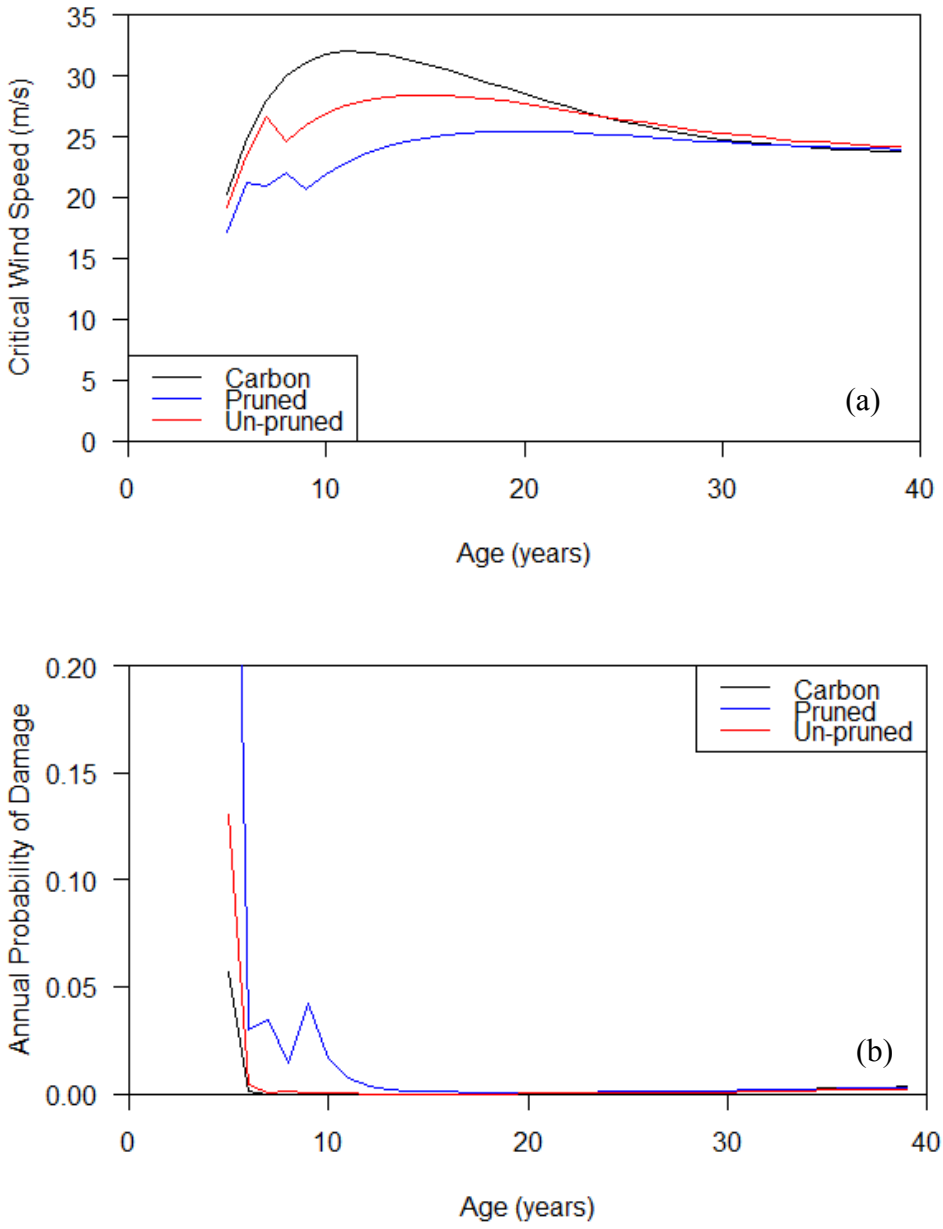

Figure 4.4.5. Comparison of (a) critical wind speed for damage and (b) the annual probability of damage for stands grown under a carbon, pruned and un-pruned regime on the same site.

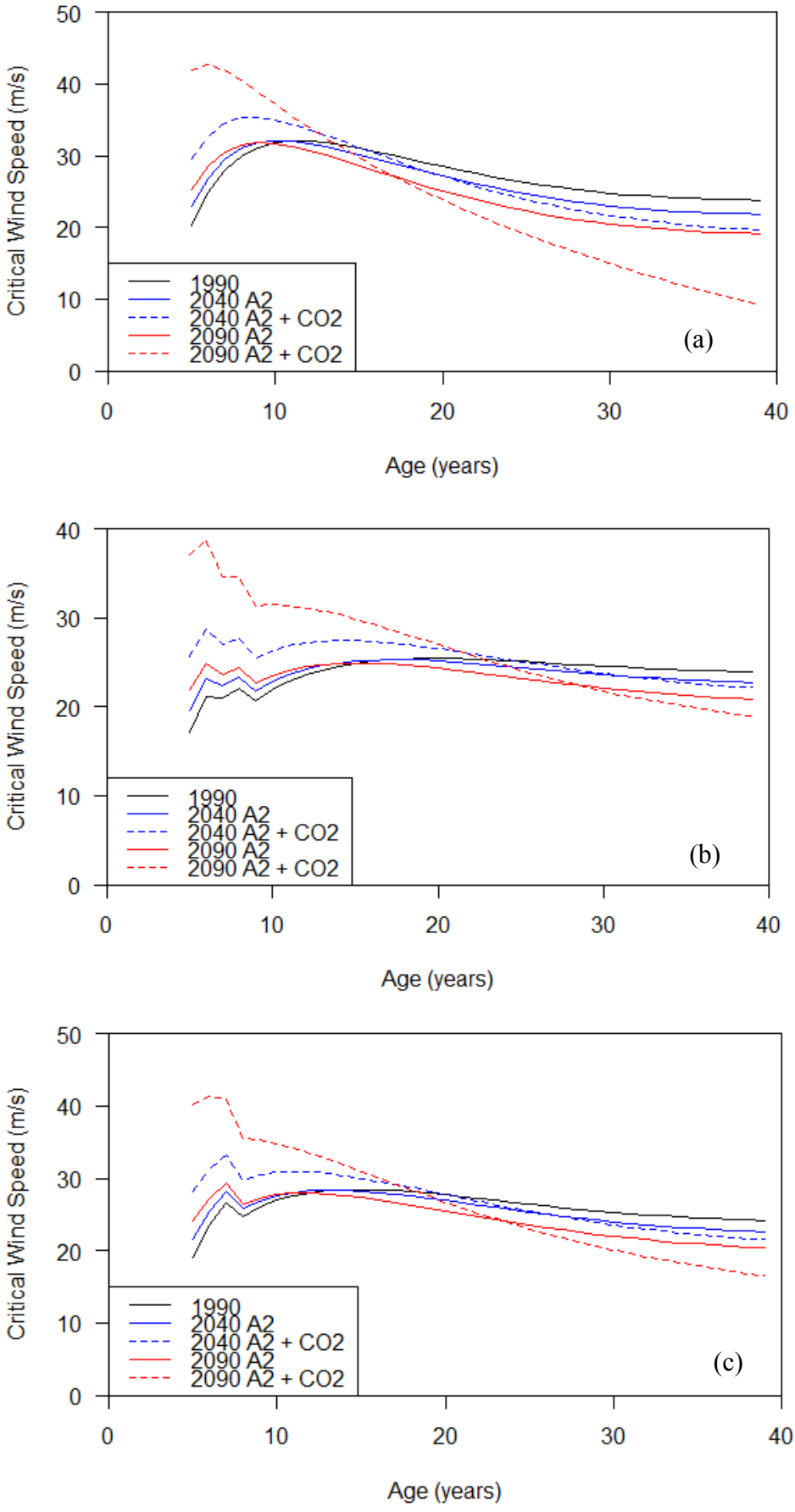

Figure 4.4.6. Comparison of the critical wind speed for damage for (a) carbon, (b) pruned and (c) un-pruned regimes under current and future conditions.

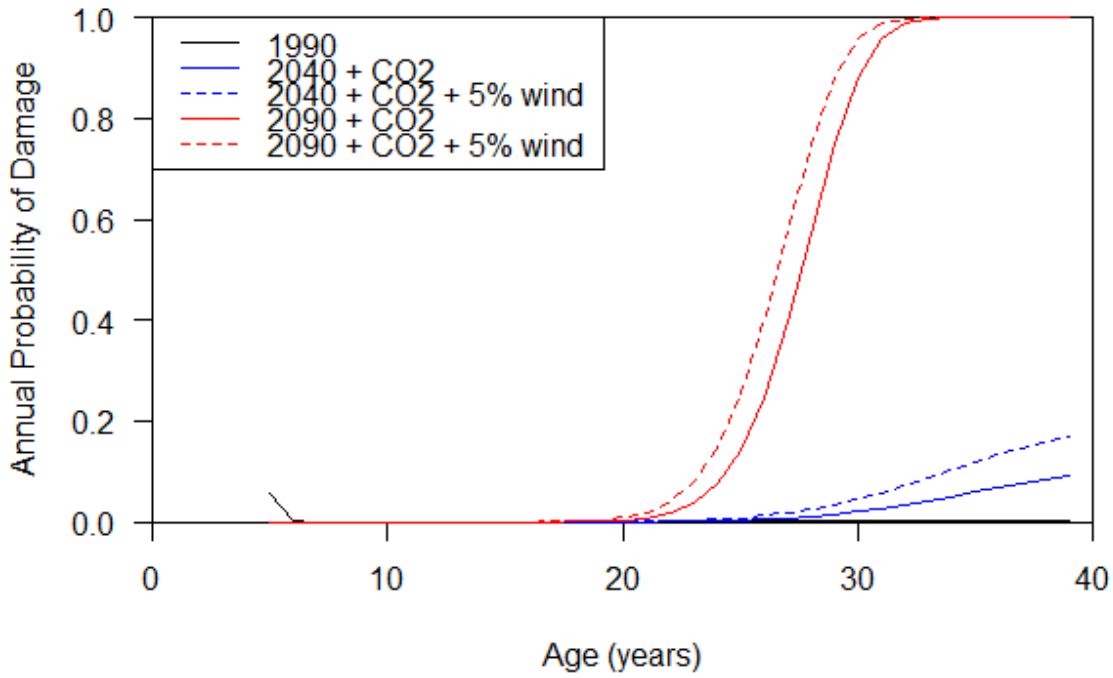

Figure 4.4.7. Annual probability of damage for the carbon regime grown under the 1990 baseline and the A2 scenario with increased CO_2. A 5% increase in the extreme wind climate was also assumed for the two future scenarios.

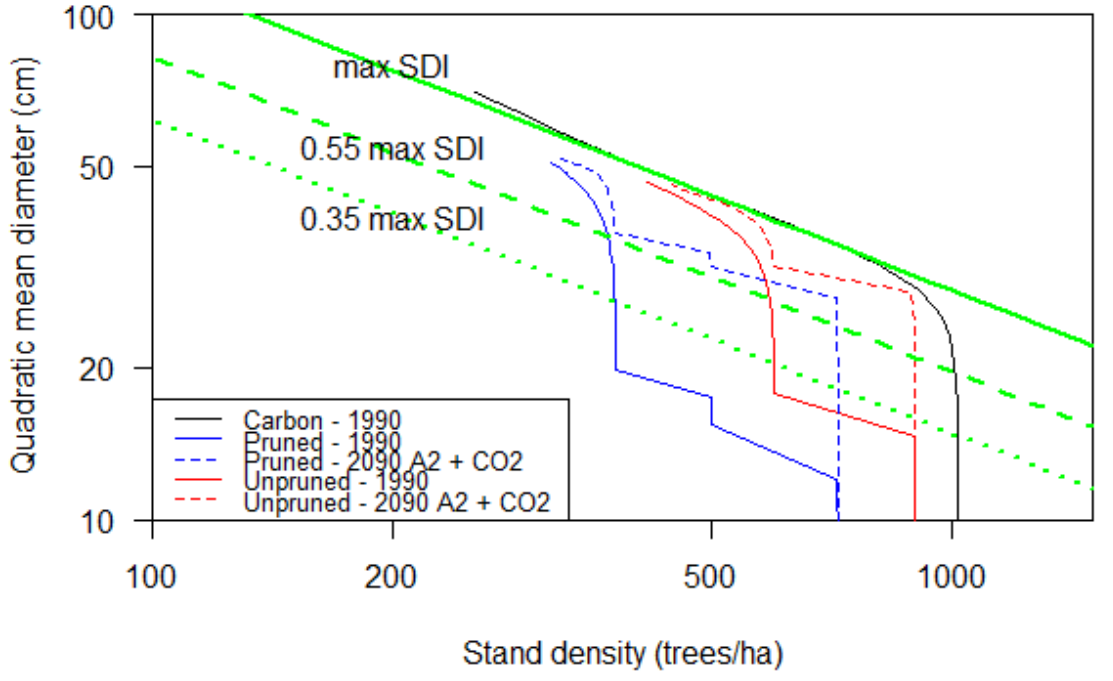

Figure 4.4.8. Density management diagram showing the development of stands grown under different silvicultural regimes and under different emissions scenarios. The solid green line shows the maximum size density limit for radiata pine, while the dashed and dotted green lines show 55% and 35% of this maximum, respectively.

The spatial variation in critical wind speed was calculated for all three regimes under the 1990 baseline conditions and under the A2 emission scenario in 2090. For each grid point on the 0.25° productivity surfaces developed in Section 3.1, the mean diameter at breast height, mean top height, stand density and volume were estimated for 30-year-old carbon, pruned

and un-pruned stands using the radiata pine meta-model. The critical wind speed was then estimated for each grid point using ForestGALES. Differences in soil type, which influence the root anchorage strength were ignored and a uniform soil type was assumed. This analysis showed that the critical wind speed was generally lowest in areas where the productivity was the highest (Figure 4.4.9) as critical wind speed generally decreases with increasing tree height. The change in critical wind speed between 1990 and 2090 was greatest for those regions exhibiting the largest changes in productivity. For example, the decrease in critical wind speed between 1990 and 2090 for the carbon regime was greatest in the Central North Island (Figure 4.4.10).

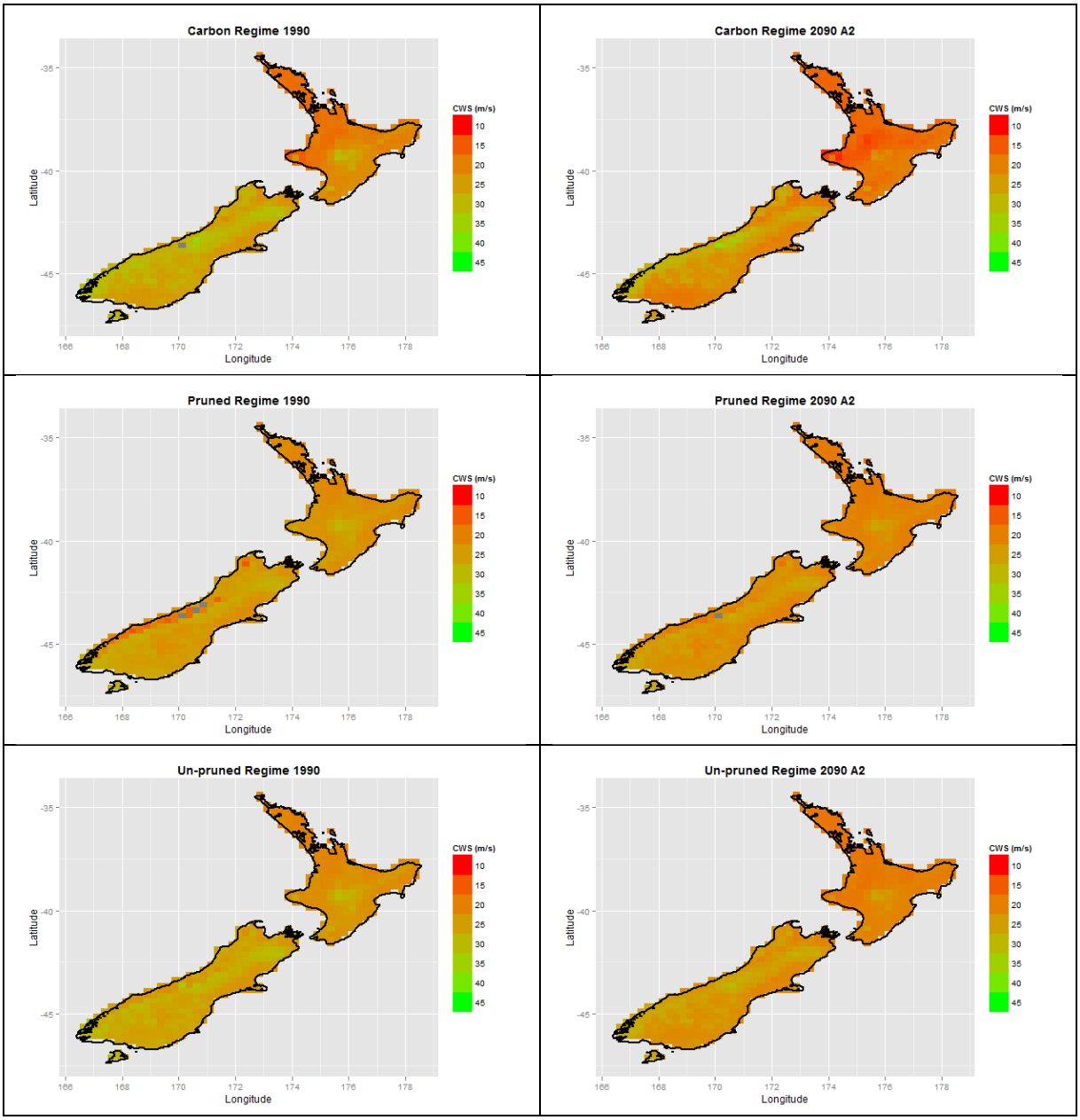

Figure 4.4.9. Comparison of the spatial pattern of critical wind speed at age 30 years for the different silvicultural regimes. Values are calculated for the 1990 conditions and 2090 conditions under the A2 emissions scenario with increased CO_2 concentration.

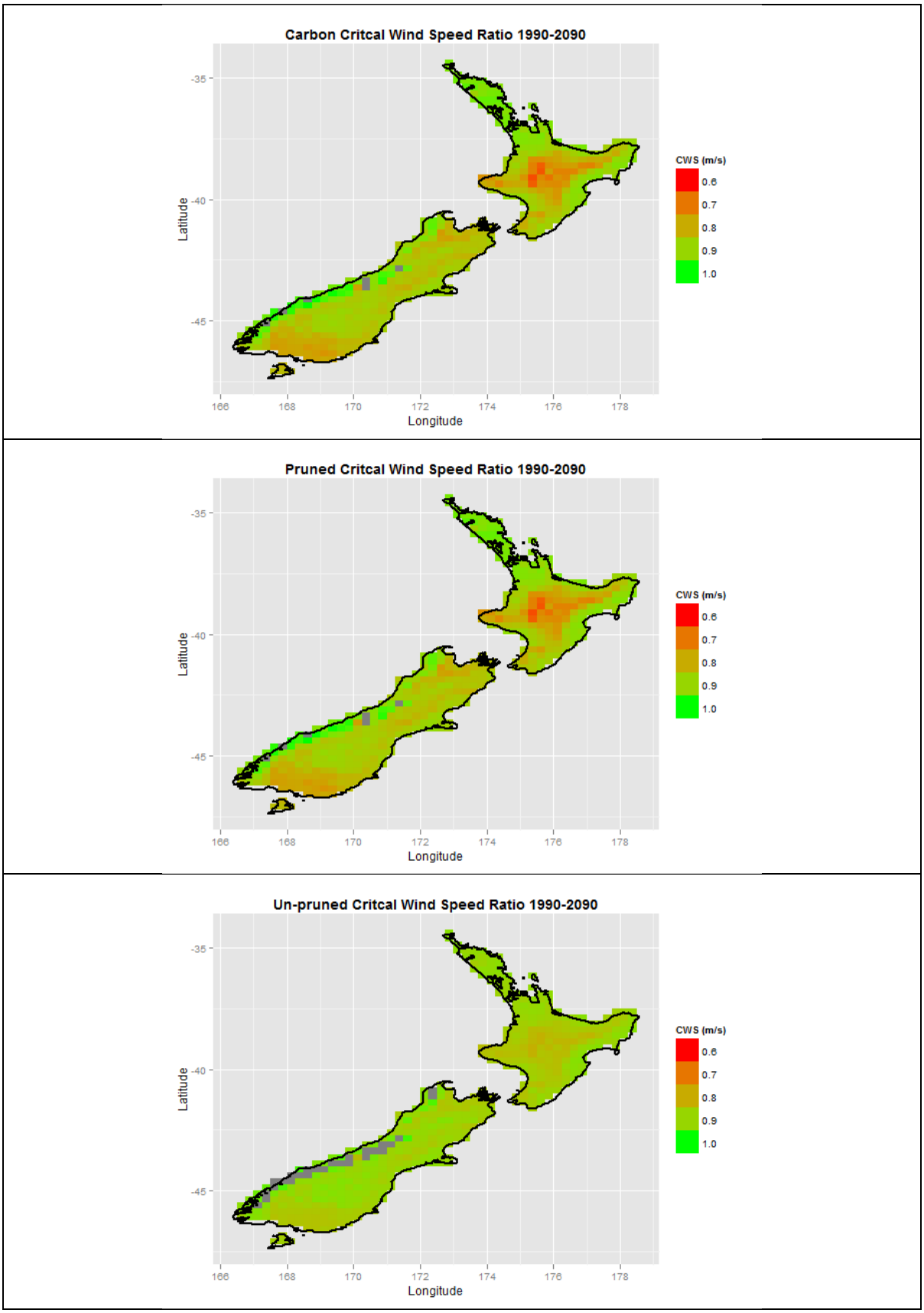

Figure 4.4.10. Change in critical wind speed for damage between 1990 and 2090 for the three regimes under the A2 scenario with increased CO_2 concentration. The change is presented as the ratio of the 2090 value to the 1990 value. Values were calculated for an age of 30 years.

Discussion

Linking growth and yield models with a mechanistic wind damage model (ForestGALES) and having estimates of forest productivity under future emission scenarios has enabled the impacts of future climate change on the risk of wind damage to be more fully investigated. The approach that has been used in this study follows a similar approach that has been used to investigate the impact of climate change on the risk of wind damage in Swedish forests (Blennow and Olofsson, 2008; Blennow et al., 2010 a,b). In contrast to the results from the Swedish studies, the major effect of future climate change on the risk of wind damage in New Zealand occurs through increased forest growth rates, which affect the vulnerability of the forests, rather than through increases in the extreme wind climate. Unfortunately, we do not have a complete understanding of what future climate change might mean for the extreme wind climate in New Zealand, but we do know that relatively small increases in extreme wind speeds can have a significant impact on the risk of damage. The passage that storms take as they pass across the country also has a significant impact on the amount of damage that occurs. Compared with Europe, our forest resource is relatively fragmented and we do not see the levels of damage that occur in Europe from storms originating in the Atlantic Ocean. However, if storm tracks shift so that more storms pass through regions with larger contiguous areas of forest, we may observe greater levels of damage even though there has been little increase in the magnitude of extreme wind climate.

Increased future growth rates of radiata pine under the different emissions scenarios appear to be the main driver of an increase in the risk of damage. Only results for the most extreme A2 scenario have been presented in order to show a “worst case scenario”. Results for the B1 and A1B scenarios are intermediate between the 1990 baseline and A2 scenario. It would be expected that increases in productivity under the future emissions scenarios would lead to changes in forest management practices that may reduce the risk of damage. This could include a reduction in rotation length, which would reduce the length of time that the stand is exposed to potentially damaging winds. Other activities include the timing and intensity of thinning operations, and the location of harvesting operations (Quine et al., 1995; Somerville, 1995). A well-known New Zealand example of management to reduce the risk of wind damage is the Selwyn Plantation Board’s Canterbury Plains forests (Studholme, 1995).

5. Development of Climate Change Decision Support System

Introduction

The Decision Support System (DSS) is a web-based tool that enables users to set-up multiple scenarios to predict forest productivity under future climate change scenarios. The spatial user interface makes it an intuitive and easy to use system that requires minimal input from the user. Information derived from both the underlying spatial layers and the data entered by users are the inputs to the various climate change scenarios. The simulation outcomes of these scenarios enable the user to determine and compare the impact various climate changes will have on forest productivity, cost structures, and profitability for a particular area. These outputs combined with the information provided on diseases, fire and wind risks under future climate change scenarios, help users determine the most optimal regime for a particular scenario. The DSS provides users with the opportunity to take advantage of the economic and market opportunities as a result of climate change.

The Decision Support System Functionality

Various models are applied by the DSS through a sequence of events to simulate climate change scenarios (Figure 5.1). The DSS is dependent on a number of inputs from the user to activate these sequences of events.

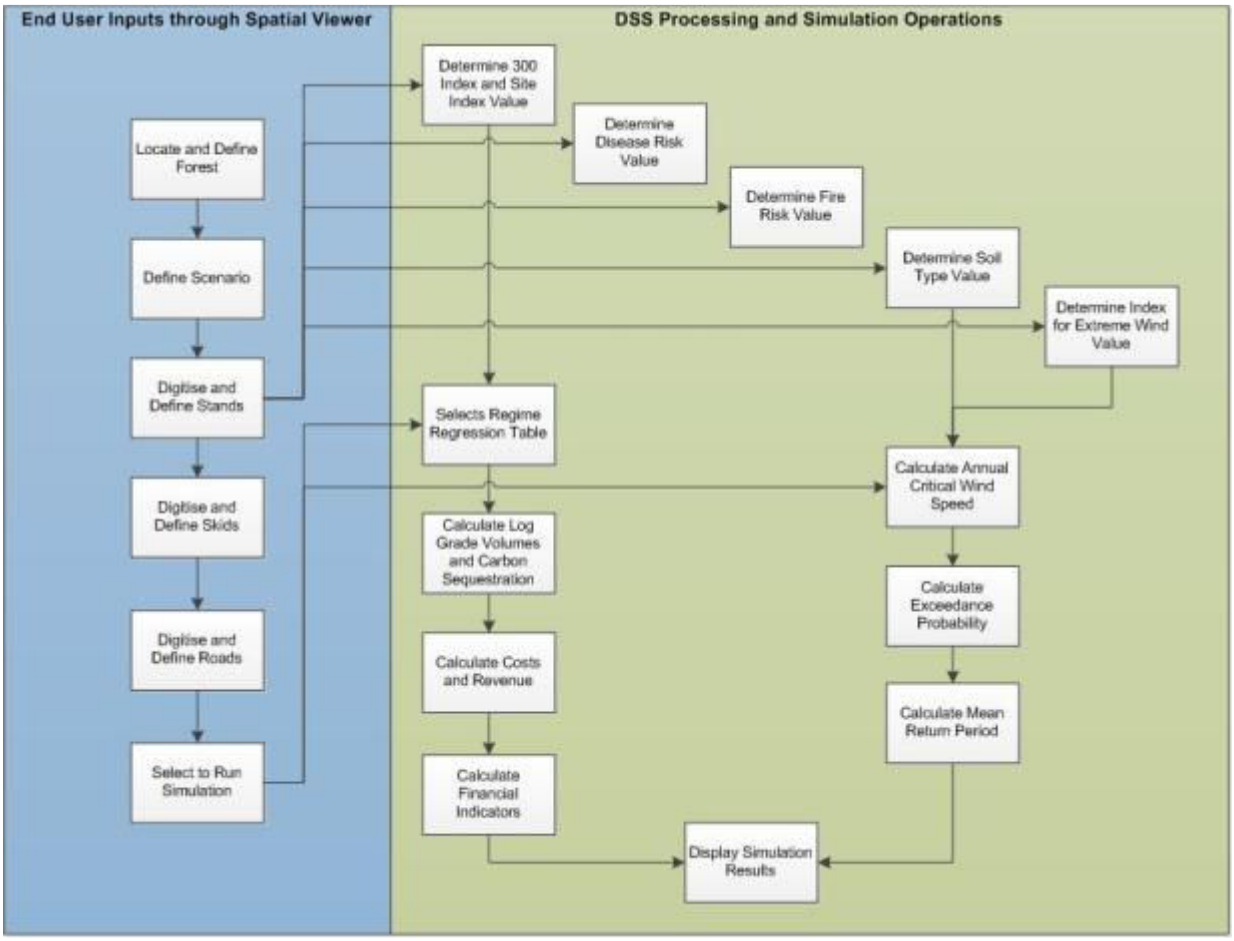

Figure 5.1: Processing and Simulation Operations executed by the Decision Support System.

Users are expected to locate and define a forest, set-up a number of climate change scenarios against the forest and digitise and define stands, skids and roads associated with each of these climate change scenarios. The following four climate change options could be applied when setting up the climate change scenarios:

(i) None - Current climate environment;
(ii) Low - Low CO_2 emissions;
(iii) Medium - Moderate CO_2 emissions; and
(iv) High - High CO_2 emissions.

Each of the above options defines the climate change productivity spatial layers that will be used to determine the 300 Index and Site Index values, used as inputs to the regression tables of the forest model. The user is also expected to enter operation costs and log and carbon prices for each climate change scenario. These costs and log and carbon prices form the basis for the calculation of the economic and financial outcomes by the forest economic model. To assist and guide users with the above the DSS provides default costs and prices that could be overwritten with user defined values. Finally the user will be able to run simulations for a single or multiple scenarios for a defined period.

Running a simulation prompts the DSS to populate the regression tables of the forest model with annual log grade volumes and carbon sequestration rates. These values are transferred to the forest economic model which together with the defined costs and prices calculates costs and revenue for carbon and wood products, and the financial indicators for each scenario.

The carbon revenue and costs represents (i) the carbon credits multiplied by the prevailing carbon price and (ii) the costs associated with participating in the ETS. Log products revenue and costs is (i) the log yield by grade multiplied by the log grade price and (ii) the costs associated with forest management, silviculture, harvesting and cartage. These values are used to represent the annual cashflow for each scenario. Lastly the forest economic model also calculates the Net Present Value (NPV), Land Expectation Value (LEV) and Internal Rate of Return (IRR) as financial indicators for each scenario.

The wind risk model determines the (i) annual critical wind speed, (ii) annual exceedance probability (AEP) and (iii) mean return period (RP) using the regression table outputs of the forest model, the soil type and Index for Extreme Wind values as inputs.

The Decision Support System Outputs

The outcomes of the simulated climate change scenarios are displayed either as a table or graphical format. These outputs enable users to easily compare various climate change scenarios. The table format is used for presenting the (i) cash flow and (ii) financial indicators for each climate change scenario as per defined simulation period. The cash flow report displays the annual net income, expenses and balance for a given year while the financial indicators report indicates the NPV, LEV and IRR for each scenario, as shown in Figure 5.2.

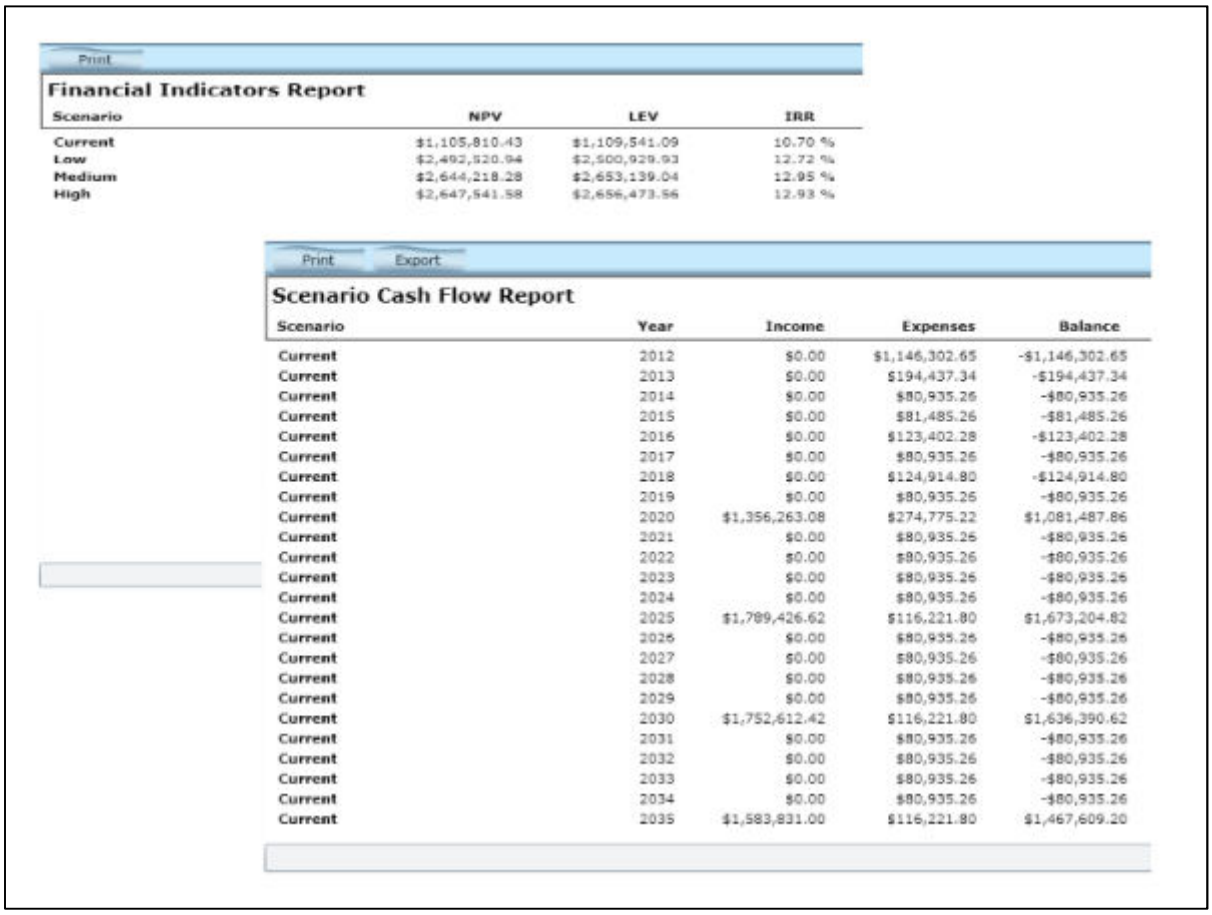

Print

Financial Indicators Report

Scenario	NPV	LEV	IRR
Current	$1,105,810.43	$1,109,541.09	10.70 %
Low	$2,492,520.94	$2,500,929.93	12.72 %
Medium	$2,644,218.28	$2,653,139.04	12.95 %
High	$2,647,541.58	$2,656,473.56	12.93 %

Print Export

Scenario Cash Flow Report

Scenario	Year	Income	Expenses	Balance
Current	2012	$0.00	$1,146,302.65	-$1,146,302.65
Current	2013	$0.00	$194,437.34	-$194,437.34
Current	2014	$0.00	$80,935.26	-$80,935.26
Current	2015	$0.00	$81,485.26	-$81,485.26
Current	2016	$0.00	$123,402.28	-$123,402.28
Current	2017	$0.00	$80,935.26	-$80,935.26
Current	2018	$0.00	$124,914.80	-$124,914.80
Current	2019	$0.00	$80,935.26	-$80,935.26
Current	2020	$1,356,263.08	$274,775.22	$1,081,487.86
Current	2021	$0.00	$80,935.26	-$80,935.26
Current	2022	$0.00	$80,935.26	-$80,935.26
Current	2023	$0.00	$80,935.26	-$80,935.26
Current	2024	$0.00	$80,935.26	-$80,935.26
Current	2025	$1,789,426.62	$116,221.80	$1,673,204.82
Current	2026	$0.00	$80,935.26	-$80,935.26
Current	2027	$0.00	$80,935.26	-$80,935.26
Current	2028	$0.00	$80,935.26	-$80,935.26
Current	2029	$0.00	$80,935.26	-$80,935.26
Current	2030	$1,752,612.42	$116,221.80	$1,636,390.62
Current	2031	$0.00	$80,935.26	-$80,935.26
Current	2032	$0.00	$80,935.26	-$80,935.26
Current	2033	$0.00	$80,935.26	-$80,935.26
Current	2034	$0.00	$80,935.26	-$80,935.26
Current	2035	$1,583,831.00	$116,221.80	$1,467,609.20

Figure 5.2: Examples of the reports generated by the Decision Support System.

The graphical format of reporting is used for presenting the (i) carbon sequestration and related revenue, (ii) log volumes and revenue per grade and (iii) the cumulative probability of damage caused by wind for each climate change scenario as per defined simulation period. These values are displayed in a number of line graphs, as shown in Figure 5.3.

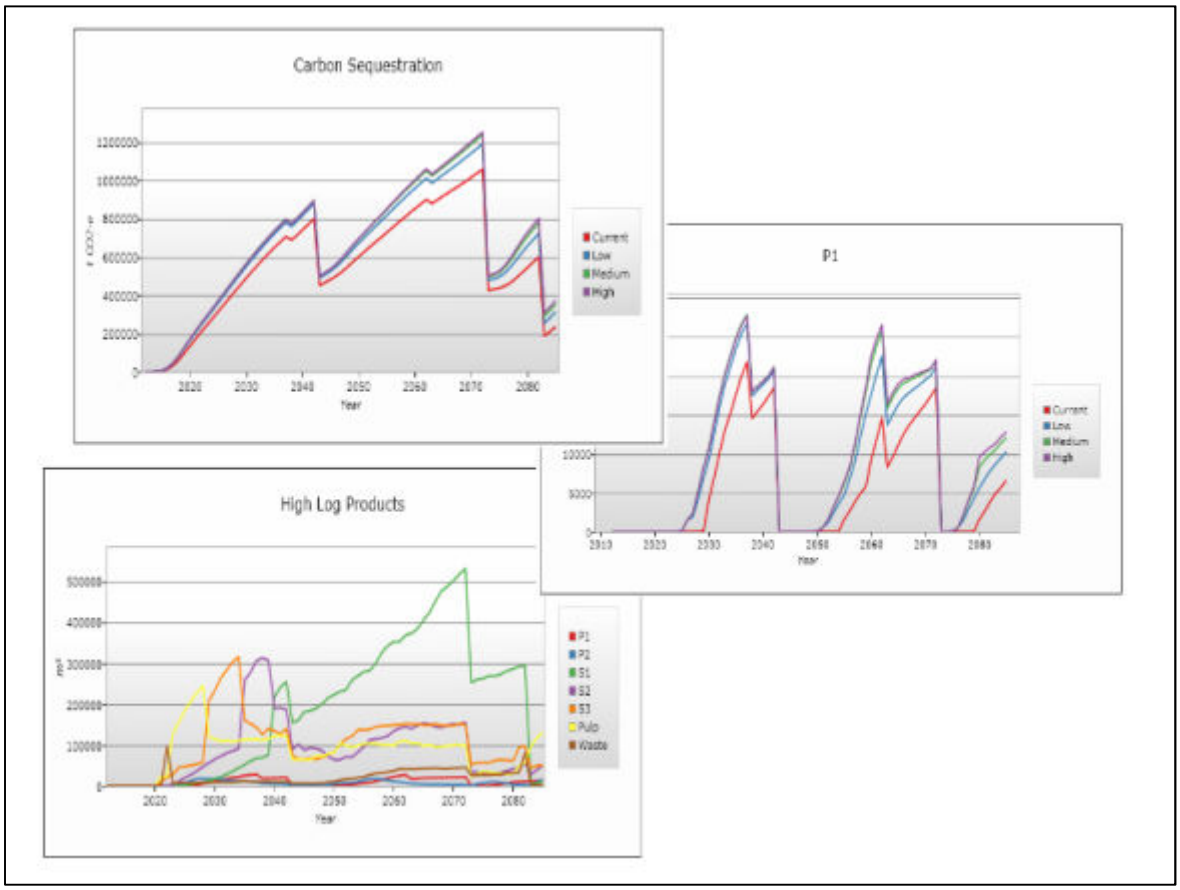

Figure 5.3: Examples of the graphs generated by the Decision Support System.

The Decision Support System Models

The DSS includes a number of models such as the (i) forest model, (ii) forest economic model and (iii) wind risk model. The forest model represents the regression tables for the various species and associated regimes such as (i) plant and leave (carbon), (ii) pruned (clearwood) and (iii) un-pruned (sawlog). It provides log volumes per grade as well as the carbon sequestered over time based on the 300 Index and Site Index values derived from the productivity spatial layers. These productivity spatial layers represent the three climate change scenarios of low, moderate and high emissions with increased CO_2. The forestry economic model calculates the cost and revenue associated the timber production and carbon forestry to provide outputs such as the (i) annual cash flow and (ii) financial indicators. The financial indicators define the NPV, LEV and IRR derived from discounted cashflow analysis. The wind risk model determines the wind risk under future climate change scenarios based on outputs from the forestry model and values derived from the soil types and Index of Extreme Wind spatial layers. The DSS also contains spatial information on how climate change affects risks associated with fire and the diseases Cyclanuesma needle cast and Dothistroma needle blight.

The Decision Support System Architecture

The DSS was developed as a web-based tool to provide users easy access via the internet, without the need to install an application on their personal computers. The system as shown in Figure 5.4 is hosted on a central server that stores the (i) spatial viewer, (ii) GIS layers and database, and (iii) modelling database.

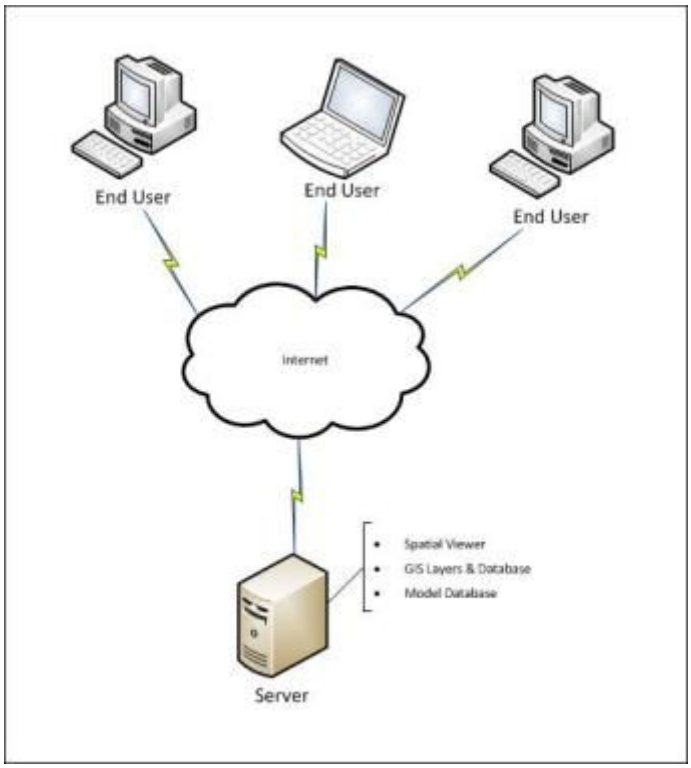

Figure 5.4: Architecture for Decision Support System.

The user interacts with the GIS layers and modelling database by making use of the spatial viewer as shown in Figure 5.5. The spatial viewer is a unique feature to the DSS in that it allows users to visually interact with the system. Information is captured through user input forms and deriving values from underlying spatial layer. The DSS database was developed to provide a flexible framework to easily accommodate other species and regimes in the future.

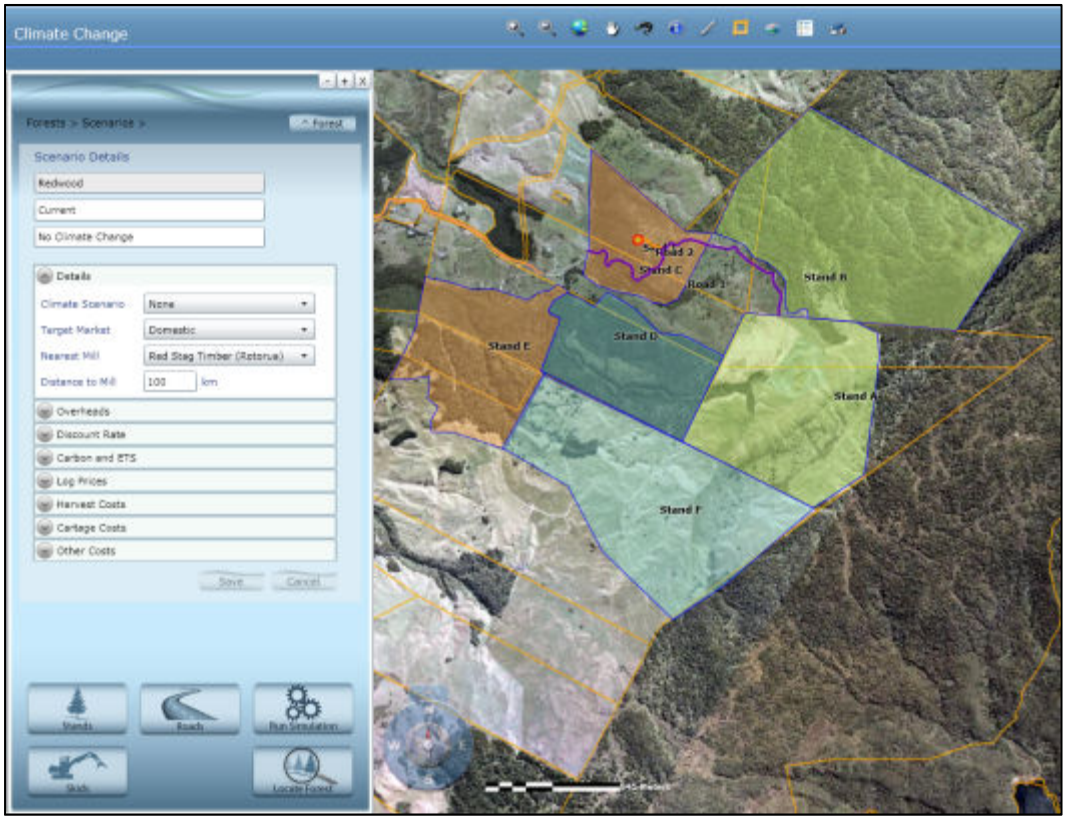

Figure 5.5: User Interface for Decision Support System.

The DSS was developed using the latest available development technologies to ensure that it is current with market development and software trends. The following were used for developing the DSS:

(i) Silverlight 4 for the rich graphical user interface;
(ii) ArcGIS Server 10 for the GIS database;
(iii) SQL Server 2008 R2 for the storage of the modelling database; and
(iv) .NET 4 for services to access the databases.

Summary

The DSS was developed as a web-based tool to provide users easy access to various scientific models such as the (i) forest model, (ii) forest economic model and (iii) wind risk model. The spatial viewer user interface, which is a unique feature of the DSS, makes the DSS an easy to use and intuitive tool for digitising and capturing information on stands, skids and roads and associated information. Each model plays an important part in predicting forest productivity under future climate change scenarios. The forest model determines the annual log grade volumes and carbon sequestration rates. These are then used by the forest economic model to calculate the cashflow and the financial indicators. The wind risk model together with fire and disease risk values provides information on the effect climate change will have on these risks. Based on the above information the user is able to make an informed decision on the most productive and profitable regime for a specific area under future climate change scenarios. This provides the user with the opportunity to take advantage of the economic and market opportunities arising as a result of climate change.

References

Ainsworth, E. A., Rogers, A., Nelson, R., & Long, S. P. (2004). Testing the "source-sink" hypothesis of down-regulation of photosynthesis in elevated [CO_2] in the field with single gene substitutions in Glycine max. *Agricultural and Forest Meteorology, 122*, 85-94.

Ainsworth, E. A., & Long, S. P. (2005). What have we learned from 15 years of free-air CO_2 enrichment (FACE)? A meta-analytic review of the responses of photosynthesis, canopy properties and plant production to rising CO_2. *New Phytologist, 165*, 351-371.

Allen, R. B., Partridge, T. R., Lee, W. G., & Efford, M. (1992). Ecology of *Kunzea ericoides* (A Rich) Thompson, J. (Kanuka) In East Otago, New-Zealand. *New Zealand Journal of Botany, 30*, 135-149.

Almeida, A. C., Sands, P. J., Bruce, J., Siggins, A. W., Leriche, A., Battaglia, M., & Batista, T. R. (2009). Use of a spatial process-based model to quantify forest plantation productivity and water use efficiency under climate change scenarios. Presentation 18th World IMACS/MODSIM Congress, Cairns, Australia 13-17 July 2009.

Anderson, S. A. J., Doherty, J. J., & Pearce, H. G. (2008). Wildfires in New Zealand from 1991 to 2007. *New Zealand Journal of Forestry, 53(3)*, 19-22.

Anon. (2009). The future may be in Redwood. *New Zealand Logger, April 2007, 19-21*.

Arp, W. J. (1991). Effects of source-sink relations on photosynthetic acclimation to elevated CO_2. *Plant Cell and Environment, 14*, 869-875.

AsureQuality. (2009). http://www.asurequality.com/geospatial-services/agribase-derived-products.cfm. Accessed 30/04/2010.

Bain, J., & Nicholas, I. (2009). Chapter 4. Health., In: I. Nicholas (ed.), Best Practice with Farm Forestry Timber Species No. 3: Redwoods. www.nzffa.org.nz/special-interest-groups/sequoia-action-group/.

Ball, J. T., Woodrow, I. E., & Berry, J. A. (1987). A model predicting stomatal conductance and its contribution to the control of photosynthesis under different environmental conditions. In: Biggins J ed. Progress in photosynthesis research. Dordrecht, The Netherlands, Martin-Nijhoff Publishers pp. 221–224.

Barnes, I., Crous, P. W., Wingfield, B. D., & Wingfield, M. J. (2004). Multigene phylogenies reveal that red band needle blight of *Pinus* is caused by two distinct species of Dothistroma, *D. septosporum* and *D. pini*. *Studies in Mycology, 50*, 551-565.

Bassett, C. (1969). *Larix decidua* a new host for *Dothistroma pini*. *Plant Disease Reporter, 53*, 706.

Battaglia, M., & Sands, P. (1997). Modelling site productivity of *Eucalyptus globulus* in response to climatic and site factors. *Australian Journal of Plant Physiology, 24*(6), 831-850.

Battaglia, M., & Sands, P. J. (1998). Process-based forest productivity models and their application in forest management. *Forest Ecology and Management, 102*(1), 13-32.

Battaglia, M., Sands, P., White, D., & Mummery, D. (2004). CABALA: a linked carbon, water and nitrogen model of forest growth for silvicultural decision support. *Forest Ecology and Management, 193*(1/2), 251-282.

Battaglia, M., Bruce, J., Brack, C., & Baker, T. (2009). Climate Change and Australia's plantation estate: analysis of vulnerability and preliminary investigation of adaptation options. *Report prepared to FWPA by CSIRO Project No: PR07.4021*.

Bednárová, M., Palovcíková, D., & Jankovský, L. (2006). The host spectrum of Dothistroma needle blight *Mycosphaerella pini* E. Rostrup - new hosts of Dothistroma needle blight observed in the Czech Republic. *Journal of Forest Science, 52*(1), 30-36.

Blennow, K., & Olofsson, E. (2008). The probability of wind damage in forestry under a changed climate. *Climatic Change, 87*, 347-360.

Blennow, K., Andersson, M., Bergh, J., Sallnas, O., & Olofson, E. (2010). Potential climate change impacts on the probability of wind damage in a south Swedish forest. *Climatic Change, 99*, 261-278.

Blennow, K., Andersson, M., Sallnas, O., & Olofson, E. (2010). Climatic change and the probability of wind damage in two Swedish forests. *Forest Ecology and Management, 259*, 818-830.

Booth, T. H., & McMurtrie, R. E. (1988). Climate change and *Pinus radiata* plantations in Australia. In: Pearman GI, ed., Greenhouse, Cambridge University Press, Melbourne. pp. 534-545. .

Bradbury, P. M. (1998). The effects of the Burnt Pine Longhorn Beetle and wood-staining fungi on fire damaged *Pinus radiata* in Canterbury. *New Zealand Journal of Forestry, 43*, 28-31.

Brown, A. (2005). Seeing red! *Forestry & British Timber, 34*(7), 16-18.

Brown, I. (2007). Redwoods-an overview. *Tree Grower, 27*.

Brown, I., Low, C., Nicholas, I., & Webster, R. (2008). Introduction. In I. Nicholas (Ed.), Best Practice with Farm Forestry Species, no. 3: Redwoods, 7-12. Wellington: New Zealand Farm Forestry Association Electronic Handbook Series.

Bulman, L. S., Gadgil, P. D., Kershaw, D. J., & Ray, J. W. (2004). Assessment and control of Dothistroma needle-blight. *Forest Research Bulletin No. 229*.

Bulman, L. S. (2006). Foliar diseases of pine - the New Zealand experience. In: Jackson, M. B. comp. 2007. Proceedings of the 54th Annual Western International Forest Disease Work Conference; 2-6 October 2006; Smithers, BC. Missoula, MT: US Department of Agriculture, Forest Service, Forest Health Protection. 57-60.

Burdon, R. D., & Bannister, M. H. (1973). Provenances of *Pinus radiata*: their early performance and silvicultural potential. *New Zealand Journal of Forestry, 18*(2).

Burdon, R. D., & Miller, J. T. (1992). Introduced forest trees in New Zealand: Recognition, Role and Seed Source. 12. Radiata pine (*Pinus radiata* D.Don). FRI Bulletin No. 124 Part 12.

Burrows, L., Carswell, F., Brignall-Theyer, M., & McKenzie, S. (2009). Changes in biomass carbon during kanuka shrubland succession to forest. Landcare Research Internal Report LC0809/084, 20 pp.

Burrows, L. E. (2010). Estimate of biomass and leaf area index (LAI) for kanuka at Avoca Station. Unpublished report, Landcare Research, 11 pp.

Cameron, G., Dudfield, M., & Pearce, G. (2007). Fire management in commercial plantations: a New Zealand perspective. Paper presented at the 4th International Wildland Fire Conference, Seville, Spain, 13-17 May 2007. 12 p.

Campion, J. M., Esprey, L. J., & Scholes, M. C. (2005). Application of the 3-PG model to a *Eucalyptus grandis* stand subjected to varying levels of water and nutrient constraints in KwaZulu-Natal, South Africa. *Southern African Forestry Journal 203*, 3-13.

Carter, P. (1989). Wind damage in Kinleith forest-effects of Cyclone Bola. In: Wind damage in New Zealand exotic forests, (Eds Alan Somerville, Stephen Wakelin and Lesley Whitehouse), FRI Bulletin 146.

Carvalho, A., Flannigan, M. D., Logan, K. A., Gowman, L. M., Miranda, A. I., & Borrego, C. (2011). The impact of spatial resolution on area burned and fire occurrence projections in Portugal under climate change. *Climatic Change, 98*, 177-197.

Chapin, F. S., McGuire, A. D., Ruess, R. W., Hollingsworth, T. N., Mack, M. C., Johnstone, J. F., Kasischke, E. S., Jones, J. B., Jorgenson, M. T., Kielland, K., Kofinas, G. P., Turstsky, M. R., Yarie, J., Lloyd, A. H., & Taylor, D. L. (2010). Resilience of Alaska's boreal forest to climate change. *Canadian Journal of Forest Research, 40*, 1360-1370.

Clutter, J. L., Fortson, J. C., Pienaar, L. V., Brister, G. H., & Bailey, R. L. (1992). Timber Management: a Quantitative Approach. Reprint edition. Krieger Publishing, Malabar.

Coakley, S. M., Scherm, H., & Chakraborty, S. (1999). Climate change and disease management. *Annual Review Phytopathology, 37*, 399-426.

Comins, H. N., & McMurtrie, R. E. (1993). Long-term biotic response of nutrient-limited forest ecosystems to CO_2-enrichment; equilibrium behaviour of integrated plant-soil models. *Ecological Applications, 3*, 666-681.

Coops, N. C., Waring, R. H., & Schroeder, T. A. (2009). Combining a generic process-based productivity model and a statistical classification method to predict the presence and absence of tree species in the Pacific Northwest, U.S.A. *Ecological Modelling, 220*, 1787-1787.

Coops, N. C., & Waring, R. H. (2010). A process-based approach to estimate lodgepole pine (*Pinus contorta* Dougl.) distribution in the Pacific Northwest under climate change. *Climatic Change 105*, 313-328.

Coops, N. C., & Waring, R. (2011). Estimating the vulnerability of fifteen tree species under changing climate in Northwest North America. *Ecological Modelling, 222*, 2119-2129.

Cornell, W. (2002). New Zealand Redwood Growers Handbook, Henderson: Diversified Forests Limited.

Covington, W. W., & Sackett, S. S. (1984). The effect of a prescribed burn in Southwestern Ponderosa Pine on organic matter and nutrients in woody debris and forest floor. *Forest Science, 30*, 183-192.

Cown, D. J. (1997). New Zealand forest management and wood quality trends. *In: Proceedings of the CTIA-IUFRO. Timber management toward wood quality and end-product value. International Wood Quality Workshop, Quebec City, Canada, August 18-22. Zhang, S.Y., Gosselin, R. and Chauret, G. (Ed.).*

Cullingham, C. I., Cooke, J. E. K., Dang, S., Davis, C. S., Cooke, B. J., & Coltman, D. W. (2011). Mountain pine beetle host-range expansion threatens the boreal forest. *Molecular Ecology 20*, 2157-2171.

Curtis, P. S., & Wang, X. (1998). A meta analysis of elevated CO_2 effects on woody plant mass, form, and physiology. *Oecologia, 113*, 299-313.

Davis, M. R., Coker, G., Parfitt, R. L., Simcock, R., Clinton, P. W., Garrett, L. G., & Watt, M. S. (2007). Relationships between soil and foliar nutrients in young densely planted mini-plots of *Pinus radiata* and *Cupressus lusitanica*. *Forest Ecology and Management, 240*(1-3), 122-130.

De Wolf, E. D., & Isard, S. A. (2007). Disease cycle approach to plant disease prediction. *Annual Review of Phytopathology, 45*, 203-220.

DeBano, L. F., Neary, D. G., & Folliott, P. F. (1998). Fire: Its Effect on Soil and Other Ecosystem Resources. New York: John Wiley. 336 pp.

Desprez-Loustau, M. L., Robin, C., Reynaud, G., Deque, M., Badeau, V., Piou, D., Husson, C., & Marcais, B. (2007). Simulating the effects of a climate-change scenario on the geographical range and activity of forest-pathogenic fungi. *Canadian Journal of Plant Pathology, 29*, 101-120.

Dixon, R. K., Brown, S., Houghton, R. A., Solomon, A. M., Trexler, M. C., & Wisniewski, J. (1994). Carbon pools and flux of global forest ecosystems. *Science, 263*, 185-190.

Doherty, J. J., Anderson, S. A. J., & Pearce, G. (2008). An analysis of wildfire records in New Zealand: 1991-2007. Scion Client Report No. 12789. Christchurch: Scion, Rural Fire Research Group. 194 pp.

Dowdy, A. J., Mills, G. A., Finkele, K., & de Groot, W. (2010). Index sensitivity analysis applied to the Canadian Forest Fire Weather Index and the McArthur Forest Fire Danger Index. *Meteorological Applications 17*, 298-312.

Drake, B. G., Gonzalez-Meler, M. A., & Long, S. P. (1997). More efficient plants: a consequence of rising atmospheric CO_2? *Annual Review of Plant Physiology and Plant Molecular Biology, 48*, 609-639.

Dubin, H., & Walper, S. (1967). *Dothistroma pini* on *Pseudotsuga menziesii*. *Plant Disease Reporter 51*, 454.

Dymond, J. R., Ausseil, A. G., Shepherd, J. D., & Buettner, L. (2006). Validation of a region-wide model of landslide susceptibility in the Manawatu-Wanganui region of New Zealand. *Geomorphology, 74*(1-4), 70-79.

Farquhar, G. D., & von Caemmerer, S. (1982). Modelling of photosynthetic response to environmental conditions. In: Lange OL, Nobel PS, Osmond CB, Ziegler H, eds., Physiological Plant Ecology II. Water Relations and Carbon Assimilation. Encyclopaedia of Plant Physiology, New Series Vol. 12B. Berlin, Heidelberg, New York, Springer-Verlag, pp. 549–588.

Flannigan, M. D., Logan, K. A., Amiro, B. D., Skinner, W. R., & Stocks, B. J. (2005). Future area burned in Canada. *Climatic Change, 72*, 1-16.

Flannigan, M. D., Logan, K. A., Stocks, B. J., Wotton, B. M., Skinner, W. R., Martell, D. L., Amiro, B. D., & Todd, J. B. (2005). Projections of future area burned in Canada. *Climatic Change, 72*, 1-16.

Fontes, L., Bontemps, J. D., Bugmann, H., Van Oijen, M., Gracia, C., Kramer, K., Lindner, M., Rotzer, T., & Skovsgaard, J. P. (2010). Models for supporting forest management in a changing environment. *Forest Systems, 19*, 8-29.

Gadgil, P. D. (1970). Survival of *Dothistroma pini* on fallen needles of *Pinus radiata*. *New Zealand Journal of Botany, 8*, 303-309.

Gadgil, P. D. (1974). Effect of temperature and leaf wetness period on infection of *Pinus radiata* by *Dothistroma pini*. *New Zealand Journal of Forestry Science, 4*(3), 495-501.

Gadgil, P. D. (1984a). Dothistroma needle blight. *In : Forest Pathology in New Zealand, Forest Research Institute, New Zealand.* .

Gadgil, P. D. (1984b). *Cyclaneusma* (*Naemacyclus*) needle cast of *Pinus radiata* in New Zealand. 1. Biology of *Cyclaneusma minus*. *New Zealand Journal of Forestry Science, 14*, 179-196.

Ganley, R., & Berndt, L. (2009). Identification of pests that could threaten selected plantation species. Internal Scion Report.

Ganley, R. J., Watt, M. S., Manning, L., & Iturritxa, E. (2009). A global climatic risk assessment of pitch canker disease. *Canadian Journal of Forest Research, 39*, 2246-2256.

Gardiner, B., Peltola, H., & Kellomaki, S. (2000). Comparison of two models for predicting the critical wind speeds required to damage coniferous trees. *Ecological Modelling, 129*(1), 1-23.

Gibson, I. A. S., Christensen, P. S., & Munga, F. M. (1964). First observations in Kenya of a foliage disease of pines caused by *Dothistroma pini* Hulbary. *Commonwealth Forestry Review*, 31-48.

Gibson, I. A. S. (1974). Impact and control of dothistroma blight of pines. *European Journal of Forest Pathology, 4*(2), 89-100.

Gilman, E. F., & Watson, D. G. (1994). *Sequoia sempervirens*, Coast redwood. USDA Forest Service, Fact Sheet ST-589. .

Gilmour, J. W. (1981). The effect of season on infection of *Pinus radiata* by *Dothistroma pini*. *European Journal of Forest Pathology, 11*, 265-269.

Goh, K. M., & Phillips, M. J. (1991). Effects of clearfell logging and clearfell logging and burning of a Nothofagus forest on soil nutrient dynamics in South Island, New Zealand - changes in forest floor organic matter and nutrient status. *New Zealand Journal of Botany, 29*, 367- 384.

Gordon, A., Nicholas, I. D., & McConnochie, R. M. (2007). Siting eucalypts. Eucalypts for high value timber, 9-12 October, 2007.

Gradwell, M. W., & Birrell, K. S. (1979). Soil Bureau laboratory methods. Part C. Methods for physical analysis of soils. New Zealand Bureau scientific report 10C. Wellington, Department of Scientific and Industrial Research.

Greer, D. H., Muir, L. A., & Harris, W. (1991). Seasonal frost hardiness in *Leptospermum scoparium* seedlings from diverse sites throughout New Zealand. *New Zealand Journal of Botany, 29*, 207-212.

Greer, D. H., & Robinson, L. A. (1995). Temperature control of the development of frost hardiness in 2 populations of *Leptospermum scoparium*. *Tree Physiology 15*, 399-404.

Griffiths, E. (1985). Interpretation of soil morphology for assessing moisture movement and storage. New Zealand Soil Bureau scientific report no. 74. Wellington, Department of Scientific and Industrial Research.

Gunderson, C. A., & Wullschleger, S. D. (1994). Photosynthetic acclimation in trees to rising atmospheric CO_2: a broader perspective. *Photosynthesis Research 39*, 369-388.

Harwood, C. E., & Jackson, W. D. (1975). Atmospheric losses of four plant nutrients during a forest fire. *Australian Forestry, 38*, 92-99.

Hasenauer, H., Nemani, R. R., Schadauer, K., & Running, S. W. (1999). Forest growth response to changing climate between 1961 and 1990 in Austria. *Forest Ecology and Management, 122*(3), 209-219.

Hasson, A. E. A., Mills, G. A., Timbal, B., & Walsh, K. (2008). Assessing the impact of climate change on extreme fire weather in southeast Australia. CAWCR Technical Report No. 7. Melbourne: Centre for Australian Weather and Climate Research. 81 pp.

Hay, A. E., Nicholas, I. D., & Shelbourne, C. J. A. (2005). Plantation forestry species: alternatives to radiata pine. In: Colley, M. (ed). NZIF Forestry Handbook, New Zealand Institute of Forestry, pp. 83-86.

Hengl, T., Heuvelink, G., & Stein, A. (2004). A generic framework for spatial prediction of soil variables based on regression-kriging. *Geoderma, 120*, 75-93.

Hepting, G. H. (1963). Climate and forest diseases. *Annual Review of Phytopathology, 1*, 31-50.

Hicke, J. A., Logan, J. A., Powell, J., & Ojima, D. S. (2006). Changing temperatures influence suitability for modeled mountain pine beetle (*Dendroctonus ponderosae*) outbreaks in the western United States. *Journal of Geophysical Research - Biogeosciences 111, Article Number: G02019.*

Hicks, D. L. (1991). Erosion under pasture, pine plantations, scrub and indigenous forest: a comparison from cyclone Bola. *New Zealand of Forestry, 26*, 21-22.

Hock, B., Payn, T., Clinton, P., & Turner, J. (2009). Towards green markets for New Zealand plantations. *New Zealand Journal of Forestry, 54*, 9 -18.

Hocking, D., & Etheridge, D. (1967). Dothistroma needle blight of Pines. I. Effect and etiology. *Annals of Applied Biology, 59*, 133-141.

Horgan, G. (2007). Financial returns and forestry planting rates. www.maf.govt.nz/climatechange/forestry/ets/returns/returns-and-new-planting-rates.pdf. Accessed 30/04/2010.

Hunter, I. R., & Gibson, A. R. (1984). Predicting *Pinus radiata* site index from environmental variables. *New Zealand Journal of Forestry Science, 14*(1), 53-64.

Hunter, I. R., Rodgers, B. E., Dunningham, A., Prince, J. M., & Thorn, A. J. (1991). An atlas of radiata pine nutrition in New Zealand. Forest Research Bulletin No. 165. Forest Research Institute, Rotorua, New Zealand, 24 pp.

IPCC. (2000). *Special report on emissions scenarios: A special report of working group III of the intergovernmental panel on climate change* Cambridge, United Kingdom: Cambridge University Press.

IPCC. (2007a). Climate change 2007: Impacts Adaptation and Vulnerability. Contribution of working group II to the fourth assessment report of the Intergovernmental Panel on Climate Change. Eds., Parry, M.L., Canziani, O.F., Palutikof, J.P, van de Linden, P.J.& Hanson, C.E. Cambridge University Press.

IPCC. (2007b). Climate Change 2007: The Physical Science Basis. Contribution of Working Group I to the Fourth Assessment Report of the Intergovernmental

Panel on Climate Change. Cambridge University Press, Cambridge, United Kingdom and New York, NY, USA.

Jackson, D. S. (1965). Species siting: climate, soil and productivity. *New Zealand Journal of Forestry, 10*, 90-102.

Jackson, D. S., & Gifford, H. H. (1974). Environmental variables influencing the increment of Radiata Pine. (1) Periodic volume increment. *New Zealand Journal of Forestry Science, 4*(1), 3-26.

Jankovský, L., Bednářová, M., & Palovčíková, D. (2004). Dothistroma needle blight *Mycosphaerella pini* E. Rostrup, a new quarantine pathogen of pines in the CR. *Journal of Forest Science 50*(7), 319-326.

Johnson, G. R., & Wilcox, M. D. (1989). Eucalyptus species trials on pumiceland. . *New Zealand Forestry, 34*, 24-27.

Johnson, I. G. (1989). The breeding strategy for radiata pine in New South Wales. Part II - proposed operations. *Technical Paper - Forestry Commission of NSW*(No. 47).

Karnosky, D. F. (2003). Impacts of elevated atmospheric CO_2 on forest trees and forest ecosystems: knowledge gaps. *Environment International, 29*, 161-169.

Kimberley, M. O., West, G., Dean, M., & Knowles, L. (2005). Site Productivity: The 300 Index - a volume productivity index for radiata pine. *New Zealand Journal of Forestry, 50*, 13-18.

King, K. J., de Ligt, R. M., & Cary, G. J. (2011). Fire and carbon dynamics under climate change in south-eastern Australia: insights from FullCAM and FIRESCAPE modelling. *International Journal of Wildland Fire, 20*, 563-577.

King, M. (1980). Eucalypts in the Wairarapa. Wairarapa Catchment Board, Masterton.

Kirschbaum, M. U. F., Medlyn, B., King, D. A., Pongracic, S., Murty, D., Keith, H., Khanna, P. K., Snowdon, P., & Raison, J. R. (1998). Modelling forest-growth response to increasing CO_2 concentration in relation to various factors affecting nutrient supply. *Global Change Biology, 4*, 23-42.

Kirschbaum, M. U. F. (1999a). Modelling forest growth and carbon storage with increasing CO_2 and temperature. *Tellus 51B*, 871–888.

Kirschbaum, M. U. F. (1999b). CenW, a forest growth model with linked carbon, energy, nutrient and water cycles. *Ecological Modelling, 118*(1), 17-59.

Kirschbaum, M. U. F. (2000). Forest growth and species distributions in a changing climate. *Tree Physiology, 20*, 309-322.

Kirschbaum, M. U. F., & Paul, K. I. (2002). Modelling carbon and nitrogen dynamics in forest soils with a modified version of the CENTURY model. *Soil Biology & Biochemistry 34*, 341-354.

Kirschbaum, M. U. F., Keith, H., Leuning, R., Cleugh, H. A., Jacobsen, K. L., van Gorsel, E., & Raison, R. J. (2007). Modelling net ecosystem carbon and water exchange of a temperate *Eucalyptus delegatensis* forest using multiple constraints. *Agricultural and Forest Meteorology, 145*, 48-68.

Kirschbaum, M. U. F., Mason, N. W. H., Watt, M. S., Tait, A., Ausseil, A. E., Palmer, D. J., & Carswell, F. E. (2010). Productivity Surfaces for *Pinus radiata* and a range of indigenous forests under current and future climatic conditions. MAF report

Kirschbaum, M. U. F., & Watt, M. S. (2011). Use of a process-based model to describe spatial variation in *Pinus radiata* productivity in New Zealand. *Forest Ecology and Management, 262*(6), 1008-1019.

Kirschbaum, M. U. F., Watt, M. S., Tait, A., & Ausseil, A. G. E. (2012). Future wood productivity of *Pinus radiata* in New Zealand under expected climatic changes. *Global Change Biology, 18*(4), 1342-1356.

Kirschbaum, S. B., & Williams, D. G. (1991). Colonization of pasture by *Kunzea ericoides* in the Tidbinbilla Valley, ACT, Australia. *Australian Journal of Ecology 24*, 79-90.

Knowles, F. B., & Miller, J. T. (1993). Introduced forest trees in New Zealand: Recognition, role, and seed source. No. 13 The redwoods. FRI Bulletin No. 124. Rotorua: New Zealand Forest Research Institute.

Körner, C. (2006). Plant CO_2 responses: an issue of definition, time and resource supply. *New Phytologist, 172*, 393-411.

Körner, C., Morgan, J., & Norby, R. (2007). CO_2 fertilization: when, where, how much? *In: Canadell JG, Pataki DE, Pitelka LF eds Terrestrical ecosystems in a changing world. Berlin/Heidelberg, Springer Verlag, pp. 9–21*.

Landcare Research. (2010). http://www.landcareresearch.co.nz/databases/LENZ/products_poster.asp. Accessed 30/04/2010.

Landsberg, J. J., & Waring, R. H. (1997). A generalized model of forest productivity using simplified concepts of radiation-use efficiency, carbon balance and partitioning. *Forest Ecology and Management, 95*, 209-228.

Landsberg, J. J., Waring, R. H., & Coops, N. C. (2003). Performance of the forest productivity model 3-PG applied to a wide range of forest types. *Forest Ecology and Management 172*, 199-214.

Lang, K. (1987). *Dothistroma pini* on young Norway spruce (*Picea abies*). *European Journal of Forest Pathology 17*, 316-317.

Leathwick, J., Morgan, F., Wilson, G., Rutledge, D., McLeod, M., & Johnston, K. (2002). Land environments of New Zealand: A technical guide. Ministry for the Environment, Wellington, and Manaaki Whenua Landcare Research, Hamilton, 184 pp.

Leathwick, J., Wilson, G., Rutledge, D., Wardle, P., Morgan, F., Johnston, K., McLeod, M., & Kirkpatrick, R. (2003). *Land environments of New Zealand.* Hamilton: Ministry for the Environment, Wellington, and Manaaki Whenua Landcare Research.

Leathwick, J. R., & Rogers, G. M. (1996). Modelling relationships between environment and canopy composition in secondary vegetation in central North Island, New Zealand. *New Zealand Journal of Ecology, 20*, 147-161.

Leathwick, J. R., & Stephens, R. T. T. (1998). Climate surfaces for New Zealand. Landcare Res. Contract Report LC9798/126. Landcare Research, Lincoln, New Zealand 19 pp.

Ledgard, N., Knowles, L., & De La Mare, P. (2005). Douglas-fir - the current New Zealand scene. *New Zealand Journal of Forestry 50*(3), 14-16.

Leitch, C. J., Flinn, D. W., & Van de Graaff, R. H. M. (1983). Erosion and nutrient loss resulting from Ash Wednesday (February 1983) wildfires: a case study. *Australian Forestry, 46*, 173-180.

Lewis, J. D., Wang, X. Z., Griffin, K. L., & Tissue, D. T. (2002). Effects of age and ontogeny on photosynthetic responses of a determinate annual plant to elevated CO_2 concentration. *Plant Cell and Environment 25*, 359-368.

Lewis, N. B., & Ferguson, I. S. (1993). *Management of radiata pine*: Inkata Press, Melbourne.

Libby, W. (1999). Redwood – an addition to exotic forestry? *New Zealand Forestry 38*, 3-7.

Littell, J. S., Oneil, E. E., McKenzie, D., Hicke, J. A., Lutz, J. A., Norheim, R. A., & Elsner, M. M. (2010). Forest ecosystems, disturbance, and climatic change in Washington State, USA. *Climatic Change 102*, 129-158.

Long, S. P., Osborne, C. P., & Humphries, S. W. (1996). Photosynthesis, rising atmospheric carbon dioxide concentration and climate change. *In: Breymeyer AI, Hall DO, Melillo JM, Ågren GI eds SCOPE 56 – Global change: effects on coniferous forests and grasslands. Chichester, John Wiley & Sons Ltd, pp. 121–159.*

Long, S. P., Zhu, X. G., Naidu, S. L., & Ort, D. R. (2006). Can improvements in photosynthesis increase crop yields? *Plant, Cell and Environment 29*, 315-330.

Luo, Y., Su, B., Currie, W. S., Dukes, J. S., Finzi, A., Hartwig, U., Hungate, B., McMurtrie, R. E., Oren, R., Parton, W. J., Pataki, D. E., Shaw, M. R., Zak, D. R., & Field, C. B. (2004). Progressive nitrogen limitation of ecosystem responses to rising atmospheric carbon dioxide. *BioScience, 54*, 731-739.

Luxmoore, R. J., Wullschleger, S. D., & Hanson, P. J. (1993). Forest responses to CO_2 enrichment and climate warming. *Water, Air, and Soil Pollution, 70*, 309-323.

Lynn, I. H., Manderson, A. K., Page, M. J., Harmsworth, G. R., Eyles, G. O., Douglas, G. B., Mackay, A. D., & Newsome, P. J. F. (2009). *Land Use Capability survey handbook - a New Zealand handbook for the classification of land. 3rd Ed. Hamilton, Agresearch; Lincoln, Landcare Research; Lower Hutt, GNS Science. 163 p.*

Magnani, F., Consiglio, L., Erhard, M., Nole, A., Ripullone, F., & Borghetti, M. (2004). Growth patterns and carbon balance of *Pinus radiata* and *Pseudotsuga menziesii* plantations under climate change scenarios in Italy. *Forest Ecology and Management, 202*, 93-105.

Manley, B., & Maclaren, P. (2009). Modelling the impact of carbon trading legislation on New Zealand's plantation estate. *New Zealand Journal of Forestry 54*, 39-44.

Marden, M., Arnold, G., Gomez, B., & Rowan, D. (2005). Pre- and post-reforestation gully development in Mangatu Forest, east coast, North Island, New Zealand. *River Research and Applications, 21*(7), 757-771.

Marks, G., & Smith, I. (1987). Effect of canopy closure and pruning on *Dothistroma septospora* needle blight of *Pinus radiata* D. Don. *Australian Forest Research, 17*, 145-150.

Martin, T. J., & Ogden, J. (2006). Wind damage and response in New Zealand forests: a review. *New Zealand Journal of Ecology*(30), 295-310.

McCarthy, H. R., Oren, R., Johnsen, K. H., Gallet-Budynek, A., Pritchard, S. G., Cook, C. W., LaDeau, S. L., Jackson, R. B., & Finzi, A. C. (2010). Re-assessment of plant carbon dynamics at the Duke free-air CO_2 enrichment site: interactions of atmospheric [CO_2] with nitrogen and water availability over stand development. *New Phytologist 185*, 514-528.

McGlone, M., Walker, S., Leathwick, J., & Briggs, C. (2004). Predicted Potential Natural Vegetation of New Zealand. Poster and electronic data produced by Manaaki Whenua Landcare Research, New Zealand, http://www.landcareresearch.co.nz/databases/lenz/products_poster.asp. Accessed 30/04/2010.

McMurtrie, R. E., Rook, D. A., & Kelliher, F. M. (1990). Modelling the yield of *Pinus radiata* on a site limited by water and nitrogen. *Forest Ecology and Management, 30*(1-4), 381-413.

Meason, D. F., Beets, P., & Dungey, H. (2010). Development of a carbon sequestration web tool for *Eucalyptus fastigata*. Unpublished report No. 17610. Rotorua: New Zealand Forest Research Institute Limited.

Meason, D. F., Almeida, A., Manning, L., & Nicholas, I. (2011). Preliminary parameterisation of the hybrid model 3-PG for *Eucalyptus fastigata* in New Zealand. Unpublished report No. 18500. Rotorua: New Zealand Forest Research Institute Limited.

Medlyn, B. E., Barton, C. V. M., Broadmeadow, M. S. J., Ceulemans, R., De Angelis, P., Forstreuter, M., Freeman, M., Jackson, S. B., Kellomaki, S., Laitat, E., Rey, A., Roberntz, P., Sigurdsson, B. D., Strassemeyer, J., Wang, K., Curtis, P. S., & Jarvis, P. G. (2001). Stomatal conductance of forest species after long-term exposure to elevated CO_2 concentration: a synthesis. *New Phytologist, 149*(2), 247-264.

Medlyn, B. E., Duursma, R. A., & Zeppel, M. J. B. (2011). Forest productivity under climate change: a checklist for evaluating model studies. *Wiley Interdisciplinary Reviews-Climate Change, 2*(3), 332-355.

Meehl, G. A., Covey, C., Delworth, T., Latif, M., McAvaney, B., Mitchell, J. F. B., Stouffer, R. J., & Taylor, K. E. (2007). The WCRP CMIP3 multimodel dataset: A new era in climate change research. *Bulletin of the American Meteorological Society, 88*, 1383–1394.

Meehl, G. A., Stocker, T. F., Collins, W. D., Friedlingstein, P., Gaye, A. T., Gregory, J. M., Kitoh, A., Knutti, R., Murphy, J. M., Noda, A., Raper, S. C. B., Watterson, I. G.,

Weaver, A. J., & Zhao, Z. C. (2007). Global Climate Projections. In: Climate Change 2007: The Physical Science Basis. Contribution of Working Group I to the Fourth Assessment Report of the Intergovernmental Panel on Climate Change [Solomon, S., D. Qin, M. Manning, Z. Chen, M. Marquis, K.B. Averyt, M. Tignor and H.L. Miller (eds.)]. Cambridge University Press, Cambridge, United Kingdom and New York, NY, USA, pp. 747-846.

Mehrotra, M. (1997). Diseases in the Forest. India. In: Hansen, E.M., Lewis, K.J. (Eds.), Compendium of Conifer Diseases. APS Press, 3340 Pilot Knob Road, St Paul, MN 55121 2097, USA, pp. 83-85.

Meyer, J. (2005). Fire effects on forest resource development in the French Mediterranean region – projections with a large-scale forest scenario model. Technical Report 16. European Forest Institute

MfE. (2008). Climate change effects and impacts assessment: A guidance manual for local government in New Zealand (2nd edition). Prepared by Mullan, B., Wratt, D., Dean, S., Hollis, M., Allan, S., Williams, T., Kenny, G. and MfE staff. Ministry for the Environment, Wellington. Report ME870, 167p.

Millar, C. S., & Minter, D. W. (1980). Naemacyclus minor. *CMI Descriptions of Pathogenic Fungi and Bacteria, 659*(66), 1-2.

Ministry for the Environment. (2007). See: http://www.mfe.govt.nz/issues/land/land-cover-dbase/classes.html. Accessed 16/05/2011.

Ministry for the Environment. (2008). Climate change effects and impacts assessment. A guidance manual for local government in New Zealand. 2nd Edition. Prepared for the Climate Change Office by B. Mullan, D. Wratt, S. Dean, M. Hollis, S. Allan, T. Williams, G. Kenny and MfE. MFE Publication ME 870. 149p. http://www.mfe.govt.nz/publications/climate/climate-change-effect-impacts-assessments-may08/climate-change-effect-impacts-assessment-may08.pdf. Accessed: April 2010.

Ministry for the Environment. (2010). Land Use and Carbon Analysis System (LUCAS): Land use classes with woody biomass satellite imagery interpretation guide. Ministry for the Environment, Wellington. See: http://koordinates.com/#/layer/1414-new-zealand-land-use-map-1990-2008-lum-v003/ <http://koordinates.com/>. Accessed 29-04-2010.

Mitchell, N. D. (1991). The derivation of climate surfaces for New Zealand, and their application to the bioclimatic analysis of the distribution of kauri (*Agathis australis*). *Journal of the Royal Society of New Zealand, 21*, 13-24.

Moore, J. R., & Somerville, A. R. (1998). Assessing the risk of wind damage to plantation forests in New Zealand. *New Zealand Forestry, 43*, 25-29.

Moore, J. R. (2000). Differences in maximum resistive bending moments of *Pinus radiata* trees grown on a range of soil types. *Forest Ecology and Management, 135*, 63-71.

Moore, J. R., Manley, B. R., Park, D., & Scarrott, C. J. (in review). Quantification of wind damage to New Zealand's planted forests.

Mullan, A. B., Wratt, D. S., & Renwick, J. A. (2002). Transient Model Scenarios of Climate Changes for New Zealand. *Weather and Climate, 21*, 3-34.

Mullan, A. B., Porteous, A., Wratt, D., & Hollis, M. (2005). Changes in drought risk with climate change. NIWA Client Report WLG2005-23. Wellington: National Institute of Water and Atmospheric Research Ltd. 58 pp.

Mullan, B., Caray-Smith, T., Griffiths, G., & Sood, A. (2011). Scenarios of storminess and regional wind extremes under climate change. NIWA Client Report WLG2010-31 prepared for the Ministry of Agriculture and Forestry.

Nash, J. E., & Sutcliffe, J. V. (1970). River flow forecasting through conceptual models part I - A discussion of principles. *Journal of Hydrology, 10*, 282-290.

Neves, N., Moniz, F., De Azevedo, N., Ferreira, M., & Ferreira, G. (1986). Present phytosanitory situation in Portuguese forests. *EPPO Bulletin 16*, 505-508.

New, D. (1989). Accounting for New Zealand plantation's risk to wind damage. In Somerville, A.R.; Wakelin, S.J.; Whitehouse, L. (eds.). Workshop on wind

damage in New Zealand exotic forests. Ministry of Forestry, Rotorua. FRI Bulletin 146. pp 62-65.
New Zealand Forest Owners Association. (2007). New Zealand Forestry Industry, Facts and Figures 2006/2007. *New Zealand Forest Owners Association, Wellington.*
New Zealand Forest Owners Association. (2010). New Zealand plantation forest industry facts and figures. New Zealand Forest Owners Association.
Newsome, P. F. J. (1987). The Vegetative Cover of New Zealand. Soil Conservation Centre, Aokautere, Ministry of Works and Development. Water and Soil Miscellaneous Publication No. 112, Wellington, New Zealand.
Newsome, P. F. J., Wilde, R. H., & Willoughby, E. J. (2008). Land resource information system spatial data layers. Data dictionary. Palmerston North; Landcare Research New Zealand.
Newsome, P. J. F., Wilde, R. H., & Willoughby, E. J. (2000). *Land resource information system spatial data layers. Volume 1: Label Format* Palmerston North: Landcare Research.
Nicholas, I. (2007). Best Practice with Farm Forestry Timber Species, No.1: Cypresses - NZFFA electronic handbook series No. 1. www.nzffa.org,nz
Nicholas, I., Silcock, P., & Gea, L. (2007). Redwood research: The way ahead. *New Zealand Tree Grower, February 2007*, 15.
Nicholas, I. (2008). Best Practice with Farm Forestry Timber Species, No. 3: Redwoods - NZFFA electronic handbook series No. 3. www.nzffa.org,nz
Nicholas, I. D. (1991). Specialty timber species for farm sites. Paper presented at the ANZIF Conference, Christchurch, October, 1991.
Nicholas, I. D., Low, C., Miller, J., & Wilkinson, A. (2005). Tabular notes on individual species. pp. 78-83 in Colley, M. (Ed.). NZIF Forestry Handbook, New Zealand Institute of Forestry.
Nicoll, B. C., Gardiner, B. A., Rayner, W., & Peace, A. J. (2006). Anchorage of coniferous trees in relation to species, soil type, and rooting depth. *Canadian Journal of Forest Research, 36*, 1871-1883.
NIWA. (2008). See: http://www.niwa.co.nz/our-science/freshwater/tools/rec. Accessed 30/04/2010.
NIWA. (2010). New Zealand temperature record. Available at <http://www.niwa.co.nz/our-science/climate/news/all/nz-temp-record> (last accessed on 25 June, 2010).
Norby, R. J., Wullschleger, S. D., Gunderson, C. A., Johnson, D. W., & Ceulemans, R. (1999). Tree responses to rising CO_2 in field experiments: implications for the future forest. *Plant Cell and Environment, 22*(6), 683-714.
Norby, R. J., DeLucia, E. H., Gielen, B., Calfapietra, C., Giardina, C. P., King, J. S., Ledford, J., McCarthy, H. R., Moore, D. J. P., Ceulemans, R., De Angelis, P., Finzi, A. C., Karnosky, D. F., Kubiske, M. E., Lukac, M., Pregitzer, K. S., Scarascia-Mugnozza, G. E., Schlesinger, W. H., & Oren, R. (2005). Forest response to elevated CO_2 is conserved across a broad range of productivity. *Proceedings of the National Academy of Sciences of the United States of America, 102*(50), 18052-18056.
Norby, R. J., Warren, J. M., Iversen, C. M., Medlyn, B. E., & McMurtrie, R. E. (2010). CO(2) enhancement of forest productivity constrained by limited nitrogen availability. *Proceedings of the National Academy of Sciences of the United States of America, 107*(45), 19368-19373.
Nowak, R. S., Ellsworth, D. S., & Smith, S. D. (2004). Functional responses of plants to elevated atmospheric CO_2 - do photosynthetic and productivity data from FACE experiments support early predictions? *New Phytologist, 162*(2), 253-280.
NWASCO. (1970). Wise land use and community development. Report of technical committee of inquiry into the problems of the Poverty Bay- East Coast District of New Zealand. Published for the National Water and Soil Conservation Organisation by the Water and Soil Division, Ministry of Works: Wellington, New Zealand; 119 pp.

NWASCO. (1979). Our Land Resources - a bulletin to accompany NZLRI worksheets. Wellington, National Water and Soil Conservation Organisation, pp. 79.

NZFOA. (2010). Facts and Figures 2010/2011. New Zealand Forest Owners Association, Wellington, 49 pp.

Odeh, I., & McBratney, A. (2000). Using AVHRR imageries for spatial prediction of clay content in the lower Namoi Valley of eastern Australia. *Geoderma, 97*, 237-254.

Osawa, A., & Allen, R. B. (1993). Allometric theory explains self-thinning relationships of mountain beech and red pine. *Ecology, 74*, 1020-1032.

Page, M. J., Reid, L. M., & Lynn, I. H. (1999). Sediment production from Cyclone Bola landslides, Waipaoa catchment. *Journal of Hydrology 38*, 289-308.

Palmer, D. J. (2008). Development of national extent terrain attributes (TANZ), soil water balance surfaces (SWatBal), and environmental surfaces, and their application for spatial modelling of *Pinus radiata* productivity across New Zealand. PhD thesis, University of Waikato, Hamilton, New Zealand. 410pp.

Palmer, D. J., Höck, B. K., Dunningham, A. G., Lowe, D. J., & Payn, T. W. (2009). Developing national-scale terrain attributes for New Zealand (TANZ). *Forest Research Bulletin, 232*, 1-81.

Palmer, D. J., Hock, B. K., Kimberley, M. O., Watt, M. S., Lowe, D. J., & Payn, T. W. (2009). Comparison of spatial prediction techniques for developing *Pinus radiata* productivity surfaces across New Zealand. *Forest Ecology and Management, 258*(9), 2046-2055.

Palmer, D. J., Watt, M. S., Hock, B. K., & Lowe, D. J. (2009). A dynamic framework for spatial modelling *Pinus radiata* soil water balance (SWatBal) across New Zealand. Scion Bulletin 234. pp. 93.

Palmer, D. J., Watt, M. S., Kimberley, M. O., Hock, B. K., Payn, T. W., & Lowe, D. J. (2010). Mapping and explaining the productivity of *Pinus radiata* in New Zealand. *New Zealand Journal of Forestry, 55*, 15-21.

Parton, W. J., Schimel, D. S., Cole, C. V., & Ojima, D. S. (1987). Analysis of factors controlling soil organic matter levels in Great Plains grasslands. *Soil Science Society of America Journal, 51*(5), 1173-1179.

Paul, I., Van Jaarsveld, A. S., Korsten, L., & Hattingh, V. (2005). The potential global geographical distribution of citrus black spot caused by *Guignardia citricarpa* (Kiely): Likelihood of disease establishment in the European Union. *Crop Protection, 24*(4), 297-308.

Payn, T. W., Skinner, M. F., Hill, R. B., Thorn, A. J., Scott, J., Downs, S., & Chapman, H. (2000). Scaling up or scaling down: the use of foliage and soil information for optimising the phosphate nutrition of radiata pine. *Forest Ecology and Management, 138*(1-3), 79-89.

Payton, I. J., Barringer, J., Lambie, S., Lynn, I., Forrester, G., & Pinkney, T. (2010). Carbon sequestration rates for post-1989-compliant indigenous forests. Landcare Research Contract Report LC0809/107, 35 pp.

Pearce, H. G., Mullan, A. B., Salinger, M. J., Opperman, T. W., Woods, D., & Moore, J. R. (2005). Impact of climate change on long-term fire danger. NZFSC Research Report No. 50. Wellington: New Zealand Fire Service Commission. 70 pp.

Pearce, H. G., Cameron, G., Anderson, S. A. J., & Dudfield, M. (2008). An overview of fire management in New Zealand forestry. *New Zealand Journal of Forestry, 53*, 7-11.

Pearce, H. G., & Clifford, V. (2008). Fire weather and climate of New Zealand. *New Zealand Journal of Forestry, 53*, 13-18.

Pearce, H. G., Kerr, J., Clark, A., Mullan, B., Ackerley, D., Carey-Smith, T., & Yang, E. (2011). Improved estimates of the effect of climate change on NZ fire danger. Scion Client Report (MAF SLMACC) No. 18087. Christchurch & Wellington: Scion, Rural Fire Research Group, in conjunction with NIWA. 84 pp.

Pearce, H. G., Kerr, J. L., Clifford, V. R., & Wakelin, H. M. (2011). Fire climate severity across New Zealand. NZFSC Research Report No. 116. Wellington: New Zealand Fire Service Commission. 78 pp.

Pearce, H. G. (2012). Initial investigation into relationships between current fire climate severity and fire occurrence. Scion, Rural Fire Research Group, unpublished data.

Peltola, H., Kellomäki, S., Hassinen, A., & Granander, M. (2000). Mechanical stability of Scots pine, Norway spruce and birch: an analysis of tree-pulling experiments in Finland. *Forest Ecology and Management, 135*, 143-153.

Peterson, G. (1967). Dothistroma needle blight of Pines in North America. Proc. 14th Congress IUFRO, Munich 1967.

Plummer, N., Salinger, M. J., Nicholls, N., Suppiah, R., Hennessy, K. J., Leighton, R. M., Trewin, B., M., P. C., & Lough, J. M. (1999). Changes in climate extremes over the Australian region and New Zealand during the Twentieth Century. *Climatic Change, 42*, 183-202.

Poorter, H., & Navas, M. L. (2003). Plant growth and competition at elevated CO_2: on winners, losers and functional groups. *New Phytologist, 157*(2), 175-198.

Quine, C., Coutts, M., Gardiner, B., & Pyatt, G. (1995). Forests and Wind: Management to Minimise Damage. Forestry Commission Bulletin 114, HMSO, London. 27 p.

Quine, C. P., & White, I. M. S. (1994). Using the relationship between the rate of tatter and topographic variables to predict site windiness in upland Britain. *Forestry, 67*, 245-256.

Quine, C. P. (2000). Estimation of mean wind climate and probability of strong winds for wind risk assessment. *Forestry, 73*(3), 247-258.

Quine, C. P., & Gardiner, B. A. (2002). Climate change impacts: storms. In: Broadmeadow, M. (ed.) Climate Change: Impacts on UK Forests. Forestry Commission Bulletin, 125, HMSO, London. Pp. 41-52.

Rahmstorf, S., Cazenave, A., Church, J. A., Hansen, J. E., Keeling, R. F., Parker, D. E., & Somerville, R. C. J. (2007). Recent climate observations compared to projections. *Science, 316*(5825), 709.

Raison, R. J. (1979). Modification of the soil environment by vegetation fires, with particular reference to nitrogen transformations: a review. *Plant and Soil, 51*, 73-108.

Rastetter, E. B., McKane, R. B., Shaver, G. R., & Melillo, J. M. (1992). Changes in C storage by terrestrial ecosystems: how C-N interactions restrict responses to CO_2 and temperature. *Water, Air, and Soil Pollution 64*, 327-344.

Richardson, B., Whitehead, D., & McCracken, I. J. (2002). Root-zone water storage and growth of *Pinus radiata* in the presence of a broom understorey. *New Zealand Journal of Forestry Science, 32*(2), 208-220.

Rogers, G. M., & Leathwick, J. R. (1994). North-Island seral tussock grasslands. 2. Autogenic succession - change of tussock grassland to shrubland. *New Zealand Journal of Botany, 32*, 287-303.

Ross, D. J., Scott, N. A., Lambie, S. M., Trotter, C. M., Rodda, N. J., & Townsend, J. A. (2009). Nitrogen and carbon cycling in a New Zealand pumice soil under a manuka (*Leptospermum scoparium*) and kanuka (*Kunzea ericoides*) shrubland. *Australian Journal of Soil Research, 47*, 725-736.

Roxburgh, S. H., Barrett, D. J., Berry, S. L., Carter, J. O., Davies, I. D., Gifford, R. M., Kirschbaum, M. U. F., McBeth, B. P., Noble, I. R., Parton, W. G., Raupach, M. R., & Roderick, M. L. (2004). A critical overview of model estimates of net primary productivity for the Australian continent. *Functional Plant Biology, 31*, 1043–1059.

Ruel, J. C., Pin, D., Spacek, L., Cooper, K., & Benoit, R. (1997). The estimation of wind exposure for windthrow hazard rating: comparison between Strongblow, MC2, Topex and a wind tunnel study. *Forestry (Oxford), 70*(3), 253-266.

Sabate, S., Gracia, C. A., & Sanchez, A. (2002). Likely effects of climate change on growth of *Quercus ilex*, *Pinus halepensis*, *Pinus pinaster*, *Pinus sylvestris* and *Fagus sylvatica* forests in the Mediterranean region. *Forest Ecology and Management, 162*(1), 23-37.

Salinger, M. J. (1981). New Zealand Climate: The instrumental record. Thesis submitted for the degree of Doctor of Philosophy at the Victoria University of Wellington, January 1981.

Sallnäs, O. (1990). A matrix growth model of the Swedish forest. Studia Forestalia Sueccia No. 183. Uppsala: Swedish University of Agricultural Sciences, Faculty of Forestry.

Sands, P. (2004). Adaptation of 3-PG to novel species: guidelines for data collection and parameter assignment. Technical Report 141. Cooperative Research Centre for Sustainable Production Forestry. CSIRO.

Sands, P. J. (1995). Modelling canopy production. II. From single-leaf photosynthesis parameters to daily canopy photosynthesis. *Australian Journal of Plant Physiology, 22*(4), 603-614.

SAS-Institute-Inc. (2000). SAS/STAT User's Guide: Version 8. *Volumes 1, 2 and 3. SAS Institute Inc., Cary, North Carolina, 3884 pp.*

Schelhaas, M. J., Nabuurs, G. J., Sonntag, M., & Pussinen, A. (2002). Adding natural disturbances to a large-scale forest scenario model and a case for Switzerland. *Forest Ecology and Management, 167*, 13-26.

Schimel, D. S., Parton, W. J., Kittel, T. G. F., Ojima, D. S., & Cole, C. V. (1990). Grassland biogeochemistry - links to atmospheric processes. *Climatic Change, 17*, 13-25.

Schwalm, C. R., & Ek, A. R. (2001). Climate change and site: relevant mechanisms and modeling techniques. *Forest Ecology and Management, 150*(3), 241-257.

Scion. (2011a). Fire climate severity. Rural Fire Research Update, 8 (July 2011). Christchurch: Scion, Rural Fire Research Group. 4 pp.

Scion. (2011b). Future fire danger. Rural Fire Research Update, 9 (November 2011). Christchurch: Scion, Rural Fire Research Group. 4 pp.

Scott, N. A., White, J. D., Townsend, J. A., Whitehead, D., Leathwick, J. R., Hall, G. M. J., Marden, M., Rogers, G. N. D., Watson, A. J., & Whaley, P. T. (2000). Carbon and nitrogen distribution and accumulation in a New Zealand scrubland ecosystem. *Canadian Journal of Forest Research-Revue Canadienne De Recherche Forestiere, 30*(8), 1246-1255.

SCRCC. (1974). Land Use Capability survey handbook. A New Zealand handbook for the classification of land. Wellington, Soil Conservation and Rivers Control Council, pp. 137.

Simioni, G., Ritson, P., Kirschbaum, M. U. F., McGrath, J., Dumbrell, I., & Copeland, B. (2009). The carbon budget of *Pinus radiata* plantations in south-western Australia under four climate change scenarios. *Tree Physiology, 29*(9), 1081-1093.

Simmons, J. H. (1927). Trees from other lands for shelter and timber in New Zealand: Eucalypts. Brett Publishing Co. Auckland.

Sinclair, S., Turner, J. A., Schnell, J., Smeaton, D., & Glennie, S. (2009). Management of carbon price exposure in the agricultural sector through the use of post-1989 forestry - case studies based on farmer data, attitudes and actions. Report Prepared for the Ministry of Agriculture and Forestry. AgResearch, Hamilton. http://www.maf.govt.nz/climatechange/reports/management-of-carbon-price-exposure-feb-2010.pdf. Accessed 29-04-10.

Sinclair, W. A., & Lyon, H. H. (2005). *Diseases of Trees and Shrubs* Ithaca, New York: Cornell University Press.

Smale, M. C. (1994). Structure and dynamics of kanuka (*Kunzea ericoides* var. *ericoides*) heaths on sand dunes in Bay of Plenty, New Zealand. *New Zealand Journal of Botany, 32*, 441-452.

Smale, M. C., McLeod, M., & Smale, P. N. (1997). Vegetation and soil recovery on shallow landslide scars in tertiary hill country, East Cape region, New Zealand. *New Zealand Journal of Ecology, 21*, 31-41.

Smith, C. T., Lowe, A. T., Skinner, M. F., Beets, P. N., Schoenholtz, S. H., & Fang, S. Z. (2000). Response of radiata pine forests to residue management and

fertilisation across a fertility gradient in New Zealand. *Forest Ecology and Management, 138*(1-3), 203-223.

Snowdon, K., McIvor, I., & Nicholas, I. (2008). Energy farming with willow in New Zealand. SFF Project (05/058).

Somerville, A. R. (1995). Wind damage in New Zealand State plantation forests. In M. P. Coutts & J. Grace (Eds.), *Wind and Trees* (pp. 460-467). Cambridge: Cambridge University Press.

Stahl, W. (1966). Needle cast fungi on conifers in the Australian Capital Territory. *Australian Forestry 30*, 20-32.

Stephens, J. M. C., Molan, P. C., & Clarkson, B. D. (2005). A review of *Leptospermum scoparium* (*Myrtaceae*) in New Zealand. *New Zealand Journal of Botany 43*, 431-449.

Stinson, G., Kurz, W. A., Smyth, C. E., Neilson, E. T., Dymond, C. C., Metsaranta, J. M., Boisvenue, C., Rampley, G. J., Li, Q., White, T. M., & Blain, D. (2011). An inventory-based analysis of Canada's managed forest carbon dynamics, 1990 to 2008. *Global Change Biology, 17*(6), 2227-2244.

Studholme, W. P. (1995). The experience of and management strategy adopted by the Selwyn Plantation Board, New Zealand. In: Coutts, M.P. and Grace, J. (eds.). Wind and Trees, Cambridge University Press, Cambridge, U.K. pp. 468-476.

Suckling, D. M., Gibb, A. R., Daly, J. M., Chen, X., & Brockerhoff, E. G. (2001). Behavioural and electrophysiological responses of Arhopalus tristis to burnt pine and other stimuli. *Journal of Chemical Ecology, 27*, 1091-1104.

Sullivan, J. J., Williams, P. A., & Timmins, S. M. (2007). Secondary forest succession differs through naturalised gorse and native kanuka near Wellington and Nelson. *New Zealand Journal of Ecology, 31*, 22-38.

Sutherst, R. W., Baker, R. H. A., Coakley, S. M., R. Harrington, R., Kriticos, D. J., & Scherm, H. (2007). Pests Under Global Change - Meeting Your Future Landlords? In *Terrestrial Ecosystems in a Changing World* (pp. 211-223): Springer, Berlin Heidelberg New York.

Tait, A., Henderson, R., Turner, R., & Zheng, Z. (2006). Thin plate smoothing interpolation of daily rainfall for New Zealand using a climatological rainfall surface. *International Journal of Climatology, 26*, 2097-2115.

Tait, A. (2008). Future projections of growing degree days and frost in New Zealand and some implications for grape growing. *Weather and Climate, 28*, 17-36.

Tait, A., & Liley, B. (2009). Interpolation of daily solar radiation for New Zealand using a satellite derived cloud cover surface. *Weather Climate 29*, 70-88.

Thompson, A. P. (1976). 500-year evidence of gales: research would identify risk areas. *Forest Industries Review, 7*, 11-16.

Thompson, S., Gruner, I., & Gapare, N. (2003). New Zealand Land Cover Database Version 2 - Illustrated Guide to Target Classes. Technical User Guide Version 4.0_April 2004, Ministry for the Environment, http://www.mfe.govt.nz/issues/land/land-cover-dbase/. Accessed 30/04/2010.

Tian, X. R., Shu, L. F., Wang, M. Y., & Zhao, F. J. (2011). Forest fire danger ratings in the 2040s for northeastern China. *Forestry Studies in China, 13*, 85-96.

Trenberth, K. E., Jones, P. D., Ambenje, P., Bojariu, R., Easterling, D., Klein, T. A., Parker, D., Rahimzadeh, F., Renwick, J. A., Rusticucci, M., Soden, B., & Zhai, P. (2007). Observations: Surface and atmospheric climate change. In: Climate Change 2007: The Physical Science Basis. Contribution of Working Group I to the Fourth Assessment Report of the Intergovernmental Panel on Climate Change [Solomon, S., D. Qin, M. Manning, Z. Chen, M. Marquis, K.B. Averyt, M. Tignor and H.L. Miller (eds.)]. Cambridge University Press, Cambridge, United Kingdom and New York, NY, USA, pp. 235-336. .

Trotter, C., Tate, K., Scott, N., Townsend, J., Wilde, H., Lambie, S., Marden, M., & Pinkney, T. (2005). Afforestation/ reforestation of New Zealand marginal pasture lands by indigenous shrublands: the potential for Kyoto forest sinks. *Annals of Forest Science, 62*, 865-871.

Tupek, B., Zanchi, G., Verkerk, P. J., Churkina, G., Viovy, N., Hughes, J. K., & Lindner, M. (2010). A comparison of alternative modelling approaches to evaluate the European forest carbon fluxes. *Forest Ecology and Management, 260*(3), 241-251.

Turner, J., & Lambert, M. J. (1986). Nutrition and nutritional relationships of *Pinus radiata*. *Annual Review of Ecology and Systematics, 17*, 325-350.

Turner, J. A., West, G., Dungey, H., Wakelin, S., Maclaren, P., Adams, T., & Silcock, P. (2008). Managing New Zealand planted forests for carbon: A review of selected management scenarios and identification of knowledge gaps. MAF report No. CC MAF POL_2008-09 (108-1).

van der Pas, J., Bulman, L., & Horgan, G. (1984). Estimation and cost benefits of spraying *Dothistroma pini* in tended stands of *Pinus radiata* in New Zealand. *New Zealand Journal of Forestry Science 14*, 23-40.

van der Pas, J. B. (1981). Reduced early growth rates of *Pinus radiata* by *Dothistroma pini*. *New Zealand Journal of Forestry Science, 11*(3), 210-220.

van der Pas, J. B., Slater-Hayes, J. D., Gadgil, P. D., & Bulman, L. (1984). *Cyclaneusma* (*Naemacyclus*) needle-cast of *Pinus radiata* in New Zealand. 2: Reduction in growth of the host, and its economic implication. *New Zealand Journal of Forestry Science, 14*, 197-209.

Vanner, A. L. (1986). An aerial spray trial to control Cyclaneusma needlecast on radiata pine. Proceedings of the 39th New Zealand Weed and Pest Control Conference: 106-107.

Venette, R. C., & Cohen, S. D. (2006). Potential climatic suitability for establishment of *Phytophthora ramorum* within the contiguous United States. *Forest Ecology and Management, 231*, 18-26.

Villebonne, D., & Maugard, F. (1999). Rapid development of Dothistroma needle blight (*Scirrhia pini*) on Corsican pine (*Pinus nigra* subsp. *laricio*) in France. La Sante des Forets, Annual Report 1998, Les Cahiers du DSF 1, DERF, Paris 30-32.

Wallin, J. R., & Waggoner, P. E. (1950). The influence of climate on the development and spread of *Phytophthora infestans* in artificially inoculated potato plots. *Plant Dis. Reptr. Suppl. , 190*, 19-33.

Waring, R., Milner, K. S., Jolly, W. M., Phillips, L., & McWethy, D. (2005). A basis for predicting site index and maximum growth potential across the Pacific and Inland Northwest U.S.A. with a MODIS satellite-dervided vegetation index. *Forest Ecology and Management, 228*, 285-291.

Watt, M. S., Whitehead, D., Mason, E. G., Richardson, B., & Kimberley, M. O. (2003). The influence of weed competition for light and water on growth and dry matter partitioning of young *Pinus radiata*, at a dryland site. *Forest Ecology and Management, 183*(1-3), 363-376.

Watt, M. S., Kirschbaum, M. U. F., Paul, T. S. H., Tait, A., Pearce, H. G., Brockerhoff, E. G., Moore, J. R., Bulman, L. S., & Kriticos, D. J. (2008). The effect of climate change on New Zealand's planted forests: Impacts, risks and opportunities. Client Report No. CC MAF POL_2008-07 (106-1) -No. 1.

Watt, M. S., Kriticos, D. J., Alcaraz, S., Brown, A. V., & Leriche, A. (2009). The hosts and potential geographic range of Dothistroma needle blight. *Forest Ecology and Management, 257*, 1505-1519.

Watt, M. S., Palmer, D. J., Dungey, H., & Kimberley, M. O. (2009). Predicting the spatial distribution of *Cupressus lusitanica* productivity in New Zealand. *Forest Ecology and Management, 258*(3), 217-223.

Watt, M. S., Palmer, D. J., Kimberley, M. O., Hock, B. K., Payn, T. W., & Lowe, D. J. (2010). Development of models to predict *Pinus radiata* productivity throughout New Zealand. *Canadian Journal of Forest Research-Revue Canadienne De Recherche Forestiere, 40*(3), 488-499.

Watt, M. S., Stone, J. K., Hood, I. A., & Palmer, D. J. (2010). Predicting the severity of Swiss needle cast on Douglas fir under current and future climate in New Zealand. *Forest Ecology and Management, 260*, 2232-2240.

Watt, M. S., Ganley, R. J., Kriticos, D. J., & Manning, L. (2011). Dothistroma needle blight and pitch canker: the current and future potential distribution of two important diseases of *Pinus* species. *Canadian Journal of Forest Research, 41*, 412-424.

Watt, M. S., & Kirschbaum, M. U. F. (2011). Moving beyond simple linear allometric relationships between tree height and diameter. *Ecological Modelling, 222*(23-24), 3910-3916.

Watt, M. S., Palmer, D. J., & Bulman, L. S. (2011). Predicting the severity of Dothistroma on *Pinus radiata* under current climate in New Zealand. *Forest Ecology and Management, 261*, 1792-1798.

Watt, M. S., Rolando, C. A., Palmer, D. J., & Bulman, L. (2012). Predicting the severity of *Cyclaneusma minus* on *Pinus radiata* under current climate in New Zealand. *Canadian Journal of Forest Research, 42*, 667-674.

Webb, J. (2007). Redwood markets in California. *New Zealand Tree Grower 28*, 13.

Webb, T. H., & Wilson, A. D. (1995). A manual of land characteristics for evaluation of rural land. Landcare research science series No. 10. Lincoln. Landcare Research New Zealand.

Weston, G. (1957). Forest Trees of New Zealand. NZ Forest Service Bulletin No. 13.

Whitehead, D., Walcroft, A. S., Scott, N. A., Towsend, J. A., Trotter, C. M., & Rogers, G. N. D. (2004*b*). Characteristics of photosynthesis and stomatal conductance in the shrubland species manuka (*Leptospermum scoparium*) and kanuka (*Kunzea ericoides*) for the estimation of annual carbon uptake. *Tree Physiology, 24*, 795-804.

Whitehead, D., & Walcroft, A. S. (2005). Forest and shrubland canopy carbon uptake in relation to foliage nitrogen concentration and leaf area index: a modelling analysis. In *Annals of Forest Science* (Vol. 62, pp. 525-535). Les Ulis France: EDP Sciences.

Wilcox, M. D., Rook, D. A., & Holden, D. G. (1980). Provenance variation in frost resistance of *Eucalyptus fastigata* Deane & Maid. Presented to IUFRO Symposium and Workshop, Genetic improvement and productivity of fast-growing tree species: 9 p.

Wilcox, M. D. (1982). Genetic variation in frost tolerance, early height growth, and incidence of forking among and within provenances of *Eucalyptus fastigata*. *New Zealand Journal of Forestry Science, 12*, 510-524.

Wilde, R. H., Willoughby, E. J., & Hewitt, A. E. (2000). Data manual for the national soils database spatial extension. Landcare Research New Zealand Ltd. Available online at: http://www.landcareresearch.co.nz/databases/nzlri.asp {Last accessed October 2010}.

Will, G. M. (1985). *Nutrient deficiencies and fertiliser use in New Zealand exotic forests* Rotorua, New Zealand: Forest Research Institute Bulletin No 97.

Wilson, A. D., & Giltrap, D. J. (1982). Prediction and mapping of soil water retention properties. New Zealand Soil Bureau district office report WN7. Wellington, Department of Scientific and Industrial Research.

Wilson, H. D. (1994). Regeneration of native forest on Hinewai Reserve, Banks Peninsula. *New Zealand Journal of Ecology 32*, 373-383.

Woods, A. (2003). Species diversity and forest health in northwest British Columbia. *Forestry Chronicle 79*, 892-897.

Woods, A., Coates, K., & Hamann, A. (2005). Is an unprecedented Dothistroma needle blight epidemic related to climate change? *BioScience 55*, 761-769.

Wratt, D., Mullen, B., Salinger, J., Allan, S., Morgan, T., & Kenny, G. (2004). Climate change effects and impacts assessment: a guidance manual for local government in New Zealand. Ministry for the Environment, Climate Change Office Report ME 513, Wellington.

Wratt, D. S., Tait, A., Griffiths, G., Espie, P., Jessen, M., Keys, J., Ladd, M., Lew, D., Lowther, W., Mitchell, N., Morton, J., Reid, J., Reid, S., Richardson, A., Sansom, J., & Shankar, U. (2006). Climate for crops: integrating climate data with

information about soils and crop requirements to reduce risks in agricultural decision-making. *Meteorological Applications, 13*(4), 305-315.

Acknowledgements

Funding was provided from the MAF contract 'Future Forest Systems' (Contract No. C04X0901). Specific acknowledgements relating to each of the chapters area as follows:

Chapter 1.

We thank Peter Hall, Ian Nicholas, James Turner, Thomas Paul (Scion), and Mark Bloomberg (University of Canterbury) for their advice and assistance in the development of the future forest scenarios. This work was jointly funded through the MAF programme, Future Forest Systems (Contract No. CO4X0901), and the Future Forest Research contract 'Positioning Future forests project (Contract No. C04X0806).

Chapter 2.

The assistance of Christine Dodunski and Carolyn Andersen, (Scion PSP administrators) in data preparation and summaries for new and existing plots is most appreciated. The field assistance of Mark Miller (Scion), Angus Gordon (NZFFA), and Tim Rose (NZFFA) was also critical in completing the establishment of the new plots. The permission from the landowners to establish new plots, use existing data and FFR for the use of PSP data has also been critical to this species selection project, their help is most appreciated.

Chapter 3.

3.1. Future wood productivity of *Pinus radiata* in New Zealand under expected climatic changes

We would like to thank Hamish Heke for preparing plots of the spatial information and David Palmer, Ian Payton and two anonymous referees for many useful comments on the manuscript.

3.2. Influence of climate change on productivity of *Eucalyptus fastigata*

We appreciate the advice and assistance of Michael Battaglia and Jody Bruce. We are also grateful to Auro Almeida, Andrew Dunningham, Carolyn Anderson, Christine Dodunski, Christine Todoroki, Mark Miller, Kane Fleet, Toby Stovold and FFR for access to the PSP database.

3.3 Influence of climate change on productivity of coast redwood

As above for 3.2.

Chapter 4.

4.1. and 4.2. Predicting the severity of Cyclanuesma needle cast and Dothistroma needle blight on *Pinus radiata* under future climate in New Zealand

The data were collected during forest health surveys funded from 1970 to 1987 by the New Zealand Forest Service and thereafter primarily by members of the New Zealand Forest Owners' Association.

4.3 Impact of climate change on fire risk

Datasets of projected changes in fire climate for weather station locations from statistical downscaling were provided by NIWA (Drs Anthony Clark and Brett Mullan). Dr Andrew Tait (NIWA) also provided advice during the initial project design. GIS maps of projected changes in fire danger were produced by Heather Wakelin and Lucy Manning (Scion). The research was funded by the Ministry of Agriculture and Forestry (MAF) under the Sustainable Land Management and Climate Change (SLMACC) Plan (Contract C04X0809, Climate Change and Fire Danger), but was also supported by funding provided by the Foundation for Research, Science and Technology (FRST) and rural fire end-users as part of contract C0X0403 (Rural Fire).

Appendix A – List of publications resulting from MAF contract

1. Watt, M.S., Palmer, D. J., Höck, B. K. (2011). Spatial description of potential areas suitable for afforestation within New Zealand and quantification of their productivity under *Pinus radiata*. *New Zealand Journal of Forestry Science*, 41, 115-129.
2. Nicholas, I., Watt, M.S. (2011) The three potentially most useful exotic forest species for south eastern North Island marginal hill country. *New Zealand Journal of Forestry* 56 (1), 15-19.
3. Kirschbaum, M.U.F., Watt, M.S. (2011) Use of a process-based model to describe spatial variation in *Pinus radiata* productivity in New Zealand. *Forest Ecology and Management*, 262, 1008-1019.
4. Kirschbaum, M.U.F., Watt, M.S., Tait, A., Ausseil, A.E. (2012) Future productivity of *Pinus radiata* in New Zealand under expected climatic changes. *Global Change Biology* 18, 1342-1356.
5. Watt, M.S., Kirschbaum, M.U.F. (2011) Moving beyond simple linear allometric relationships between tree height and diameter. *Ecological Modelling* 222, 3910-3916.
6. Watt, M.S., Palmer, D.J. (2012) Use of regression kriging to develop a Carbon: Nitrogen ratio surface for New Zealand. *Geoderma* 183-184, 49-57.
7. Watt, M.S., Palmer, D.J., Bulman, L.S. (2011) The ecomomic cost of Dothistroma needle blight to the New Zealand forest industry. *New Zealand Journal of Forestry* 56 (1), 20-22.
8. Watt, M.S., Palmer, D.J., Bulman, L.S. (2011) Predicting the severity of Dothistroma on *Pinus radiata* under current climate in New Zealand. *Forest Ecology and Management* 261, 1792-1798.
9. Watt, M.S., Palmer, D. J., Bulman, L.S. (2011) Predicting the severity of Dothistroma needle blight on *Pinus radiata* under future climate in New Zealand. *New Zealand Journal of Forestry Science*, 41, 207-215.
10. Watt, M.S., Rolando, C., Palmer, D.J., Bulman, L.S. (2012) Predicting the severity of *Cyclanuesma minus* on *Pinus radiata* under current climate in New Zealand. *Canadian Journal of Forest Research* 42, 667-674.
11. Watt, M.S., Palmer, D.J., Bulman, L.S., Harrison, D. (in press) Predicting the severity of Cyclanuesma needle cast on *Pinus radiata* under future climate in New Zealand. New Zealand Journal of Forestry Science.

Appendix B – Mean regional variation in 300 Index for current forests and the three future forest scenarios

Region	300 Index (m^{-3} ha^{-1} yr^{-1})			
	Current forests	Scenario 1	Scenario 2	Scenario 3
Northland	26.8	29.9	29.4	28.4
Auckland	27.4	30.8	30.0	28.9
Waikato	27.5	32.3	31.0	30.5
Gisborne	32.2	32.5	32.7	32.7
Bay of Plenty	27.2	32.0	31.1	31.0
Hawkes Bay	31.3	31.2	31.6	31.8
Taranaki	31.2	31.2	29.8	29.6
Manawatu-Wanganui	28.3	30.2	29.8	29.6
Wellington	27.6	29.0	28.9	28.4
Nelson	26.3	28.8	28.9	28.6
Tasman	25.8	27.3	26.5	26.3
Marlborough	26.8	23.1	24.0	25.7
West Coast	23.3	23.5	23.6	23.6
Canterbury	22.2	24.4	23.7	24.4
Otago	23.6	22.3	21.2	21.2
Southland	25.6	26.0	25.5	25.0

Appendix C – Parameters used for kanuka/mānuka simulations

The parameters given below were used to give the best description of the full present data set.

Parameter description	**kanuka/ mānuka**	**Units**
Minimum foliage turn-over	0.14	yr^{-1}
Fine-root turn-over	0.5	yr^{-1}
Branch turn-over	0.05	yr^{-1}
Bark turn-over	0.04	yr^{-1}
Low-light senescence limit	1.0	MJ m^{-2} d^{-1}
Max daily low-light senescence	1	% d^{-1}
Max drought foliage death rate	1.3	% d^{-1}
Soil water stress threshold (W_{crit})	0.63	-
Respiration ratio	0.41	-
Specific leaf area	9.1	m^2 $(kgDW)^{-1}$
Foliage albedo	10	%
Transmissivity	2	%
Loss as volatile organic carbon	0.5	%
Threshold N concentrations (N_o)	10	gN $(kgDW)^{-1}$
Non-limiting N concentration (N_{sat})	30	gN $(kgDW)^{-1}$
Light-saturated maximum photosynthetic rate (A_{max})	39.5	µmol m^{-2} s^{-1}
Maximum quantum yield	0.08	mol mol^{-1}
Curvature in light response function	0.73	-
Ball-Berry stomatal parameter (unstressed)	9.5	-
Ball-Berry stomatal parameter (stressed)	5	-
Age-based decline	70	years
Exponential term in age-based decline	4.0	-
Size-based decline	240	tDM ha^{-1}
Exponential term in size-based decline	4.0	-
Minimum temperature for photosynthesis (T_n)	5.3	°C
Lower optimum temperature for photosynthesis ($T_{opt,\ lower}$)	12.9	°C
Upper optimum temperature for photosynthesis ($T_{opt,\ upper}$)	24	°C
Maximum temperature for photosynthesis (T_x)	35	°C
Frost damage threshold temperature (F_0)	0	°C
High-temperature damage threshold temperature (S_0)	35	°C
Temperature damage sensitivity (s_T)	0.03	-
Temperature damage repair rate (R_T)	0.46	d^{-1}
Heavy-rain damage threshold (R_{crit})	60	mm d^{-1}
Heavy-rain damage sensitivity (s_R)	0.05	-
Heavy-rain damage repair rate (D_{repair})	1.5	d^{-1}
Max repair length (for complete damage)	40	d
Water-logging threshold (L_{log})	0.975	-
Water-logging sensitivity (s_L)	0.5	-

Parameter description	kanuka/ mānuka	Units
Foliar lignin concentration	30	%
Root lignin concentration	30	%
Wood lignin concentration	30	
Atmospheric N deposition	3	kgN ha^{-1} yr^{-1}
Volatilisation fraction	5	%
Leaching fraction	0.75	-
Litter water-holding capacity	2	g gDW^{-1}
Mulching effect of litter	5	% tDW^{-1}
Canopy aerodynamic resistance	40	s m^{-1}
Canopy rainfall interception	0.45	mm LAI^{-1}
Organic matter transfer in the soil for top three layers, decreasing with depth	5/ 3/ 1	% cm^{-1} yr^{-1}
Organic matter transfer from surface to soil	5	% yr^{-1}
Critical C:N ratio	7.5	
Ratio of C:N ratios in structural and metabolic pools	5	
Exponential term in lignin inhibition	3	
Residual decomposition under dry conditions	0.1	
Mineral N immobilised	1	% d^{-1}
Maximal height of weed layer	2.56	m
Weeds reach half max. height at weed leaf biomass	1.69	tDW ha^{-1}
Weed foliage turn-over	1.5	yr^{-1}
Weed allocation to foliage	0.369	-
Foliage: branch ratio	1.84	-
Stem: branch	4.7	-
Coarse roots: stem wood	0.2	-
Bark: stem wood	0.05	-
Allocation to seed and seed capsules	0.03	-
Allocation to pollen	0.03	-
Minimum wood allocation	0.15	-
Fine root: foliage ratio (nitrogen-unstressed)	0.2	-
Fine root: foliage ratio (nitrogen-stressed)	0.41	-
Initial slope in height:diameter (h:d) allometric relationship	0.43	-
Intercept in initial h:d allometric relationship	1.13	-
Height:diameter relationship constant	0.43	-
Minimum value for h:d relationship	0.01	-
Maximum value for h:d relationship	1.5	-
Wood density	800	kg m^{-3}